AWARD NUMBER: W81XWH-15-1-0621

TITLE: Brain Consequences of Spinal Cord Injury with and without Neuropathic Pain: Translating Animal Models of Neuroinflammation onto Human Neural Networks and Back

PRINCIPAL INVESTIGATOR: Nils Clas Linnman

CONTRACTING ORGANIZATION: Boston Children´s Hospital
Boston, MA 02115

REPORT DATE: October 2018

TYPE OF REPORT: Annual Report

PREPARED FOR: U.S. Army Medical Research and Materiel Command
Fort Detrick, Maryland 21702-5012

REPORT DOCUMENTATION PAGE

Form Approved
OMB No. 0704-0188

1. REPORT DATE	2. REPORT TYPE	3. DATES COVERED
Oct 2018	Annual	15Sep2017 - 14Sep2018

4. TITLE AND SUBTITLE

Brain Consequences of Spinal Cord Injury with and without Neuropathic Pain: Translating Animal Models of Neuroinflammation Onto Human Neural Networks and Back

5a. CONTRACT NUMBER
W81XWH-15-1-0621

5b. GRANT NUMBER
SC140194

5c. PROGRAM ELEMENT NUMBER

6. AUTHOR(S)
Nils Clas Linnman
Teng Yang

E-Mail:clas.linnman@childrens.harvard.edu

5d. PROJECT NUMBER

5e. TASK NUMBER

5f. WORK UNIT NUMBER

7. PERFORMING ORGANIZATION NAME(S) AND ADDRESS(ES)
Boston Children´s Hospital
300 Longwood Avenue, Boston,
MA 02115

8. PERFORMING ORGANIZATION REPORT NUMBER

9. SPONSORING / MONITORING AGENCY NAME(S) AND ADDRESS(ES)

U.S. Army Medical Research and Materiel Command
Fort Detrick, Maryland 21702-5012

10. SPONSOR/MONITOR'S ACRONYM(S)

11. SPONSOR/MONITOR'S REPORT NUMBER(S)

12. DISTRIBUTION / AVAILABILITY STATEMENT

Approved for Public Release; Distribution Unlimited

13. SUPPLEMENTARY NOTES

14. ABSTRACT
This project aims to investigate the consequence of spinal cord injury with regards to alterations in brain network function and expression of activated microglia, both human patients and in an animal model. During year three we have continued our collection of PET-MR data on spinal cord injured subjects, completed the rodent spinal cord injury surgeries and imaging procedures. Human imaging data is of consistently high quality and is reliably collected, albeit with some concerns regarding patient recruitment being slower than anticipated. The animal behavioral and imaging data is of high quality, and histological analysis is ongoing in parallell with neuroimaging analysis.

15. SUBJECT TERMS
microglia, Positron Emission Tomography, functional Magnetic Resonance Imaging, translational medicine, spinal cord injury, rat, human

16. SECURITY CLASSIFICATION OF:			17. LIMITATION OF ABSTRACT	18. NUMBER OF PAGES	19a. NAME OF RESPONSIBLE PERSON
a. REPORT	b. ABSTRACT	c. THIS PAGE			USAMRMC
Unclassified	Unclassified	Unclassified	Unclassified	111	19b. TELEPHONE NUMBER *(include area code)*

Table of Contents

1. INTRODUCTION

The goal of this project is to develop a translational framework where we define targets in SCI patients with and without neuropathic pain using a combination of clinical assessment, microglial Positron Emission Tomography (PET) and functional- structural- and diffusion- Magnetic Resonance Imaging (fMRI, MR, DTI). These measures of neural dysfunction and microglial activation are also acquired in a rodent model of pre-SCI, subacute and chronic SCI and sham surgery. In the animal model, behavioral, sensorimotor function and histopathological / immunopathological staining data derived from tissue samples collected will be evaluated as the gold standard for neuronal and microglial alterations. Using this approach, imaging will serve as the "language of translation", allowing us to define human markers of disease and map them, via imaging in the animal model, onto detailed biological pathology. The direct comparisons between human and rat will define the utility of imaging to translate between bedside and bench. Detailed histology will further inform on the interpretation of imaging metrics.

2. KEYWORDS: microglia, positron emission tomography, magnetic resonance imaging, spinal cord injury, neuropathic pain, inflammation, microglial activation, pathology, translational medicine, thalamus, sensory cortex, anterior cingulate, resting state functional connectivity, brain structure, immunohistochemistry, motor, human, rat

3. ACCOMPLISHMENTS

Below we list the aims and sub-tasks from the statement of work on the grant, and the accomplishments in relation to the goals and timelines. The animal surgical model, behavioral, PET and MRI components have been completed, with data analysis ongoing. Human patient recruitment has been slower than anticipated. Preliminary results are promising.

Specific Aim 1A: Define microglial activation as assessed by 11C-PBR28 PET in spinal cord injured patients with and without neuropathic pain.

Specific Aim 2A: Define brain structural, diffusion and functional network changes in the SCI populations.

Goal 1:Human PET-MR imaging of microglia and functional consequences in spinal cord injury with and without neuropathic pain.

Subtask 1: Obtaining IRB and HRPO approval for human studies (month 1-6)

Human IRB approval was obtained on 30/11/2015. USAMRMCORP HRPO of human protocol was approved on 14/12/2015.
IRB annual continuing review of the protocol was submitted on March 8, 2017 and approved March 30
HRPO approved continuing review of project on March 21, 2017.
IRB annual continuing review of the protocol was submitted on Jan 15, 2018, and approved on March 14, 2018.

The annual review was been submitted to HRPO on March 21, 2018, and approved on April 16, 2018
Current IRB protocol expires on Feb 21. 2019

Subtask 2: Recruitment, screening and scheduling of 1-3 patients per month (month 6-30)

41 subjects have been consented, whereof 24 have completed PET-MR investigations (13 patients and 11 healthy controls).
Notably, patient recruitment has been slower than anticipated. This is likely due to multiple factors, including a) strict inclusion/exclusion criteria b) multiple co-morbidities in the SCI patient population, c) no direct medical benefit for SCI subjects volunteering in study, d) an approximate 10% loss of subjects due to incompatible genotyping, and e) a possible saturation of SCI studies in the Boston area.
For recruitment, we are actively engaging the SCI community via multiple channels: Volunteering at the Greater Boston Chapter for Spinal Cord Injury, contacts with physicians at Spaulding rehab hospital, and distributing recruitment material via the Boston University Health & Disabilities Research Institute, the Abilities expo in Boston, the Northeast passage (a recreational therapy non-profit in Durham New Hampshire), and to Adaptive Sports New England.

Subtask 3: PET-MR imaging, initial data quality control (month 6-30) and Subtask 4: Data analysis

We perform data quality control continually with data collection, and have found the brain MR and PET data to be of consistently high quality.

Archiving of data: Data is continuously backed up on a dual RAID system and a physically separate cluster storage space.

We have performed preliminary data analysis in the obtained subjects, below, to further ensure data quality and to develop analytical strategies. Final data analysis will be performed when the data collection is completed as planned.

<u>Preliminary findings</u>

Microglial activation and spinal cord injury in humans

Compared to healthy controls (HC), spinal cord injured subjects had a significantly increased uptake of 11C-PBR28 in the bilateral posterior hippocampus.

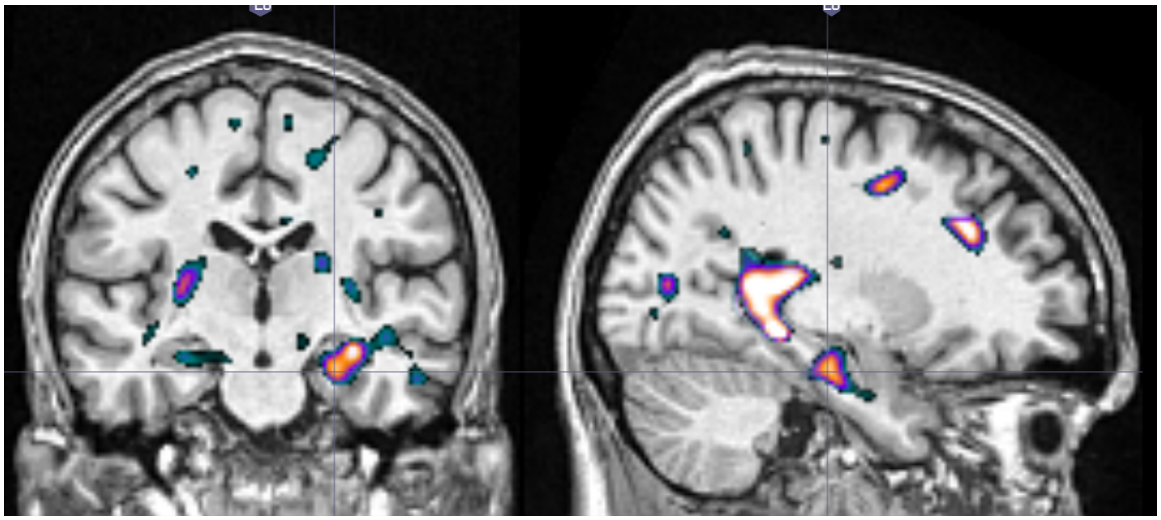

Figure 1. Regions with elevated 11C-PBR28 uptake in chronic spinal cord injury, as contrasted to a healthy control group, overlaid on a simultaneously acquired structural MRI. This is the first evidence of neuroinflammation in human SCI. Of particular interest is the bilateral hippocampal activation (at crosshairs).

We are cautious in our interpretation of these results, as the sample is still small. Nonetheless, there is a compelling animal literature on the role of the hippocampus in SCI: In rodents, SCI induces widespread neuroinflammation and impacts hippocampal function and neurogenesis. For example, SCI causes chronic microglial activation in the hippocampus and cerebral cortex, where microglia with hypertrophic morphologies and M1 phenotype predominated. There was also significant neuronal loss in the hippocampus at 12 weeks after injury [57]. SCI reduces the levels of the molecular substrates of synaptic plasticity, including synapsin I [58] and BDNF expression in the hippocampus [58,59]. In subacute SCI, hippocampal neurogenesis is reduced, while there is an increase of neurogenesis in the dorsal vagal complex of the hindbrain, where most of the newly generated cells are identified as microglia. Moreover, in chronic SCI, hippocampal neurogenesis remains reduced [60]. Neurogenesis and hippocampal glial responses are also dependent on the intensity of SCI, with neurogenesis impacted by moderate SCI, and severe SCI impacting both neurogenesis and significant neuronal loss in the hippocampus, effects that persist into the chronic phase of injury[61]. Functionally, SCI impairs synaptic plasticity in the hippocampus, as evidenced by a profound loss of silent synapses in the hippocampus post SCI [62].
As such, these first results in humans may map well onto the animal literature, and we seek to confirm hippocampal neuroinflammation in our animal model.
We plan to relate our findings in SCI subjects to previously reported metrics of brain structure, resting state functional connectivity alterations and microglial expression, once we have acquired a sufficiently large patient material.

Resting state functional connectivity after spinal cord injury in humans

A regional graphical analysis was conducted on the resting state data. Preliminary results indicate that SCI subjects have an altered resting state connectivity within the Salience network (particularly the anterior insula and the supramarginal gyrus) and, compared to healthy subjects, a lower connectivity between the salience network and the "default mode" network and regions of occipital networks. The behavioral correlates of these alteration are not clear, but our working hypothesis is that ongoing nociceptive signaling creates a competition between the "resting state" system, and a salience detection network , Figure 2

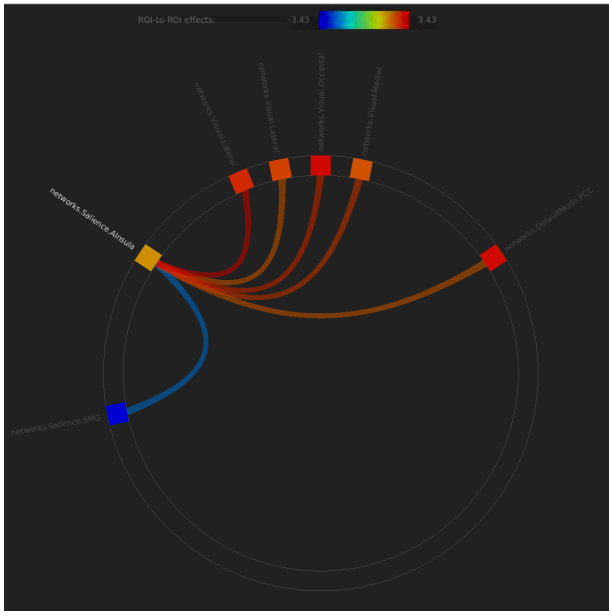

Figure 2. Graphical representation of altered salience network properties in SCI subjects.

A seed based resting state connectivity analysis was carried out investigating regions likely to be most affected after a spinal cord injury based on their implication in motor and sensory processing as well as pain. With a seed-based analysis in the Right lateral sensorymotor region, we found that SCI sunjets have significantly decreased connectivity to the bilateral superior parietal lobule (left parietal p_{FWE}=0.00191, right parietal p_{FWE}=0.00264), and also to the left frontal pole (p_{FWE}=0.00360), suggesting that the disruption of the thalamocortical sensory tract leads to global network changes at rest (Figure 3)

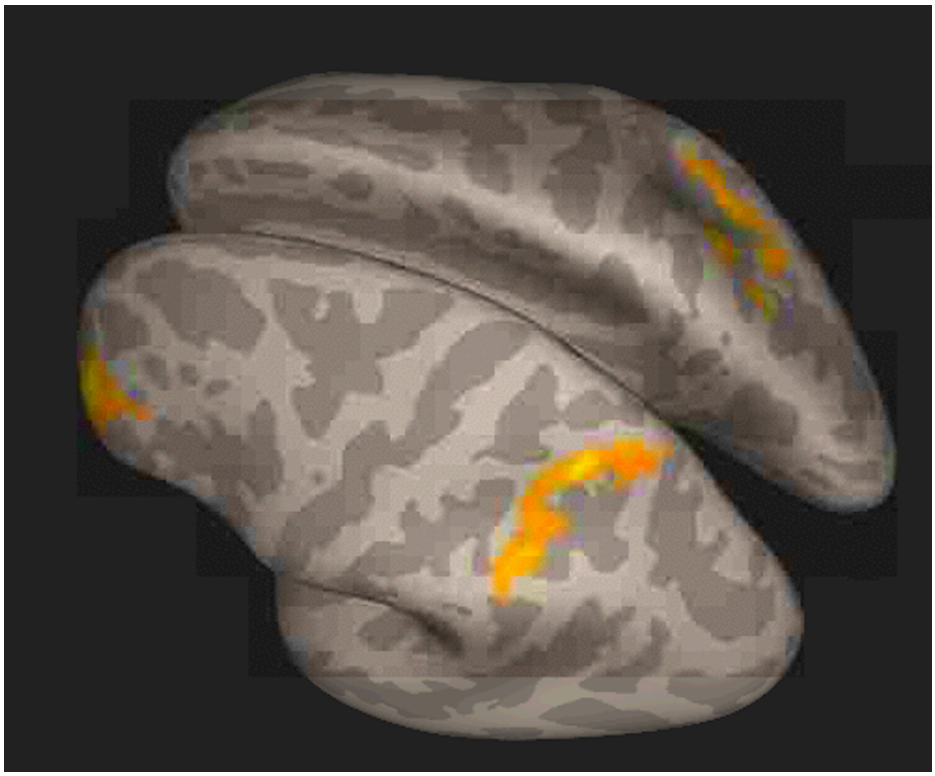

Figure 3. Altered somatosensory cortex resting state functional connectivity, projected on an inflated brain surface. The color map represents regions with higher resting state connectivitity in healthy subjects as contrasted to subjects with SCI, thresholded at P<0.005 for illustrative purposes.

Structural data analyses

As previously reported, structural data analysis indicates decreased gray matter density in the somatosenory cortex representing the lower limbs, consistent with prior literature reports, Figure 4.

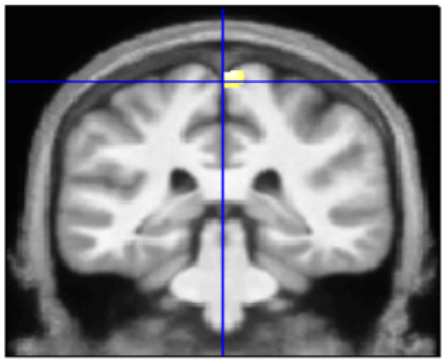

Figure 4. Decreased gray matter density in SCI subjects as compared to healthy controls, as per a preliminary DARTEL optimized voxel based morphometric analysis

Spinal cord and spine data analysis

It has been proven problematic to measure microglial activation of the lesioned spinal cord in people with SCI, as the absolute majority of SCI subjects have implanted steel or titanium rods, plates and screws to stabilize the injured spine. As a proxy to determine spinal cord atrophy, we have employed measures of spinal cord volume, cross-sectional area, left-right width and anterior-posterior length using the recently developed Spinal Cord Toolbox [1]. Compared to healthy controls (HC), spinal cord injured subjects had an approximately 20% lower spinal cord cross-section thickness at the C2 level (p=0.005) and the C3 level (p=0.007)

Review and meta-analysis

Our registered review of brain imaing fingings in spinal cord injury was published in Neuroscience and Biobehavioral Reviews (see appendix). We found a sufficient homogeneity in the littereture for meta-analysis of fMRI motor and motor imagery tasks, with results indicative of consistently elevated motor, parietal and cerebellar responses in SCI. We further found multiple, qualitatively overlapping reports of structural alterations, and evidence that plasticity following injury can be affected by pain. Sample sizes are typically small. We recommend a streamlining of research methdos, with more standardized protocols across labs to minimize heterogeneity in studies, allow for comparisons, and data sharing.

Specific aim 1B: Microglial activation as assessed by 11C-PBR28 PET in a Surgical Model of Moderate Static Compression SCI compared with non-operated controls.

Based on agreement initiated by Dr. Linnman, Project PI and concurred by Dr. Teng, Co-PI, (Spaulding Rehab Hospital and Brigham and Women's Hospital) all rodent purchasing, surgery, and imaging are performed at facilities of the Boston Children´s Hospital (BCH), respectively. This arrangement, while necessary to bring together the significant neuroimaging and SCI model combined expertise, has resulted in some extra regulatory work in order to be compliant with all regulating institutions.

Major Task 2: Animal model and imaging

Subtask 1: Obtaining IACUC and ACURO approval for animal protocol (month 1-3)
Boston Children´s Hospital IACUC approved 01/21/2016

- ACURO was approved on 04/18/2016 and communicated to us on 04/25/2016.
- The BCH IACUC performed an annual review, and renewed the protocol on January 17, 2017.
- Amendments to the protocol were submitted to ACURO, and approved on July 19, 2017.
- Annual Renewal was reviewed and approved according to Boston Children's Hospital (BCH) Institutional Animal Care and Use Committee (IACUC) policy October 24, 2017
- Amendment to use Buprenorphine Slow Release as an alternative analgesic was approved by BCH IACUC on April 10, 2018.
- Amendment was filed with ACURO on April 10, 2018, and approved on April 11, 2018.

Subtask 2: Training Post doc II in Surgical Model of Moderate Static Compression (month 1-3).

Dr. Teng trained and guided his two fellows to complete all BCH IACUC surgery qualifications by practicing surgical procedures at his labs. Specifically, Dr. Wang and Dr. Abd-El-Barr successfully passed Observation of Aseptic Procedures of Surgery Preparation and Rodent Spinal Cord Compression Injury evaluated by BCH's Animal Research Facility veterinary doctor and staff members.

Dr. Teng' Lab successfully graduated his postdoc fellow Muhammad Ebd-El-Barr, M.D., Ph.D. (from Brigham & Women's Hospital and Harvard Medical School) February, 2018.

Between April and June, Dr. Teng further trained and guided his postdoctoral fellow Dr. Wang to perform 3 new groups of surgeries for in vivo modeling of spinal cord injury (SCI) and to complete all planned post-SCI tissue preservation, classification, storage, cryostat section, and immunohistochemical assays of neuroinflammation responses, in addition to continued analyses of data of behavioral tests and statistical analysis.

Between June and September, Dr. Teng' Lab effectively set Dr. A. Semeano, PGY0 postdoc fellow from University of Sao Paulo, Brazil and University of Lisbon, Portugal on track to carry on all the analytical studies of the project. Dr. Teng has also enrolled O. Imir newly graduated from University of Illinois Urbana-Champaign as a research assistant intern for the study.

Between April and June, Dr. Teng further trained and guided his postdoctoral fellow Dr. Wang to perform 3 new groups of surgeries for in vivo modeling of spinal cord injury (SCI) and to complete all planned post-SCI tissue preservation, classification, storage, cryostat section, and immunohistochemical assays of neuroinflammation responses, in addition to continued analyses of data of behavioral tests and statistical analysis.

Between July and September, Dr. Teng further trained and guided his postdoctoral fellow Dr. Wang to successfully complete the entire in vivo SCI modeling surgery, behavioral tests and tissue collection, in addition to the ongoing data analysis.

All went well for post-SCI tissue preservation, classification, storage, cryostat section, immunohistochemical assays of neuroinflammation responses, data of behavioral tests, and statistical analysis.

Dr. Teng's Team also completed all the cleaning, reorganization and paperwork to sign the project off the project's surgical, behavioral and tissue processing rooms at BCH's Animal Research Facility (ARCH), which was praised by the BCH veterinary doctor and staff members in coordination with occupational health offices at SRH and BCH.

Post-operative care and behavioral evaluations have been according to plans.

Subtask 3: microPET-CT imaging of SCI animals with Surgical Model of Moderate Static Compression (month 3-30)

Dr. Linnman and his post-doctoral fellow Dr. Dahlberg completed 60 PET-CT scans, whereof 22 baseline animals, 24 subacute animals and 24 chronic animals.

MicroPET-CT imaging for the project was completed in August, 2018, and data analysis is ongoing.

Milestone #1: Define preliminary translational capacity of PET imaging system (month 7-30)
Microglial PET imaging has been achieved in both spinal cord injured and healthy humans or animals, respectively. The translational capacity between human and animal SCI microglial imaging, i.e., comparable changes in microglial expression magnitude and region specificity, remains to be defined once the human and animal data collection is complete. Of note, we have preliminary data from the human component indicative of elevated hippocampal microglia activity in the PET signal (Figure 1) and Nissl stain-based histopathology of the hippocampus in the animal model (Figure X) also indicated elevated neural inflammatory reactions at this level of the neural axis.

Specific aim 2B: Brain structural, diffusion and functional network changes in the SCI model and control animals.
Major task 3: Awake rat fMRI
Subtask 1: Animal training (month 6-24)

Due to concerns about data reliability and animal safety in this sensitive animal model, all functional MRI animal data was collected under light isoflurane (1-1.5%) anesthesia). As the animal model induces significant stress and neuropathic pain phenotype, we have found, in a parallel project, that awake imaging has severe motion artifacts and the stressor of sustained constraint in awake animals may be too stressful, thereby inducing secondary complications in the animal model. The light anesthesia approach was a successful compromise between animal protection and data quality in previous studies, and necessary to obtain high quality data.

Subtask 2: Control animal imaging (month 6-24)
Dr. Linnman and his post-doctoral fellow Dr. Dahlberg completed acquiring baseline structural, resting state fMRI and diffusion data in 23 animals. Imaging quality is excellent. Data analysis is ongoing

Subtask 3: Pilot and define SCI animal imaging procedures (month 3-9)
Piloting of animal imaging procedures is completed.

Subtask 4: Sub-acute and control animals (month 12-30)
Dr. Linnman and his post-doctoral fellow Dr. Dahlberg completed structural, functional and diffusion and PET data in 23 animals in the subacute stage. Data analysis is ongoing

Subtask 5: Chronic animal imaging (month 12-30)
Dr. Linnman and his post-doctoral fellow Dr. Dahlberg completed structural, functional and diffusion data in 25 animals in the chronic stage. Data analysis is ongoing.

Specific aim 3: Determine correlations between imaging findings and those of behavioral, sensorimotor function and histopathological / immunopathological

staining results derived from tissue samples collected in animals from Aim 1B and 2B.

Major task 4: Histology and translation
Subtask 1: functional tests, histological, cellular and molecular assays, and data analyses

The basic science modeling and SCI pathophysiologic data component of the project is headed by Dr. Teng of the Spaulding Rehabilitation Hospital (SRH) and the Brigham and Women's Hospital (BWH), Harvard Medical School's teaching institutions, he provided detailed daily training of neuroscience procedures and skills to his three postdoctoral fellows and a B.S. college graduate intern at his lab for surgery skill training, behavioral assays, behavioral data analysis, spinal cord and brain tissue perfusion, spinal cord sample preservation, tissue processing, histochemical assays, and immunochemical assessments. The following figures are representative data presentation for the rat SCI study.

Immunohistochemical Assessment of Extensive Microglia Activation and Severe Reactive Astrogliosis Resulting from T9-10 Compression Injury of the Rat Spinal Cord.
Figure 5 reveals T9-10 compression injury caused extensive microglia activation as detected by immunocytochemical (ICC) assay using antibodies against iba-1, a activated microglia/macrophage marker. In addition, there was severe reactive astrogliosis that was depicted by ICC using antibodies against GFAP (glial fibrillary acidic protein). In tissue sections 3mm rostral to the lesion site and inside areas that housed sensory neurites and secondary sensory neurons, iba-1 (upper panel) and GFAP (lower panel) immunoreactivities were discernibly higher in the SCI group (b-i, c-i, e-I and f-I, respectively), relative to those in the sham surgical group (b-ii, c-ii, e-ii and f-ii, respectively).
Activated microglia (iba-1 immunopositive) and reactive astrocytes (GFAP immunopositive) with obviously hypertrophic cell morphologic features were selected from the dorsal part of the gray matter or higher magnification presentations (insets: b-i, c-i, e-i and f-I, respectively). Scale bar equals 50 μm.

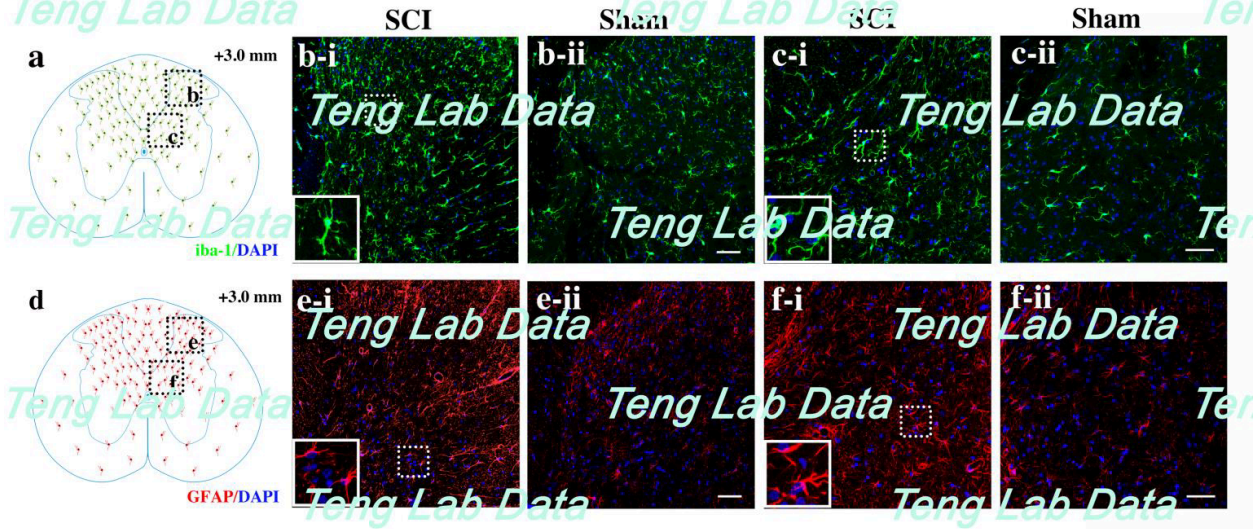

Figure 5. Immunohistochemical Assays of microglia activation and reactive astrogliosis resulting from T9-10 compression injury of the rat spinal cord.

ICC Assessment of Extensive Neuroinflammation in T9-10 Compression Injured Rat Spinal Cords.

Figure 6 shows that compared to laminectomy controls T9-10 compression injury (a and b: T8 segment of spinal cord; lesion pathology indicated in c-f) resulted in reactive gliosis hallmarked by hypertrophic astrocytes (with increased GFAP ICC level) that also expressed inducible nitric oxide synthase (iNOS), a major inflammatory mediator in specific anatomical areas that housed sensory neurons and pathways or other neural components (c-n) of T8 spinal cord. Moreover, microglia activation was also detected by ICC assay using antibodies against iba-1, an activated microglia/macrophage marker. The activated microglia produced tumor necrosis factor alpha (TNFα) that can trigger diffused inflammatory response in its target regions. Magnification: 20X.

Histochemical Assessment of brain functional centers that play important roles in developing and mediating neuropathic pain after traumatic spinal cord injury.

At the functional centers of the nucleus raphe magnus and gracile nucleus the H&E/Fast Blue histochemical stains depicted the cytoarchitecture of the tissue for evaluating the cellular, neurite and extracellular matrix components. The anatomical location details helped us to analyze neuroinflammatory responses via immunohistochemical reactions. Figure 7. Histochemical Assay of the

histopathology of brain and brainstem regions of the nucleus raphe magnus (upper) and gracile nucleus (lower) of rats with T10 moderate compression injury of the rat spinal cord.

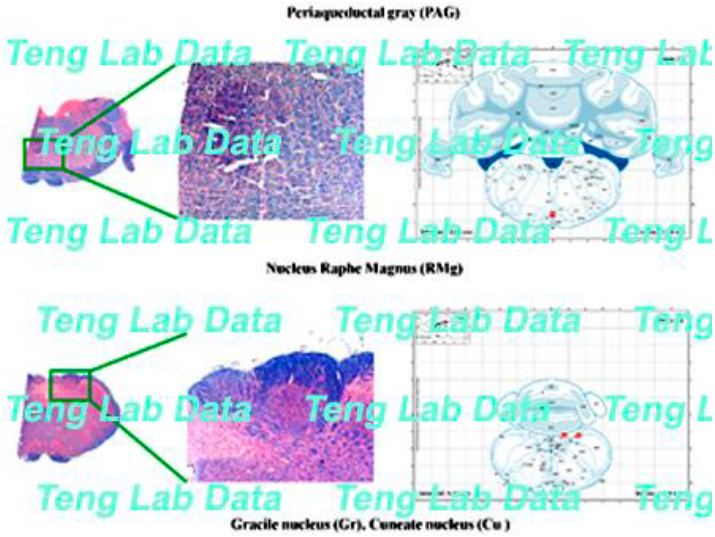

Figure 7 Immunohistochemical Assessment of spinal cord functional centers that play important roles in developing and mediating neuropathic pain after traumatic spinal cord injury.

Immunohistochemical (IHC) Assessment of Extensive Neuroinflammation in the Nucleus Raphe Magnus and the Periaqueductal Gray Matter in Rats with T9-10 Compression Injury of the Spinal Cords

Figure 8 shows that T9-10 compression injury resulted in microglia activation detected by IHC assay using antibodies against iba-1, an activated microglia/macrophage marker. The activated microglia can trigger diffused inflammatory response in the adjacent regions, inducing reactive gliosis hallmarked by hypertrophic astrocytes (with increased GFAP IHC level in) in the gracile nucleus of the lesioned spinal cord.

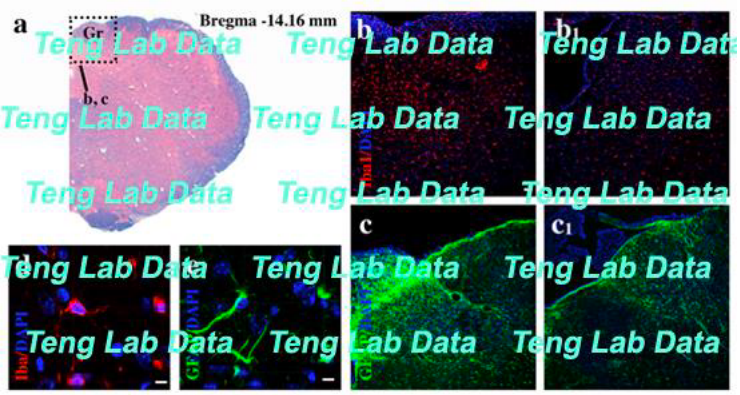

Figure 8. Histopathology of the gracile nucleus (a: Gr). IHC using antibodies against Iba-1 (b and b1) and GFAP (c and c1) detected microglia activation and extensive astrocyte reaction, respectively in rats with T10 moderate compression injury of the rat spinal cord.

Figure 9 shows that T9-10 compression injury resulted in microglia activation detected by IHC assay using antibodies against iba-1, an activated microglia/macrophage marker. The activated microglia can trigger diffused inflammatory response in the adjacent regions, inducing reactive gliosis hallmarked by hypertrophic astrocytes (with increased GFAP IHC level) in the periaqueductal gray matter of the lesioned spinal cord.

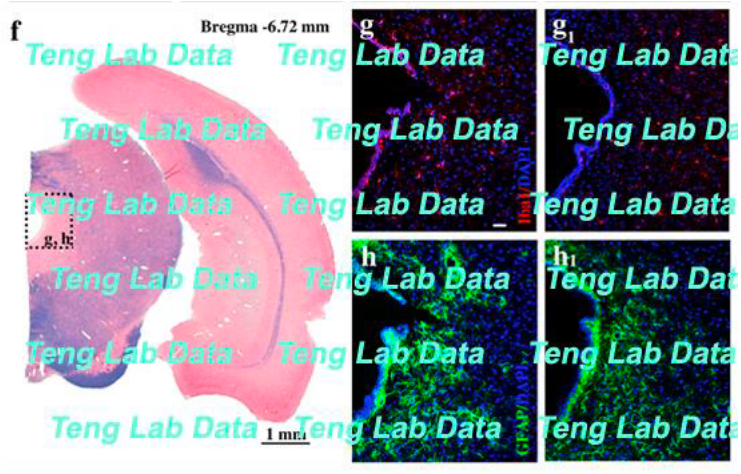

Figure 9. Histopathology of periaqueductal gray matter IHC using antibodies against 1 (g and g1) and GFAP (h h1) detected microglia activation and extensive astrocyte reaction, respectively in rats with T10 moderate compression injury of the rat spinal cord.

the (f). Iba- and

At the functional centers of the dorsal horn gray and white matter dorsal funiculi immunohistochemical stains detected that compression SCI triggered neural inflammation in regions that house sensory neurons and ascending neural pathways. The anatomical location specifics suggested that the neuroinflammatory responses in these anatomical structures can be responsible for pain-like behavioral signs shown by the SCI rats

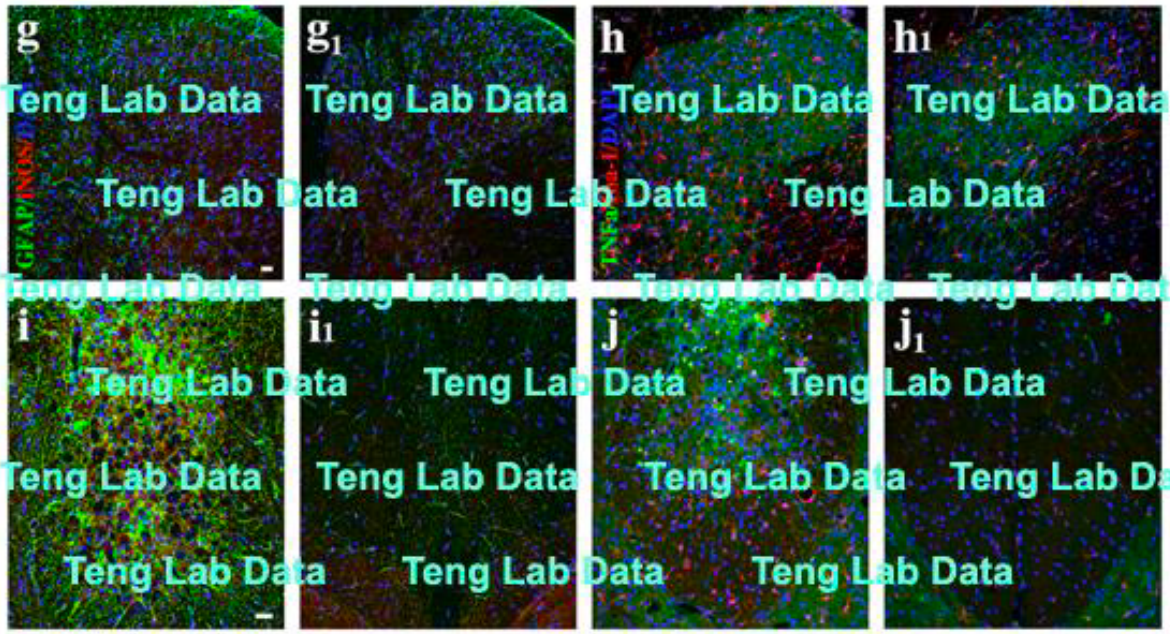

Figure 10 Immunohistochemical Assay of the dorsal horn (DH) gray matter (GM) region of the rat spinal cord after T10 moderate compression injury. Both the DHGM (g and i) and DH white matter (WH; h and j) of the injured spinal cords showed increased expre of GFAP and iNOS, relative to laminectomy controls (g1 and i1). Similar levels of differences were also observed for TNFα and iba-1 in the same areas between the SCI group and control group.

Nissl Stain Assessment of Neuroinflammation Profile in the Hippocampus in Rats with T9-10 Compression Injury or laminectomy Alone in the Spinal Cords.

Figure 11 shows that T9-10 compression injury resulted in enhanced Nissl substance expression and cell number in the hippocampus and brainstem in rats with lower thoracic compression SCI. By contrast, control rats receiving T9-10 laminectomy only did not show any elevated responses in Nissl staining in the two regions holding important function for nociception signal processing. The data indicated that SCI could induce neural inflammatory reactions in much higher levels of the neural axis and in functional centers that are involved in pain signaling and processing.

Figure 11. Nissl stain-based histopathology of the hippocampus (**upper left panel**) and brainstem (**lower left panel**) of the SCI group versus the laminectomy control group (**upper and lower right panels, respectively**). T10 moderate compression injury of the rat spinal cord.

Dr Teng, his postdoctoral fellows Dr Wang and Dr Liu and his research assistant intern Mr Ozan Imir worked together to complete all spinal cord injury modeling surgeries. Dr Semeano also started to learn surgery and behavioral and pathological data processing. Most importantly, they successfully completed the surgical tasks, and are continuously processing and sectioning the spinal cord tissue samples, in order to produce systematically analyzed behavioral, histopathological and immuno-histochemical data for comparing the SCI rats versus those of sham surgical controls. These results produced and will continuously provide critical information for the upcoming correlative examinations with those of MRI imaging analysis in the future. Teng lab team has, in addition, made new progresses in securing performing unbiased scientific data analysis; the results demonstrates that sensory neural components and pathways had abnormities in rats with T9-10 SCI besides motor disorders that had intraspinal cord parenchyma neuroinflammation as one of the mechanistic underpinnings.

Upon the completion of in vivo SCI study, Teng Lab is continuing to analyze tangible behavioral, histopathological, cellular and molecular data. The outcomes not only demonstrate motor function deficits but also sensory abnormalities including hypersensitivity/pain resulting from T9-10 SCI. Importantly, they have now uncovered key neuropathology and neuroinflammation evidence. In-depth training has been provided for tissue preservation, processing, sectioning, and

histopathology and immunohistochemistry analytical methods to enhance the team's readiness for the current stage where pathological and neuroinflammatory outcomes will be verified as main underlying mechanisms for the development and escalation of neuropathic pain following SCI. The lab team is continuing its enhancement of mechanistic knowledge and insight on correlative comparison between behavioral sensory disorders (e.g., hypersensitivity/pain-like behavior) and histological (e.g., sensory neural pathway), cellular (e.g., reactive gliosis, activated microglia), and molecular (e.g., pro-inflammatory molecules such as TNF-alpha, GFAP, iba-1 and iNOS) marker changes, based on the labs' existing data. Identification of these mediators or activators of post-SCI neuropathic pain will provide therapeutic targets for developing clinical therapies to treat sensory disorder after traumatic SCI.

Somatosensorimotor disorders resulting from T9-10 compression SCI in adult rats.

Figure 12 clearly shows that T9-10 moderate compression injury resulted in long-term deficits in coordinated hindlimb functions represented by inability to maintain a stable body posture when facing downwards on an inclined board fixed at a particular angle for the SCI rats, compared to laminectomy control rats (A). This functional loss was caused by paraplegic pathophysiology, not by general physical strength reduction post surgery since when facing upwards the two groups of rats showed similar angles upon which they could remain stable (i.e., they showed comparable levels of front limb strengths; B). There was discernible hypersensitivity/pain that was detected in the hind paws in SCI rats via a brief pinch-triggered spinal reflex (C). Similarly, either pressure (D) or extension (E) stimulus-induced spinal reflex showed abnormalities in the SCI rats, relative to sham surgery controls. Lastly, T9-10 moderate compression produced long lasting deficits in contact righting reflex as shown in (F), confirming disability in the brain and spinal cord coordination system. Group sizes were N = 4-5/SCI group (red) and N = 4-5/Sham surgery group (blue).

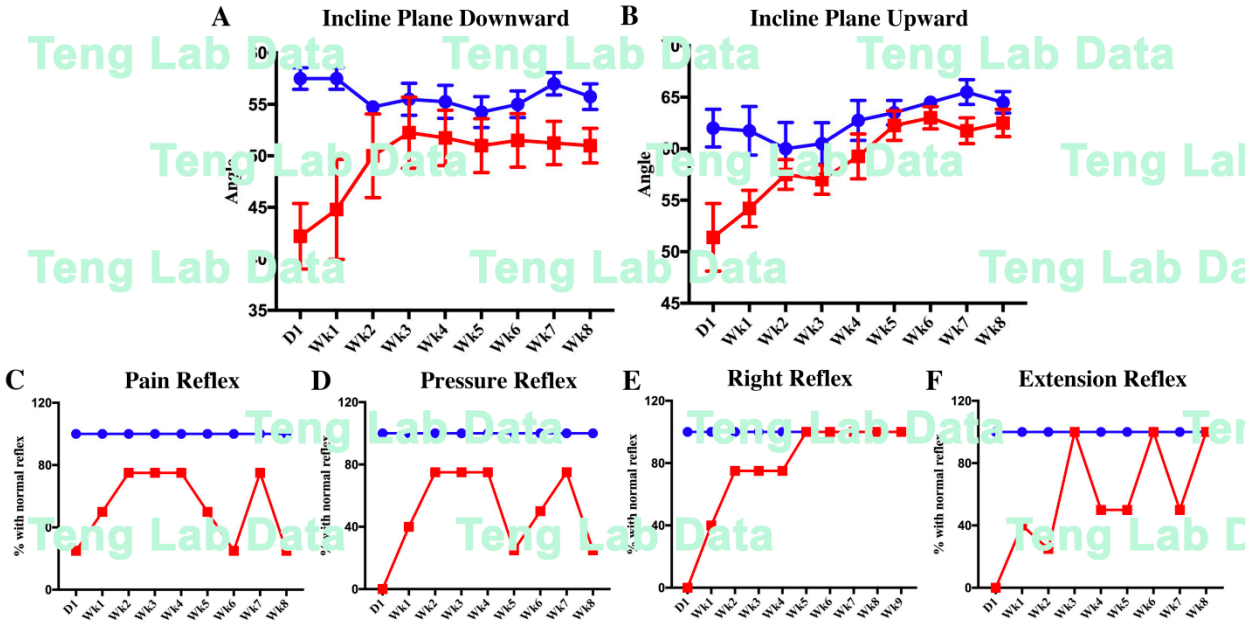

Fig. 12 General Somoatomotosensory Function of Adult Rats after T9-10 Compression SCI

4. What opportunities for training and professional development has the project provided?

Dr. Linda Dahlberg, post-doctoral fellow in the human project, has been trained in rat functional MRI imaging and rat PET imaging methods, as well as post-operative care. Dr. Dahlberg has further developed her skills in both human and animal MR and PET data analysis, including automated spinal cord segmentation methods. Dr Dahlberg completed her Post-doctoral fellowship in September 2018 and has subsequently moved to a position at the Montreal Neurological Institute.

Dr .Anna Dahl Myrvag, pre-doctoral Fullbright fellow, was successfully trained in human structural and Diffusion Tensor Imaging data analysis by Dr. Linnman (together with Dr. Yedenki, Massachusetts General Hospital) , and is currently completing her PhD at the Arctic University of Tromsö.

Dr. Abd-El-Barr was trained in Rodent Spinal Cord Compression Injury model, and successfully completed his postdoc (from Brigham & Women's Hospital and Harvard Medical School) in February, 2018. Dr. Ebd-El-Barr is now Assistant Professor of Neurosurgery of Duke University Medical Center and VA Durham Medical Center.
Dr. Teng' Lab effectively set Dr. A. Semeano, PGY0 postdoc fellow from University of Sao Paulo, Brazil and University of Lisbon, Portugal on track to carry on all the analytical studies of the project. Dr. Teng has also enrolled O. Imir newly graduated from University of Illinois Urbana-Champaign as a research assistant intern for the study.
Dr. Wang, under Dr Tengs close mentorship, successfully completed training in the rodent SCI model and post-operative care. He completed his postdoctoral in August 2018 and is back in operation room as an academic neurosurgeon to help patients with neurotrauma and neurological conditions.

5. IMPACT

The long-term goal of this project is to develop a pipeline for translating promising therapeutics candidates in animal models of spinal cord injury onto the human condition. We currently focus on the role of microglial activity in SCI with neuropathic pain, but the general framework developed will be applicable to evaluate the translation potential of multiple agents. This approach can reduce the risk of running up blind alleys and putting patients at risk, allows using lower numbers of patients, and allows for a more informed approach in early clinical trials. We now have very preliminary translational evidence for a shared microglial response in the human and animal paradigms, and with PET and MRI completed in animals and far along in the human arm, the project is marching steadily towards that goal. We foresee multiple joint projects using the methods developed here in the near future.
The techniques that are being developed (microglial PET-MR in human, rat functional imaging and rad in-vivo microglial PET) are likely to make an impact on multiple other disciplines, as neuroinflammatory responses are a key component of multiple neurological and neurodegenerative diseases, including traumatic brain injury and Alzheimer's.

Technology transfer
Nothing to report to date.

Impact on society beyond science and technology
Nothing to report to date.

6. CHANGES/PROBLEMS
Changes in approach and reasons for change
There are no changes in the human side of the study, or in the general approach of the study in the basic science/laboratory side of the project.

Actual or anticipated problems or delays and actions or plans to resolve them

The human neuroimaging component of the study is running well, although recruitment of spinal cord injured volunteers is slower than anticipated. We continue to reach out to physicians within the Harvard Medical School network, to Boston University, and to patient organizations in the New England are to increase recruitment rates. It is noted that SCI patients are interested in the study, but several potential subjects have had complications such as pressure wounds, causing them to hold of on participation.
The animal surgical model and data collection component, after initial delays due to personnel turnover, has been completed. Further histological investigations are ongoing, as are neuroimaging data analysis.

Changes that had a significant impact on expenditures
Nothing to report

Significant changes in use or care of vertebrate animals

Nothing to report.

7. PRODUCTS
Publications, conference papers, and presentations

Linnman lab

SCI related work:
Publications
Dahlberg L.S. , Becerra, L., Borsook, D., Linnman, C. Brain changes after spinal cord injury, a quantitative meta-analysis and review Neurosci Biobehav Rev. 2018 Jul;90:272-293.

Presentations
Linnman C, Dahlberg L, Morse L. Spinal cord atrophy after spinal cord injury, a meta-analysis and replication (Abstract presented at American Spinal Injury Association annual meeting 2018)

Dahlberg L, Linnman C. Heritability in spinal cord thickness – a twin study (Abstract presented at American Spinal Injury Association annual meeting 2018)
*not included in appendix

Methods related non-SCI work:
Linnman C., Catana C., Petkov M.P., Chonde D.B., Becerra L., Hooker J., Borsook D. Molecular and functional PET-fMRI measures of placebo analgesia in episodic migraine: Preliminary findings. Neuroimage Clin. 2017 Nov 15;17:680-690
*not included in appendix

Dahlberg L.S., Linnman C., Lee D., Burstein R., Becerra L., Borsook D., Responsivity of Periaqueductal Gray Connectivity Is Related to Headache Frequency in Episodic Migraine. Frontiers In Neurology 2018 Feb 13;9:61
*not included in appendix

Hoppe J.M., Frick A., Åhs F., **Linnman C**., Appel L., Jonasson M., Lubberink M., Långström B., Frans Ö., von Knorring L., Fredrikson M., Furmark T. Association between amygdala neurokinin-1 receptor availability and anxiety-related personality traits. Translational Psychiatry 2018 Aug 28;8(1):168
*not included in appendix

Teng lab
Cancer Stem Cells or **Tumor Survival Cells**?
Teng YD, Wang L, Kabatas S, Ulrich H, **Zafonte** RD.
Stem Cells Dev. **2018** Sep 25. doi: 10.1089/scd.**2018**.0129. [Epub ahead of print]

Pathophysiological Bases of **Comorbidity**: Traumatic Brain Injury and **Post-TraumaticStress** Disorder.
Kaplan GB, Leite-Morris KA, Wang L, Rumbika KK, Heinrichs SC, Zeng X, Wu L, Arena DT, Teng YD.

J Neurotrauma. 2018 Jan 15;35(2):210-225. doi: 10.1089/neu.2016.4953. Epub **2017** Nov 3.

Establishing an Organotypic System for Investigating Multimodal Neural Repair Effects of Human Mesenchymal Stromal Stem Cells.
Thakor DK, Wang L, Benedict D, Kabatas S, **Zafonte** RD, **Teng YD**.
Curr Protoc Stem Cell Biol. 2018 Jul 18:e58. doi: 10.1002/cpsc.58. [Epub ahead of print]

Spinal cord astrocytomas: progresses in experimental and clinical investigations for developing recovery neurobiology-based novel therapies.
Teng YD, **Abd-El-Barr** M, Wang L, Hajiali H, Wu L, Zafonte RD.
Exp Neurol. 2018 Sep 21;311:135-147. doi: 10.1016/j.expneurol.2018.09.010. [Epub ahead of print] Review.

Updates on Human Neural Stem Cells: From Generation, Maintenance, and Differentiation to Applications in Spinal Cord Injury Research.
Teng YD, Wang L, Zeng X, Wu L, Toktas Z, Kabatas S, Zafonte RD.
Results Probl Cell Differ. 2018;66:233-248. doi: 10.1007/978-3-319-93485-3_10.
*not included in appendix

Presentations and book-chapters

Toktaş ZO, Yılmaz B, Ekşi MS, Wang L, Akakın A, Yener Y, Konakçı M, Ayan E, Kılıç T, Konya D, and Teng YD. An ioMRI-assisted Case of Cervical Intramedullary Diffuse Glioma Resection
*not included in appendix

Teng YD, Wang L, Zeng X, Wu LQ, Toktas Z, Kabatas S, and Zafonte RD. Chapter 3: Updates on human neural stem cells: from generation to research and translational applications in SCI studies. In: Leonora Buzanska editor. Human neural stem cells - from generation through differentiation to application. Results & Progress in Cell Differentiation (RPCD) Series. Springer-Verlag-GmbH: Berlin, 2018 in press.
*not included in appendix

Teng YD. Oncolytic Targets Identified by Genetically Engineered hNSCs in a Rodent Model of Spinal Cord Glioma. Turkish Society of Stem Cell and Cell Therapy Annual Congress, October 2017; Trabzon, Turkey.
*not included in appendix

Teng, YD. (2018) The role of endogenous neurogenesis in neural recovery following treatment of an experimental medical gas therapy after traumatic spinal cord injury. Szczecin, Poland
*not included in appendix

Teng, YD (2018) Recovery neurobiology of injured adult spinal cord. Munich, Germany
*not included in appendix

Teng, YD (2018) Recovery Neurobiology-based cellular treatment of spinal cord astrocytoma. Frankfurt, Germany
*not included in appendix

8. PARTICIPANTS & OTHER COLLABORATING ORGANIZATIONS

Name: Clas Linnman
Project role: PI
Researcher Identifier: 0000-0001-8449-894X
Nearest person month worked: 9
Funding Support: DoD
Contribution to project: Dr. Linnman has led the effort with regards to project planning, human IRB and animal IACUC approvals, setup and execution of PET-MR imaging of patients, setup and execution of PET imaging of rats, post-doctoral training, data quality control and analysis, and project reporting

Name: Yang D. Teng
Project role: Co-PI
Researcher Identifier: 0000-0002-1257-4461
Nearest person month worked: 2
Funding Support: DoD
Contribution to project: Dr. Teng has led the effort on development, refinement and execution of the experimental SCI model, post-doctoral training in animal surgery and care, histology and contributed to project reporting.

Name: Lino Becerra
Project role: Co-investigator
Researcher Identifier: 0000-0002-5840-1160
Nearest person month worked: 1
Funding Support: DoD
Contribution to project: Dr. Becerra left to an industry position in November, 2017. Dr Linnman subsequently assumed his responsibilities in the project

Name: David Borsook
Project role: Co-investigator
Researcher Identifier:
Nearest person months worked: 1
Funding Support: DoD
Contribution to project: Dr. Borsook has contributed to grants management and oversight.

Name: Linda Solstrand Dahlberg
Project role: Post-doctoral fellow
Researcher Identifier: 0000-0002-1090-7138
Nearest person months worked: 12
Contribution to project: Dr. Dahlberg has recruited human patients, performed screening, consenting (together with a Nurse Practitioner, as per IRB protocol),

patient booking, human PET-MR scanning, PET and MRI data analysis, and manuscript preparation. Dr. Dahlberg has further, with Dr. Linnman, performed animal PET and MR imaging, and contributed to data analysis of animal imaging.

Name: Lei Wang
Project role: Post-doctoral fellow
Researcher Identifier:
Nearest person months worked: n.a.
Funding Support: Non-DoD fellowship support
Contribution to project: Dr. Wang has led the day to day animal SCI surgeries, post-operative care, behavioral measures, tissue collection, and reporting.

What other organizations were involved as partners?
Organization Name: Spaulding Rehab Hospital
Location of Organization: Boston, MA
Partner's contribution to the project: The spinal cord injury model was developed by Dr. Yang Teng at Spaulding Rehab Hospital facilities, and his lab provides the expertise and personnel to perform this surgical model and post-operative care. Dr. Tengs lab is further responsible for behavioral testing and histological analysis of spinal cord and brain tissue.
We have further established extensive contacts with clinicians at SRH for patient recruitment.

Neuroscience and Biobehavioral Reviews 90 (2018) 272–293

Contents lists available at ScienceDirect

Neuroscience and Biobehavioral Reviews

journal homepage: www.elsevier.com/locate/neubiorev

Brain changes after spinal cord injury, a quantitative meta-analysis and review

Linda Solstrand Dahlberg[a,b,*], Lino Becerra[a,b,c,d], David Borsook[a,b,c,d], Clas Linnman[a,b,e]

[a] Department of Anesthesiology, Perioperative and Pain Medicine, Boston Children's Hospital, Harvard Medical School, Boston, MA, USA
[b] Departments of Psychiatry and Radiology, Massachusetts General Hospital, Harvard Medical School, MA, USA
[c] Center for Pain and the Brain, Boston Children's Hospital and Massachusetts General Hospital (MGH), Harvard Medical School, Boston, MA, USA
[d] Athinoula A. Martinos Center for Biomedical Imaging, Department of Radiology, Massachusetts General Hospital and Harvard Medical School, Charlestown, MA, USA
[e] Spaulding Rehabilitation Hospital, Harvard Medical School, Charlestown, MA, USA

ARTICLE INFO

Keywords:
Spinal cord injury
Neuroimaging
Meta-analysis
Plasticity
Cortical reorganization
MRI

ABSTRACT

Spinal Cord Injuries (SCI) lead to alterations in brain structure and brain function by direct effects of nerve damage, by secondary mechanisms, and also by longer term injury consequences such as paralysis and neuropathic pain. Here, we review neuroimaging studies of patients with traumatic spinal cord injuries, perform a quantitative meta-analysis of motor and motor imagery studies, summarize structural studies, evidence of cortical reorganization, and provide an overview of diffusion and spectroscopy studies. The meta-analysis showed significantly altered motor cortex, as well as cerebellar and parietal lobe changes, and qualitatively consistent reports of alterations in somatosensory brain structure, cortical reorganization, white matter diffusion and thalamic metabolites. Larger samples in combination with standardized imaging protocols and data sharing will further our understanding of brain changes after SCI and help in defining short and long-term changes in brain systems in SCI patients. Such data would provide a basis for clinical trials, treatment outcomes, and guide novel interventions.

1. Introduction

Neuroimaging of brain changes following spinal cord injury (SCI) has a long history (Merlis and Watson, 1949; Roelcke et al., 1997), with continuing improvements in hardware, software and the specificity of scientific inquires. Here, we attempt to summarize and synthesize the field, with a focus on studies using Magnetic Resonance Imaging (MRI) to study human brain function after traumatic SCI. A quantitative meta-analysis was performed on studies of evoked responses to motion and to imagined motion. As the field is relatively small and rapidly evolving in terms of imaging hardware, data acquisition, experimental paradigms and analytical approaches, we also include a narrative review on structural alterations, resting state functional alterations, diffusion, spectroscopy and brain metabolism, with an emphasis on how pain may exacerbate post-injury brain changes. We discuss current controversies, obstacles and future directions for a more coherent and collaborative approach.

The review is registered with PROSPERO http://www.crd.york.ac.uk/PROSPERO/) CRD42016032967 and follows Preferred Reporting Items for Systematic Reviews and Meta-Analyses (PRISMA) guidelines (http://www.prisma-statement.org).

Imaging of the injured spinal cord has been thoroughly reviewed elsewhere (Martin et al., 2016; Stroman et al., 2014; Wheeler-Kingshott et al., 2014) and is not included in this review.

1.1. A brief overview of SCI

Epidemiology: The United States of America is estimated to have the highest incidence of SCI in the world with 54 new cases per million a year, or 17 000 new SCI cases every year. There are approximately 282

Abbreviations: ACC, Anterior Cingulate Cortex; ASIA, American Spinal Injury Association; BOLD, Blood Oxygen Level Dependent; Cho, Choline; Cr, Creatine; DLPFC, Dorsolateral Prefrontal Cortex; DTI, Diffusion Tensor Imaging; DWI, Diffusion Weighted Imaging; ED, Euclidian Distance; Fa, Fractional Anisotropy FDG - ^{18}F-fluorodeoxyglucose; FDG, ^{18}F-fluorodeoxyglucose; fMRI, Functional Magnetic Resonance Imaging; GLM, General Linear Model; Glx, Glutamate-glutamine; HC, Healthy Control; Ins, Myo-inositol; IPL, Inferior Parietal Lobe; ISCIP, International Spinal Cord Injury Pain; MNI, Montreal Neurological Institute; MRI, Magnetic Resonance Imaging; MRS, Magnetic Resonance Spectroscopy; Naa, *N*-acetylaspartate; PET, Positron Emission Tomography; PFC, Prefrontal Cortex; PMC, Premotor Cortex; rCBF, regional Cerebral Blood Flow; ReHo, Regional Homogeneity; ROI, Region of Interest; RSFC, Resting State Functional Connectivity; RSFMRI, Resting State Fmri; SCI, Spinal Cord Injury; SDM, Signed Differential Mapping; SMA, Supplementary Motor Area; SPECT, Single Photon Emission Computed Tomography; tDCS, Transcranial Direct Current Stimulation; VBM, Voxel-based Morphometry

* Corresponding author at: Building 120, 2nd Ave, Charlestown, Boston, MA, 02129, USA.
E-mail address: ldahlberg@mgh.harvard.edu (L. Solstrand Dahlberg).

https://doi.org/10.1016/j.neubiorev.2018.04.018
Received 25 September 2017; Received in revised form 21 February 2018; Accepted 23 April 2018
Available online 24 April 2018
0149-7634/

000 spinal cord injured persons currently living with a SCI in the US (DeVivo et al., 1980; Singh et al., 2014; "Spinal Cord Injury Facts and Figures at a Glance", 2013). Motor vehicle accidents are the leading cause of injury, particularly in the younger (< 30 years) population, while falls are the primary cause in the elderly population (Jain et al., 2015). Although the incidence rate of traumatic SCI has been stable (Jain et al., 2015), there has been a marked decline in mortality during the critical first 2 years after injury (Strauss et al., 2006), and life expectancies have improved considerably in the last six decades. The most frequent neurological categories, in order, are incomplete quadriplegia, complete paraplegia, incomplete paraplegia followed by complete quadriplegia ("Spinal Cord Injury Facts and Figures at a Glance", 2013).

Clinical Presentation: Every spinal cord injury is unique in terms of extent, clinical presentation, secondary injury, stabilization and recovery. The American Spinal Injury Association (ASIA, asia-spinalinjury.org) classification is the most widely used scale, with 5 categories: A: complete, B: sensory incomplete (sensory but not motor function is preserved below the neurological level and includes the sacral segments S4-S5), C: motor incomplete (motor function is preserved below the neurological level, and more than half of key muscles below the neurological level have a muscle function grade less than 3), D: motor incomplete (motor function is preserved below the neurological level, and at least half of key muscles below the neurological level have a muscle function grade of 3 or more), and E: normal. The consequence of injury largely depends on the location and severity of the initial trauma, and the extent of multiple secondary injury mechanisms (swelling, hemorrhage, posttraumatic ischemia, and inflammation) causing further tissue damage and cell death. See Oyinbo (2011) for a comprehensive discussion of secondary injury mechanisms.

Other physical consequences: In addition to sensory and motor dysfunction, autonomic functions are often impacted, especially in higher-level injuries. The most common causes of morbidity in chronic SCI are diseases of the cardiovascular system, followed by respiratory complications (Garshick et al., 2005). Patients may be in a state of low grade chronic inflammation (Davies et al., 2007), especially in SCI subjects with neuropathic pain, as evidenced by elevated interleukin-6 (IL-6) and C-reactive protein levels (Neefkes-Zonneveld et al., 2015). This can be attributed to a combination of lost lymphoid innervation, endocrine impairment, and prolonged physical inactivity (Allison and Ditor, 2015). The loss of load bearing on lower extremities leads to a rapid reduction in bone mass and a more than five-fold increased risk of fractures (Troy and Morse, 2015). With decreased gastric motility, chronification of gastrointestinal problems occurs in the majority of the SCI population (Hou and Rabchevsky, 2014; Stiens et al., 1997). Lack of intact somatic and autonomic nerves following SCI frequently results in micturition dysfunction and problems pertaining to the lower urinary tract (Hou and Rabchevsky, 2014). Incontinence can be a major obstacle for normal sexual function in female patients (Cramp et al., 2015), whereas males commonly report erectile dysfunction and anejaculation after injury (Cobo Cuenca et al., 2015; Virseda-Chamorro et al., 2013). Sexual dysfunction also influences patients' quality of life (QOL) (Cramp et al., 2015).

Psychological impact: Reactive anxiety and depression following injury typically peaks in the acute phase and is heavily affected by the length of stay in the hospital (Kennedy and Rogers, 2000). Persistent anxiety is also reported to increase gradually from time of injury, reaching above diagnostic cut-off scores (Kennedy and Rogers, 2000). Depression is somewhat more common in SCI patients compared to unaffected individuals; whereas lifetime prevalence of major depressive disorder in the general population is estimated to be 16.2% in the United States (Kessler et al., 2003), prevalence of depression following SCI is reported to be 22% (Williams and Murray, 2015). Depressive reactions and post-traumatic distress may occur after spinal injuries, and as symptoms usually improve over time, it has been suggested that they reflect transient adjustment problems (Schönenberg et al., 2014). Post-traumatic stress disorder (PTSD) occurs in 8–11% of the SCI population (Migliorini et al., 2008; Otis et al., 2012). Furthermore, cognitive dysfunction is a common consequence of the injury with cases reported in up to 60% of the SCI population (Davidoff et al., 1985, 1992; Dowler et al., 1997). In many cases this is due to a concomitant traumatic brain injury with the SCI (Davidoff et al., 1985), however, it may also be an effect of altered cardiovascular autonomic control (Wecht and Bauman, 2013), and neurodegeneration related to neuroinflammation (Wu et al., 2014).

Pain in SCI: Pain following SCI can be classified with the International Spinal Cord Injury Pain (ISCIP) classification (Bryce et al., 2012), based on type and source of the pain. Nociceptive pain is pain from musculoskeletal or visceral tissues, and is the most commonly reported type of pain after SCI (Siddall et al., 2003). In the sub-acute phase of injury, patients frequently report pressure ulcers during rehabilitation (Chen et al., 1999). In paralyzed patients, the use of, and transfer to and from a wheel chair is associated with shoulder pain, especially if overweight (Ferrero et al., 2015). Shoulder pain is further associated with depressive symptoms and worsened self-perceived health (Wang et al., 2015). In stable SCI patients, low self-efficacy and high pain intensity are most detrimental on QOL, sometimes more so than any other physical dysfunction (Middleton et al., 2007). Musculoskeletal pain often manifests itself in the early stages after the injury, but late onset is also reported, likely as a result of unnatural use and posturing of the body (Siddall et al., 2003).

Neuropathic Pain from both central (spinal cord) and peripheral nerve (dorsal roots/dorsal root entry zone) damage is common in SCI patients. Neuropathic pain is frequently described as excruciating and more severe than nociceptive pain. Neuropathic pain is reported in approximately 50% of the SCI population (Siddall et al., 2003). The pain is typically chronic, and often refractory to pharmacological treatment. Pain is also associated with great costs to both society and the individual patient (Mann et al., 2013). For example, in a study including 1357 SCI patients receiving initial rehabilitation, those with severe pain spent less time in rehab, and had more treatment sessions adjusted in goal or content because of pain (Zanca et al., 2013). Chronic pain in SCI patients has a cascading effect on other aspects relating to an individuals' well being such as general functioning (Turner et al., 2001a), increased depression and anxiety (Avluk et al., 2014; Tran et al., 2016), sleep quality (Avluk et al., 2014) and daily activities (Widerström-Noga et al., 2001).

Given the major impact of a spinal lesion, along with physiological and psychological consequences of a SCI, it is not surprising that changes in brain function and structure occur. The complexity of alterations in spine and brain that occur after a spinal cord lesion include *i*) direct effects of injury to spinal tracts and cell death to those projection neurons in the spinal cord, *ii*) effects on the endocrine system (in particular the hypothalamic-pituitary-adrenal axis) which interacts with immune function that together may impact neuronal signaling, *iii*) adaptive or maladaptive plasticity over the duration of illness, *iv*) potential changes induced by altered cardiovascular function, *v*) indirect changes due to SCI symptoms and altered behaviors such as disuse, depression and pain, and *vi*) alterations induced by medications. Below, we provide a brief background on brain imaging methods, and review the evidence towards brain alterations in SCI.

1.2. Neuroimaging metrics

Early neuroimaging studies on SCI utilized Positron Emission Tomography (PET) with glucose or cerebral blood flow measures (Bruehlmeier et al., 1998; Roelcke et al., 1997). PET can also provide dynamic information of molecular processes to study neurochemical alterations but use of the technology in the SCI population has not been published. With MRI) methods becoming increasingly accurate, accessible and affordable, it is the mainstay technology in human neuroimaging research for cortical and subcortical brain imaging. MRI is currently mainly used for four types of applications in brain imaging:

(1) Structural imaging (Lauterbur, 1989) is used to define regional brain volumes, gray matter density and cortical thickness. Typically, a method called Voxel-Based Morphometry (VBM) (Ashburner and Friston, 2000) has been used to quantify gray matter density in order to assess the effect of SCI on brain morphology. However, surface based metrics, such as cortical thickness, may be better suited to study cortical gray matter atrophy (Dale et al., 1999).
Tensor-based morphometry (TBM) (Ashburner and Ridgway, 2012) and/or specific longitudinal surface analysis streams (Reuter et al., 2012) are particularly well suited for tracking patients over time to directly asses brain plasticity and/or effects of rehabilitation interventions,
(2) Brain function is typically measured using regional alterations in blood-oxygen-level dependent (BOLD) (Ogawa et al., 1990) functional MRI (fMRI) signal or arterial spin labeling (ASL) (Williams et al., 1992) providing a measure of cerebral blood flow. The hemodynamic response is correlated to local field potentials, primarily reflecting the incoming input and the local processing in a given brain region (Logothetis, 2003). Functional connectivity typically utilizes the BOLD signal to define regions with synchronous low-frequency fluctuations of signal intensities as a metric of co-activation or functional connectivity (Biswal et al., 1997).
(3) Diffusion imaging (Le Bihan et al., 1986) quantifies the apparent rate and direction of water diffusion in tissue, allowing for metrics on white matter integrity (such as fractional anisotropy (FA)) and tracking white matter bundle orientations using diffusion tensor imaging (DTI).
(4) Magnetic Resonance Spectroscopy (MRS) (Purcell et al., 1946) provides measures of metabolite 1H chemical shifts including choline, creatine, glutamate and glutamine, myo-inositol, and *N*-acetylaspartate (Naa). This method allows the determination of brain metabolite concentrations in specific structures of the brain, and is a useful technique to investigate clinical populations as biochemical changes might precede structural ones.

Many studies employ multiple MRI metrics in the same population and structural characteristics such as gray matter volume, as well as white matter properties, and functional measurements of brain activity and metabolites likely interact. Below, we present data from the meta-analysis on brain activity related to motor execution and imagination, and provide an overview of results organized per the above measures in separate sections.

2. Meta-analytical methods

The neuroimaging field has developed tremendously in the last decades, with improvements in image acquisition and analytical approaches as well as in the way results are reported. Thus, stratification and clear criteria for inclusion are essential for a reliable meta-analysis. We identified homogeneous studies in terms of experimental paradigms, metrics and analysis in order to determine consistent and replicable brain changes following SCI.

2.1. Eligibility criteria, information sources and search strategy

Only studies from peer-reviewed articles published in English with online access were included. Included studies were published between 1998 (when the first study describing functional differences was published) and early 2016. Exhaustive searches of literature were performed on the PubMed database. Further, relevant publication reference lists were searched to identify further publications. The search was performed on March 5th 2016 identifying 356 potential studies.

We identified studies on human spinal cord injury employing brain imaging with Magnetic Resonance Imaging (MRI), functional MRI (fMRI), diffusion weighted imaging (DWI, DTI), Magnetic Resonance Spectroscopy (MRS), Positron Emission Tomography (PET), and Single Photon Emission Computed Tomography (SPECT). We searched PubMed using the search phrases:[Brain AND “Spinal Cord Injury” AND “magnetic resonance imaging” AND human],[Brain AND “Spinal Cord Injury” AND (“functional magnetic resonance imaging” OR “fMRI”)], [Brain AND “Spinal Cord Injury” AND (“Diffusion weighted Imaging” OR vDiffusion Tensor Imaging”)],[Brain AND “Spinal Cord Injury” AND “Magnetic Resonance Spectroscopy”],[Brain AND “Spinal Cord Injury” AND (“Positron Emission Tomography” OR “PET”)], [Brain AND “Spinal Cord Injury” AND “Single Photon Emission Computed Tomography”].

2.2. Study selection

After initial review of the literature indicating a limited and diverse set of studies on brain changes following SCI, we opted to only include studies investigating differences in functional MR brain activation of SCI patients versus healthy subjects. Inclusion criteria for the quantitative analysis were i) inclusion of spinal cord injured patients, ii) brain imaging using fMRI, iii) reports of brain alterations in the form of MNI or Talairach coordinates, iv) comparisons with healthy controls. The functional studies included in the meta-analysis were limited to movement or attempted movement paradigms, comparing the differences in activation in each group.

We also performed a narrative review of fMRI studies using other paradigms and/or not reporting brain imaging findings in coordinate form. A handful of structural and functional studies using VBM, DTI or studies examining metabolic changes measured by PET or MRS were identified and are included in the narrative review. Including SPECT into the search term provided two articles, one of which was excluded, as it was a methods review paper.

2.3. Meta-analysis data

Information on differences in activation between SCI patients and healthy controls from functional paradigms involving movement or imagined movement was extracted from the result tables in the respective articles. Studies eligible for inclusion in the meta-analysis were analyzed using signed differential mapping (SDM). SDM is a software based on previous meta-analytic methods such as multilevel kernel density analysis (MKDA) and activation likelihood estimation (ALE), which can include both positive and negative results from the same coordinates, and use effect sizes to improve accuracy (Radua et al., 2012). In order to produce a SDM map based on the included studies, coordinates of peaks with the maximum intensity from clusters of activation found to differ between the groups are entered into the software. Effect size and variance, which contribute to the recreation of statistical brain maps, are calculated based on the reported cluster t-statistic. To be as inclusive as possible, we opted to include studies using a region of interest (ROI) approach in the meta-analysis. In this approach, analyses are performed in regions selected based on a-priori hypotheses, in contrast to the whole brain. Although this may bias the results towards positive findings, however, it is less sensitive to false positives which whole-brain analyses are more prone to.

Coordinates of peak voxels and t-values from each study, sample size of each group and thresholding (corrected/uncorrected) were used as inputs in the SDM software.

SDM carries out sensitivity and replicability tests of the results with a jackknife analysis, as well as measuring inter-study heterogeneity by weighing the study by their sample sizes. The jackknife analysis explores robustness of the results by excluding one study at the time in the mean analysis. An assumption of reliability can be made if the same findings persists and are unaffected by the discarded studies in the jackknife analysis.

The recreation of effect-size maps was carried out with a Monte-Carlo randomization method using 500 iterations, and a full width at

half maximum (FWHM) of 20 mm. This threshold was chosen based on the recommendations by the SDM software as it is described to be the optimal balance of specificity and sensitivity, and a similar threshold is also standard for activation likelihood estimation analyses and multi-level kernel density analysis, of which SDM is based on (Radua et al., 2012). An uncorrected significance threshold of $p < 0.005$ was used, with a cluster extent of > 10 voxels.

2.4. Risk of bias in individual studies

We did not assess individual studies for risk of bias, publication bias or measures of consistency. Multiple methods have been used to study changes in the SCI brain, including activation changes, Euclidean distances in somatosensory representations, volume of activation and center of gravity. Only differences in activation intensity were included in the meta-analysis, however, studies describing other measurements are discussed in the narrative review.

3. Results

From an initial 268 identified unique studies, 58 were identified as relevant, whereof 7 studies reported sufficient data to be included in the quantitative meta-analysis (see Fig. 1, and Table 1 for an overview of the 7 studies).

3.1. Meta-analytical results

The meta-analysis included results from 75 SCI subjects (whereof 19 women), with an average age of 38 years, investigated at an average of 8 years since injury (see Fig. 2). Patients with SCI display significantly increased activation of the left postcentral gyrus (motor cortex), bilateral parts of the cerebellum, right superior parietal gyrus and left inferior parietal gyrus in response to active or imagined right-sided movement, as compared with healthy controls (see Fig. 3 and Table 2 for details). The increased activation likely reflects adaptive changes in cortical function following SCI. More specifically, when attempting right-sided movement, an increase in cortical engagement is seen from the contralateral sensorimotor and bilateral cerebellar regions.

Another consistent finding was increased activity in the ipsilateral superior parietal gyrus, and the contralateral inferior parietal gyrus. Interestingly, the superior parietal lobe on the ipsilateral side (right side) of movement is commonly activated in response to imagined movement in healthy individuals (Anderson and Lenz, 2011), and the region is implicated in internal representation of the body state (Wolpert et al., 1998), a function necessary to perform imagined movements.

Furthermore, a cluster in the left inferior parietal gyrus also showed consistently increased activity in the SCI group compared to healthy controls (HC) during active and/or imagined movement paradigms. There is increasing evidence that the inferior parietal lobule is involved with action intention when it comes to movement, and the feeling of

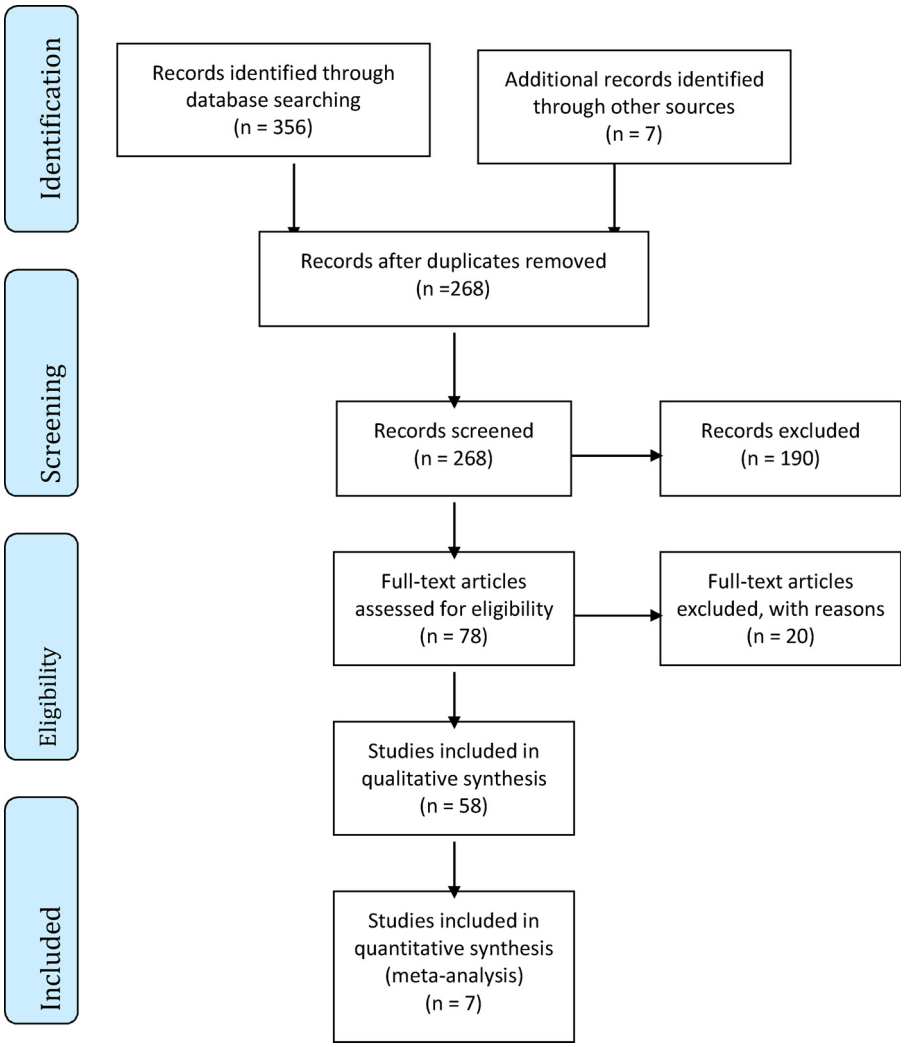

Fig. 1. Articles identified, screened and included in the meta-analysis and qualitative synthesis.

Table 1
Description of the 7 studies included in the meta-analysis.

Study	SCI (n)	Mean age (SD)	M:F SCI	TSI (years)	HC (n)	Mean age (SD)	M:F HC	Task
Sabre et al. (2016)	10	29.1 (± 4.8)	9:1	5.1 (± 2.9)	18	28.5 (± 4.2)	16:2	Flexion/extension of right hand fingers and right ankle.
Chen et al. (1999)	17	38.3 (± 12.2)	10:7	1.4 (± 1.6)	17	38.2 (± 12.3)	10:7	Kinesthetic MI task (imagining dorsiflexion of right ankle), and ME task (for controls, attempted for SCI)
Freund et al. (2011b)	10	47.1 (± 10.7)	10:0	14.6 (± 6.9)	16	39.3 (± 15.4)		Grip task
Hotz-Boendermaker et al. (2011)	9	35 (± 6)	6:3	9	12	29 (± 3.7)	7:5	Execution (HC) or attempt (SCI) of dorsal/plantar flexion of right food. Observe video of same foot flexing movement.
Gustin et al. (2010)	11	48 (± 13.3)	9:2	16.8 (± 15.8)	19	36 (± 13.1)	18:1	Movement imagery: plantar and dorsal flexion of right ankle (after 7 days of training)
Hotz-Boendermaker et al. (2008)	9	35 (± 6)	6:3	9.8 (± 5.1)	12	29 (± 3.7)	7:5	Imagined and attempted movement (executed movement in controls) (dorsal and plantar flexion of right foot)
Curt et al. (2002a)	9	30.3 (± 6.9)	6:3	3.4 (± 3.1)	12	29.9 (± 4.1)	6:6	Flexion and extension of right wrist, right elbow, repetitive and sequential finger to thumb movement and right-left movements with tongue

F, Female; HC, healthy control; M, Male; ME, Motor Execution; MI, Motor Imagery; N, number; SCI, Spinal Cord Injury; SD, Standard Deviation; TSI, Time Since Injury.

Fig. 2. Average time since injury in patients from each study included in the meta-analysis depicted in a forest plot displaying mean (years) ± standard deviation. Gray line represents mean time since injury of all subjects from all studies. Hotz-Boendermaker (2011) only listed average years since injury for the SCI group, but reported a range between 2–20 years.

Fig. 3. SDM analyses revealed consistently increased activation in the precentral gyrus, cerebellum and superior and inferior parietal cortex in response to attempted/imagined movement in patients with spinal cord injury compared to healthy controls.

"wanting to move" or movement preparation (see (Desmurget and Sirigu, 2012) for a review on the inferior parietal lobe's (IPL) involvement in motor intention). The inferior parietal gyrus cluster appeared on the contralateral side of the movement, which is in accordance with a previous study that describes stimulation of the right IPL to result in a strong wanting of moving the left arm, hand or foot (Desmurget et al., 2009).

The result of the current meta-analysis suggests that deafferentation and the loss of sensorimotor functions after SCI not only directly impacts the sensorimotor system, but also secondary areas with indirect implication in motor ability relating to envisioning, urging, preparing and coordinating movement. This is also supported by previous studies that found that both the sensorimotor and the limbic system are affected following an SCI (Freund et al., 2013; Grabher et al., 2015).

Further insight to the mechanisms behind the observed increase in motor system activation in SCI may be gained from other disease states. In amputees, there is reorganization of sensory and motor cortices (Raffin et al., 2016), and hyperactivation of the motor cortex to imagined phantom limb movement has been observed in some (Lotze et al., 2001) but not all (Raffin et al., 2016) studies. In amyotrophic lateral sclerosis (ALS) impacting motor neurons, there is evidence of elevated

Table 2
Attempted or imagined movement evoked increased levels of activity in the following areas in the SCI group compared to healthy controls. Jackknife analysis describes the frequency of cluster activation occurrence when each one of the studies were excluded in analysis.

Region	Hemi-sphere	MNI coordinates			Voxels	SDM-Z	p-value	Jackknife Analysis
		x	y	z				
Middle Cerebellar Peduncles		*16*	*−38*	*−32*	*6428*	*3.473*	*0.000000119*	*7/7*
Local peaks in cluster:								
Middle Cerebellar Peduncles		*16*	*−38*	*−32*		*3.473*	*0.000000119*	
Cerebellum, hemispheric lobule IV/V	*Right*	*22*	*−36*	*−28*		*3.424*	*0.000000119*	
Undefined		*10*	*−46*	*−32*		*3.419*	*0.000000179*	
Cerebellum, hemispheric lobule VI	*Left*	*−22*	*−62*	*−18*		*2.565*	*0.00003022*	
Cerebellum, hemispheric lobule VI	*Left*	*−6*	*−68*	*−14*		*2.24*	*0.000239611*	
Cerebellum, hemispheric lobule IV/V	*Left*	*−6*	*−54*	*−18*		*2.176*	*0.000342429*	
Cerebellum, hemispheric lobule IV/V	*Left*	*−8*	*−52*	*−22*		*2.138*	*0.000422299*	
Middle Cerebellar Peduncles		*30*	*−50*	*−42*		*1.956*	*0.001188517*	
Middle Cerebellar Peduncles		*28*	*−54*	*−42*		*1.934*	*0.001378059*	
Undefined		*26*	*−50*	*−44*		*1.878*	*0.00196147*	
Postcentral Gyrus	*Left*	*−20*	*−28*	*64*	*1754*	*3.487*	*0.000000119*	*7/7*
Local peaks in cluster:								
Postcentral Gyrus	*Left*	*−20*	*−28*	*64*		*3.487*	*0.000000119*	
Paracentral Lobule	*Left*	*−2*	*−26*	*54*		*2.525*	*0.00003922*	
Precuneus	*Left*	*−4*	*−40*	*66*		*2.346*	*0.000127971*	
Superior Parietal Gyrus	*Right*	*28*	*−62*	*60*	*163*	*2.004*	*0.000878632*	*4/7*
No other peaks								
Inferior Parietal Gyri	*Left*	*−36*	*−56*	*52*	*59*	*1.806*	*0.003002286*	*5/7*
Local peaks in cluster:								
Inferior Parietal Gyrus	*Left*	*−36*	*−56*	*52*	*59*	*1.806*	*0.003002286*	
Superior Parietal Gyrus	*Left*	*−30*	*−56*	*56*		*1.799*	*0.003121078*	

MNI, Montreal Neurological Institute; SDM, Signed Differential Mapping.

motor system activation to attempted or imagined movement (Shen et al., 2015). This may indicate that motor neuron damage is sufficient to induce elevated motor cortex activation, with or without lacking somatosensory feedback. Notably, Cosittini et al. found primary motor cortex atrophy and hypo-activation in ALS, but enhanced activation of the fronto-parietal pre-motor circuit, which suggest that this may be driven by loss of inhibitory inter-neurons (Cosottini et al., 2012). Likewise, in patients with pure peripheral motor neuropathy, an elevated cortical motor system response to movement is observed (Reddy et al., 2002). In an experimental study examining movements without proprioceptive feedback using ischemic nerve block, there was preserved activation of primary somatosensory cortex, and increased activation of primary motor cortex, premotor cortex, parietal cortex, midcingulate and the cerebellum during nerve block (Christensen et al., 2007).

Taken together, it is possible that it is the disruption of descending corticospinal tract neurons that leads to elevated cerebral motor cortex activation. However, disruption of sensory and proprioceptive feedback, and engagement of motor preparation and sensory-motor integration networks likely also contribute to the observed hyperactivations in SCI. Human spinal cord injuries are heterogenerous, and recent evidence suggests that below injury stimulation can still result in somatosensory cortex activation in a sub-portion of clinically complete SCI (Wrigley et al., 2018), suggesting that nerves remain, but are silent or dysfunctioning. Thus, as clearly described in the work by Lemon (2008), alterations after lesions to descending pathways are best interpreted as a combination of the disruption of the lesioned pathway, adaptive changes in uninjured fibers, and compensatory changes in the motor network as a whole.

3.2. Functional alterations following SCI not included in meta-analysis

3.2.1. Studies of motor cortex representations

Nineteen additional studies on motor and sensory responses in SCI patients were identified (see Table 3). In pioneering work Sabbah et al. and Curt et al. investigated the ability to activate somatosensory and motor cortices to attempted or imagined movement of lower limbs in patients with complete injury (Sabbah et al., 2002, 2000) or motor activation of regions above the lesion level (Curt et al., 2002a). Sabbah et al. demonstrated that lower limb cortical networks can be activated in complete SCI patients, and Curt et al. demonstrated that cortical representation of the upper limb muscles is altered, with elevated functional responses. Subsequent studies (both included and not included in the quantitative meta-analysis) have identified increased motor cortex activation to movement in SCI patients. In one of the larger studies (n = 17 SCI patients, 7 HC). Lundell et al. (2011) found that the observed increase in ipsilateral somatosensory and motor cortex was correlated with the degree of atrophy of the spinal cord, and premotor cortex activation also correlated to clinical motor scores. There are, however, a couple of studies that did not find elevated motor cortex activation: Cramer et al. (2005) found apparent *reduced* sensorimotor activation in SCI subjects during attempted right foot movement, although directly contrasting SCI subjects and controls did not reveal significant differences. Alkadhi et al. (2005) and Mikulis et al. (2002) found no difference between SCI subjects and non-SCI subjects in motor cortex activation to motion. Turner et al. reported greater modulation of BOLD signal in somatosensory areas during a motor and sensory task in SCI patients compared to controls, in addition to a posterior shift in activity in response to the motor task (Turner et al., 2003). During the sensory task, controls showed increased activation compared to SCI patients.

In an intriguing study on the clinical utility of fMRI to predict functional outcomes, Lee et al. (2015) investigated the effect of repeated passive movement of the toe, i.e. a proprioceptive and somatosthetic stimulation in 49 patients with SCI before and after surgical decompression and fixation. 17 of the 49 patients showed improvements in ASIA score after surgery. None of the 49 patients displayed fMRI responses to the toe stimulation before surgery, but after surgery, 6 of the 49 patients had contralateral somato-motor cortex responses to passive toe movement, and those six patients subsequently showed improved ASIA scores. Hence, the cortical response to below-lesion proprioceptive stimulation suggests preserved sensory tracts and

Table 3
An overview of fMRI studies on brain changes following SCI that were not eligible for the meta-analysis.

Study	SCI (n)	Mean age (SD)	M:F SCI	TSI (years)	HC (n)	Mean age (SD)	M:F HC	Objective	Outcome
fMRI studies not included in meta-analysis									
Eick and Richardson (2015)	3	29 (± 3.6)	2:1	2.9 (± 3.5)	5	31.6 (± 7.8)	2:3	fMRI in SCI with thoracic injuries were conducted during a visual illusion walking paradigm where subjects were presented with illusory walking and sitting conditions. The same paradigm was carried out on controls.	The illusory walking evoked SMC activation when compared to illusory sitting in SCI. HC showed activation in the premotor and frontal areas in the same contrast.
Jutzeler et al. (2015)	Total: 24, w/ NP: 12, wo/ NP: 12	Total: 43.6 (± 11.4), w/ NP: 45.8 (± 12.2), wo/ NP: 41.5 (± 10.5)	22:2	Total: 13.1 (± 8.6), w/ NP: 13.6 (± 8.7), wo/ NP: 12.7 (± 8.9)	31	31.9 (± 9.9)	17:14	Cortical activation in SCI patients with and without neuropathic pain as well as healthy controls was recorded during sensory (brushing and heat) and motor (wrist extension) tasks.	No differences were seen in response to both sensory and motor tasks between SCI and HC. A lateral shift of peak activation was observed in M1 and S1 in the SCI group compared to HC. The shift of activation during the motor task was negatively correlated with pain intensity.
Lee et al. (2015)	Total: 49, A: 6, B: 21, C: 22	A: 42.33 (± 15.65), B: 46.52 (± 13.22), C: 40.14 (± 14.34)	A: 4:2, B: 20:1, C: 15:7	Peri- and postoperative	–	–	–	fMRI determined if activity during toe stimulation in SCI could predict neurological outcome. 3 groups were categorized based on responses: A - showed contralateral SMC activation in The post-op MRI. B - showed activity in other regions. C - no activation.	The group with contralateral activation to toe stimulation were more likely to show greater improvement compared to group B and C.
Sabre et al. (2013)	6	27.3 (± 10.9)	6:0	< 1	12	27.1 (± 10.1)	12:0	SCI were scanned at 1, 3 and 12 months after injury. Cortical reorganization was assessed with BOLD to flex/extension of hand, fingers and ankle. VOA, COG, max intensity and weighted laterality indexes were calculated.	VOA in the M1 correlated with the ASIA impairment scale at 1 and 3 months after injury. Within the year, there was a broadening and shift of activation.
Freund et al. (2011a)	10	47.1 (± 10.7)	10:0	14.6 (± 6.9)	16	39.3 (± 15.4)		Cortical responses to hand-grip task and stimulation of the tibial and median nerve were recorded in subjects with a cervical SCI and compared with HC.	Hand grip evoked increased M1 activation in the leg representation area, and the S1 face area in response to median nerve stimulation in SCI. Increased response to the grip task and median nerve stimulation, plus reduced activity to the tibial stimulation were associated with smaller cord area.
Lundell et al. (2011)	19	46 (± 12)	18:1	13	7	42 (± 18)	7:0	Relationship between cortical responses to dorsiflexion of the ankle and spinal cord reduction as well as functional recovery (as measured by motor scores) was investigated in SCI and HC.	Clinical motor scores negatively correlated with responses in the ipsilateral M1 and bilateral PMC. Responses in the ipsilateral M1, S1 and PMC negatively correlated with cord width.
Jurkiewicz et al. (2010)	4	29.5	3:1	< 1	7	–	–	Attempted right ankle dorsiflexion was used to investigate changes in cortical activation throughout the first year following a SCI.	BOLD response to attempted ankle movements in SCI was similar to HC in early stages after the injury. Activity in associated sensorimotor areas and M1 reduced over time after the injury.
Cramer et al. (2005)	10	30 (± 12.7)		5.5 (± 4.7)	20	31.5 (± 15.7)			

(*continued on next page*)

Table 3 (*continued*)

Study	SCI (n)	Mean age (SD)	M:F SCI	TSI (years)	HC (n)	Mean age (SD)	M:F HC	Objective	Outcome
								fMRI before and after 7 days of motor imagery training of food and tongue examined changes in cortical activation in SCI patients compared with controls with and without training.	Increased putamen activation was found in both trained groups but not the untrained HC group during attempted foot movements. No change was seen in M1/S1.
Jurkiewicz et al. (2007)	6	28 (± 9)	5:1	< 1	10	29 (± 7)	4:6	A wrist extension task was used to investigate changes in cortical activation throughout the first year following a SCI.	Little M1 activation was seen in the early stages after the injury, whereas associated sensorimotor areas showed increased activation compared to controls in response to the wrist extension task. An inverted pattern more similar to controls was seen with improved motor functioning.
Cramer et al. (2005)	11	47 (± 6)	11:0	22 (± 6.6)	12	42 (± 15)	12:0	Potential changes to the cortical motor system function were assessed in SCI and healthy during attempted and imagined foot movements.	In SCI, the volume of activation in the SMC was reduced during the task. Activation patterns outside the expected areas of activation were seen both in attempted and imagined movement in SCI.
Alkadhi et al. (2005)	8	31.3	5:3	2.6	8	29.6	4:4	Brain activation in response to movement imagery with extension and flexion of right ankle was tested in patients with complete SCI's contrasted with healthy controls.	SCI showed increased activity in primary and associated motor regions plus subcortical structures compared to controls. Motor imagery in SCI and executed movements in controls activated the M1 to the same degree.
Turner et al. (2003)	13	42 (± 8)	0:13	15. (± 8)	13	44 (± 11)		Cortical reorganization of responses to a hand movement and sensory task was tested in paraplegic patients and compared to controls.	In comparison to the activation seen in HC, SCI subjects had smaller and more variable activation and location to both tasks. The activity was found to be more posterior in the M1 and SMA in the motor task.
Curt et al. (2002a,b)	9	30.3 (± 6.9)	3:6	3.4 (± 37.6)	12	29.9 (± 4.1)	6:6	Cortical reorganization of non-affected body limb representation was investigated with flexion and extension of wrist, elbow, finger tapping and tongue movements in SCI and controls.	Increased volume of activation in the M1 was observed in SCI during finger movements. Motor regions, the parietal cortex and cerebellum showed increased activity during all except tongue movements. No shift in activation was seen during upper limb or tongue movements.
Mikulis et al. (2002)	11	41 (± 16)		7 (± 7.4)	14	28.9 (± 7)		Motor cortex adaption following a cervical SCI was examined using a wrist and tongue movement task to look at changes in motor cortex representation of the two parts.	BOLD to wrist movement did not differ between the groups. A shift of activation was indicated by a difference in location of maximum activation during tongue movement in the SCI group.
Sabbah et al. (2002)	9	36.4 (± 8.7)	9:0	10.1 (± 12)	–	–	–	Activity in response to attempted and imagined movement as well as stimulation with and without visual feedback of toes were recorded in patients with SCI.	All patients showed activity in SMC, PMC and SMA. Passive proprio-somesthesic stimulation also evoked activity posterior to the central sulcus.
Turner et al. (2001a,b)	Total: 8, tetra: 2, para: 3, amputee: 3	46.6	7:1	7 - 29	6		4:2		

(*continued on next page*)

Table 3 (*continued*)

Study	SCI (n)	Mean age (SD)	M:F SCI	TSI (years)	HC (n)	Mean age (SD)	M:F HC	Objective	Outcome
								Subjects executed or attempted movement of wrists, feet and tongue during fMRI to assess changes in limb representation.	All patient groups showed some evidence of cortical reorganization. SCI showed reduced activity in activation area and intensity while attempting to move paralyzed limbs, while activation patterns of amputees during movement of lost limbs were more similar to controls.
Moore et al. (2000)	4	42.5	4:0		–	–	–	The link between cortical reorganization and phantom sensations following SCI was examined with fMRI during tactile stimulation in 4 thoracic SCI patients.	The findings provided some evidence to cortical representation of phantom sensation based on co-activation of unstimulated body regions.
Sabbah et al. (2000)	5	32.8 (± 5.0)	5:0	7.5 (± 9.6)	–	–	–	fMRI was conducted during movement of upper limb movement, and attempted, imagined or stimulated movement of toes.	Activation of M1, PMC and SMA were seen both during movement and imagined movement of upper limbs, as well as during attempted and imagined movements of toes.

BOLD, Blood Oxygen Level Dependent; COG, Center of Gravity; F, Female; HC, healthy control; M, Male; ME, Motor Execution; MI, Motor Imagery; N, number; PMC, Premotor Cortex; SCI, Spinal Cord Injury; SD, Standard Deviation; SMA, Supplementary Motor Area; SMC, Sensorimotor Cortex; TSI, Time Since Injury; VOA – Volume of Activation.

associated symptom improvements.

Two longitudinal studies Jurkiewicz et al. (2007), Sabre et al. (2016) have investigated the temporal development of sensorimotor cortical activation in human SCI. Jurkiewicz et al. investigated four (non-recovering) quadriplegic individuals on up to four consecutive occasions, at 1, 3, 6 and 12 months post injury, while patients attempted right ankle dorsiflexion. In the early stages post-injury, SCI subjects displayed elevated primary motor cortex activation, but this elevated response diminished over time to be lower than healthy controls at 12 months post-injury. Sabre et al. investigated six SCI subjects at 1, 3 and 12 months after injury, with a right hand and a right ankle and flexion/extension task (Sabre et al., 2013). Three of the subjects improved, and results indicate that primary motor cortex activation increased over time in the recovering patients. Neither of the longitudinal studies report direct comparisons between healthy subjects and SCI subjects, but relied on volume of activation as an outcome metric. Unfortunately, volume of activation has been found to be a rather unstable measure (Cohen and DuBois, 1999) that does not account for the magnitude of activation within each counted voxel. In combination with the inconsistent findings between studies, and the small sample sizes, this review cannot draw any firm conclusions on the temporal development of motor cortex responses after SCI.

3.2.2. Studies on somatosensory cortex representations

After an injury, when afferent sensory and proprioceptive information no longer reaches the brain, the somatosensory cortical regions representing the corresponding regions become deafferented and receptive fields from spared regions take over primary sensory representation. This somatosensory cortex reorganization was first demonstrated in rats with nucleus gracilis injury by Wall and Eger in 19,717 (Wall and Egger, 1971), where forelimb representations invaded hindlimb cortical representations within seven weeks after injury. This process has been documented in numerous SCI models (see Endo et al. (2009), and Nardone et al. (2013) for recent reviews).

Pennfield and Boldreys classical studies of somatic and sensory representations in the human cerebral cortex (1937) have been largely confirmed using transcranial magnetic stimulation (Metman et al., 1993; Penfield and Boldrey, 1937) and functional imaging recordings (Tal et al., 2017), but Ddefining subtle changes in cortical representations is challenging: The general linear model (GLM) —currently the dominant way to analyze fMRI data— models individual voxel signal time series as a linear combination of a) the experimental paradigm and a canonical hemodynamic response function, and b) other sources of variance such as experimental control conditions and noise estimates (typically motion and scanner drift). While the approach is effective in determining stimulus-induced activation, it may be less sensitive when examining cortical reorganization: Wrigley et al. (2009b) investigated whether the degree of primary somatosensory cortex reorganization following SCI correlated with on-going neuropathic pain intensity. To do so, they evaluated responses to light brushing of the little finger, thumb and lip. While no significant differences in evoked responses were found between healthy subjects, SCI patients with and without neuropathic pain using a GLM analysis, they did observe evidence for cortical reorganization: the Euclidean distance (ED) of locally evoked responses was measured from an anatomical landmark, i.e. the convergence of the central sulcus with the longitudinal fissure, to the maximally activated voxel's coordinates during a specific task or stimuli (i.e. little finger brush, thumb brush or lip brush). While lip representation remained intact in all SCI patients, there was a medial shift in S1 responses (i.e. decreased ED) to little finger stimulation in the SCI group with neuropathic pain. In contrast, Jutzeler et al. conducted a similar study on 24 SCI patients and 31 healthy controls, using active and passive wrist extension to elicit motor cortex activations, and brush and heat stimuli to the hand to elicit somatosensory cortex activation. There were no differences in the extent of activation as assessed by a GLM, there was, however evidence of lateral shifts (i.e. increased ED) in

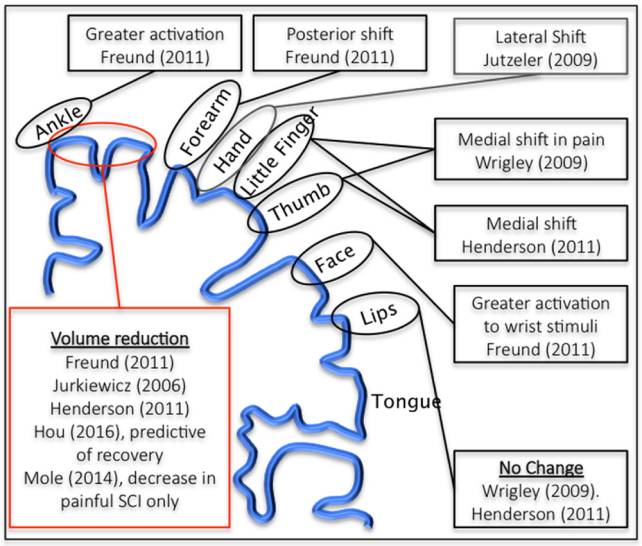

Fig. 4. Illustration of evidence for atrophy and reorganization of the primary somatosensory cortex. Due to the multiplicity of methods, meta-analytical confirmation of observed effects was not possible.

the somatosensory cortex hand representation. However, no relation between somatosensory reorganization and the severity of neuropathic pain was observed. Interestingly, SCI patients without neuropathic pain showed greater cortical reorganization of the M1 compared to SCI patients with neuropathic pain, whose shift of activation was closer to that of controls during a wrist extension paradigm (Jutzeler et al., 2015).

Similarly, in a study including 20 SCI patients with thoracic injuries, Henderson et al. reported a medial shift of thumb and little finger representation, measured with ED, which was associated with sensory deprivation and time since injury (Henderson et al., 2011). Of note, Freund et al. found increased activation of the primary sensory cortex (face region) to median nerve stimulation, but no differences in activation during tibial nerve stimulation between SCI patients and controls (Freund et al., 2011b). In the same subjects, alterations in the corticomotor representation areas were also assessed by transcranial magnetic stimulation. Results indicated that forearm representation was located more posteriorly towards the anatomical hand representation of M1 in SCI. These findings are summarized in Fig. 4.

Deafferentation and neuropathic pain has been hypothesized to be impacted by the cortical reorganization that occurs due to altered signaling to and from the sensory cortex in individuals with sensory deprivation from the extremities. This is supported by studies showing pain ratings to be significantly correlated with measures of cortical reorganization of the S1 in both SCI (Wrigley et al., 2009a) and amputees (Turner et al., 2001b). In contrast, Jutzeler et al. examined changes in ED in patients with and without neuropathic pain, and found a negative correlation between pain and ED measures (Jutzeler et al., 2015). Thus, the maladaptive plasticity hypothesis of neuropathic pain appears insufficient (see also (Makin et al., 2015)), suggesting other influences on neuropathic pain than somatosensory cortical plasticity.

3.2.3. Resting State functional MRI studies

Neural activity in the absence of goal directed cognition or tasks can be studied using resting state functional connectivity (rsFC), based on low frequency spontaneous fluctuations in the BOLD signal. Intra-regionally correlated spontaneous fluctuations indicate that regions are functionally connected. Thus, rsFC provides an indirect measurement of brain connectivity that allows for characterization of distinct functional networks (Van Dijk et al., 2010). As resting state functional connectivity does not require task probes, the design of studies are inherently similar across studies, which would appear ideal for data-sharing initiatives and for meta-analyses. However, the field is still young with regards to clinical investigations of brain consequences of SCI, and a wide range of preprocessing and analytical approaches are used (such as seed-based methods with a-priori defined seeds, independent component analyses, regional homogeneity and frequency based analyses). These methods address different aspects of functional connectivity and activity during rest, and we did not find enough consistency across rsfMRI studies on SCI to conduct a coordinate based meta-analysis.

One assessment of resting state activity evaluates local connectivity between neighboring voxels as a measure of regional homogeneity (ReHo). ReHo in SCI patients have recently been reported to be disrupted in widespread regions of the brain, such as M1 and S1, the dorsolateral prefrontal cortex (DLPFC), brainstem, insula, anterior cingulate cortex (ACC), supplementary motor area (SMA), the cerebellum, among others (Zhu et al., 2015). The international standards for the neurological classification of spinal cord injury (ISNCSCI) motor scores of subjects were found to be negatively correlated with ReHo values in the thalamus and insula, implicating increased cortical reorganization is associated with increased motor impairments. Similarly, a study in newly injured SCI patients (Hou et al., 2014) (time since injury < 15 weeks) reported widespread resting state activity and connectivity differences in SCI patients. Altered amplitude of low-frequency fluctuations (ALFF) during rest was found in the primary sensorimotor cortex, orbitofrontal cortex and the cerebellum in SCI patients, where ALFF activation in the cerebellum was negatively correlated with motor scores in the patients (Hou et al., 2014). Connectivity measures from the same study showed increased connectivity between the primary sensorimotor cortex of both hemispheres, as well as increased functional connectivity between sensory and motor regions, some of which were seen to correlate with ASIA motor scores in SCI patients compared to controls.

Somewhat contradicting these results, another study in eighteen patients with incomplete cervical SCI (49 ± 33 weeks post-injury) found increased connectivity between motor regions, but decreased connectivity between sensory areas (Min et al., 2015a,b).

Global brain connectivity with graph theory approaches has also been used to examine resting state connectivity networks in SCI patients, reporting more or less unaffected global and economic efficiency and functional segregation in comparison to that of healthy controls (Min et al., 2015a,b). These findings are indicative of preservation of areas not directly impacted by cortical deafferentation.

One study examined resting state functional and structural reorganization in SCI patients in the acute stage of the injury (< 9 weeks post injury), as well as changes associated with motor recovery in the first six months after injury (Hou et al., 2016). Functional connectivity was found to be reduced in the primary and association motor cortices in patients who had poor motor recovery after 6 months, whereas an opposite pattern of increased connectivity between these areas were seen in good recoverees.

To sum, rsfMRI studies suggest alterations in neural activity following SCI are evident both in changes to resting state activity and connectivity. RSFC measures offer a promising avenue of SCI research, but there is a need for between-lab methods alignment to define replicable results.

3.3. Structural alterations following SCI

3.3.1. Structural changes in gray matter and spinal cord

After a spinal cord injury, there is rapid atrophy of the corticospinal tracts and sensorimotor areas, with reductions in spinal cord cross section evident within months after injury (Freund et al., 2013; Hou et al., 2016). The initial rate of atrophy, evaluated in subacute patients tracked longitudinally, corresponded to a spinal cord cross section reduction of about 0.4 mm^2 (or 0.5%) per month in the first 12 months (Freund et al., 2013). In another study, an 8% reduction in spine cross-

section was reported in patients approximately 9 weeks post-injury, with larger reductions associated with poor motor recovery (Hou et al., 2016). In chronic patients (14 years after injury), cord cross section reductions of 20–30% have been reported (Freund et al., 2011b; Lundell et al., 2011), suggesting that the rate of cord atrophy plateaus, although long-term longitudinal studies are missing. The degree of cord atrophy correlates with clinical outcomes (Freund et al., 2013, 2011b; Hou et al., 2016; Jutzeler et al., 2016). Beyond the relatively simple measure of spinal cord cross section area, diffusion imaging of the injured spinal cord indicates alterations in fractional anisotropy and cord white matter diffusion properties are also altered (Ohn et al., 2013; Petersen et al., 2012), indicating demyelination and axonal degeneration of spinal tracts. See (Martin et al., 2016) and (Vedantam et al., 2014) for recent reviews on diffusion imaging of the injured spine. One recent study on the structural characteristics of the lesion area itself (Huber et al., 2017) indicates that lesion size and midsagittal tissue bridges at 1 month after injury predicted clinical outcome and recovery. At the brainstem level, there is volume loss in the corticospinal tract and the medial lemniscus, and myelin reductions in the periaqueductal gray, dorsal pons and dorsal medulla, some of which were found to be related to functional impairment (Grabher et al., 2017).

At the level of the brain, extensive structural alterations have been observed using voxel-based morphometry. In parallel with clinical presentations, reductions of gray matter volume in the primary somatosensory cortex lower body, leg and foot areas have been reported (Freund et al., 2011b; Henderson et al., 2011; Hou et al., 2016; Jurkiewicz et al., 2007; Jutzeler et al., 2016), but there are some discrepancies: Mole et al. only observed decreased volume of this area in SCI patients with neuropathic pain (Mole et al., 2014), and in a longitudinal study over the first 12 months post SCI, Freund et al. found gray matter volume reductions in the leg area of the primary motor cortex, but not the somatosensory cortex (Freund et al., 2013). Moreover, progressive reductions over time were observed in the thalamus, anterior cingulate, secondary somatosensory cortex, insula and pons (Grabher et al., 2015). Such changes in volume related quantitatively to sensory deficits, but there were no correlations between neuropathic pain and volumetric declines during the first year of injury. Jutzeler et al. reported reductions in ACC, insula, S2 and thalamus volume in SCI patients with and without neuropathic pain compared to controls. Neuropathic pain was associated with increases in ACC and M1 Gy matter, as well as reductions in S1 and thalamic gray matter (Jutzeler et al., 2016). On the other hand, in a sample of 19 chronic SCI patients and 7 healthy controls, Lundell et al. found no significant differences in regional gray matter volume (Lundell et al., 2011).

Although inconclusive, the above studies indicate that structural reductions occur in both cortical (sensorimotor cortex, ACC, insula) and subcortical (thalamus, pons) areas following a SCI that seem to be influenced by time since injury and the clinical state (i.e. presence of neuropathic pain). Table 4 provides an overview of study findings, and the results are illustrated in Fig. 4.

3.3.2. Structural changes in white matter

Diffusion tensor imaging (DTI) is an imaging technique that allows for exploration of water diffusivity, usually along the white matter tracts. Fractional anisotropy (FA) is related to fiber loss, whereas mean diffusivity (MD) measures the diffusion rate of molecules in the selected voxels. A combination of reduced Fractional anisotropy (FA) values and increased mean diffusivity (MD) are commonly found in damaged fiber tracts, likely reflecting loss of fiber integrity.

A few studies have reported DTI changes in SCI: One study found decreased FA in the centrum semiovale in a sample of complete and incomplete SCI patients compared to orthopedically injured controls (Koskinen et al., 2014). The decreased white matter FA was detected in approximation to the sensorimotor cortex. Changes in white matter diffusivity were related to the clinical state of the SCI patients.

Yoon et al. (2013 – see also PET section below) reported a widespread decrease in MD in SCI patients with neuropathic pain compared to healthy controls (Yoon et al., 2013). Reduced MD in the prefrontal white matter correlated with medial prefrontal cortex mPFC metabolites, suggesting ongoing changes in pain modulation in patients.

Freund et al. also reported decreased FA values in the corticospinal tract in the brain as well as the cervical regions of the spinal cord of patients with a cervical SCI compared to controls (Freund et al., 2012). Remarkably, the FA reduction correlated with upper limb ability, which was not linked to spinal cord reduction.

Henderson et al. found increased cortical reorganization (as measured during a functional imaging during brushing of the skin) of the S1 following thoracic SCI to be associated with reduced FA measures in the white matter beneath the hand representation area (Henderson et al., 2011). However, FA values were not significantly different between patients and controls. Further, no change in FA values in the white matter connecting the S1 region to the ventroposterior thalamus was seen between the groups. Interestingly, diffusion direction of water molecules in the area representing the little finger in the S1 was found to differ from the controls with a direction towards the typical leg representation area reported in the SCI subjects.

Similarly, the same researchers also found increased MD and reduced FA values in a group of 15 SCI subjects with injury to the thoracic level, compared to 27 controls (Wrigley et al., 2009a). Increased MD values were observed in the cerebellum white matter as well as in white matter near the M1 region radiating to the spinal cord region innervating leg muscles in SCI patients compared to control subjects. This was seen in combination with gray matter volume reductions in same M1 region. Moreover, the corticospinal and the corticopontine tracts showed reduced FA values in SCI subjects compared to the healthy sample. The values were not seen to be associated with time since injury.

Gustin et al. reported widespread changes in MD values in the brain when comparing SCI subjects with and without neuropathic pain (Gustin et al., 2010). The affected areas are typically linked to nociceptive processing, and changes were found to correlate with the severity of pain. Tractography changes were also observed in regions associated with reward processes.

Taken together, DTI studies reveal widespread changes in white matter microstructure with studies reporting a general decrease in FA in the corticospinal tracts as well as in areas adjacent to the sensorimotor cortex. Changes in MD are also observed, and both MD and FA measures are in several studies reported to be associated with the clinical state of the patients. Two studies also linked white matter alterations to pain in SCI, indicating profound effects of pain that even affects the white matter fibers in the brain. An overview of findings from DTI, resting state fMRI, MRS, PET and SPECT imaging is found in Table 5.

3.4. Blood flow, metabolic and neurochemical alterations following SCI

3.4.1. Positron emission tomography studies in SCI

Positron emission tomography (PET) uses gamma rays to detect signal from radioactive isotopes in an injectable tracer in the blood stream. This technique allows localization and quantification of tracer distribution, indicative of, for example, regional blood flow, metabolism, receptor expression, neuroinflammation or endogenous neurotransmitter release.

Using $H_2{}^{15}O$–PET as a marker of regional cerebral blood flow (rCBF) to active brain areas, a comparison of healthy subjects, SCI patients with normal hand function (paraplegics) and SCI patients without normal hand function (quadriplegic) during a hand motor task, revealed SCI induced cortical changes that are not specific to site of injury (Curt et al., 2002b). During a motor task, patients with paraplegia showed widespread changes including increased activation in the sensorimotor cortex, thalamus, and the cerebellum among others. The authors suggest that the reorganization may be due to general loss of

Table 4
An overview of MRI studies on structural brain changes following a SCI.

Study	SCI (n)	Mean age (SD)	M:F SCI	TSI (years)	HC (n)	Mean age (SD)	M:F HC	Task	Outcome
MRI									
Jutzeler et al. (2016)	30	46.3 (± 11.9)	27:3	12.5 (± 8.2)	31	42.1 (± 9.9)	23:8	Anatomical data of the brain and the cervical spinal cord was gathered from SCI and HC to assess the relationship between structural changes and NP following a SCI.	The SCI group showed decreased GM volumes in the ACC, bilateral thalamus, left S2 and the left insula. Increased GM volume in the left ACC and right M1 (linked to the amount of reported NP), as well as decreased volumes in the right S1 and thalamus was found in SCI patients with NP.
Grabher et al. (2015)	14	45.6 (± 20)	13:1	< 1	18	34.1 (± 9.5)	12:6	Morphometric measures of the brain and spinal cord were conducted 4 times during the first year following a SCI and compared with HC. Measurements were also assessed in relation to sensory function at each time point as well as pain. Longitudinal relaxation rate (R1) and magnetization transfer (MT) investigated myelin integrity at all time points.	Between baseline and 12 months there was a progressive decline in volume of brain structures implicated in the sensory system (the thalamus, ACC, S2, insula and the brainstem). At 12 months, pinprick scores were found to be associated with the rate of cerebellar volume change.
Hou et al. (2014)	20	36.3 (± 5.6)	11:9	< 12 weeks	30	35.2 (± 8.9)	17:13	Early structural changes (within 12 weeks of injury) were examined in this study. Alterations in GM and WM were investigated, also in relation to sensorimotor functioning in SCI and HC.	SCI patients showed significant morphometrical alterations with reduction in M1, S1, SMA and thalamus GM. M1 GM volume significantly correlated with ASIA motor scores in patients. Reductions in WM were reported in the corticospinal tracts.
Mole et al. (2014)	Total: 30, w/ NP: 18, wo/ NP: 12	Total: 52.5 (± 12.6), w/ NP: 51.3 (± 8.4), wo/ NP: 54.3 (± 17.6)		Total: 13.7 (± 10.5), w/ NP: 11.1 (± 8.7), wo/ NP: 17.7 (± 11.9)	18	Matched		A voxel-based morphometric analysis was conducted on the brains of SCI patients with and without neuropathic pain, as well as age- and gender-matched controls.	Compared to patients without pain, patients with pain showed reduced somatosensory cortex gray matter that correlated with pain intensity. Pain related GM and WM changes in corticospinal tracts and the visual cortex were reported.
Freund et al. (2013)	13	46.9 (± 20.2)	12:1	< 1	18	35 (± 9.3)	12:6	Acute SCI patients were scanned at 4 time points within one year of injury. Measures of GM in the sensorimotor cortices, WM in corticospinal tracts, and MT and R1 methods for myelin assessment were carried out in patients and controls. Anatomical changes were also investigated in relation to functional improvement.	GM volume in the left M1, as well as WM volumes in the corticospinal tracts declined at a faster pace in SCI compared to controls. Indications towards widespread atrophy of myelinated axons were found by MT and R1 measurements at 12 months. A significant progression of spinal cord area was also seen in patients throughout the year. Improvement in motor functioning was correlated with less spinal cord area reduction, and white matter volume reduction over time.
Freund et al. (2011a,b)	10	47.1 (± 10.7)	10:0	14.6 (± 6.9)	16	39.3 (± 15.4)		Anatomical changes in the brain and spinal cord and its association with functional changes in the sensorimotor cortex to a motor and stimulations task were investigated in SCI and controls.	GM volume reduction and cortical thinning was observed in the leg area of M1 and S1 in SCI in contrast to HC. In comparison to HC, the SCI group had 30% reduced cord area and decreased WM in the left cerebellar peduncle and bilateral pyramids.
Lundell et al. (2011)	19	46 (± 12)	18:1	13	7	42 (± 18)	7:0	With a focus on brain activation to a motor task, associations to measurements of structural volume of the spinal cord were made in SCI and HC. Changes in GM volume was made between the groups.	No differences in GM volume was found between the groups, and no correlations were found to motor scores. BOLD responses in the ipsilateral M1, S1 and PMC negatively correlated with cord width in the left-right direction in SCI patients.

(*continued on next page*)

Table 4 (*continued*)

Study	SCI (n)	Mean age (SD)	M:F SCI	TSI (years)	HC (n)	Mean age (SD)	M:F HC	Task	Outcome
Wrigley et al. (2009a,b)	15	41 (± 11.6)	15:0	12.5 (± 10.8)	27	37 (± 15.6)	27:0	Changes to brain anatomy following SCI was assessed in 15 SCI patients with thoracic injuries. VBM (and DTI) methods were employed to investigate alterations in the motor cortices and in motor pathways.	SCI patients showed reduced GM volume in left M1, bilateral medial prefrontal, bilateral anterior temporal cortex, insula, lateral hypothalamus and the ACC compared to controls. No region was found to have smaller GM in controls compared to SCI.
Crawley et al. (2004)	17	33.1 (± 8.9)		4.25 (± 4.25)	16	27.9 (± 7.7)	8:8	Anatomical changes in GM and WM in the M1 of cervical SCI patients and controls were investigated. Specifically the region of the precentral knob, the hand motor area, was looked into. Both an automated and manual based morphometric analyses were carried out.	Both the automated and manual method did not detect any significant anatomical changes in GM and WM volume between the two groups.

ACC, Anterior Cingulate Cortex; BOLD, Blood Oxygen Level Dependent; DTI, Diffusion Tensor Imaging; F, Female; GM, Gray Matter; HC, healthy control; M, Male; ME, Motor Execution; MI, Motor Imagery; MT, Magnetization Transfer; N, number; NP, Neuropathic Pain; R1, Longitudinal Relaxation Rate; SCI, Spinal Cord Injury; SD, Standard Deviation, TSI, Time Since Injury; VBM, Voxel-based Morphometry; WM, White Matter.

afferent bodily input in these patients.

Similarly, an earlier report from the same sample using $H_2{}^{15}O$ to examine differences in rCBF to a motor task in both paraplegic and quadriplegic patients found that both patient groups had activity in the thalamus and cerebellum that was not seen in healthy controls (Bruehlmeier et al., 1998). Moreover, the motor task evoked activation in the sensorimotor cortex region normally representing the leg, indicating an expansion of the hand representative area to "unused" cortical regions. The degree of activation outside of the expected pattern of activation evoked by the particular motor task was associated with the extent of deafferented body parts (Bruehlmeier et al., 1998).

Another PET study investigated cerebral glucose metabolism using ^{18}F-fluorodeoxyglucose (FDG) during rest in a group of both paraplegic and quadriplegic patients compared to controls (Roelcke et al., 1997). Absolute global glucose metabolism was found to be lower in the patient group, likely due to neurological deprivation. On the other hand, an increase in regional metabolism was observed in the SMA, ACC and the putamen, whereas midbrain, the cerebellum and the temporal cortex showed decreased metabolism in patients relative to healthy controls.

With the focus to alleviate neuropathic pain, transcranial direct current stimulation (tDCS) was applied in a sample of SCI subjects. Anodal stimulation was delivered for 20 min, two times a day, for 10 days over the motor cortex. The effect of active and sham treatments was measured with FDG-PET that was performed before and after the stimulation. Compared to sham stimulation, active stimulation resulted in decreased left DLPFC and increased medulla, insular and subgenual ACC metabolism. A decrease in pain ratings was also observed (Yoon et al., 2014), but long term results were not reported.

In a multimodal imaging study using FDG-PET, MRI and DTI, Yoon et al. focused on imaging neural mechanisms of neuropathic pain (Yoon et al., 2013). Ten SCI patients with neuropathic pain were compared with ten healthy controls in this study. Amongst their findings, they report that in comparison to healthy controls, patients with SCI had reduced gray matter and metabolism in the left DLPFC, while reduced metabolism in the medial PFC was correlated with reductions in mean diffusivity of the prefrontal white matter. Regions of differential structure and metabolism in this study are typically associated with pain modulation; however, it is not clear whether the changes are a consequence of neuropathic pain.

Taken together, PET-studies provide further evidence of cortical reorganization following SCI, and findings report altered global and regional metabolism. Interestingly, three of the studies reported regional changes in areas associated with pain modulation (Roelcke et al., 1997; Yoon et al., 2014, 2013), whereof two of the study report a direct link between metabolism in these areas and neuropathic pain levels in SCI patients.

The use of PET ligands to measure more specific targets, such as aspects of dopamine, serotonin and opioid receptor systems, or microglial and astrocyte function, have yet to be reported in the SCI population.

3.4.2. *Magnetic resonance spectroscopy studies in SCI*

Magnetic resonance spectroscopy (MRS) provides metabolic information to the structural information provided by MRI. Changes in metabolite concentrations can be used as biological markers for more widespread physiological changes in the brain.

Alterations in thalamic metabolites have been found in SCI patients, with consistently decreased *N*-acetylaspartate (NAA) levels in patients with neuropathic pain (Gustin et al., 2014; Pattany et al., 2002; Widerstrom-Noga et al., 2015). Further, NAA/Ins ratios in the thalamus (Pattany et al., 2002) and the ACC (Widerstrom-Noga et al., 2013) are different in patients with and without neuropathic pain. Together the studies indicate that NAA concentrations changes significantly following injury, and thalamic NAA are closely linked with neuropathic pain.

Table 5
An overview of studies on brain changes following a SCI as revealed by DTI, resting state fMRI, MRS, PET and SPECT imaging.

Study	Patients (n)	Mean age (SD)	M:F SCI	TSI (years)	HC (n)	Mean age (SD)	M:F HC	Task	Outcome
DTI									
Koskinen et al. (2014)	Total: 34, AIS A: 10, AIS B-E: 24	Total: 57.5 (± 12.2), AIS A: 51.3 (± 15.7), AIS B-E: 60.1 (± 13.4)	Total: 27:7, AIS A: 7:3, AIS B-E: 20:4	Total: 13.9 (± 12.1), AIS A: 23.5 (± 13.1), AIS B-E: 9.9 (± 9.3)	40	40.6 (± 12.2)	20:20	DTI was used to assess white matter tracts in patients with complete and incomplete SCI to controls with orthopedic injury. Metrics were examined in relation to injury severity.	FA reductions were found in the centrum semiovale in both SCI groups compared to controls. FA reductions were also seen in the white matter adjacent to the sensorimotor cortex. Diffusivity changes correlated with the clinical state of the patients.
Yoon et al. (2013)	10	40.8 (± 5.7)	7:3	1.5 (± 0.5)	10	39.5 (± 8.6)	6:4	White matter tracts were investigated with DTI in SCI patients with neuropathic pain to controls.	Extensive reduction in white matter MD were found in SCI compared to HC. Reductions included areas in the prefrontal white matter, suggesting altered pain modulation in these patients with neuropathic pain.
Freund et al. (2012)	9	45.7 (± 9.7)	9:0	14.8 (± 7.2)	10	38.8 (± 15.5)	10:0	Whole brain and ROI assessments of white matter were investigated in cervical SCI subjects and controls. Regression analyses examined relationships between FA and clinical state.	Compared to controls, SCI patients showed decreased FA in the corticospinal tract that correlated with upper limb ability.
Freund et al. (2012)	9	47.1 (± 10.7)	9:0	14.6 (± 6.9)	14	40.1 (± 16.2)	10:0	White matter integrity was examined in the same cohort of 9 cervical SCI subjects in comparison to controls. White matter changes were examined in relation to motor function as measured with a handgrip task.	Significant white matter changes (reduced FA, axial diffusivity AD and increased radial diffusivity RD) were observed in SCI patients in the hand area, the cerebral peduncle, internal capsule and the pyramids in comparison to HC. The white matter change was found to correlate with cortical reorganization.
Henderson et al. (2011)	20	41.55 (± 11.7)	18:2	12.9 (± 10.7)	23		20:3	White matter anatomy changes in relation to functional cortical reorganization were investigated in 20 thoracic SCI subjects compared to healthy controls.	FA values did not differ between groups. Cortical representation of the little finger was seen to move towards the lower limb area. This change correlated with FA values in the area of the S1 little finger representation. In SCI, the direction of diffusivity was towards the area typically representing the legs.
Gustin et al. (2010)	Total: 23, w/ NP: 12, wo/ NP: 11	Total: 43.2 (± 14.4), w/ NP: 48 (± 13.9), wo/ NP: 38 (± 10)	19:4	Total: 14.1 (± 12.2), w/ NP: 15.7 (± 15.5), wo/ NP: 12.5 (± 7.6)	45	33 (± 13.4)	28:17	DTI was used to investigate the association between anatomical white matter changes and neuropathic pain following SCI in 23 patients with thoracic injury and 45 controls.	Widespread significant differences were found in MD values between NP and no NP patients, as well as all SCI compared to HC. MD values in certain regions were found to correlate with pain intensity in the SCI subjects.
Wrigley et al. (2009a,b)	15	41 (± 11.6)	15:0	12.5 (± 10.8)	27	37 (± 15.6)	27:0	Changes to brain anatomy following SCI was assessed in 15 thoracic patients. DTI and VBM methods were employed to investigate alterations in the motor cortex and in pathways.	

(*continued on next page*)

Table 5 (*continued*)

Study	Patients (n)	Mean age (SD)	M:F SCI	TSI (years)	HC (n)	Mean age (SD)	M:F HC	Task	Outcome
									Decreased FA was found in the corticospinal and corticopontine tracts in SCI compared to HC. Increased MD, and gray matter reductions, was found in the cerebellum and M1 region that signals to the spinal cord area innervating the legs in SCI.
Resting State									
Zhu et al. (2015)	Total: 12, para: 6, tetra: 6	46.67 (± 12.12)	12:0	16.83 (± 4.34) days	16	46.06 (± 9.44)	16:0	ReHo during rest was assessed in the whole brain, and in association with clinical scores in patients in the acute stage of a SCI in comparison with HC.	Patients had lower ReHo in the M1, S1, SMA, DLPFC, dACC, caudate and inferior frontal cortex compared to HC. Increased ReHo was seen in the precuneus, insula, thalamus and cerebellum, as well as the cingulate motor area, brainstem /hippocampus, inferior parietal lobe. Motor scores negatively correlated with ReHo in the thalamus and insula.
Min et al. (2015a)	18	57.7 (± 11.94)	12:6	0.95 (± 0.64)	18	52.1 (± 13.8)	10:8	Seed-based resting state methods was employed to investigate changes to the SMC following SCI.	Increased connectivity between the M1 to other motor areas, and decreased connectivity between the S1 and secondary somatosensory cortex were observed in the SCI group compared to controls.
Min et al. (2015b)	20	55 (± 14.1)	14:6	1.1 (± 1)	20	52.9 (± 13.6)	10:10	Graph-theory approach was used to examine whole-brain functional connectivity networks in SCI patients and controls.	Measurements of global efficiency, small-worldness and clustering coefficients were unaffected in SCI. Only the normalized characteristic path length to random network was found to be longer in the SCI group compared to controls.
Hou et al. (2014)	25	36.9 (± 5.8)	13:12	9.3 (± 2.9) weeks	25	36.2 (± 8.3)	13:12	Spontaneous neural activity during rest was assessed with ALFF and functional connectivity was investigated with a seed-based approach in SCI and HC.	Newly injured SCI patients displayed decreased ALFF values in the primary SMC, cerebellum and orbitofrontal cortex compared to HC. Connectivity analyses showed increased functional connectivity in SCI between both primary SMC's, and between motor and sensory regions where some correlated with motor scores in SCI.
Hou et al. (2014)	Total: 25, good rec: 10, poor rec: 15	Good rec: 37.9 (± 13.9), poor rec: 35.8 (± 11.5)	Good rec: 6:4, poor rec: 8:7	Good red: 9.2 (± 3.5), poor rec: 8.8 (± 2.6)	25	36.5 (± 9.3)	15:10	Functional reorganization was assessed by seed-based connectivity in acute SCI. Comparison was made between good and poor recovery and HC.	A decrease in functional connectivity between M1 and SMA and PMC was seen in poor recoverers, whereas increased connectivity amongst these areas was revealed in good recoverers.
Spectroscopy									
Widerström-Noga et al. (2001)	Low NP: 35, High NP: 19	Low NP: 35.7 (± 12.4), High NP: 43 (± 12.5)	Low NP: 28:7, High NP: 16:3	Low NP: 13.1 (± 9.7), High NP: 12 (± 9.7)	24	34.4 (± 8.6)	19:5		

(*continued on next page*)

Table 5 (*continued*)

Study	Patients (n)	Mean age (SD)	M:F SCI	TSI (years)	HC (n)	Mean age (SD)	M:F HC	Task	Outcome
								MR spectroscopy was used to examine the relationship between thalamic Glx/Ins levels in SCI with high and low NP with sensory function below injury level.	Lower thalamic Glx/Ins and Naa/Ins ratios were found in the high NP group compared to those with low NP and controls. Glx/Ins ratios negatively correlated with momentary pain intensive and average pain levels.
Gustin et al. (2014)	22	54 (± 14.1)	16:6		21	51 (± 9.2)	13:8	GABA levels were examined in the thalamus of SCI with and without NP, and in HC.	Reductions in Naa and GABA concentrations in the thalamus was found in patients with NP compared to those without and HC.
Widerstrom-Noga et al. (2013)	No NP: 18, Low NP: 31, High NP:19	No NP: 36.8 (± 11), Low NP: 37.5 (± 13.4), High NP: 40.4 (± 11.8)	No NP: 14:4, Low NP: 26:5, High NP: 14:5	No NP: 16.2 (± 9.5), Low NP: 10.6 (± 9.1), High NP: 12 (± 9.9)	24	34.4 (± 8.6)	19:5	Metabolite concentrations in the ACC as an indicator of neural and/or glial dysfunction were investigated in patients with high-, low- and no NP, as well as controls.	Increased concentrations of Ins, Cr, Cho and reduced levels of Naa/Ins and Glx/Ins ratios were found in the ACC of patients with high levels of NP compared to patients with low levels of NP. Glx/Ins ratios correlated with level of NP severity.
Stanwell et al. (2010)	Total: 10, w/ pain: 5, wo/ pain: 5	36.4 (± 10.4)		Total: 5.1 (± 4), w/ pain: 5.3 (± 4.1), wo/ pain: 4.9 (± 5)	10	27.4 (± 6.8)		Wavelet-based decomposition models were used to discriminate between SCI and HC, and SCI with and without pain based on biochemical concentrations from the thalamus, ACC and the PFC.	SCI and non-SCI subjects could be distinguished by metabolites in the thalamus with high specificity and accuracy. ACC and PFC measures could distinguish between SCI patients with and without pain with high accuracy.
Pattany et al. (2002)	Total: 16, w/ pain: 7, wo/ pain: 9	W/pain: 46.2 (± 16.2), wo/ pain: 34.8 (± 10)	16:0	W/ pain: 7.6 (± 6.3), wo/ pain: 11.3 (± 9.6)	10	42.3 (± 10.5)	10:0	Spectroscopy was used to assess the effects of SCI on thalamic metabolite concentrations.	Lower levels of thalamic Naa was observed in the SCI group with chronic pain compared to those without, and negatively correlated with pain intensity. Ins levels correlated positively with pain intensity measures.
Puri et al. (1998)	6	47.8 (± 11.7)	6:0	1.2 (± 0.6)	5	42 (± 6.6)	5:0	Metabolites in the motor cortex were examined in patients with SCI compared to healthy controls.	The hand representation area of the M1 showed increased Naa/Cr ratios in SCI compared to HC, and in comparison with the occipital cortex within the SCI group. Cho/Cr ratios were higher in the M1 compared to the occipital cortex, this was not found in SCI patients.
PET									
Yoon et al. (2014)	Active tDCS: 10	41.5 (± 8.5)	7:3	Active: 2.5 (± 3.1) / Sham: 2.1 (± 1.4)	Sham tDCS: 6	48.3 (± 7.6)	5:1	Anodal and sham tDCS was applied over the M1 for 20 treatments over 2 weeks to assess effects on NP. ^{18}FDG PET was conducted before and at the end of treatment.	Pain ratings decreased in the active stimulation group. Decreased metabolism was observed in the DLPFC, and reduced metabolism in the medulla in the active group compared with sham.
Yoon et al. (2013)	10	40.8 (± 5.7)	7:3	1.5 (± 0.5)	10	39.5 (± 8.6)	6:4	^{18}FDG PET compared metabolism in SCI patients with neuropathic pain to controls.	Hypometabolism was found in the mid. frontal gyrus, extending to the DLPFC in patients compared to controls. No areas showed hypermetabolism.
	7 para, 7 tetra				8	Median: 27	8:00		

(*continued on next page*)

Table 5 (*continued*)

Study	Patients (n)	Mean age (SD)	M:F SCI	TSI (years)	HC (n)	Mean age (SD)	M:F HC	Task	Outcome
Curt et al. (2002b)		Median - Para: 32, Tetra: 26	Para: 4:3; Tetra: 7:0	Median - Para: 2.9; Tetra: 4.7				$H_2{}^{11}O$ PET assessed activity in the brain of paraplegic, quadriplegic and controls during right hand wrist extension.	Increased activity of the SMC, thalamus, cerebellum and the superior parietal lobe was observed in paraplegics when compared to HC. Quadriplegics showed increased activity only in the SMA. Extent of disability in quadriplegics correlated with reduction of SMA and cerebellar activity.
Bruehlmeier et al. (1998)	7 para, 7 tetra	Para: 32, Tetra: 26	Para: 4:3; Tetra: 7:0	Par: 2.9; Tetra: 4.7		27	27:0	$H_2{}^{11}O$ PET assessed activity in the brain of paraplegic, tetraplegic and controls while moving a joystick with their right hand.	The task evoked activation in a part of the SMC that typically represents the leg area in paraplegic and tetraplecic patients. This spread of activation correlated with the amount of dysfunctional body parts.
Roelcke et al. (1997)	11 (7 para, 4 tetra)	31 (± 11)	9:2	4.6 (± 5.6)	12	34 (± 11)		Resting brain metabolism was examined with ^{18}FDG PET in a group consisting of both paraplegic and quadriplegic patients, compared to controls.	Global glucose metabolism was reduced in SCI compared to HC. Regional increases in metabolism were observed in the putamen, ACC, and the SMA in SCI compared to HC, while a decrease was found in the cerebellum, midbrain and temporal cortex.
Spect									
Ness et al. (1998)	1	40	0:1	16	N.A	N.A.	N.A.	Alteration in brain blood flow was examined in a patient's on and off periods in his reported pain cycles.	There was an increase in rCBF in the thalamus, ACC and S1, as well as a reduction in the caudate during the pain period compared to the pain free period.

ACC, Anterior Cingulate Cortex; ALFF, Amplitude of Low Frequency Fluctuations; BOLD, Blood Oxygen Level Dependent; Cho, Choline; Cr, Creatine; dACC, dorsal ACC; DLPFC, Dorsolateral Prefrontal Cortex; DTI, Diffusion Tensor Imaging; F, Female; FA, Fractional Anisotropy; FDG, ^{18}F-fluorodeoxyglucose; Glx, Glutamate-glutamine; HC, healthy control; M, Male; MD, Mean Diffusivity; N, number; N.A., Not Applicable; Naa, N-acetylaspartate; NP, Neuropathic Pain; Para, Paraplegic; PMC, Premotor Cortex; rCBF, regional Cerebral Blood Flow; ReHo, Regional Homogeneity; SCI, Spinal Cord Injury; SD, Standard Deviation; SMA, Supplementary Motor Area; SMC, Sensorimotor Cortex; tDCS, transcranial Direct Current Stimulation; Tetra, tetraplegic; TSI, Time Since Injury.

Widerstrom-Noga et al. investigated glutamate-glutamine/myo-inositol (Glx/Ins) ratios in the ACC anterior cingulate cortex in SCI patients with severe, moderate and no neuropathic pain as well as healthy controls (Widerstrom-Noga et al., 2013). Significantly higher levels of Ins, creatine (Cr), choline (Cho) and lower NAA/Ins and Glx/Ins ratios were observed in SCI patients with severe neuropathic pain compared to those with low neuropathic pain. Interestingly, the Glx/Ins ratio was found to be associated with the severity of neuropathic pain.

Glx/Ins ratios were also examined in the thalamus in SCI patients with high and low levels of neuropathic pain and its relation to somatosensory functioning of areas below injury level (Widerstrom-Noga et al., 2015). SCI patients with high levels of neuropathic pain compared to those with low levels and healthy controls had significantly lower thalamic Glx/Ins and NAA/Ins ratio. Glx/Ins ratios were found to negatively correlate with the subject's average and momentary pain intensity measures. The authors therefore suggest that the metabolite concentrations are associated with neuropathic pain, and not solely to the injury. Interestingly, it was also reported that the SCI group with high pain levels had greater sensory functioning than those with low pain levels, indicating a relationship between residual functioning after the injury and neuropathic pain levels.

Similar results were found in a study by Gustin et al. (Gustin et al., 2014), who reported reduced NAA and gamma amino butyric acid (GABA) levels in the thalamus in SCI patients with neuropathic pain compared to those without pain and healthy controls. Moreover, the NAA/Cr levels were positively correlated with the GABA/Cr ratio. In a previous study that also focused on thalamic metabolites in SCI with neuropathic pain, the researchers report significantly lower levels in NAA concentrations in SCI patients with neuropathic pain compared to those without (Pattany et al., 2002). However, a significant difference between healthy controls and patients without pain was not seen, whereas the difference between healthy controls and patients with neuropathic pain showed a numerical significant difference. Ins concentrations were different in patients with and without pain, but were not significant. NAA/Ins ratios were also found to be different between patients with and without neuropathic pain, but not different from controls. Moreover, the NAA concentration was inversely correlated, and Ins was positively correlated with pain intensity measurements.

One study investigated whether SCI subjects with and without neuropathic pain, and healthy controls could be differentiated based on brain chemistry in the thalamus, ACC and PFC (Stanwell et al., 2010). Using wavelet-based decomposition methods, spectroscopy measures in the thalamus could distinguish between SCI and non-SCI patients with high accuracy and specificity, whereas spectroscopy measures in the ACC and PFC could distinguish between neuropathic pain and non-neuropathic pain patients also with great accuracy.

Another study investigated metabolites in the motor cortex of SCI patients and controls (Puri et al., 1998). NAA/Cr ratios in the hand representation area of the motor cortex were increased in SCI patients compared to the occipital cortex, as well as in comparison to the motor cortex in healthy controls. The authors speculate that this is due to increased levels of NAA instead of decreased Cr levels, as NAA is typically found in neurons in both the developing and adult brain. This could therefore indicate adaptive processes at a microscopic level at work in the motor cortex following a SCI.

In sum, MRS studies provide evidence of altered brain chemistry linked to SCI in several brain regions. Changes in brain chemistry are in many studies reported to be linked with neuropathic pain following SCI as differences in metabolite concentrations are found in those with pain compared to those without pain (primarily in the thalamus) after the injury. As most MRS studies to date have been space constrained and only provided information of a select region, there are several unexplored paths to study in relation to SCI using MRS.

3.4.3. Single photon emission computed tomography studies in SCI

Single photon emission computed tomography (SPECT) has been used in clinical and research settings to examine blood flow in both brain and body organs. Including SPECT into the search term provided two articles, one of which was excluded, as it was a methods review paper. The relevant research article is an early investigation of SCI focusing on neuropathic pain in a single subject, performing imaging in the patients' on and off phases of his reported pain cycles. The authors reported higher rCBF in the ACC, bilateral thalamus and in the contralateral S1, and decreased blood flow in the bilateral caudate in the pain period compared with the subjects' pain free period, describing the relationship between pain and rCBF (Ness et al., 1998). No further studies using SPECT were found.

4. Summary discussion

Both the present quantitative meta-analyses and several non-included studies indicate hyperactivation of motor cortical and subcortical regions during motor execution and motor imagery tasks in SCI. Disruption of descending corticospinal tract neurons appears to drive this hyperactivation but changes in cortico-cortical (feedback) inhibition mechanisms and lost sensory and proprioceptive input are likely also involved. As demonstrated by Freund et al. (Freund et al., 2011a), transcranial magnetic stimulation of the M1 leg area, — the same area that was hyperactive upon voluntary hand movement — did not result in upper limb muscle activation. Thus, the observed hyperactivation was not directly indicative of a reorganized motor cortex with upper limb functions now represented in former lower limb areas. Rather, observed hyperactivations in lower limb areas may be represent a lack of tight motor cortex regulation in denervated areas. In line with this, the observed hyperactivity seen in motor areas upon *imagining or attempting execution* of movement of denervated limbs may arise from both the lack-of-feedback regulation, but from also behavioral effects such as SCI individuals actively making reoccurring, but failing attempts to move a denervated limb.

Resting state studies indicate alterations in low-frequency fluctuations and functional connectivity in sensory and motor related regions, whereas regions with no direct relation to sensorimotor function are mostly spared.

Structural imaging studies indicate loss of cortical gray matter in somatosensory cortices, primarily in regions representing the lower trunk and limbs. There was no evidence for altered glucose metabolism in the somatosensory cortex in SCI.

A curious observation is the possible relation between gray matter loss on structural imaging, and elevated activation on functional imaging, i.e. less is more. The relationships between gray matter structure and functional activation have been explored in healthy subjects (Segall et al., 2012), and in ALS (Cosottini et al., 2012), but we are not aware of any studies directly relating gray matter loss in motor and somatosensory areas to motor and somatosensory hyperactivation in SCI.

Diffusion weighted imaging studies typically identify alterations in fractional anisotropy in thalamocortical somatosensory radiations, but also in cerebellar and motor regions. Magnetic Resonance Spectroscopy studies have primarily focused on the thalamus and anterior cingulate, with consistent reductions in Naa levels, commonly linked to the severity of neuropathic pain after SCI. Unfortunately, only one publication on MRS investigating the motor cortex in SCI was found. Further studies including the motor and/or somatosensory cortex using MRS should be conducted, which could potentially shed light on the observations of somatosensory function, structure and diffusion.

Potential confounds and caveats specific to Spinal Cord Injury

Functional MRI is based on the Blood-Oxygenation Level Dependent (BOLD) signal, detecting relative levels of oxyhemoglobin and deoxyhemoglobin, which in turn are related to the relationship between local neural activity and subsequent changes in cerebral blood (neurovascular coupling). Insult to the brain or spinal cord typically results in astrocytioc gliosis and neuroinflammation, which may impact the normal neurovascular coupling (D'Esposito et al., 2003), and

consequentially may influence the BOLD signal. Cardiovascular and autonomic dysfunction is common after high-level spinal cord injury, and there is emerging evidence that changes in sympathetic vascular control can disrupt neurovascular coupling in SCI (Phillips et al., 2013). Thus, to attribute altered BOLD changes to altered neuronal function, further studies utilizing combinations of metabolic imaging (^{18}FDG PET), blood-flow imaging ($H_2{}^{15}O$ PET or Arterial Spin Labeling MRI), fMRI, EEG, Near Infrared Spectroscopy, or their combination, are needed to define this potentially crucial caveat.

In traumatic spinal cord injury, up to 60% of patients also have co-occurring mild to severe traumatic brain injury (Macciocchi et al., 2008), which may impact multiple brain metrics and thus needs to be taken into account.

Another consideration in SCI imaging is the presence of implanted pumps and stimulators, which are not MR safe, thereby limiting and biasing the available patient population. While current spine stabilization hardware is generally MR safe at 1.5 and 3T (but always verify!), implants can significantly impact MR signal, especially high-level hardware in diffusion and functional imaging sequences). Metal implants further cause attenuation of PET signal that may be difficult to quantify.

In our experience, not all SCI patients fit comfortably in scanners, due to difficulties in transferring, the relatively tight bore of the camera, and long imaging time on a flat, hard scan bed. While patients often are more than willing to endure some discomfort for an experiment, spasticity and being uncomfortable typically induces subject motion and thus abnormal/additional fMRI signals related to increased stress or pain. Future studies will benefit from incorporating prospective and retrospective motion correction methods (Tisdall et al., 2016).

Finally, when comparing SCI subjects to healthy individuals, task difficulty and performance may impact results; for example, it is not evident that the process of “imagining you are wiggling your toes” is the same in paralyzed individuals, and resulting brain activations may differ accordingly, see Lotze and Halsband, (2006) for a thoughtful review of motor imagery. In this context, and for data sharing efforts, resting state fMRI approaches may be preferential.

5. Conclusions and future directions

Taken together, neuroimaging has provided ample evidence that SCI has profound effects also on underlying brain structure, suggesting adaptive and/or maladaptive plasticity following injury, primarily affecting the thalamocortical and somatosensory/motor regions. There is some evidence of alterations in prefrontal cortices and subcortical anatomical structures, possibly exacerbated by the magnitude of neuropathic pain. Such changes are likely a function of both the loss of somatosensory inflow and motor feedback, and the impact of (mal-) adaptive cortical reorganization, where longitudinal studies may allow to define the sequence of events (Freund et al., 2013).

For studies on cortical reorganization after SCI, a limitation of the Euclidian distance approach used in prior studies is that measures are taken without consideration of white matter boundaries and cortical folding, Thus, the metric is less physiologically relevant, an mapping the cortex as an (un)folded surface, rather than a volume, seem preferable going forward (Makin et al., 2015).

The predictive nature of brain alterations to therapeutic outcomes, and the possibility to track mechanisms of therapeutic success are promising avenues of study. But neuroimaging research is cost- and labor-intensive, typically resulting studies that are rather small. Studies of 12–20 patients, what appears to be a de-facto standard, may be underpowered (Button et al., 2013). The situation is exacerbated in SCI studies, where recruitment is often more challenging and there is large variability with regards to injury location and completeness, time since injury, medical history, secondary symptoms, medication and MR compatibility of surgical implants. That said, this meta-analysis and review still found consistent statistical evidence of altered motor responses, and, while not quantifiable, consistent reports of alterations in somatosensory brain structure, cortical reorganization, diffusion and thalamic metabolite alterations.

Neuroimaging hardware and software solutions are developing rapidly, allowing the community to pose new and exciting questions, thereby perhaps missing the less rewarding work of replicating prior work. Accordingly, neuroimaging in general, and SCI brain imaging in particular, contains incomplete, inconsistent and sometimes contradicting results. The neuroimaging community response to these challenges has been to begin synchronizing protocols and sharing data more openly (Poldrack and Gorgolewski, 2014). Such efforts are ongoing in the pre-clinical SCI community (Callahan et al., 2017). In clinical studies, pioneered by dementia- and psychiatric-neuroimaging groups, there are now very large data depositories with phenotypic, genotypic and multi-modal neuroimaging data, made freely available to other researchers after rigorous de-identification. Further, several largescale ($>$ 1000 subjects) datasets of healthy subjects (behavior, MRI and genetics) are available to the scientific community. Future SCI studies would benefit from employing matching hardware and scan sequences, allowing for comparisons to normative data. While new SCI imaging studies may want to focus on more specific hypotheses, or on more refined imaging technologies, going forward, the SCI community would benefit tremendously by also adopting an open-data approach and harmonizing data collection methods and analytical approaches with these larger neuroimaging efforts. With sensitive and specific imaging biomarkers, clinical trials can be replicable neuroimaging findings can provide a basis to improve the sensitivity of clinical trials (Huber et al., 2015).

Funding

This study was supported by the Promobilia Foundation, Wings for Life, The Ellen R and Melvin J Gordon foundation/Spaulding hospital and by the Department of Defense (DOD) Office of Congressionally Directed Medical Research Programs (CDMRP) SC140194.

Conflicts of interests

The authors declare no competing interest.

References

Alkadhi, H., Brugger, P., Boendermaker, S.H., Crelier, G., Curt, A., Hepp-Reymond, M.-C.C., Kollias, S.S., 2005. What disconnection tells about motor imagery: evidence from paraplegic patients. TL-15. Cereb. Cortex 15, 131–140. http://dx.doi.org/10.1093/cercor/bhh116.

Allison, D.J., Ditor, D.S., 2015. Immune dysfunction and chronic inflammation following spinal cord injury. Spinal Cord 53, 14–18. http://dx.doi.org/10.1038/sc.2014.184.

Anderson, W.S., Lenz, F.A., 2011. Review of motor and phantom-related imagery. Neuroreport 22, 939–942. http://dx.doi.org/10.1097/WNR.0b013e32834ca58d.

Ashburner, J., Friston, K.J., 2000. Voxel-based morphometry—the methods. Neuroimage 11, 805–821. http://dx.doi.org/10.1006/nimg.2000.0582.

Ashburner, J., Ridgway, G.R., 2012. Symmetric diffeomorphic modeling of longitudinal structural MRI. Front. Neurosci. 6, 197. http://dx.doi.org/10.3389/fnins.2012.00197.

Avluk, O.C., Gurcay, E., Gurcay, A.G., Karaahmet, O.Z., Tamkan, U., Cakci, A., 2014. Effects of chronic pain on function, depression, and sleep among patients with traumatic spinal cord injury. Ann. Saudi Med. 34, 211–216. http://dx.doi.org/10.5144/0256-4947.2014.211.

Biswal, B.B., Van Kylen, J., Hyde, J.S., 1997. Simultaneous assessment of flow and BOLD signals in resting-state functional connectivity maps. NMR Biomed. 10, 165–170.

Bruehlmeier, M., Dietz, V., Leenders, K.L., Roelcke, U., Missimer, J., Curt, A., 1998. How does the human brain deal with a spinal cord injury? Eur. J. Neurosci. 10, 3918–3922.

Bryce, T.N., Biering-Sørensen, F., Finnerup, N.B., Cardenas, D.D., Defrin, R., Lundeberg, T., Norrbrink, C., Richards, J.S., Siddall, P., Stripling, T., Treede, R.-D.D., Waxman, S.G., Widerström-Noga, E., Yezierski, R.P., Dijkers, M., 2012. International spinal cord injury pain classification: part I. Background and description. Spinal Cord 50, 413–417. http://dx.doi.org/10.1038/sc.2011.156.

Button, K.S., Ioannidis, J.P.A., Mokrysz, C., Nosek, B.A., Flint, J., Robinson, E.S.J., Munafo, M.R., 2013. Power failure: why small sample size undermines the reliability

of neuroscience. Nat. Rev. Neurosci. http://dx.doi.org/10.1038/nrn3475.
Callahan, A., Anderson, K.D., Beattie, M.S., Bixby, J.L., Ferguson, A.R., Fouad, K., Jakeman, L.B., Nielson, J.L., Popovich, P.G., Schwab, J.M., Lemmon, V.P., 2017. Developing a data sharing community for spinal cord injury research. Exp. Neurol. 295, 135–143. http://dx.doi.org/10.1016/j.expneurol.2017.05.012.
Chen, D., Apple, D.F., Hudson, L.M., Bode, R., 1999. Medical complications during acute rehabilitation following spinal cord injury—current experience of the model systems. Arch. Phys. Med. Rehabil. 80, 1397–1401.
Christensen, M.S., Lundbye-Jensen, J., Geertsen, S.S., Petersen, T.H., Paulson, O.B., Nielsen, J.B., 2007. Premotor cortex modulates somatosensory cortex during voluntary movements without proprioceptive feedback. Nat. Neurosci. 10, 417–419. http://dx.doi.org/10.1038/nn1873.
Cobo Cuenca, A.I., Sampietro-Crespo, A., Virseda-Chamorro, M., Martín-Espinosa, N., 2015. Psychological impact and sexual dysfunction in men with and without spinal cord injury. J. Sex. Med. 12, 436–444. http://dx.doi.org/10.1111/jsm.12741.
Cohen, M.S., DuBois, R.M., 1999. Stability, repeatability, and the expression of signal magnitude in functional magnetic resonance imaging. J. Magn. Reson. Imaging 10, 33–40.
Cosottini, M., Pesaresi, I., Piazza, S., Diciotti, S., Cecchi, P., Fabbri, S., Carlesi, C., Mascalchi, M., Siciliano, G., 2012. Structural and functional evaluation of cortical motor areas in amyotrophic lateral sclerosis. Exp. Neurol. 234, 169–180. http://dx.doi.org/10.1016/j.expneurol.2011.12.024.
Cramer, S.C., Lastra, L., Lacourse, M.G., Cohen, M.J., 2005. Brain motor system function after chronic, complete spinal cord injury. Brain 128, 2941–2950. http://dx.doi.org/10.1093/brain/awh648.
Cramp, J.D., Courtois, F.J.J., Ditor, D.S., 2015. Sexuality for women with spinal cord injury. J. Sex. Marital Ther. 41, 238–253. http://dx.doi.org/10.1080/0092623X.2013.869777.
Crawley, A.P., Jurkiewicz, M.T., Yim, A., Heyn, S., Verrier, M.C., Fehlings, M.G., Mikulis, D.J., 2004. Absence of localized grey matter volume changes in the motor cortex following spinal cord injury. Brain Res. 1028, 19–25. http://dx.doi.org/10.1016/j.brainres.2004.08.060.
Curt, A., Alkadhi, H., Crelier, G.R.R., Boendermaker, S.H., Hepp-Reymond, M.-C.C., Kollias, S.S., 2002a. Changes of non-affected upper limb cortical representation in paraplegic patients as assessed by fMRI. Brain 125, 2567–2578 VN-r.
Curt, A., Bruehlmeier, M., Leenders, K.L., Roelcke, U., Dietz, V., 2002b. Differential effect of spinal cord injury and functional impairment on human brain activation. J. Neurotrauma 19, 43–51. http://dx.doi.org/10.1089/089771502753460222.
D'Esposito, M., Deouell, L.Y., Gazzaley, A., 2003. Alterations in the BOLD fMRI signal with ageing and disease: a challenge for neuroimaging. Nat. Rev. Neurosci. 4, 863–872. http://dx.doi.org/10.1038/nrn1246.
Dale, A.M., Fischl, B., Sereno, M.I., 1999. Cortical surface-based analysis. I. Segmentation and surface reconstruction. Neuroimage 9, 179–194. http://dx.doi.org/10.1006/nimg.1998.0395.
Davidoff, G., Morris, J., Roth, E., Bleiberg, J., 1985. Cognitive dysfunction and mild closed head injury in traumatic spinal cord injury. Arch. Phys. Med. Rehabil. 66, 489–491.
Davidoff, G.N., Roth, E.J., Richards, J.S., 1992. Cognitive deficits in spinal cord injury: epidemiology and outcome. Arch. Phys. Med. Rehabil. 73, 275–284.
Davies, A.L., Hayes, K.C., Dekaban, G.A., 2007. Clinical correlates of elevated serum concentrations of cytokines and autoantibodies in patients with spinal cord injury. Arch. Phys. Med. Rehabil. 88, 1384–1393. http://dx.doi.org/10.1016/j.apmr.2007.08.004.
Desmurget, M., Reilly, K.T., Richard, N., Szathmari, A., Mottolese, C., Sirigu, A., 2009. Movement intention after parietal cortex stimulation in humans. Science 324 (80), 811–813. http://dx.doi.org/10.1126/science.1169896.
Desmurget, M., Sirigu, A., 2012. Conscious motor intention emerges in the inferior parietal lobule. Curr. Opin. Neurobiol. 22, 1004–1011. http://dx.doi.org/10.1016/j.conb.2012.06.006.
DeVivo, M.J., Fine, P.R., Maetz, H.M., Stover, S.L., 1980. Prevalence of spinal cord injury: a reestimation employing life table techniques. Arch. Neurol. 37, 707–708.
Dowler, R.N., Harrington, D.L., Haaland, K.Y., Swanda, R.M., Fee, F., Fiedler, K., 1997. Profiles of cognitive functioning in chronic spinal cord injury and the role of moderating variables. J. Int. Neuropsychol. Soc. 3, 464–472.
Eick, J., Richardson, E.J., 2015. Cortical activation during visual illusory walking in persons with spinal cord injury: a pilot study. TL - 96. Arch. Phys. Med. Rehabil. 750–753. http://dx.doi.org/10.1016/j.apmr.2014.10.020. 96VN-readcube.com.
Endo, T., Tominaga, T., Olson, L., 2009. Cortical changes following spinal cord injury with emphasis on the nogo signaling system. Neuroscientist 15, 291–299. http://dx.doi.org/10.1177/1073858408329508.
Ferrero, G., Mijno, E., Actis, M.V., Zampa, A., Ratto, N., Arpaia, A., Massè, A., 2015. Risk factors for shoulder pain in patients with spinal cord injury: a multicenter study. Musculoskelet. Surg. 99 (Suppl. (1)), 6. http://dx.doi.org/10.1007/s12306-015-0363-2.
Freund, P., Rothwell, J., Craggs, M., Thompson, A.J., Bestmann, S., 2011a. Corticomotor representation to a human forearm muscle changes following cervical spinal cord injury. Eur. J. Neurosci. 34, 1839–1846. http://dx.doi.org/10.1111/j.1460-9568.2011.07895.x.
Freund, P., Schneider, T., Nagy, Z., Hutton, C., Weiskopf, N., Friston, K., Wheeler-Kingshott, C., Thompson, A.J., 2012. Degeneration of the injured cervical cord is associated with remote changes in corticospinal tract integrity and upper limb impairment. PloS One 7, e51729. http://dx.doi.org/10.1371/journal.pone.0051729.
Freund, P., Weiskopf, N., Ashburner, J., Wolf, K., Sutter, R., Altmann, D.R., Friston, K., Thompson, A., Curt, A., 2013. MRI investigation of the sensorimotor cortex and the corticospinal tract after acute spinal cord injury: a prospective longitudinal study. Lancet. Neurol. 12, 873–881. http://dx.doi.org/10.1016/S1474-4422(13)70146-7.
Freund, P., Weiskopf, N., Ward, N.S., Hutton, C., Gall, A., Ciccarelli, O., Craggs, M., Friston, K., Thompson, A.J., 2011b. Disability, atrophy and cortical reorganization following spinal cord injury. TL-134. Brain 134, 1610–1622. http://dx.doi.org/10.1093/brain/awr093.
Garshick, E., Kelley, A., Cohen, S.A., Garrison, A., Tun, C.G., Gagnon, D., Brown, R., 2005. A prospective assessment of mortality in chronic spinal cord injury. Spinal Cord 43, 408–416. http://dx.doi.org/10.1038/sj.sc.3101729.
Grabher, P., Blaiotta, C., Ashburner, J., Freund, P., 2017. Relationship between brainstem neurodegeneration and clinical impairment in traumatic spinal cord injury. NeuroImage Clin. 15, 494–501. http://dx.doi.org/10.1016/j.nicl.2017.05.026.
Grabher, P., Callaghan, M.F., Ashburner, J., Weiskopf, N., Thompson, A.J., Curt, A., Freund, P., 2015. Tracking sensory system atrophy and outcome prediction in spinal cord injury. Ann. Neurol. 78, 751–761. http://dx.doi.org/10.1002/ana.24508.
Gustin, S.M., Wrigley, P.J., Siddall, P.J., Henderson, L.A., 2010. Brain anatomy changes associated with persistent neuropathic pain following spinal cord injury. Cereb. Cortex 20, 1409–1419. http://dx.doi.org/10.1093/cercor/bhp205.
Gustin, S.M., Wrigley, P.J., Youssef, A.M., McIndoe, L., Wilcox, S.L., Rae, C.D., Edden, R.A.E., Siddall, P.J., Henderson, L.A., 2014. Thalamic activity and biochemical changes in individuals with neuropathic pain after spinal cord injury. Pain 155, 1027–1036. http://dx.doi.org/10.1016/j.pain.2014.02.008.
Henderson, L.A., Gustin, S.M., Macey, P.M., Wrigley, P.J., Siddall, P.J., 2011. Functional reorganization of the brain in humans following spinal cord injury: evidence for underlying changes in cortical anatomy. J. Neurosci. 31, 2630–2637. http://dx.doi.org/10.1523/JNEUROSCI.2717-10.2011.
Hotz-Boendermaker, S., Hepp-Reymond, M.-C., Curt, A., Kollias, S.S., 2011. Movement observation activates lower limb motor networks in chronic complete paraplegia. Neurorehabil. Neural Repair 25, 469–476. http://dx.doi.org/10.1177/1545968310389184.
Hou, J.-M.M., Sun, T.-S.S., Xiang, Z.-M.M., Zhang, J.-Z.Z., Zhang, Z.-C.C., Zhao, M., Zhong, J.-F.F., Liu, J., Zhang, H., Liu, H.-L.L., Yan, R.-B.B., Li, H.-T.T., 2014. Alterations of resting-state regional and network-level neural function after acute spinal cord injury. Neuroscience 277, 446–454. http://dx.doi.org/10.1016/j.neuroscience.2014.07.045.
Hou, J., Xiang, Z., Yan, R., Zhao, M., Wu, Y., Zhong, J., Guo, L., Li, H., Wang, J., Wu, J., Sun, T., Liu, H., 2016. Motor recovery at 6 months after admission is related to structural and functional reorganization of the spine and brain in patients with spinal cord injury. Hum. Brain Mapp. 37, 2195–2209. http://dx.doi.org/10.1002/hbm.23163.
Hou, S., Rabchevsky, A.G., 2014. Autonomic consequences of spinal cord injury. Compr. Physiol. 4, 1419–1453. http://dx.doi.org/10.1002/cphy.c130045.
Huber, E., Curt, A., Freund, P., 2015. Tracking trauma-induced structural and functional changes above the level of spinal cord injury. Curr. Opin. Neurol. 28, 365–372. http://dx.doi.org/10.1097/WCO.0000000000000224.
Huber, E., Lachappelle, P., Sutter, R., Curt, A., Freund, P., 2017. Are midsagittal tissue bridges predictive of outcome after cervical spinal cord injury? Ann. Neurol. 81, 740–748. http://dx.doi.org/10.1002/ana.24932.
Jain, N.B., Ayers, G.D., Peterson, E.N., Harris, M.B., Morse, L., O'Connor, K.C., Garshick, E., 2015. Traumatic spinal cord injury in the United States, 1993–2012. JAMA 313, 2236–2243. http://dx.doi.org/10.1001/jama.2015.6250.
Jurkiewicz, M.T., Mikulis, D.J., Fehlings, M.G., Verrier, M.C., 2010. Sensorimotor cortical activation in patients with cervical spinal cord injury with persisting paralysis. Neurorehabil. Neural Repair 24, 136–140. http://dx.doi.org/10.1177/1545968309347680.
Jurkiewicz, M.T., Mikulis, D.J., McIlroy, W.E., Fehlings, M.G., Verrier, M.C., 2007. Sensorimotor cortical plasticity during recovery following spinal cord injury: a longitudinal fMRI study. Neurorehabil. Neural Repair 21, 527–538. http://dx.doi.org/10.1177/1545968307301872.
Jutzeler, C.R., Freund, P., Huber, E., Curt, A., Kramer, J.L., 2015. Neuropathic pain and functional reorganization in the primary sensorimotor cortex after spinal cord injury. TL-16. J. Pain 1256–1267. http://dx.doi.org/10.1016/j.jpain.2015.08.008.
Jutzeler, C.R., Huber, E., Callaghan, M.F., Luechinger, R., Curt, A., Kramer, J.L.K., Freund, P., 2016. Association of pain and CNS structural changes after spinal cord injury. Sci. Rep. 6, 18534. http://dx.doi.org/10.1038/srep18534.
Kennedy, P., Rogers, B.A., 2000. Anxiety and depression after spinal cord injury: a longitudinal analysis. Arch. Phys. Med. Rehabil. 81, 932–937. http://dx.doi.org/10.1053/apmr.2000.5580.
Kessler, R.C., Berglund, P., Demler, O., Jin, R., Koretz, D., Merikangas, K.R., Rush, A.J., Walters, E.E., Wang, P.S., Replication, N.C.S., 2003. The epidemiology of major depressive disorder: results from the National Comorbidity Survey Replication (NCS-R). JAMA 289, 3095–3105. http://dx.doi.org/10.1001/jama.289.23.3095.
Koskinen, E.A., Hakulinen, U., Brander, A.E., Luoto, T.M., Ylinen, A., Ohman, J.E., 2014. Clinical correlates of cerebral diffusion tensor imaging findings in chronic traumatic spinal cord injury. TL-52. Spinal Cord 52, 202–208. http://dx.doi.org/10.1038/sc.2013.163. VN-r.
Lauterbur, P.C., 1989. Image formation by induced local interactions. Examples employing nuclear magnetic resonance. 1973. Clin. Orthop. Relat. Res. 3–6.
Le Bihan, D., Breton, E., Lallemand, D., Grenier, P., Cabanis, E., Laval-Jeantet, M., 1986. MR imaging of intravoxel incoherent motions: application to diffusion and perfusion in neurologic disorders. Radiology 161, 401–407. http://dx.doi.org/10.1148/radiology.161.2.3763909.
Lee, J.K., Oh, C.H., Kim, J.Y., Park, H.-C.C., Yoon, S.H., 2015. Brain activation evoked by sensory stimulation in patients with spinal cord injury: functional magnetic resonance imaging correlations with clinical features. TL-58. J. Korean Neurosurg. Soc. 58, 242–247. http://dx.doi.org/10.3340/jkns.2015.58.3.242.
Lemon, R.N., 2008. Descending pathways in motor control. Annu. Rev. Neurosci. 31, 195–218. http://dx.doi.org/10.1146/annurev.neuro.31.060407.125547.

Logothetis, N.K., 2003. The underpinnings of the BOLD functional magnetic resonance imaging signal. J. Neurosci. 23, 3963–3971.
Lotze, M., Flor, H., Grodd, W., Larbig, W., Birbaumer, N., 2001. Phantom movements and pain. An fMRI study in upper limb amputees. Brain 124, 2268–2277.
Lotze, M., Halsband, U., 2006. Motor imagery. J. Physiol. Paris 99, 386–395. http://dx.doi.org/10.1016/j.jphysparis.2006.03.012.
Lundell, H., Christensen, M.S., Barthélemy, D., Willerslev-Olsen, M., Biering-Sørensen, F., Nielsen, J.B., 2011. Cerebral activation is correlated to regional atrophy of the spinal cord and functional motor disability in spinal cord injured individuals. Neuroimage 54, 1254–1261. http://dx.doi.org/10.1016/j.neuroimage.2010.09.009.
Macciocchi, S., Seel, R.T., Thompson, N., Byams, R., Bowman, B., 2008. Spinal cord injury and co-occurring traumatic brain injury: assessment and incidence. Arch. Phys. Med. Rehabil. 89, 1350–1357. http://dx.doi.org/10.1016/j.apmr.2007.11.055.
Makin, T.R., Scholz, J., Henderson Slater, D., Heidi, J.-B., Tracey, I., 2015. Reassessing cortical reorganization in the primary sensorimotor cortex following arm amputation. Brain 138, 2140–2146. http://dx.doi.org/10.1093/brain/awv161.
Mann, R., Schaefer, C., Sadosky, A., Bergstrom, F., Baik, R., Parsons, B., Nalamachu, S., Stacey, B.R., Tuchman, M., Anschel, A., Nieshoff, E.C., 2013. Burden of spinal cord injury-related neuropathic pain in the United States: retrospective chart review and cross-sectional survey. Spinal Cord 51, 564–570. http://dx.doi.org/10.1038/sc.2013.34.
Martin, A.R., Aleksanderek, I., Cohen-Adad, J., Tarmohamed, Z., Tetreault, L., Smith, N., Cadotte, D.W., Crawley, A., Ginsberg, H., Mikulis, D.J., Fehlings, M.G., 2016. Translating state-of-the-art spinal cord MRI techniques to clinical use: a systematic review of clinical studies utilizing DTI, MT, MWF, MRS, and fMRI. NeuroImage Clin. 10, 192–238. http://dx.doi.org/10.1016/j.nicl.2015.11.019.
Merlis, J.K., Watson, C.W., 1949. The electroencephalogram after injury to the spinal cord in man. Arch. Neurol. Psychiatry 61, 695–698.
Metman, L.V., Bellevich, J.S., Jones, S.M., Barber, M.D., Streletz, L.J., 1993. Topographic mapping of human motor cortex with transcranial magnetic stimulation: homunculus revisited. Brain Topogr. 6, 13–19.
Middleton, J., Tran, Y., Craig, A., 2007. Relationship between quality of life and self-efficacy in persons with spinal cord injuries. Arch. Phys. Med. Rehabil. 88, 1643–1648. http://dx.doi.org/10.1016/j.apmr.2007.09.001.
Migliorini, C., Tonge, B., Taleporos, G., 2008. Spinal cord injury and mental health. Aust. N. Z. J. Psychiatry 42, 309–314. http://dx.doi.org/10.1080/00048670801886080.
Mikulis, D.J., Jurkiewicz, M.T., McIlroy, W.E., Staines, W.R., Rickards, L., Kalsi-Ryan, S., Crawley, A.P., Fehlings, M.G., Verrier, M.C., 2002. Adaptation in the motor cortex following cervical spinal cord injury. Neurology 58, 794–801.
Min, Y.-S., Park, J.W., Jin, S.U., Jang, K.E., Nam, H.U., Lee, Y.-S., Jung, T.-D., Chang, Y., 2015a. Alteration of resting-state brain sensorimotor connectivity following spinal cord injury: a resting-state functional magnetic resonance imaging study. J. Neurotrauma 32, 1422–1427. http://dx.doi.org/10.1089/neu.2014.3661.
Min, Y.-S.S., Chang, Y., Park, J.W., Lee, J.-M.M., Cha, J., Yang, J.-J.J., Kim, C.-H.H., Hwang, J.-M.M., Yoo, J.-N.N., Jung, T.-D.D., 2015b. Change of brain functional connectivity in patients with spinal cord injury: graph theory based approach. Ann. Rehabil. Med. 39, 374–383. http://dx.doi.org/10.5535/arm.2015.39.3.374.
Mole, T.B., MacIver, K., Sluming, V., Ridgway, G.R., Nurmikko, T.J., 2014. Specific brain morphometric changes in spinal cord injury with and without neuropathic pain. NeuroImage Clin. 5, 28–35. http://dx.doi.org/10.1016/j.nicl.2014.05.014.
Moore, C.I., Stern, C.E., Dunbar, C., Kostyk, S.K., Gehi, A., Corkin, S., 2000. Referred phantom sensations and cortical reorganization after spinal cord injury in humans. Proc. Natl. Acad. Sci. U. S. A. 97, 14703–14708. http://dx.doi.org/10.1073/pnas.250348997.
Nardone, R., Höller, Y., Brigo, F., Seidl, M., Christova, M., Bergmann, J., Golaszewski, S., Trinka, E., 2013. Functional brain reorganization after spinal cord injury: systematic review of animal and human studies. Brain Res. 1504, 58–73. http://dx.doi.org/10.1016/j.brainres.2012.12.034.
Neefkes-Zonneveld, C.R., Bakkum, A.J., Bishop, N.C., van Tulder, M.W., Janssen, T.W., 2015. Effect of long-term physical activity and acute exercise on markers of systemic inflammation in persons with chronic spinal cord injury: a systematic review. Arch. Phys. Med. Rehabil. 96, 30–42. http://dx.doi.org/10.1016/j.apmr.2014.07.006.
Ness, T.J., San Pedro, E.C., Richards, J.S., Kezar, L., Liu, H.G., Mountz, J.M., 1998. A case of spinal cord injury-related pain with baseline rCBF brain SPECT imaging and beneficial response to gabapentin. Pain 78, 139–143.
Ogawa, S., Lee, T.M., Nayak, A.S., Glynn, P., 1990. Oxygenation-sensitive contrast in magnetic resonance image of rodent brain at high magnetic fields. Magn. Reson. Med. 14, 68–78.
Ohn, S.H., Kim, D.Y., Shin, J.C., Kim, S.M., Yoo, W.-K.K., Lee, S.-K.K., Park, C.-H.H., Jung, K.-I.I., Jang, K.U., Seo, C.H., Koh, S.H., Jung, B., 2013. Analysis of high-voltage electrical spinal cord injury using diffusion tensor imaging. J. Neurol. 260, 2876–2883. http://dx.doi.org/10.1007/s00415-013-7081-1.
Otis, C., Marchand, A., Courtois, F., 2012. Risk factors for posttraumatic stress disorder in persons with spinal cord injury. Top. Spinal Cord Inj. Rehabil. 18, 253–263. http://dx.doi.org/10.1310/sci1803-253.
Oyinbo, C.A., 2011. Secondary injury mechanisms in traumatic spinal cord injury: a nugget of this multiply cascade. Acta Neurobiol. Exp. (Wars) 71, 281–299.
Pattany, P.M., Yezierski, R.P., Widerstrom-Noga, E.G., Bowen, B.C., Martinez-Arizala, A., Garcia, B.R., Quencer, R.M., 2002. Proton magnetic resonance spectroscopy of the thalamus in patients with chronic neuropathic pain after spinal cord injury. AJNR Am. J. Neuroradiol. 23, 901–905.
Penfield, W., Boldrey, E., 1937. Somatic motor and sensory representation in the cerebral cortex of man as studied by electrical stimulation. Brain 60, 389–443. http://dx.doi.org/10.1093/brain/60.4.389.
Petersen, J.A., Wilm, B.J., von Meyenburg, J., Schubert, M., Seifert, B., Najafi, Y., Dietz, V., Kollias, S., 2012. Chronic cervical spinal cord injury: DTI correlates with clinical and electrophysiological measures. J. Neurotrauma 29, 1556–1566. http://dx.doi.org/10.1089/neu.2011.2027.
Phillips, A.A., Ainslie, P.N., Krassioukov, A.V., Warburton, D.E.R., 2013. Regulation of cerebral blood flow after spinal cord injury. J. Neurotrauma 30, 1551–1563. http://dx.doi.org/10.1089/neu.2013.2972.
Poldrack, R.A., Gorgolewski, K.J., 2014. Making big data open: data sharing in neuroimaging. Nat. Neurosci. 17, 1510–1517. http://dx.doi.org/10.1038/nn.3818.
Purcell, E.M., Torrey, H.C., Pound, R.V., 1946. Resonance absorption by nuclear magnetic moments in a solid. Phys. Rev. 69, 37–38.
Puri, B.K., Smith, H.C., Cox, I.J., Sargentoni, J., Savic, G., Maskill, D.W., Frankel, H.L., Ellaway, P.H., Davey, N.J., 1998. The human motor cortex after incomplete spinal cord injury: an investigation using proton magnetic resonance spectroscopy. J. Neurol. Neurosurg. Psychiatry 65, 748–754.
Radua, J., Mataix-Cols, D., Phillips, M.L., El-Hage, W., Kronhaus, D.M., Cardoner, N., Surguladze, S., 2012. A new meta-analytic method for neuroimaging studies that combines reported peak coordinates and statistical parametric maps. Eur. Psychiatry 27, 605–611. http://dx.doi.org/10.1016/j.eurpsy.2011.04.001.
Raffin, E., Richard, N., Giraux, P., Reilly, K.T., 2016. Primary motor cortex changes after amputation correlate with phantom limb pain and the ability to move the phantom limb. Neuroimage 130, 134–144. http://dx.doi.org/10.1016/j.neuroimage.2016.01.063.
Reddy, H., Bendahan, D., Lee, M.A., Johansen-Berg, H., Donaghy, M., Hilton-Jones, D., Matthews, P.M., 2002. An expanded cortical representation for hand movement after peripheral motor denervation. J. Neurol. Neurosurg. Psychiatry 72, 203–210.
Reuter, M., Schmansky, N.J., Rosas, H.D., Fischl, B., 2012. Within-subject template estimation for unbiased longitudinal image analysis. Neuroimage 61, 1402–1418. http://dx.doi.org/10.1016/j.neuroimage.2012.02.084.
Roelcke, U., Curt, A., Otte, A., Missimer, J., Maguire, R.P., Dietz, V., Leenders, K.L., 1997. Influence of spinal cord injury on cerebral sensorimotor systems: a PET study. J. Neurol. Neurosurg. Psychiatry 62, 61–65.
Sabbah, P., De, S.S., Leveque, C., Gay, S., Pfefer, F., Nioche, C., Sarrazin, J.L., Barouti, H., Tadie, M., Cordoliani, Y.S., 2002. Sensorimotor cortical activity in patients with complete spinal cord injury: a functional magnetic resonance imaging study. TL-19. J. Neurotrauma 19, 53–60. http://dx.doi.org/10.1089/089771502753460231.
Sabbah, P., Lévêque, C., Pfefer, F., Nioche, C., Gay, S., Sarrazin, J.L., Barouti, H., Tadie, M., Cordoliani, Y.S., 2000. Functional MR imaging and traumatic paraplegia: preliminary report. J. Neuroradiol. 27, 233–237.
Sabre, L., Tomberg, T., Korv, J., Kepler, J., Kepler, K., Linnamagi, U., Asser, T., 2016. Brain activation in the chronic phase of traumatic spinal cord injury. Spinal Cord 54, 65–68. http://dx.doi.org/10.1038/sc.2015.158.
Sabre, L., Tomberg, T., Korv, J., Kepler, J., Kepler, K., Linnamagi, U., Asser, T., 2013. Brain activation in the acute phase of traumatic spinal cord injury. Spinal Cord 51, 623–629. http://dx.doi.org/10.1038/sc.2013.41.
Schönenberg, M., Reimitz, M., Jusyte, A., Maier, D., Badke, A., Hautzinger, M., 2014. Depression, posttraumatic stress, and risk factors following spinal cord injury. Int. J. Behav. Med. 21, 169–176. http://dx.doi.org/10.1007/s12529-012-9284-8.
Segall, J.M., Allen, E.A., Jung, R.E., Erhardt, E.B., Arja, S.K., Kiehl, K., Calhoun, V.D., 2012. Correspondence between structure and function in the human brain at rest. Front. Neuroinf. 6, 10. http://dx.doi.org/10.3389/fninf.2012.00010.
Shen, D., Cui, L., Cui, B., Fang, J., Li, D., Ma, J., 2015. A systematic review and meta-analysis of the functional MRI investigation of motor neuron disease. Front. Neurol. 6, 246. http://dx.doi.org/10.3389/fneur.2015.00246.
Siddall, P.J., McClelland, J.M., Rutkowski, S.B., Cousins, M.J., 2003. A longitudinal study of the prevalence and characteristics of pain in the first 5 years following spinal cord injury. Pain 103, 249–257.
Singh, A., Tetreault, L., Kalsi-Ryan, S., Nouri, A., Fehlings, M.G., 2014. Global prevalence and incidence of traumatic spinal cord injury. Clin. Epidemiol. 6, 309–331. http://dx.doi.org/10.2147/CLEP.S68889.
Spinal Cord Injury Facts and Figures at a Glance, 2013. J. Spinal Cord Med. 36, 1–2. http://dx.doi.org/10.1179/1079026813Z.000000000136.
Stanwell, P., Siddall, P., Keshava, N., Cocuzzo, D., Ramadan, S., Lin, A., Herbert, D., Craig, A., Tran, Y., Middleton, J., Gautam, S., Cousins, M., Mountford, C., 2010. Neuro magnetic resonance spectroscopy using wavelet decomposition and statistical testing identifies biochemical changes in people with spinal cord injury and pain. Neuroimage 53, 544–552. http://dx.doi.org/10.1016/j.neuroimage.2010.06.051.
Stiens, S.A., Bergman, S.B., Goetz, L.L., 1997. Neurogenic bowel dysfunction after spinal cord injury: clinical evaluation and rehabilitative management. Arch. Phys. Med. Rehabil. 78, 102.
Strauss, D.J., Devivo, M.J., Paculdo, D.R., Shavelle, R.M., 2006. Trends in life expectancy after spinal cord injury. Arch. Phys. Med. Rehabil. 87, 1079–1085. http://dx.doi.org/10.1016/j.apmr.2006.04.022.
Stroman, P.W., Wheeler-Kingshott, C., Bacon, M., Schwab, J.M., Bosma, R., Brooks, J., Cadotte, D., Carlstedt, T., Ciccarelli, O., Cohen-Adad, J., Curt, A., Evangelou, N., Fehlings, M.G., Filippi, M., Kelley, B.J., Kollias, S., Mackay, A., Porro, C.A., Smith, S., Strittmatter, S.M., Summers, P., Tracey, I., 2014. The current state-of-the-art of spinal cord imaging: methods. Neuroimage 84, 1070–1081. http://dx.doi.org/10.1016/j.neuroimage.2013.04.124.
Tal, Z., Geva, R., Amedi, A., 2017. Positive and negative somatotopic BOLD responses in contralateral versus ipsilateral penfield homunculus. Cereb. Cortex 27, 962–980. http://dx.doi.org/10.1093/cercor/bhx024.
Tisdall, M.D., Reuter, M., Qureshi, A., Buckner, R.L., Fischl, B., van der Kouwe, A.J.W., 2016. Prospective motion correction with volumetric navigators (vNavs) reduces the bias and variance in brain morphometry induced by subject motion. Neuroimage 127, 11–22. http://dx.doi.org/10.1016/j.neuroimage.2015.11.054.
Tran, J., Dorstyn, D.S., Burke, A.L., 2016. Psychosocial aspects of spinal cord injury pain: a meta-analysis. Spinal Cord 54, 640–648. http://dx.doi.org/10.1038/sc.2016.66.

Troy, K.L., Morse, L.R., 2015. Measurement of bone: diagnosis of sci-induced osteoporosis and fracture risk prediction. Top. Spinal Cord Inj. Rehabil. 21, 267–274. http://dx.doi.org/10.1310/sci2104-267.

Turner, J.A., Cardenas, D.D., Warms, C.A., McClellan, C.B., 2001a. Chronic pain associated with spinal cord injuries: a community survey. Arch. Phys. Med. Rehabil. 82, 501–509. http://dx.doi.org/10.1053/apmr.2001.21855.

Turner, J.A., Lee, J.S., Martinez, O., Medlin, A.L., Schandler, S.L., Cohen, M.J., 2001b. Somatotopy of the motor cortex after long-term spinal cord injury or amputation. IEEE Trans. Neural Syst. Rehabil. Eng. 9, 154–160. http://dx.doi.org/10.1109/7333.928575.

Turner, J.A., Lee, J.S., Schandler, S.L., Cohen, M.J., 2003. An fMRI investigation of hand representation in paraplegic humans. Neurorehabil. Neural Repair 17, 37–47. http://dx.doi.org/10.1177/0888439002250443.

Van Dijk, K.R., Hedden, T., Venkataraman, A., Evans, K.C., Lazar, S.W., Buckner, R.L., 2010. Intrinsic functional connectivity as a tool for human connectomics: theory, properties, and optimization. J. Neurophysiol. 103, 297–321. http://dx.doi.org/10.1152/jn.00783.2009.

Vedantam, A., Eckardt, G., Wang, M.C., Schmit, B.D., Kurpad, S.N., 2014. High cervical fractional anisotropy as an imaging marker for spinal cord injury. Neurosurgery 61, 167–170. http://dx.doi.org/10.1227/NEU.0000000000000413.

Virseda-Chamorro, M., Salinas-Casado, J., Lopez-Garcia-Moreno, A.M., Cobo-Cuenca, A.I., Esteban-Fuertes, M., 2013. Sexual dysfunction in men with spinal cord injury: a case-control study. Int. J. Impot. Res. 25, 133–137. http://dx.doi.org/10.1038/ijir.2013.1.

Wall, P.D., Egger, M.D., 1971. Formation of new connexions in adult rat brains after partial deafferentation. Nature 232, 542–545.

Wang, J.-C.C., Chan, R.-C.C., Tsai, Y.-A.A., Huang, W.-C.C., Cheng, H., Wu, H.-L.L., Huang, S.-F.F., 2015. The influence of shoulder pain on functional limitation, perceived health, and depressive mood in patients with traumatic paraplegia. J. Spinal Cord Med. 38, 587–592. http://dx.doi.org/10.1179/2045772314Y.0000000271.

Wecht, J.M., Bauman, W.A., 2013. Decentralized cardiovascular autonomic control and cognitive deficits in persons with spinal cord injury. J. Spinal Cord Med. 36, 74–81. http://dx.doi.org/10.1179/2045772312Y.0000000056.

Wheeler-Kingshott, C.A., Stroman, P.W., Schwab, J.M., Bacon, M., Bosma, R., Brooks, J., Cadotte, D.W., Carlstedt, T., Ciccarelli, O., Cohen-Adad, J., Curt, A., Evangelou, N., Fehlings, M.G., Filippi, M., Kelley, B.J., Kollias, S., Mackay, A., Porro, C.A., Smith, S., Strittmatter, S.M., Summers, P., Thompson, A.J., Tracey, I., 2014. The current state-of-the-art of spinal cord imaging: applications. Neuroimage 84, 1082–1093. http://dx.doi.org/10.1016/j.neuroimage.2013.07.014.

Widerstrom-Noga, E., Cruz-Almeida, Y., Felix, E.R., Pattany, P.M., 2015. Somatosensory phenotype is associated with thalamic metabolites and pain intensity after spinal cord injury. Pain 156, 166–174. http://dx.doi.org/10.1016/j.pain.0000000000000019.

Widerstrom-Noga, E., Pattany, P.M., Cruz-Almeida, Y., Felix, E.R., Perez, S., Cardenas, D.D., Martinez-Arizala, A., 2013. Metabolite concentrations in the anterior cingulate cortex predict high neuropathic pain impact after spinal cord injury. Pain 154, 204–212. http://dx.doi.org/10.1016/j.pain.2012.07.022.

Widerström-Noga, E.G., Felipe-Cuervo, E., Yezierski, R.P., 2001. Chronic pain after spinal injury: interference with sleep and daily activities. Arch. Phys. Med. Rehabil. 82, 1571–1577.

Williams, D.S., Detre, J.A., Leigh, J.S., Koretsky, A.P., 1992. Magnetic resonance imaging of perfusion using spin inversion of arterial water. Proc. Natl. Acad. Sci. U. S. A. 89, 212–216.

Williams, R., Murray, A., 2015. Prevalence of depression after spinal cord injury: a meta-analysis. Arch. Phys. Med. Rehabil. 96, 133–140. http://dx.doi.org/10.1016/j.apmr.2014.08.016.

Wolpert, D.M., Goodbody, S.J., Husain, M., 1998. Maintaining internal representations: the role of the human superior parietal lobe. Nat. Neurosci. 1, 529–533. http://dx.doi.org/10.1038/2245.

Wrigley, P.J., Gustin, S.M., Macey, P.M., Nash, P.G., Gandevia, S.C., Macefield, V.G., Siddall, P.J., Henderson, L.A., 2009a. Anatomical changes in human motor cortex and motor pathways following complete thoracic spinal cord injury. Cereb. Cortex 19, 224–232. http://dx.doi.org/10.1093/cercor/bhn072.

Wrigley, P.J., Press, S.R., Gustin, S.M., Macefield, V.G., Gandevia, S.C., Cousins, M.J., Middleton, J.W., Henderson, L.A., Siddall, P.J., 2009b. Neuropathic pain and primary somatosensory cortex reorganization following spinal cord injury. TL-141. Pain 141, 52–59. http://dx.doi.org/10.1016/j.pain.2008.10.007.

Wrigley, P.J., Siddall, P.J., Gustin, S.M., 2018. New evidence for preserved somatosensory pathways in complete spinal cord injury: a fMRI study. Hum. Brain Mapp. 39, 588–598. http://dx.doi.org/10.1002/hbm.23868.

Wu, J., Zhao, Z., Sabirzhanov, B., Stoica, B.A., Kumar, A., Luo, T., Skovira, J., Faden, A.I., 2014. Spinal cord injury causes brain inflammation associated with cognitive and affective changes: role of cell cycle pathways. J. Neurosci. 34, 10989–11006. http://dx.doi.org/10.1523/JNEUROSCI.5110-13.2014.

Yoon, E.J., Kim, Y.K., Kim, H.-R.R., Kim, S.E., Lee, Y., Shin, H.I., 2014. Transcranial direct current stimulation to lessen neuropathic pain after spinal cord injury: a mechanistic PET study. Neurorehabil. Neural Repair 28, 250–259. http://dx.doi.org/10.1177/1545968313507632.

Yoon, E.J., Kim, Y.K., Shin, H.I., Lee, Y., Kim, S.E., 2013. Cortical and white matter alterations in patients with neuropathic pain after spinal cord injury. Brain Res. 1540, 64–73. http://dx.doi.org/10.1016/j.brainres.2013.10.007.

Zanca, J.M., Dijkers, M.P., Hammond, F.M., Horn, S.D., 2013. Pain and its impact on inpatient rehabilitation for acute traumatic spinal cord injury: analysis of observational data collected in the SCIRehab study. Arch. Phys. Med. Rehabil. 94, 44. http://dx.doi.org/10.1016/j.apmr.2012.10.035.

Zhu, L., Wu, G., Zhou, X., Li, J., Wen, Z., Lin, F., 2015. Altered spontaneous brain activity in patients with acute spinal cord injury revealed by resting-state functional MRI. PLoS One 10. http://dx.doi.org/10.1371/journal.pone.0118816.

Spinal cord atrophy after spinal cord injury, a meta-analysis and replication.

Clas Linnman, PhD [1, 2]

clinnman@partners.org

Linda Solstrand Dahlberg, PhD [1]

Leslie Morse, DO [3]

[1] Department of Anesthesiology, Perioperative and Pain Medicine, Boston Children´s Hospital, Harvard Medical School, Boston, MA, USA.
[2] Department of Psychiatry, Massachusetts General Hospital, Harvard Medical School, MA, USA.
[3] Craig Center for Regenerative Research Craig Hospital, Englewood, CO, and University of Colorado, Denver, CO, USA

References

1.Song KJ, Choi BW, Kim SJ, Kim GH, Kim YS, Song JH. The relationship between spinal stenosis and neurological outcome in traumatic cervical spine injury. *Clin Orthop Surg.* 2009;1(1):11-18.

2.Freund P, Weiskopf N, Ward NS, et al. Disability, atrophy and cortical reorganization following spinal cord injury. *Brain : a journal of neurology.* 2011;134(Pt 6):1610-1622.

3.Lundell H, Barthelemy D, Skimminge A, Dyrby TB, Biering-Sorensen F, Nielsen JB. Independent spinal cord atrophy measures correlate to motor and sensory deficits in individuals with spinal cord injury. *Spinal Cord.* 2011;49(1):70-75.

4.Petersen JA, Wilm BJ, von Meyenburg J, et al. Chronic cervical spinal cord injury: DTI correlates with clinical and electrophysiological measures. *Journal of neurotrauma.* 2012;29(8):1556-1566.

5.Freund P, Weiskopf N, Ashburner J, et al. MRI investigation of the sensorimotor cortex and the corticospinal tract after acute spinal cord injury: a prospective longitudinal study. *Lancet neurology.* 2013;12(9):873-881.

6.Ohn SH, Kim DY, Shin JC, et al. Analysis of high-voltage electrical spinal cord injury using diffusion tensor imaging. *Journal of neurology.* 2013;260(11):2876-2883.

7.Jutzeler CR, Huber E, Callaghan MF, et al. Association of pain and CNS structural changes after spinal cord injury. *Scientific reports.* 2016;6:18534.

8.Hou J, Xiang Z, Yan R, et al. Motor recovery at 6 months after admission is related to structural and functional reorganization of the spine and brain in patients with spinal cord injury. *Human brain mapping.* 2016;37(6):2195-2209.

9.Huber E, David G, Thompson AJ, Weiskopf N, Mohammadi S, Freund P. Dorsal and ventral horn atrophy is associated with clinical outcome after spinal cord injury. *Neurology.* 2018.

10.Ziegler G, Grabher P, Thompson A, et al. Progressive neurodegeneration following spinal cord injury: Implications for clinical trials. *Neurology.* 2018;90(14):e1257-e1266.

11.De Leener B, Levy S, Dupont SM, et al. SCT: Spinal Cord Toolbox, an open-source software for processing spinal cord MRI data. *NeuroImage.* 2017;145(Pt A):24-43.

Background

After a spinal cord injury, there is rapid atrophy of the spinal cord above the site of the lesion. Here, we review the literature on Magnetic Resonance Imaging (MRI) measures of the cervical cord after SCI, and provide new data on spinal cord cross-sectional area (CSA) at the level of the second cervical vertebra (C2) in 21 patients.

Review methods and results

Through literature searches, we identified ten publications[1-10] on cervical spinal cord cross-sectional area in patients with traumatic spinal cord injury. A total of 158 patients and 173 healthy controls were included in the meta-analysis. On average, patients showed a 15 mm^2, or 18%, reduction in cross-sectional area of the spinal cord at the C2 level, corresponding to an Cohens D effect size of 1.59 (range 0,78 to 5.69).

Larger reductions in CSA have been associated with poor motor recovery[8], in individuals with tetraplegia as compared to paraplegia[7], and with the presence of neuropathic pain in paraplegic individuals[7].

Time since injury

The magnitude of CSA reduction was highly consistent across studies, but quantitative measures of CSA varies substantially, possibly attributable to differences in segmentation protocol between study sites or scan sequence specifics. The average time since injury was 4,7 years (range 35 days to 30 years). The rate of atrophy, evaluated in subacute patients tracked longitudinally [5, 10], indicates a reduction of CSA of 0.4 to 0.6 mm^2/month. A 6.9 mm^2 reduction was been reported in patients investigated approximately 9 weeks post-injury[8]. Lundell et al [6] studied 19 patients at between one and 28 years post-injury, but did not find a relation between atrophy and duration.

In the meta-analysis, time since injury ranged from 35 days to 30 years. While individual data points were typically not available, combining cross-sectional studies with the longitudinal studies suggests a logarithmic relation, with cord atrophy plateauing years after injury.

Meta-analysis Results

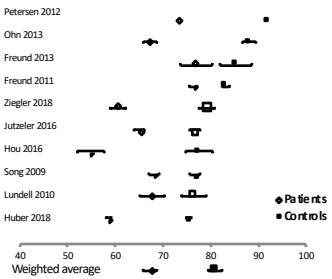

C2 spinal cord cross-sectional area (CSA) in mm^2 across 10 studies. Studies are ordered according to CSA of the healthy control group for visual clarity.

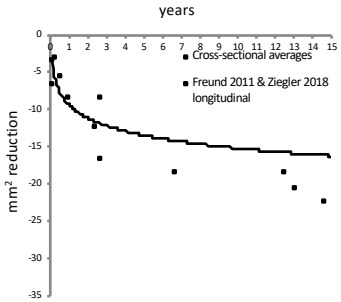

Decline in CSA (mm^2 difference to control group) as a function of time since injury, across 9 studies. Please note that the time since injury varied substantially in several studies. The fit line approximates a logarithmic decline in CSA

Replication Results

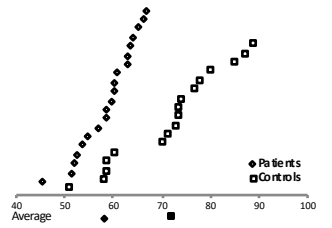

C2 spinal cord cross-sectional area (CSA) in mm^2 in 21 individuals with SCI and 17 healthy subjects. Subjects are ordered in falling CSA order for visual clarity.

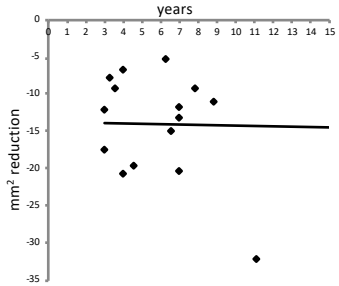

CSA as a function of time since injury in 21 subjects. The fit line indicates no correlation between cord atrophy and time since injury in this cohort of chronic individuals.

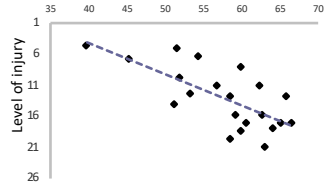

CSA as a function of level of injury in 21 individuals with SCI. Higher injuries display significantly lower C2 CSA, p=0.0004.

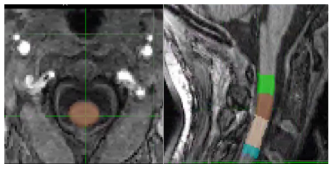

Example of an automated spinal cord segmentation using the Spinal Cord Toolbox [11].

Replication methods and results

Data was collected in two ongoing trials, with neuroimaging conducted at the Martinos Center for Biomedical Imaging in Charlestown, MA, and at Swedish Medical Center in Englewood CO on Siemens 3T scanners (Biograph mMR and Trio), using an MPRAGE and a T1 Grappa sequence. The Spinal Cord Toolbox [11] was used to segment the spinal cord, and provided measures of CSA. Data from 9 SCI subjects and 11 healthy controls (Boston site) were pooled with 12 SCI subjects and 6 healthy controls (Denver site).

The 21 SCI subjects (whereof 2 women) ranged in age between 23 and 59 yrs. (average 37) and were investigated between 3 and 37 years after injury (average 11). Injury location was between C4 and L1, ASIA A-D.

The average CSA was 57.8 mm^2 in the SCI group, and 72.0 mm^2 in the healthy control group ($p<0.00001$), corresponding to a Cohen´s D effect size of 1.68.

There was a significant correlation between the level of injury and cord atrophy, in that the higher the level of the lesion, the lower the CSA at C2, r=0.70, p=0.0004.

We did not observe a correlation between the time since injury and CSA. While individuals with neuropathic pain had a numerically lower CSA than individuals without neuropathic pain, this difference was not significant.

Conclusion

The magnitude of spinal cord atrophy is highly consistent in the published literature, and we further replicated the effect in a new sample. Longitudinal studies indicate that the cord atrophies rapidly in the first year after injury, a finding that is difficult to capture in studies of chronic SCI.

In the new cohort, the degree of atrophy in chronic SCI was closely related to the level of injury, with more extensive atrophy in higher level lesions. Given the magnitude and consistency of the effect, C2 cord CSA is a sensitive marker for injury. We are currently evaluating if rehab interventions can slow the rate of cord atrophy.

STEM CELLS AND DEVELOPMENT
Volume 00, Number 00, 2018
Mary Ann Liebert, Inc.
DOI: 10.1089/scd.2018.0129

Cancer Stem Cells or Tumor Survival Cells?

Yang D. Teng,[1–3] Lei Wang,[1–3] Serdar Kabatas,[1–3] Henning Ulrich,[4] and Ross D. Zafonte[1]

Abstract

Research endeavors originally generated stem cell definitions for the purpose of describing normally sustainable developmental and tissue turnover processes in various species, including humans. The notion of investigating cells that possess a vague capacity of ''stamm (phylum)'' can be traced back to the late 19th century, mainly concentrating on cells that could produce the germline or the entire blood system. Lately, such undertakings have been recapitulated for oncogenesis, tumor growth, and cancer cell resistance to oncolytic therapies. However, due to the complexity and basic life-origin mechanisms comprising the genetic and epigenetic repertoire of the stemness in every developing or growing cell, presently there are ongoing debates regarding the biological essentials of the stem cell-like tumor initiation cells (ie, cancer stem cells; CSCs). This conceptual analysis focuses on the potential pitfalls of extrapolating that CSCs bear major traits of stemness. We propose a novel nomenclature of *Tumor Survival Cells* (TSCs) to further define tumor cells behaving like CSCs, based on the ruthless and detrimental features of *Cancer Cell Survivology* that appears fundamentally different from stem cell biology. Hence, precise academic separation of TSCs from all the stem cell-related labels applied to these unique tumor cells may help to improve scientific reasoning and strategies to decode the desperado-like survival behaviors of TSCs to eventually overcome cancer.

Keywords: cancer stem cell, tumor survival cell, cancer cell survivology, dedifferentiation, stem cell, stemness

Background

Ernst Haeckel (1834–1919), a German biologist, physician, naturalist, artist, and philosopher, is considered a pioneer in developmental cell biology research. He proposed the nomenclature of ''Stammzellen'' (stem cells) in his published lectures on ''Natürliche Schöpfungsgeschichte'' (1868) for unicellular organisms or protozoa that he thought to be the phylogenetic ancestors of multicellular organisms [1]. He considered that the name stem cell seemed to be the most explicit and appropriate one for a pluripotent cell phenotype, from which all other cells stem. They are, in the most literal sense, the stem father and the stem mother of all the infinitive generations of cells that the multicellular organism is ultimately built with [1]. The term was created to distinguish the unique profile of the fertilized egg cell from the original egg cell. Following the doctrine, the human stem cell directly represented the whole future child [2,3].

Haeckel's neologism was derived from the metaphorical language popularly used back then in medical and philosophical discussions about cells and the human body. Scholars (eg, Rudolf Virchow: 1821–1902) often compared cells in a given organism with human individuals within an established state system [4]. For the first time, the concept of a stem cell defined cell state in a hierarchical and centralized format, departing from the previous conception of a liberal and relatively egalitarian profile. It is worth noticing that (1) stem cells are primordial biological entities destined to build a homeostatic system that can reproduce itself, and (2) the metaphorical implication of the stem cell concept not only has its general public education value, but more importantly, its usage deeply impacts the way scientists frame and orient their reasoning.

For example, at the turn of the 19th century, Artur Pappenheim (1870–1916), Alexander Maximow (1874–1928), Ernst Neumann (1798–1895), and other scholars proposed a progenitor cell-based theory for the common origin of all hematopoietic lineages. In the beginning of the 20th century, the advancements in the field of hematopoiesis and leukemia research further distinguished the stem cell definition, underscoring *a common central capacity for self-renewal and phenotypic differentiation* [2].

[1]Department of Physical Medicine and Rehabilitation, Harvard Medical School and Spaulding Rehabilitation Hospital Network, Brigham and Women's Hospital, and Massachusetts General Hospital, Boston, Massachusetts.
[2]Department of Neurosurgery, Harvard Medical School, Boston, Massachusetts.
[3]Division of SCI Research, VA Boston Healthcare System, Boston, Massachusetts.
[4]Departamento de Bioquímica, Instituto de Química, Universidade de São Paulo, São Paulo, Brazil.

The Evolving Theory of Cancer Stem Cells

Possible underlying relations between embryonic stem cells (ESCs) and normal tissue or cancer-like neoplasm were also speculated in the late 19th century. The notion concerned the chances for development deviations of ESCs to contribute to malformation or tumorigenesis [5]. However, key components of this tumorigenic theory (eg, the displacement of embryonic cells) were questioned by gathering experimental evidence around World War II [6]. In the 1950s and early 1960s, systematical investigation of murine teratoma cells resulted in successful isolation of mouse ESCs and basic characterization techniques. The research progression further cultivated the postulation of existence of the so called cancer stem cells (CSCs) [7]. By the early 1980s, murine ESCs could be reliably isolated and maintained in vitro [8,9], which, together with the identification of human neural stem cell and human ESC lines laid down the foundation for opening the contemporary chapter of stem cell research [10–12].

In parallel, the concept of CSCs was gradually shaped out in the 1960s. For instance, Kleinsmith and Pierce demonstrated that donor embryonal carcinoma cells (ECCs) could give rise to both somatic tissue cells and ECCs [7]. It was reported that only $\sim$0.1%–1% of murine myeloma cells could give rise to new clones in vitro, and only $\sim$1%–4% of leukemia cells formed macroscopic colonies in the spleen after transplantation in nonobese diabetic/SCID (severe combined immune deficiency) mice [13]. Noticeably, the data showed certain similarities with the formation of nodules that was observed in the spleens of irradiated mice following administration of bone marrow cells. The number of nodules generated was found to be dose dependent on the quantity of the injected bone marrow cells. Thus, the investigators hypothesized that a single hematopoietic stem cell (ie, colony-forming unit) might be able to develop into a cell colony that gradually formed an individual nodule [14]. These findings combinatorially inferred the possibility that a limited number of tumor cells might have ''stem cell-like'' oncological behavior and act as a ringleader for tumor initiation. Taken together, these discoveries promoted the establishment of the CSC theory.

By the mid-1970s, the clonal evolution theory of cancer growth was additionally enriched by uncovering that mutations in oncogenes and tumor suppressor genes played important roles in tumorigenesis [15]. Fearon and Vogelstein proposed that the stepwise acquisition of mutations in specific oncogenes was critical in the progression and malignization of early adenoma, based on their clonal evolution model of colon cancer [16]. The feature of colon cancers indeed exhibited a generally linear tumor evolution with incremental genetic mutations following inactivation of adenomatous polyposis coli as the most common gene mutation. Elucidating these genetic mechanisms helped to address the question of why a given malignant tumor lesion may contain a subpopulation of cells that show everescalating malignant behavior [16]. By contrast, breast cancers retain discernible levels of intratumoral heterogeneity [17]: for example, amplification of HER2 (human epidermal growth factor receptor 2), mutation of PIK3CA (phosphoinositide-3-kinase, catalytic, alpha polypeptide), etc. Moreover, similar heterogeneity exists in leukemia. Nearly all subtypes of acute myeloid leukemia (AML) can be implanted in immunodeficient mice by engraftment of a $CD34^+CD38^-$ fraction of AML cells (ie, acute myelogenous leukemia stem cells, LSCs: $\sim$1/million AML cells) [18].

At the beginning of the 21st century, the concept of CSC or tumor stem cell was refined based on the evidence that certain developmental signaling pathways governing regular stem cells might also function in CSCs for tumor formation [19]. Therefore, CSCs, as a small subpopulation of tumor cells, were proposed as the primary force fueling oncogenesis and were characterized by their capability of infinite self-renewal and drug resistance [19]. For example, to initiate a new tumor in a mouse, only $\sim$100 $CD44^+CD24^{-/low}$ human breast cancer cells are required, indicating their potent cancerogenic potential relative to other phenotypes of tumor cells that fail to grow tumors even under thousandfold higher quantity [20]. The consensus definition of a CSC was first established by the participants of the 2006 American Association of Cancer Research Workshop on Cancer Stem

FIG. 1. Established molecular markers of TSCs (also called CSCs; *left panel*) and ESCs (*right panel*). In support to our hypothesis, TSCs possess genes either uniquely to themselves (markers in *red zone* and *red font*) or shared with ESCs (molecules in *yellow zone*) that are predominantly related to cell survival functions (eg, proliferation, migration, invasive growth, drug resistance, etc.; markers in *red fonts*). They play critical roles in cancer metastasis, reoccurrence, and oncolytic treatment failure. Although TSCs in different types of malignant tumors share numerous molecular markers with ESCs (markers in *yellow zone*), they are deficient in molecules that are essential for the maintenance of pluripotent status, self-renew, and lineage-specific differentiation, key features of authentic stemness for physiological development and reproduction of biological organisms/entities, including humans (markers in *green fonts*). This unbalanced desperado-like survival strategy of TSCs disrupts homeostasis and exhausts resources essential for host life, which inevitably leads to demises of both host and tumor cells (*left panel* flowcharts). By contrast, totipotent stem cells, inner cell mass-derived ESCs, carry stemness genes mostly for physiological development (markers in *green font* and *green zone*) and keep an effective balance between cell development (markers in *green font*), tissue formation (eg, markers in *yellow*: for cell differentiation), and survival (markers in *red font*; note: functions of the marker molecule in *black font* are presently unclear). These genes work in consortium to drive proper cell proliferation and migration, lineage differentiation, organ genesis and systemic homeostasis, and to make the biological species sustainable. For example, human ESCs differentiate into progenitor cells of the three primary germ layers that subsequently establish functional tissues, organs, and systems. With a new embryo implantation and growth, the whole process of ESC-originated development results in a sustainable life circle for human race (*right panel* flowcharts). The process defines the authentic stemness capacity (ie, stamm or phylum). CSC, cancer stem cell; Drug Resi., drug resistance; ESC, embryonic stem cell; Gpj, gap junction; HSC, hematopoietic stem cell; MDR, multiple drug resistance; NSC, neural stem cell; PT, posttreatment; TSC, tumor survival cell. Color images available online at www.liebertpub.com/scd

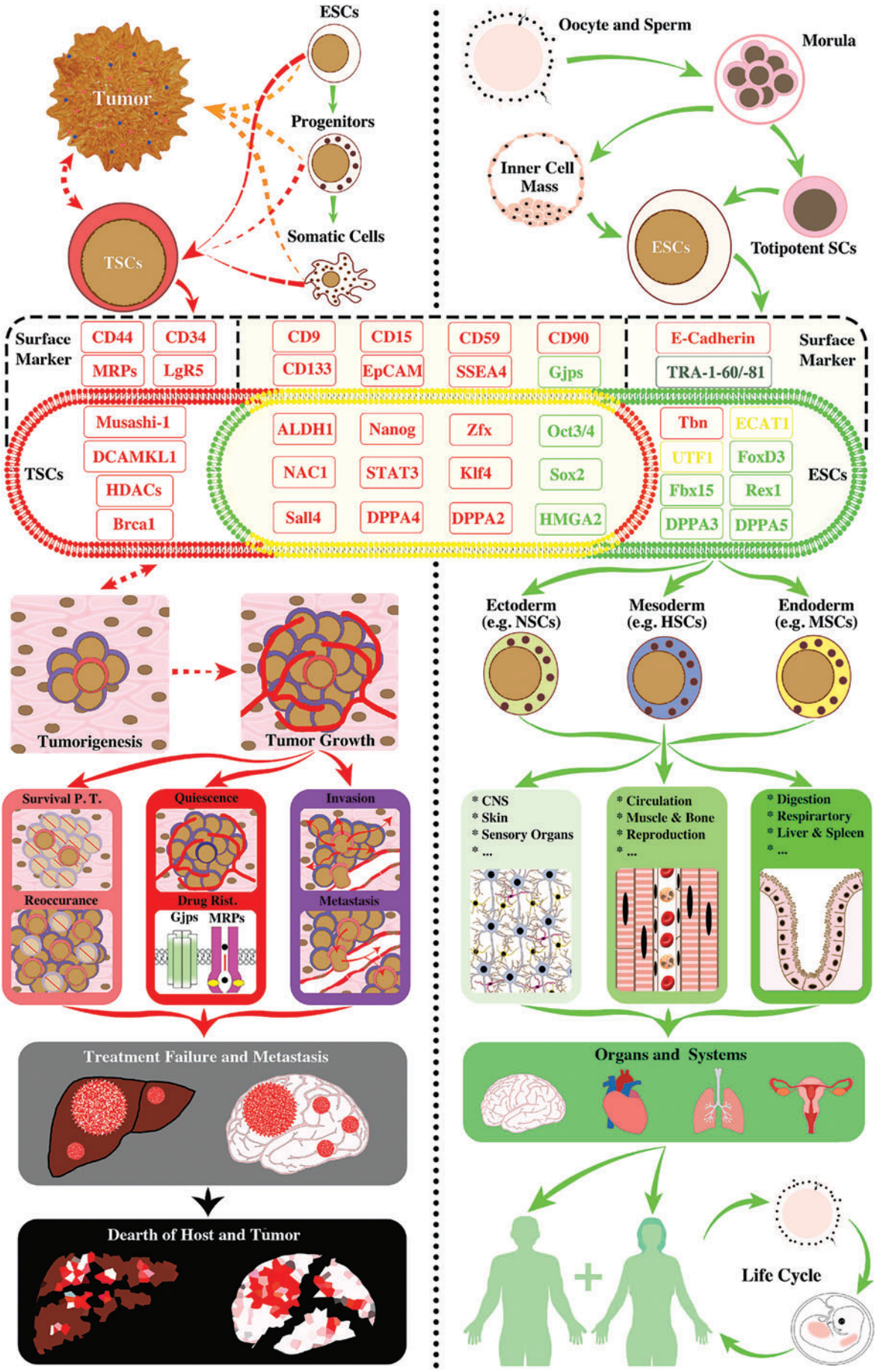
ESCs
Tumor
Progenitors
Somatic Cells
TSCs
Oocyte and Sperm
Morula
Inner Cell Mass
ESCs
Totipotent SCs
Surface Marker
CD44
CD34
MRPs
LgR5
CD9
CD15
CD59
CD90
CD133
EpCAM
SSEA4
Gjps
E-Cadherin
TRA-1-60/-81
Surface Marker
Musashi-1
DCAMKL1
HDACs
Brca1
TSCs
ALDH1
Nanog
Zfx
Oct3/4
NAC1
STAT3
Klf4
Sox2
Sall4
DPPA4
DPPA2
HMGA2
Tbn
ECAT1
UTF1
FoxD3
Fbx15
Rex1
DPPA3
DPPA5
ESCs
Tumorigenesis
Tumor Growth
Ectoderm (e.g. NSCs)
Mesoderm (e.g. HSCs)
Endoderm (e.g. MSCs)
Survival P. T.
Reoccurance
Quiescence
Drug Rist.
Gjps
MRPs
Invasion
Metastasis
* CNS
* Skin
* Sensory Organs
* ...
* Circulation
* Muscle & Bone
* Reproduction
* ...
* Digestion
* Respirartory
* Liver & Spleen
* ...
Treatment Failure and Metastasis
Organs and Systems
Dearth of Host and Tumor
Life Cycle

Cells. The definition states that CSCs should possess the properties of tumorigenicity, self-renewal capacity, continuous passage ability, multilineage differentiation potential to generate the heterogeneous subpopulations of cancer cells that comprise malignant tumors, and unique and reliable surface markers [20–23].

Reciprocal Interaction Between CSC and Normal Stem Cell Research Studies

The CSC theory, besides its academic impact, has practically revealed new therapeutic targets for designing specific therapies to treat cancer. To this end, knowledge gleaned from investigating normal stem cells has markedly improved the understanding of the heterogeneous nature of cancer cells [19,23]. It is believed that CSCs hold higher oncologic plasticity than regular cancer cells; this plasticity may be powered mainly by stemness-like capabilities, promoting efforts to identify key triggers of neoplasm occurrence/recurrence, metastasis, and drug resistance [19–25]. Therefore, it is pivotal to investigate whether or to which scale CSCs may genetically overlap with normal stem cells. Ultimate understanding of these mechanisms will facilitate therapeutic development for managing cancer.

Indeed, a subgroup of CSCs has been found to behave as tumor metastasis and recurrence (or drug resistance)-initiating cells due to their quiescent state, tumorigenicity, and migration capabilities. The cells express markers of epithelial mesenchymal transition (EMT), including collagen IV α1, α-SMA, β-catenin, etc. [24]. EMT describes the process of the transdifferentiation of stationary epithelial cells into motile mesenchymal cells. Over EMT evolvement, epithelial cells lose their tight junctions and apical–basal polarity, reorganize their cytoskeleton, and experience changes in the signaling cascades that control cellular morphological features and gene expression programs. These alterations share main features of *dedifferentiation*, increasing the motility of individual cells, and enabling them to develop into phenotypes with invasive behaviors that are crucial for *cell survival*. EMT process can be regulated or influenced by multiple pathways that are activated by TGF-β, HGF, EGF, FGF, VEGF, Wnt, Shh, IL6, HIF1α, and other signaling molecules through SNAI1/Snail, ZEB1/ZEB2, and/or basic helix-loop-helix proteins-mediated transcription activity [25]. EMT events are crucial in major biological courses of embryonic development, postnatal growth, tissue regeneration, lesion healing, and stem cell homeostasis. EMT-like mechanisms have also been implicated in triggering oncology of malignancies and pathophysiology of fibrosis [25]. The involvement of dedifferentiation as a stem cell-like feature (ie, stemness) in some cancer cells to drive tumorigenesis has been further validated by new findings published in The Pan-Cancer Atlas, the official data portal of The Cancer Genome Atlas (TCGA) consortium. Specifically, TCGA tumors' (ie, 11,000 tumors from 33 of the most prevalent forms of cancer) epigenetic and expression-based stemness indices measured oncogenic dedifferentiation and revealed association with oncogenic dedifferentiation. The investigators reported that the dedifferentiated oncogenic phenotype was generally most prominent in metastatic tumors. The indices identified novel targets for designing potential therapies to augment tumor differentiation [26]. Importantly, it has been recognized that dedifferentiation is likely a mechanism for cell survival [27]. We, therefore, suggest to also focus on survival benefits that can be derived from the intratumor molecular heterogeneity determined by the stemness indices reported [26], to dissect it from classically defined stemness indices of developmental biology that emphasize differentiation [28].

CSCs Do Not Possess Authentic Stemness Biology

Researchers have determined a variety of surface markers for identifying CSCs. As examples, currently well-accepted markers for glioma CSCs include CD15, CD90, CD133, nestin, and integrin-α6. CD44, ALDH, CD117, CD133, and CD24 are utilized to profile ovarian CSCs. For malignant melanoma CSCs, ABCB5, ALDH1, CD20, CD133, and CD271 are commonly enlisted. ALDH1, CD44, CD24, CD90, and CD133 are highlighted as markers for breast CSCs. There are some shared CSC markers frequently expressed in different types of malignant tumors. Among them, CD133 appears to be the most common one, which coincidently is also a marker of normal stem cells (eg, undifferentiated ESCs, HSCs, and NSCs).

However, in spite of accumulation of published data that is in favor of the CSC concept, the validity of the stemness biology in CSCs has been constantly challenged by observations concerning discrepancies regarding the biological characteristic, phenotype, genetic profile, and subpopulation proportion ratio of the alleged ''original'' CSC. Studies showed that successful isolation rate of glioma CSCs was dependent on microenvironmental specifics, including cell–cell interaction, culture medium composition, and cell incubation temperature [29,30]. The data begin to contest the existing CSC theory and arguably suggest that these cells could be a reactive dedifferentiation consequence of regular cancer cells driven by microenvironmental stress, attempting to maximize the survival probability of the tumor, rather than an outcome of a conventionally defined hierarchical cascade of tumor cell development. In fact, CSC-produced intratumor heterogeneity is incapable to form any truly sustainable biological system such as normal tissues or organs. The dedifferentiated tumor cells seemed to be destined to refill the pool of previous CSCs upon their depletion resulting from regular cancer cell differentiation, host immune counteraction, and/or anticancer treatment [31]. Thereby, we *hypothesized* that the commonly defined CSCs might mostly retain genes underlying cell survival (eg, dedifferentiation, proliferation/self-renewal, migration, engraftment, and drug resistance) relative to those of normal stem cells that fundamentally concern lineage-oriented differentiation, homeostasis, stemness, and sustainability through self-renewal and reproduction (Figs. 1 and 2 and Table 1). To test this hypothesis, we systematically examined a total of 50 established molecular markers of CSCs and/or ESCs. The results demonstrated that (1) CSC exclusive markers are genes that support cancer cell migration, metastasis and invasion, and/or enable drug resistance capability (see Figs. 1 and 2 for red markers) [32–42], and only two of them bear uncertain functions (gray markers: CD96 [43] and PSCA [44]; Fig. 2); (2) the majority of markers shared by CSCs and ESCs are genes that are also related to cell migration and metastasis or engraftment (see Figs. 1 and 2 for

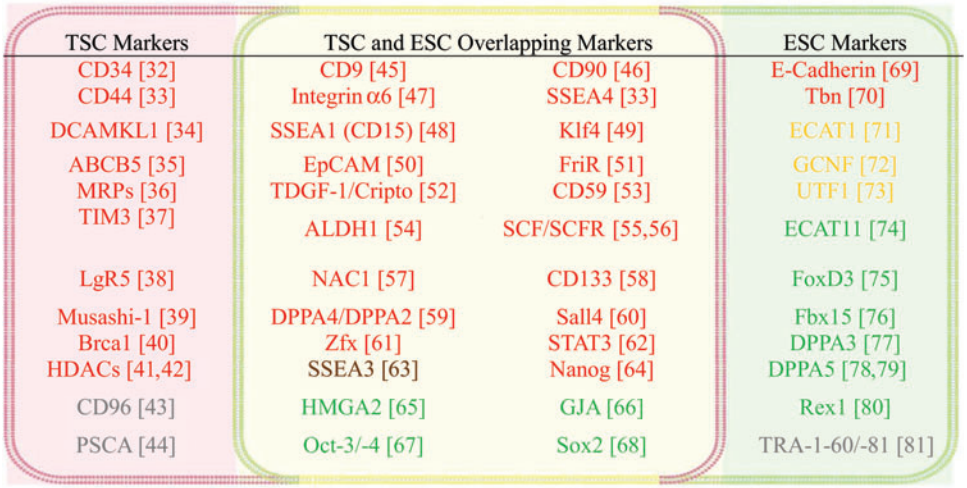

FIG. 2. Common molecular markers of TSCs and ESCs. Color codes: (1) *Green*: genes related to self-renewal and maintenance of pluripotent status or dedifferentiation; (2) *Yellow*: genes important for cell differentiation; (3) *Brown*: genes that support cell survival and cell proliferation but are not essential for the maintenance of pluripotent status of cells; (4) *Red*: genes enabling cancer cell migration, metastasis and invasion, and/or drug resistance; (5) *Gray*: specific genetic markers that are presently unclear for their functions. Color images available online at www.liebertpub.com/scd

red markers [42–59,61]) [45–63], with one related to proliferation but not stemness (brown marker: stage-specific embryonic antigen-3; SSEA3; Fig. 2) [64], and a few concerning self-renewal and maintenance of pluripotent status or dedifferentiation (green markers: HMGA2 [65], GJA [66], Oct-3/-4 [67], and Sox [68]; Fig. 2); and (3) notably, of markers selective for ESCs, there are two molecules for cell migration and engraftment (red markers; Fig. 2) [69,70], three factors important for cell differentiation (yellow markers; Fig. 2) [71–73], and mostly, genes enabling self-renewal and maintenance of pluripotent status or lineage differentiation (green markers; Fig. 2) [74–80], except for one gene with unclear function (gray marker: TRA-1-60/-81; Fig. 2) [81].

Therefore, the analytical outcome in general confirms our postulation. Although CSCs share many genetic markers with ESCs, deeper dissection revealed that CSC-specific genes are predominantly in charge of cell survival activities typically involving invasive growth, cell migration, and survival adaptation (eg, intratumoral heterogeneity and drug resistance), which jointly play critical roles in cancer metastasis, reoccurrence, and insensitivity to chemotherapy and host immune counteractions. By contrast, inner cell mass-derived ESCs exhibit a balanced profile between genes responsible for authentic stemness maintenance emphasizing pluripotency, self-renewal, capability of lineage-specific differentiation and development into reproducible organisms, and genes empowering cell homeostatic survival (Fig. 1; see detailed information in Table 1). Evidently, the biological trajectories of CSCs, which are hallmarked by unilateral attempts for self-survival at the expense of regular cancer and host cells, do not match natural paradigms of developmental biology-related stem cells. Normal stem cells, alongside their proliferation, migration, and differentiation, constantly build homeostasis with surrounding cells through their functional multipotency [82]; and once differentiated into terminal phenotypes, they will not dedifferentiate under physiological conditions.

In corroboration with our analysis, published experimental results clearly demonstrate that all colonies derived from randomly selected single cells of murine lung and breast cancer cell lines can form tumors following allografting in histocompatible mice [83]. A recent study reported that using an approach that integrated major immunogenomics methods (ie, total lymphocytic infiltrate assessed from genomic and haemotoxylin and eosin staining image data, immune cell fractions from deconvolution analysis of mRNA-sequencing data, immune gene expression signatures, neoantigen prediction, T cell receptor and B cell receptor repertoire inference, viral RNA expression, and somatic DNA alterations) to characterize the immune tumor microenvironment (TME) (ie, the immune subtype), investigators identified six immune subtypes that span TCGA cancer tissue types and molecular subtypes [84]. Cancer immune subtypes differ by somatic aberrations, TME, and survival, but not by differentiation. The six immune subtypes are wound healing, IFN-γ dominant, inflammatory, lymphocyte depleted, immunologically quiet, and TGF-β dominant, all being characterized by differences in macrophage or lymphocyte signatures, Th1:Th2 cell ratio, extent of intratumoral heterogeneity, aneuploidy, extent of neoantigen load, overall cell proliferation, expression of immunomodulatory genes, and prognosis [84]. Again, the heterogeneous features of tumor–immune cell interactions are mechanisms underlying cell survival, not sustainable development and organ genesis [85]. Interestingly, TME by definition contains the anatomically distinct regions defined as CSC niches that maintain CSCs by preserving their self-renewal, clonal tumor initiation capacity, and clonal long-term repopulation and metastatic potential, as well as by shielding them from immune surveillance [86]. It has been shown that cells within the CSC niches produce factors that stimulate CSC self-renewal, induce angiogenesis, regulate immune cells, and recruit other stromal cells that secrete additional factors to promote

Table 1. Common Molecular Markers of Tumor Survival Cells and Embryonic Stem Cells and Their Functions

Abbreviation	*Full name*	*Subcellular location*	*Function*	*Refs.*
TSC-specific markers				
CD34	CD34	Cell surface	Cell adhesion and migration	[32]
CD44	CD44	Cell surface	Cell adhesion, migration and metastasis	[33]
DCAMKL1	Doublecortin like kinase 1	Cytoplasm	Epithelial–mesenchymal transition, cancer invasion and metastasis	[34]
ABCB5	ATP-binding cassette subfamily B member 5	Cell surface	Drug resistance	[35]
MRPs	Multidrug resistance pumps	Cell surface	Drug resistance	[36]
TIM3	T cell immunoglobulin and mucin domain 3	Cell surface	Drug resistance, tumorigenesis, self-renewal in leukemic stem cells	[37]
LgR5	Leucine-rich repeat-containing G-protein-coupled receptor 5	Cell surface	WNT signaling and related cancer metastasis	[38]
Musashi-1	RNA-binding protein Musashi homolog 1	Nucleus and cytoplasm	Posttranscriptional regulation of self-renewal and differentiation	[39]
Brca1	Breast cancer 1	Nucleus	DNA repair of double-strand breaks and mismatch	[40]
HDACs	Histone deacetylases	Nucleus	Histone modification, drug resistance, cell proliferation, and growth	[41,42]
CD96	Tactile	Cell surface	Cell adhesive interaction and specific TSCs marker	[43]
PSCA	Prostate stem cell antigen	Cell surface	TSC-specific marker	[44]
Overlapping markers				
CD9	CD9 antigen	Cell surface	Cell adhesion, migration, and regulation of cell development	[45]
CD90	Thy-1 cell surface antigen	Cell surface	Cell adhesion, migration, and metastasis	[46]
Integrin α6	Integrin alpha 6	Cell surface	Cell adhesion, differentiation, polarity, proliferation, survival/ apoptosis	[47]
SSEA4 SSEA1	Stage-specific embryonic antigen 4&1	Cell surface	Cell adhesion and migration	[33,48]
Klf4	Kruppel-like factor 1	Nucleus and cytoplasm	Tumor migration, invasion, and ESCs self-renewal	[49]
EpCAM	Epithelial cell adhesion molecule	Cell surface	Cell adhesion, and WNT signaling	[50]
FriR	Frizzled receptors	Cell surface	WNT signaling receptors, related to cell proliferation, migration, and survival.	[51]
TDGF1/Cripto	Teratocarcinoma-derived growth factor 1	Cell surface and cytoplasm	Tumor anchorage-independent growth and proliferation	[52]
CD59	CD59	Cell surface	Cell survival and inhibit homologous complement-mediated cytolysis	[53]
ALDH1	Aldehyde dehydrogenase 1	Cytoplasm	Retinoid metabolism and self-renewal, cell proliferation, drug resistance	54]
SCF	Stem cell factor	Cytoplasm	Drug resistance, cell migration and stemness	[55,56]
SCFR	Mast/stem cell growth factor receptor, CD117	Cell surface	Drug resistance, cell migration and stemness	[55,56]

(*continued*)

Table 1. (Continued)

Abbreviation	*Full name*	*Subcellular location*	*Function*	*Refs.*
NAC1	Nucleus accumbens-associated protein1	Nucleus	Drug resistance and ESCs self-renewal	[57]
CD133	CD133	Cell surface and cytoplasm	Cell proliferation and dedifferentiation	[58]
DPPA2/4	Developmental pluripotency-associated 2/4	Nucleus	Tumor cell initiation, proliferation and ESCs maintenance of pluripotency	[59]
Sall4	Spalt-like transcription factor 4	Nucleus	Cell proliferation, drug resistance, and ESCs self-renewal	[60]
Zfx	Zinc finger protein X-linked	Nucleus	Cell proliferation	[61]
STAT3	Signal transducer and activator of transcription 3	Cytoplasm and nucleus	Tumor cell proliferation, survival, invasion, and ESCs self-renewal	[62]
SSEA3	Stage-specific embryonic antigen 3	Cell surface	Cell survival and cell proliferation but not necessary for maintenance of pluripotent status	[63]
Nanog	Homebox protein nanog	Nucleus	Self-renewal, maintenance of pluripotency, and drug resistance	[64]
HMGA2	High-mobility group AT-hook 2	Nucleus	Self-renewal and differentiation	[65]
GJA	Gap junction protein	Cell surface	Self-renewal and intercellular communication	[66]
Oct-3/-4	Octamer-binding transcription factor 3/4	Nucleus	Dedifferentiation and ESCs self-renewal	[67]
Sox2	(Sex-determining region Y)-box 2	Nucleus	Tumor initiation and ESCs self-renewal	[68]
ESC-specific markers				
E-Cadherin	E-Cadherin	Cell surface	Cell adhesion, migration, and pluripotency	[69]
Tbn	Taube nuss	Nucleus	Cell survival, regulating the extent of programmed cell death	[70]
ECAT1	ES cell associated transcript 1	Nucleus	Oocyte maturation and preimplantation development	[71]
GCNF	Germ cell nuclear factor	Nucleus	Differentiation	[72]
UTF1	Undifferentiated embryonic cell transcription factor 1	Nucleus	ESCs self-renewal and differentiation	[73]
ECAT11	ES cell-associated transcript 11	Nucleus	ESCs self-renewal	[74]
FoxD3	Forkhead box protein D3	Nucleus	ESCs self-renewal	[75]
Fbx15	F-box-only protein	Nucleus	ESCs self-renewal	[76]
DPPA3/5	Developmental pluripotency-associated 3/5	Nucleus	Acquisition and maintenance of pluripotency	[77–79]
Rex1	Reduced expression 1	Nucleus	Acquisition and maintenance of pluripotency	[80]
TRA-1-60/80	Podocalyxin-like protein 1	Cell surface	ESC-specific marker	[81]

tumor cell survival (eg, invasion and metastasis), Conversely, cells composing normal stem cell niches (eg, neural stem cell niches) affect stem cell differentiation in addition to preserving their self-renewal through numerous biophysical and biochemical mechanisms [87]. Presentation of systematical comparisons between CSC niches and those of regular stem cells is beyond the scope of the current work; however, such analytical outcomes will undoubtedly help us to better understand the fundamental biology of CSCs. The data have kept kindling our intention to suggest that the fundamental developmental biology principles should caution application of the stem cell concept in labeling any terminal oncological and pathological cell phenomena [83].

Present Definitions of CSCs

To substantiate our proposal of defining an alternative term for CSCs, we have analyzed the following definitions currently used to describe CSCs [88].

1. CSCs may directly derive from normal stem cells through genetic mutation. Thus, these cells have the ability for self-renewal and differentiation into all heterogeneous tumor cell phenotypes of a particular cancer (note: intratumoral heterogeneity maximizes cancer cell survival through constant adaptation without real possibility to form any sustainable system that can be stemmed for).
2. CSCs may directly derive from normal progenitor cells that may acquire tumor ''stemness-like'' biology through further accumulation of genetic abnormalities, including mutations and/or abnormal epigenetic modifications.
3. CSCs may directly derive from normal growing or static adult cells through genetic mutations and other mechanisms to trigger dedifferentiation. For example, by expression of hTERT, H-RasV12, and SV40LT and ST, human skin fibroblasts can be reprogrammed to have properties of CSCs [89].
4. Mathematical modeling and data analyses of thermal conditioning of glioblastoma cells suggested that stem cell-like tumor initiation cells, regardless of origin, may not be a fixed population of neoplastic cells [30]. Instead, CSC capacities such as expressions of representative markers, metastasis, oncolytic drug resistance and symmetric or asymmetric cell division may likely be a cluster of transient events occurring in a subpopulation of cancer cells when stressed or induced by environmental, epigenetic, genetic, and therapeutic impacts. Thus, the actual number of CSCs existing in a given tumor for a particular time point is determined by the optimal probability of the unilateral survival and growth of the entire tumor [90,91].
5. CSCs can emerge under varied combinatorial regimens that comprise all the aforementioned scenarios, which is a rational extrapolation that we made.

With the introduction of the fourth and fifth definitions of CSCs, data previously used as evidence to question real existence of CSCs can now be turned into valuable information to suggest an alternative concept. As an example, CSC composition ratio in different tumors might range from 0.2% to 82.5%. Using standardized limiting dilution assays, researchers uncovered that this ratio actually increased in breast cancers along their Stage I to Stage III progression. In contrast to Stage III–IV melanomas, tumorigenic cell ratios remained steadily at around 30% [92]. It has been known that CSCs in the same tumor could carry overlapping, nonoverlapping, or even varied characteristic markers [93,94].

CSCs Are Tumor Survival Cells

In addition to the aforedescribed results, reports showed that the specific molecular mechanisms underlying commonly targeted tumor cell ''stemness'' are unstable. The observations of genetic instability imply a real possibility that different new parental CSC lines may continuously be produced in high-grade malignant tumors. This explains why expressions of some CSC markers are time dependent [95]. With regard to the latter point, an informative comparison case can be made by examining key profiles of ESCs versus those of ECCs that have been traditionally portrayed as opposite sides of the same coin [95].

ECCs have been identified as the ''stem cells of teratocarcinomas'' and as the malignant counterparts of ESCs for mammals. Unlike ESCs that are derived from the inner cell mass of early blastocyst-stage embryos, ECCs are isolated from embryonal teratocarcinomas. It is only after prolonged in vitro culture under certain regimens that some human ESCs (hESCs) start acquiring karyotypic modifications that can be observed in human ECCs (hECCs). Over the chronic incubation process, hESCs can manifest faster proliferation rate and become more maintainable in vitro. Markedly, the more transformed hESCs can form teratocarcinoma-like neoplasms in SCID mice following transplantation. Conversely, the donor hESC-derived teratocarcinoma was able to give rise to characterizable hESCs in vitro. It was therefore concluded that hESCs under particular in vitro induction conditions could develop in similar ways that hECCs do during tumorigenesis [96].

Our analysis, based on a crossdisciplinary approach of stem cell biology and developmental neurobiology, suggests that the in vitro transforming process may actually be a journey for ESCs to gradually lose their repertoire of authentic stemness biology, for which ECCs either do not own or are in severe deficiency. This postulation renders the two types of cells not at all belonging to ''opposite sides of the same coin'' (ie, both ESCs and ECCs possess stemness biology). The conclusion is corroborated by findings from more advanced investigations. In a study of the hECC lines, NT2/D1 and NT2/B9, which were clonally derived from a xenograft tumor of the teratocarcinoma cell line Tera-2, extensive differentiation could be induced in vitro by retinoic acid treatment [97]. This differentiation was particularly marked by the disappearance of SSEA-3 that is typically expressed by hECCs. Among the differentiated cell phenotypes, hECC-produced neuron-like cells showed morphological features of neurites and expressed tetanus toxin receptors and neurofilament proteins [97]. But these NT2/N neurons did not further mature into true neurons that could express phosphorylated neurofilament heavy (NF-H) proteins after engraftment in young adult or developmental rodent brains [98]. They nevertheless survived for >12 weeks to >1 year in rat brains under immunosuppression [98,99] and for more than 27 months in a poststroke human brain [99].

The fact that NT2/N cells showed much longer graft survival duration in the brain relative to that of freshly isolated primary neurons or neural progenitor cells indicates that they might have obtained additionally augmented individual survival efficacy, albeit reduction of neural stemness (ie, diminished ability to differentiate into mature neurons) [98–101]. Accordingly, the NT2/N neurons, not the predifferentiated NT2 progenitor cells, constitutively synthesized intracellular beta/A4 peptide, a major pathologic peptide accumulating in Alzheimer disease (AD) brains, and released it into the cell culture medium [102]. The secreted form (sAPP) of the AD amyloid beta/A4 protein precursor (APP) is a potent player in promoting neurite extension, synaptic formation, overall neurotropic support, and antiexcitotoxicity effect for neuronal cells, as well as in enhancing fibroblast growth [103–108]. Clearly, the gain of function in the

ECC and ECC-derived neuron-like cells is the self-survival capability (eg, production of sAPP, enhanced grafting, etc.). Contrariwise, the loss of function for ECC and ECC-differentiated neuron-like cells is the diminished capacity of authentic stemness (eg, their inability to become mature neurons, defect in functional integration, etc.). Following this novel route of logical reasoning, cautions are deemed necessary when trying to use the NT2/N cells in vitro for investigating NSC and adult neuronal properties, modeling neuronal diseases, or discovering neuronal therapeutics [109,110]. We believe that data extrapolation without factoring the essential cell biology discrepancy could yield misleading information because changes in survival metabolic events may induce alterations of stemness marker presentations. For example, expression of CD9 gene and protein, a cell transmembrane molecule family mediating signal transductions, showed selective upregulation in human glioblastoma stem cell-like cells. CD9 silencing in three CD133+ glioblastoma cell lines triggered amelioration of cancer cell proliferation, survival, invasion, and self-renewal ability through impacting activation patterns of the Akt, MapK, and Stat3 signaling transducers, in which the signaling pathways are mainly involved in cell survival functions, which in turn resulted in expression alternations of CD133, nestin, and SOX2 [45].

Collectively, the metabolic, mitotic, and survival behavioral features as well as the overall life journey endpoints of the currently termed CSCs are vitally different from those of conventionally defined stem cells. Due to the permeating influence of stemness as an established concept that has been academically inscribed for characterizing normal primordial or tissue-specific germ cells, the use of CSC as a nomenclature may cast shadow over conscious and subconscious reasoning of investigators when they aim to tackle malignant essentials of tumor cells. Moreover, the concept of CSC certainly does not hold the original metaphorical implication of stem cells for their capacity to give rise to homeostatic and reproducible multicellular organisms, including human bodies. Therefore, establishing a new nomenclature of tumor survival cell (TSC) to replace CSC appears to be highly valuable since unilateral tumor cell survival essentials consist of endeavors of self-renewal, proliferation, limited differentiation to generate adaptive heterogeneity, migration, metastasis, immune diversity, and drug resistance.

Potential Benefits of Adopting TSC as a New Nomenclature to replace or Coexist with CSC

Application of TSC as an academically and scientifically further justified nomenclature may benefit the intellectual and research fields for its clarity and uniqueness that are tangibilized by the following perspectives.

1. To add special insight to the word ''stem'' when it is used to describe cancer cells for research and therapeutic development [110].
2. To dissect the definitive difference between TSCs and normal stem cells.

TSCs have pathologically maximized levels of individual and group survival ability and utterly perished capacity for authentic stemness biology. TSCs behave like desperados, tumor cell outlaws that act desperately to survive and appear unstoppable, but they are eventually wiped out in their self-rendered catastrophic circumstances. By contrast, ESCs or tissue-specific progenitor cells maintain a homeostatic equilibrium between its stemness biology and individual survival drive to build a sustainable and reproducible entity.

3. To reveal the lack of real stemness capability in CSCs. This will help to refocus on unilateral cell survival mechanisms when devising therapies to block cancer metastasis [111]. As *a testable hypothesis*, what is truly needed for curing the so called CSCs may likely be resurrection of authentic stemness biology and mitigation of the abnormally augmented survival biology inside tumor cells.
4. To emphasize the endpoint of the essential functions of the TSCs that is to carry out desperado-like survival behaviors (DSB). DSB as a novel term of cancer cell oncology describes the state or process of being able to live by all means available, mostly in spite of unfavorable accidents and tribulations, actually in a self-triggered perturbing, stressful, and unsustainable environment. Manifestly, tumor cell DSB do not lead to any real continuity of individual tumor cells or tumor mass as an entity. Through a single spearheaded DSB-driven relentless proliferation, growth, and metastasis, malignant tumor cells will eventually cause the imminent demise of their host organism, followed by reaching the termination of their own journey of survival. Hence, the actual use of the term TSC may further improve the fine-tuning of the direction of our reasoning in search of the oncological prerequisites of these cells in addition to providing the needed demarcation of principal differences between them and the classically entitled stem cells.

Summary

There have been increasingly convincing experimental and clinical data that validate the genetic, epigenetic, and phenotypic heterogeneity of cells comprising malignant tumors. Although questions remain with regard to the consistency and expression levels of specific markers in a subpopulation of cancer cells behaving like stem cell-like tumor initiation cells (ie, CSCs) as well as complexity of CSC oncology, they have not been able to shake the foundation of the concept of CSCs. The current CSC models illuminate tumor generation capabilities of subpopulations of self-renewable and tumor differentiable cells that drive cancer progression via producing oncologic heterogeneity, resistance to oncolytic assaults, and the ultimate death of tumor cells due to host decease. The uncertain oncological feature and conflicting genetic signature of the CSCs (eg, CSC markers mostly are genes in charge of survival, not stemness) suggest a necessity of inaugurating a new nomenclature for the demarcation of the fundamental difference between these cells and physiological stem cells to promote cancer and stem cell research.

What emerged from our analysis is a fine but definitive line between the authentic stemness biology and the newly defined cancer cell survivology. We hereby recommend introducing the term of TSCs (*Tumor Survival Cells*). Implementation of this proposal may facilitate future work to

focus on investigating key events that have gone awry in TSCs to uncover differences between the three bodies of mechanisms underlying normal stem cell biology, cancer cells, and DSB of CSCs/TSCs, respectively (Fig. 1 and Table 1). Furthermore, by weighing the characteristics of limited ''developmental hierarchy'' in cancer cells and full-scale ''functional multipotency'' of normal stem cells, researchers may explore consequences of nongenetic variability, rare clones, and clonal dynamics within a particular tumor, as well as between the tumor clones and the host microenvironment. Such undertakings may determine the oncological essentials of TSCs in terms of their endpoint of survival, defects in authentic stemness biology, and the impacts on the host. The findings will reveal crucial targets (eg, stemness defect, stemness resurrection, unchecked survival drive, etc.) for assessing risk-based patient selection for receiving a particular medical procedure and developing efficacious targeted treatment for malignant tumors [10,82,112,113].

Acknowledgments

This paper was generated from the accumulated reading notes of Y.D.T. alongside cross-disciplinary research collaborations with his colleagues and trainees. Research projects at Dr. Teng's Laboratories are funded by DoD, CASIS-NASA, and VA RRD, and by the Brain Science Foundation and the Gordon Project to Treat Clinical Paralysis (with Dr. Zafonte) at the HMS and SRHN. L.W. was additionally supported by fellowships provided by Wuhan Union Hospital and H.Z.U.S.T. (Sponsor: Y.D.T.). CSC-TSC phenotype targeting in Dr. Ulrich's laboratory is funded by a grant from the São Paulo Research Foundation (FAPESP project no. 2012/50880-4), Brazil.

Author Disclosure Statement

No competing financial interests exist.

References

1. Haeckel E, ed. (1868). *Natürliche Schöpfungsgeschichte (Natural History of Creation), 15th Lecture*. Georg Reimer, Berlin, DE.
2. Ramalho-Santos M and H Willenbring. (2007). On the origin of the term ''stem cell''. Cell Stem Cell 1:35–38.
3. Richards RJ, ed. (2008). *The Tragic Sense of Life: Ernst Haeckel and the Struggle Over Evolutionary Thought*. University of Chicago Press, Chicago, IL.
4. Johach E, ed. (2008). *Krebszelle und Zellenstaat: Zur medizinischen und politischen Metaphorik in Rudolf Virchows Zellularpathologie (Cancer Cells and Cell State: To the Medical and Political Use of Metaphor in Rudolf Virchow's Cellular Pathology)*. Rombach Verlag Kg, Freiburg im Breisgau, DE.
5. Cohnheim J, ed. (1877–1880). *Vorlesungen über allgemeine Pathologie: Ein Handbuch für Ärzte und Studierende (Lectures on general Pathology: A handbook for physicians and students)*. Hirschwald, Berlin, DE.
6. Witschi E. (1948). Migration of the germ cells of human embryos from the yolk sac to the primitive gonadal folds. Contrib Embryol 32:67–80.
7. Kleinsmith LJ and GB Pierce, Jr. (1964). Multipotentiality of single embryonal carcinoma cells. Cancer Res 24: 1544–1551.
8. Evans MJ and MH Kaufman. (1981). Establishment in culture of pluripotential cells from mouse embryos. Nature 292:154–156.
9. Martin GR. (1981). Isolation of a pluripotent cell line from early mouse embryos cultured in medium conditioned by teratocarcinoma stem cells. Proc Natl Acad Sci U S A 78:7634–7638.
10. Teng YD, FN Santos, PM Black, D Konya, KI Park and RL Sidman. (2008). Neural stem cells: multipotency beyond self-renewal and phenotypic differentiation. In: *Principles of Regenerative Medicine* Atala A, R Lanza, Thomson, RM Nerem, eds. Elsevier, San Diego, CA, pp 300–317.
11. Shamblott MJ, J Axelman, S Wang, EM Bugg, JW Littlefield, PJ Donovan, PD Blumenthal, GR Huggins and JD Gearhart. (1998). Derivation of pluripotent stem cells from cultured human primordial germ cells. Proc Natl Acad Sci U S A 95:13726–13731.
12. Thomson JA, J Itskovitz-Eldor, SS Shapiro, MA Waknitz, JJ Swiergiel, VS Marshall and JM Jones. (1998). Embryonic stem cell lines derived from human blastocysts. Science 282:1145–1147.
13. Bruce WR and H Van Der Gaag. (1963). A quantitative assay for the number of murine lymphoma cells capable of proliferation in vivo. Nature 199:79–80.
14. Till JE and EA McCulloch. (1961). A direct measurement of the radiation sensitivity of normal mouse bone marrow cells. Radiat Res 14:213–222.
15. Nowell PC. (1976). The clonal evolution of tumor cell populations. Science 194:23–28.
16. Fearon ER and B Vogelstein. (1990). A genetic model for colorectal tumorigenesis. Cell 61:759–767.
17. Eirew P, A Steif, J Khattra, G Ha, D Yap, H Farahani, K Gelmon, S Chia, C Mar, et al. (2015). Dynamics of genomic clones in breast cancer patient xenografts at single-cell resolution. Nature 518:422–426.
18. Lapidot T, C Sirard, J Vormoor, B Murdoch, T Hoang, J Caceres-Cortes, M Minden, B Paterson, MA Caligiuri and JE Dick. (1994). A cell initiating human acute myeloid leukaemia after transplantation into SCID mice. Nature 367:645–648.
19. Reya T, SJ Morrison, MF Clarke and IL Weissman. (2001). Stem cells, cancer, and cancer stem cells. Nature 414:105–111.
20. Al-Hajj M, MS Wicha, A Benito-Hernandez, SJ Morrison and MF Clarke. (2003). Prospective identification of tumorigenic breast cancer cells. Proc Natl Acad Sci U S A 100:3983–3988.
21. Shipitsin M and K Polyak. (2008). The cancer stem cell hypothesis: in search of definitions, markers, and relevance. Lab Invest 88:459–463.
22. Shah A, S Patel, J Pathak, N Swain and S Kumar. (2014). The evolving concepts of cancer stem cells in head and neck squamous cell carcinoma. Sci World J 2014:842491.
23. Clevers H. (2011). The cancer stem cell: premises, promises and challenges. Nat Med 17:313–319.
24. Ye X, WL Tam, T Shibue, Y Kaygusuz, F Reinhardt, E Ng Eaton and RA Weinberg. (2015). Distinct EMT programs control normal mammary stem cells and tumour-initiating cells. Nature 525:256–260.
25. Stefania D and D Vergara. (2017). The many-faced program of epithelial-mesenchymal transition: a system biology-based view. Front Oncol 7:274.
26. Malta TM, A Sokolov, AJ Gentles, T Burzykowski, L Poisson, JN Weinstein, B Kamińska, J Huelsken, L

Omberg, et al. (2018). Machine learning identifies stemness features associated with oncogenic dedifferentiation. Cell 173:338–354.e15.
27. Bensellam M, JC Jonas and DR Laybutt. (2018). Mechanisms of beta-cell dedifferentiation in diabetes: recent findings and future research directions. J Endocrinol 236: R109–R143.
28. Chosa N and A Ishisaki. (2018). Two novel mechanisms for maintenance of stemness in mesenchymal stem cells: SCRG1/BST1 axis and cell-cell adhesion through N-cadherin. Jpn Dent Sci Rev 54:37–44.
29. Molina ES, MM Pillat, V Moura-Neto, TT Lah and H Ulrich. (2014). Glioblastoma stem-like cells: approaches for isolation and characterization. J Cancer Stem Cell Res 1:e1007.
30. Zeng X, I Han, M Abd-El-Barr, Z Aljuboori, JE Anderson, JH Chi, RD Zafonte and YD Teng. (2016). The effects of thermal preconditioning on oncogenic and intraspinal cord growth features of human glioma cells. Cell Transplant 25:2099–2109.
31. Chen X, R Liao, D Li and J Sun. (2017). Induced cancer stem cells generated by radiochemotherapy and their therapeutic implications. Oncotarget 8:17301–17312.
32. Cho SY, M Xu, J Roboz, M Lu, J Mascarenhas and R Hoffman. (2010). The effect of CXCL12 processing on CD34+ cell migration in myeloproliferative neoplasms. Cancer Res 70:3402–3410.
33. Noto Z, T Yoshida, M Okabe, C Koike, M Fathy, H Tsuno, K Tomihara, N Arai, M Noguchi and T Nikaido. (2013). CD44 and SSEA-4 positive cells in an oral cancer cell line HSC-4 possess cancer stem-like cell characteristics. Oral Oncol 49:787–795.
34. Sureban SM, R May, SA Lightfoot, AB Hoskins, M Lerner, DJ Brackett, RG Postier, R Ramanujam, A Mohammed, et al. (2011). DCAMKL-1 regulates epithelial-mesenchymal transition in human pancreatic cells through a miR-200a-dependent mechanism. Cancer Res 71:2328–2338.
35. Frank NY, A Margaryan, Y Huang, T Schatton, AM Waaga-Gasser, M Gasser, MH Sayegh, W Sadee and MH Frank. (2005). ABCB5-mediated doxorubicin transport and chemoresistance in human malignant melanoma. Cancer Res 65:4320–4333.
36. Kondo T, T Setoguchi and T Taga. (2004). Persistence of a small subpopulation of cancer stem-like cells in the C6 glioma cell line. Proc Natl Acad Sci U S A 101:781–786.
37. Jan M, MP Chao, AC Cha, AA Alizadeh, AJ Gentles, IL Weissman and R Majeti. (2011). Prospective separation of normal and leukemic stem cells based on differential expression of TIM3, a human acute myeloid leukemia stem cell marker. Proc Natl Acad Sci U S A 108:5009–5014.
38. de Sousa e Melo F, AV Kurtova, JM Harnoss, N Kljavin, JD Hoeck, J Hung, JE Anderson, EE Storm, Z Modrusan, et al. (2017). A distinct role for Lgr5(+) stem cells in primary and metastatic colon cancer. Nature 543:676–680.
39. Kuang RG, Y Kuang, QF Luo, CJ Zhou, R Ji and JW Wang. (2013). Expression and significance of Musashi-1 in gastric cancer and precancerous lesions. World J Gastroenterol 19:6637–6644.
40. Bai F, HL Chan, A Scott, MD Smith, C Fan, JI Herschkowitz, CM Perou, AS Livingstone, DJ Robbins, AJ Capobianco and XH Pei. (2014). BRCA1 suppresses epithelial-to-mesenchymal transition and stem cell dedifferentiation during mammary and tumor development. Cancer Res 74:6161–6172.
41. Song KH, CH Choi, HJ Lee, SJ Oh, SR Woo, SO Hong, KH Noh, H Cho, EJ Chung, et al. (2017). HDAC1 upregulation by NANOG promotes multidrug resistance and a stem-like phenotype in immune edited tumor cells. Cancer Res 77:5039–5053.
42. Witt AE, CW Lee, TI Lee, DJ Azzam, B Wang, C Caslini, F Petrocca, J Grosso, M Jones, et al. (2017). Identification of a cancer stem cell-specific function for the histone deacetylases, HDAC1 and HDAC7, in breast and ovarian cancer. Oncogene 36:1707–1720.
43. Hosen N, CY Park, N Tatsumi, Y Oji, H Sugiyama, M Gramatzki, AM Krensky and IL Weissman. (2007). CD96 is a leukemic stem cell-specific marker in human acute myeloid leukemia. Proc Natl Acad Sci U S A 104:11008–11013.
44. Guzmán-Ramírez N, M Völler, A Wetterwald, M Germann, NA Cross, CA Rentsch, J Schalken, GN Thalmann and MG Cecchini. (2009). In vitro propagation and characterization of neoplastic stem/progenitor-like cells from human prostate cancer tissue. Prostate 69:1683–1693.
45. Podergajs N, H Motaln, U Rajčević, U Verbovšek, M Koršič, N Obad, H Espedal, M Vittori, C Herold-Mende, et al. (2016). Transmembrane protein CD9 is glioblastoma biomarker, relevant for maintenance of glioblastoma stem cells. Oncotarget 7:593–609.
46. Zhang K, S Che, Z Su, S Zheng, H Zhang, S Yang, W Li and J Liu. (2018). CD90 promotes cell migration, viability and sphereforming ability of hepatocellular carcinoma cells. Int J Mol Med 41:946–954.
47. Gómez-Miragaya J, M Palafox, L Paré, G Yoldi, I Ferrer, S Vila, P Galván, P Pellegrini, H Pérez-Montoyo, et al. (2017). Resistance to taxanes in triple-negative breast cancer associates with the dynamics of a CD49f+ tumor-initiating population. Stem Cell Rep 8:1392–1407.
48. Son MJ, K Woolard, DH Nam, J Lee and HA Fine. (2009). SSEA-1 is an enrichment marker for tumor-initiating cells in human glioblastoma. Cell Stem Cell 4:440–452.
49. Yu F, J Li, H Chen, J Fu, S Ray, S Huang, H Zheng and W Ai. (2011). Kruppel-like factor 4 (KLF4) is required for maintenance of breast cancer stem cells and for cell migration and invasion. Oncogene 30:2161–2172.
50. Maetzel D, S Denzel, B Mack, M Canis, P Went, M Benk, C Kieu, P Papior, PA Baeuerle, M Munz and O Gires. (2009). Nuclear signalling by tumour-associated antigen EpCAM. Nat Cell Biol 11:162–171.
51. Cantilena S, F Pastorino, A Pezzolo, O Chayka, V Pistoia, M Ponzoni and A Sala. (2011). Frizzled receptor 6 marks rare, highly tumourigenic stem-like cells in mouse and human neuroblastomas. Oncotarget 2:976–983.
52. Francescangeli F, P Contavalli, ML De Angelis, M Baiocchi, G Gambara, A Pagliuca, A Fiorenzano, C Prezioso, A Boe, et al. (2015). Dynamic regulation of the cancer stem cell compartment by Cripto-1 in colorectal cancer. Cell Death Differ 22:1700–1713.
53. Chen J, P Ding, L Li, H Gu, X Zhang, L Zhang, N Wang, L Gan, Q Wang, W Zhang and W Hu. (2017). CD59 regulation by SOX2 is required for epithelial cancer stem cells to evade complement surveillance. Stem Cell Rep 8: 140–151.
54. Jiang F, Q Qiu, A Khanna, NW Todd, J Deepak, L Xing, H Wang, Z Liu, Y Su, SA Stass and RL Katz. (2009). Aldehyde dehydrogenase 1 is a tumor stem cell-associated marker in lung cancer. Mol Cancer Res 7:330–338.
55. Siemens H, R Jackstadt, M Kaller and H Hermeking. (2013). Repression of c-Kit by p53 is mediated by miR-34

and is associated with reduced chemoresistance, migration and stemness. Oncotarget 4:1399–1415.
56. Krivtsov AV, D Twomey, Z Feng, MC Stubbs, Y Wang, J Faber, JE Levine, J Wang, WC Hahn, et al. (2006). Transformation from committed progenitor to leukaemia stem cell initiated by MLL–AF9. Nature 442:818–822.
57. Yap KL, SI Fraley, MM Thiaville, N Jinawath, K Nakayama, J Wang, TL Wang, D Wirtz and IeM Shih. (2012). NAC1 is an actin-binding protein that is essential for effective cytokinesis in cancer cells. Cancer Res 72:4085–4096.
58. Angelastro JM and MW Lamé. (2010). Overexpression of CD133 promotes drug resistance in C6 glioma cells. Mol Cancer Res 8:1105–1115.
59. Tung PY, NV Varlakhanova and PS Knoepfler. (2013). Identification of DPPA4 and DPPA2 as a novel family of pluripotency-related oncogenes. Stem Cells 31:2330–2342.
60. Oikawa T, A Kamiya, M Zeniya, H Chikada, AD Hyuck, Y Yamazaki, E Wauthier, H Tajiri, LD Miller, et al. (2013). Sal-like protein 4 (SALL4), a stem cell biomarker in liver cancers. Hepatology 57:1469–1483.
61. Wang C, SY Fu, MD Wang, WB Yu, QS Cui, HR Wang, H Huang, W Dong, WW Zhang, et al. (2017). Zinc finger protein X-linked promotes expansion of EpCAM(+) cancer stem-like cells in hepatocellular carcinoma. Mol Oncol 11:455–469.
62. Zhou J, J Wulfkuhle, H Zhang, P Gu, Y Yang, J Deng, JB Margolick, LA Liotta, E Petricoin, 3rd and Y Zhang. (2007). Activation of the PTEN/mTOR/STAT3 pathway in breast cancer stem-like cells is required for viability and maintenance. Proc Natl Acad Sci U S A 104:16158–16163.
63. Chiou SH, ML Wang, YT Chou, CJ Chen, CF Hong, WJ Hsieh, HT Chang, YS Chen, TW Lin, HS Hsu and CW Wu. (2010). Coexpression of Oct4 and Nanog enhances malignancy in lung adenocarcinoma by inducing cancer stem cell-like properties and epithelial-mesenchymal transdifferentiation. Cancer Res 70:10433–10444.
64. Cheung SK, PK Chuang, HW Huang, WW Hwang-Verslues, CH Cho, WB Yang, CN Shen, M Hsiao, TL Hsu, CF Chang and CH Wong. (2016). Stage-specific embryonic antigen-3 (SSEA-3) and beta3GalT5 are cancer specific and significant markers for breast cancer stem cells. Proc Natl Acad Sci U S A 113:960–965.
65. Yu H, HH Lim, NO Tjokro, P Sathiyanathan, S Natarajan, TW Chew, T Klonisch, SD Goodman, U Surana and P Dröge. (2014). Chaperoning HMGA2 protein protects stalled replication forks in stem and cancer cells. Cell Rep 6:684–697.
66. Hitomi M, LP Deleyrolle, EE Mulkearns-Hubert, A Jarrar, M Li, M Sinyuk, B Otvos, S Brunet, WA Flavahan, et al. (2015). Differential connexin function enhances self-renewal in glioblastoma. Cell Rep 11:1031–1042.
67. Kumar SM, S Liu, H Lu, H Zhang, PJ Zhang, PA Gimotty, M Guerra, W Guo and X Xu. (2012). Acquired cancer stem cell phenotypes through Oct4-mediated dedifferentiation. Oncogene 31:4898–4911.
68. Boumahdi S, G Driessens, G Lapouge, S Rorive, D Nassar, M Le Mercier, B Delatte, A Caauwe, S Lenglez, et al. (2014). SOX2 controls tumour initiation and cancer stem-cell functions in squamous-cell carcinoma. Nature 511:246–250.
69. Redmer T, S Diecke, T Grigoryan, A Quiroga-Negreira, W Birchmeier and D Besser. (2011). E-cadherin is crucial for embryonic stem cell pluripotency and can replace OCT4 during somatic cell reprogramming. EMBO Rep 12:720–726.
70. Voss AK, T Thomas, P Petrou, K Anastassiadis, H Schöler and P Gruss. (2000). Taube nuss is a novel gene essential for the survival of pluripotent cells of early mouse embryos. Development 127:5449–5461.
71. Liu C, M Li, T Li, H Zhao, J Huang, Y Wang, Q Gao, Y Yu and Q Shi. (2016). ECAT1 is essential for human oocyte maturation and pre-implantation development of the resulting embryos. Sci Rep 6:38192.
72. Akamatsu W, B DeVeale, H Okano, AJ Cooney and D van der Kooy. (2009). Suppression of Oct4 by germ cell nuclear factor restricts pluripotency and promotes neural stem cell development in the early neural lineage. J Neurosci 29:2113–2124.
73. van den Boom V, SM Kooistra, M Boesjes, B Geverts, AB Houtsmuller, K Monzen, I Komuro, J Essers, LJ Drenth-Diephuis and BJ Eggen. (2007). UTF1 is a chromatin-associated protein involved in ES cell differentiation. J Cell Biol 178:913–924.
74. Närvä E, N Rahkonen, MR Emani, R Lund, JP Pursiheimo, J Nästi, R Autio, O Rasool, K Denessiouk, et al. (2012). RNA-binding protein L1TD1 interacts with LIN28 via RNA and is required for human embryonic stem cell self-renewal and cancer cell proliferation. Stem Cells 30:452–460.
75. Zhu L, S Zhang and Y Jin. (2014). Foxd3 suppresses NFAT-mediated differentiation to maintain self-renewal of embryonic stem cells. EMBO Rep 15:1286–1296.
76. Tokuzawa Y, E Kaiho, M Maruyama, K Takahashi, K Mitsui, M Maeda, H Niwa and S Yamanaka. (2003). Fbx15 is a novel target of Oct3/4 but is dispensable for embryonic stem cell self-renewal and mouse development. Mol Cell Biol 23:2699–2708.
77. Xu X, L Smorag, T Nakamura, T Kimura, R Dressel, A Fitzner, X Tan, M Linke, U Zechner, W Engel and DV Pantakani. (2015). Dppa3 expression is critical for generation of fully reprogrammed iPS cells and maintenance of Dlk1-Dio3 imprinting. Nat Commun 6:6008.
78. Qian X, JK Kim, W Tong, LG Villa-Diaz and PH Krebsbach. (2016). DPPA5 supports pluripotency and reprogramming by regulating NANOG turnover. Stem Cells 34:588–600.
79. Miharada K, V Sigurdsson and S Karlsson. (2014). Dppa5 improves hematopoietic stem cell activity by reducing endoplasmic reticulum stress. Cell Rep 7:1381–1392.
80. Scotland KB, S Chen, R Sylvester and LJ Gudas. (2009). Analysis of Rex1 (zfp42) function in embryonic stem cell differentiation. Dev Dyn 238:1863–1877.
81. Schopperle WM and WC DeWolf. (2007). The TRA-1-60 and TRA-1-81 human pluripotent stem cell markers are expressed on podocalyxin in embryonal carcinoma. Stem Cells 25:723–730.
82. Teng YD, D Yu, AE Ropper, J Li, S Kabatas, DR Wakeman, J Wang, MP Sullivan, DE Redmond Jr., et al. (2011). Functional multipotency of stem cells: a conceptual review of neurotrophic factor-based evidence and its role in translational research. Curr Neuropharmacol 9:574–585.
83. Yoo MH and DL Hatfield. (2008). The cancer stem cell theory: is it correct? Mol Cells 26:514–516.
84. Thorsson V, DL Gibbs, SD Brown, D Wolf, DS Bortone, TH Ou Yang, E Porta-Pardo, GF Gao, CL Plaisier, et al. (2018). The immune landscape of cancer. Immunity 48: 812–830.e14.
85. Li Q and BA Barres. (2018). Microglia and macrophages in brain homeostasis and disease. Nat Rev Immunol 18: 225–242.

86. Plaks V, N Kong, Z Werb. (2015). The cancer stem cell niche: how essential is the niche in regulating stemness of tumor cells? Cell Stem Cell 16:225–238.
87. Falk S and M Götz. (2017). Glial control of neurogenesis. Curr Opin Neurobiol 47:188–195.
88. Verga Falzacappa MV, C Ronchini, LB Reavie and PG Pelicci. (2012). Regulation of self-renewal in normal and cancer stem cells. FEBS J 279:3559–3572.
89. Zhao JJ, OV Gjoerup, RR Subramanian, Y Cheng, W Chen, TM Roberts and WC Hahn. (2003). Human mammary epithelial cell transformation through the activation of phosphatidylinositol 3-kinase. Cancer Cell 3:483–495.
90. Poleszczuk J, P Hahnfeldt and H Enderling. (2015). Evolution and phenotypic selection of cancer stem cells. PLoS Comput Biol 11:e1004025.
91. Fusi A, S Ochsenreither, A Busse, A Rietz and U Keilholz. (2010). Expression of the stem cell marker nestin in peripheral blood of patients with melanoma. Br J Dermatol 163:107–114.
92. Cherciu I, A Bărbălan, D Pirici, C Mărgăritescu and A Săftoiu. (2014). Stem cells, colorectal cancer and cancer stem cell markers correlations. Health Sci J 40:153–161.
93. Anguille S, VF Van Tendeloo and ZN Berneman. (2012). Leukemia-associated antigens and their relevance to the immunotherapy of acute myeloid leukemia. Leukemia 26: 2186–2196.
94. Meacham CE and SJ Morrison. (2013). Tumour heterogeneity and cancer cell plasticity. Nature 501:328–337.
95. Andrews PW, MM Matin, AR Bahrami, I Damjanov, P Gokhale and JS Draper. (2005). Embryonic stem (ES) cells and embryonal carcinoma (EC) cells: opposite sides of the same coin. Biochem Soc Trans 33:1526–1530.
96. Andrews PW. (1984). Retinoic acid induces neuronal differentiation of a cloned human embryonal carcinoma cell line in vitro. Dev Biol 103:285–293.
97. Trojanowski JQ, JR Mantione, JH Lee, DP Seid, T You, LJ Inge and VM Lee. (1993). Neurons derived from a human teratocarcinoma cell line establish molecular and structural polarity following transplantation into the rodent brain. Exp Neurol 122:283–294.
98. Nelson PT, D Kondziolka, L Wechsler, S Goldstein, J Gebel, S DeCesare, EM Elder, PJ Zhang, A Jacobs, et al. (2002). Clonal human (hNT) neuron grafts for stroke therapy: neuropathology in a patient 27 months after implantation. Am J Pathol 160:1201–1206.
99. Brundin P and A Björklund. (1987). Survival, growth and function of dopaminergic neurons grafted to the brain. Prog Brain Res 71:293–308.
100. Moriarty N, A Pandit and E Dowd. (2017). Encapsulation of primary dopaminergic neurons in a GDNF-loaded collagen hydrogel increases their survival, re-innervation and function after intra-striatal transplantation. Sci Rep 7: 16033.
101. Wertkin AM, RS Turner, SJ Pleasure, TE Golde, SG Younkin, JQ Trojanowski and VM Lee. (1993). Human neurons derived from a teratocarcinoma cell line express solely the 695-amino acid amyloid precursor protein and produce intracellular beta-amyloid or A4 peptides. Proc Natl Acad Sci U S A 90:9513–9517.
102. Roch JM, E Masliah, AC Roch-Levecq, MP Sundsmo, DA Otero, I Veinbergs and T Saitoh. (1994). Increase of synaptic density and memory retention by a peptide representing the trophic domain of the amyloid beta/A4 protein precursor. Proc Natl Acad Sci U S A 91:7450–7454.
103. Ghiso J, A Rostagno, JE Gardella, L Liem, PD Gorevic and B Frangione. (1992). A 109-amino-acid C-terminal fragment of Alzheimer's-disease amyloid precursor protein contains a sequence, -RHDS-, that promotes cell adhesion. Biochem J 288:1053–1059.
104. Koo EH, L Park and DJ Selkoe. (1993). Amyloid beta-protein as a substrate interacts with extracellular matrix to promote neurite outgrowth. Proc Natl Acad Sci U S A 90: 4748–4752.
105. Araki W, N Kitaguchi, Y Tokushima, K Ishii, H Aratake, S Shimohama, S Nakamura and J Kimura. (1991). Trophic effect of beta-amyloid precursor protein on cerebral cortical neurons in culture. Biochem Biophys Res Commun 181:265–271.
106. Milward EA, R Papadopoulos, SJ Fuller, RD Moir, D Small, K Beyreuther and CL Masters. (1992). The amyloid protein precursor of Alzheimer's disease is a mediator of the effects of nerve growth factor on neurite outgrowth. Neuron 9:129–137.
107. Mattson MP, B Cheng, AR Culwell, FS Esch, I Lieberburg and RE Rydel. (1993). Evidence for excitoprotective and intraneuronal calcium-regulating roles for secreted forms of the beta-amyloid precursor protein. Neuron 10:243–254.
108. Schwartz CM, CE Spivak, SC Baker, TK McDaniel, JF Loring, C Nguyen, FJ Chrest, R Wersto, E Arenas, et al. (2005). NTera2: a model system to study dopaminergic differentiation of human embryonic stem cells. Stem Cells Dev 14:517–534.
109. Stern M, A Gierse, S Tan and G Bicker. (2014). Human Ntera2 cells as a predictive in vitro test system for developmental neurotoxicity. Arch Toxicol 88:127–136.
110. Breitbach M, K Kimura, TC Luis, CJ Fuegemann, PS Woll, M Hesse, R Facchini, S Rieck, K Jobin, et al. (2018). In vivo labeling by CD73 marks multipotent stromal cells and highlights endothelial heterogeneity in the bone marrow niche. Cell Stem Cell 22:262–276.e7.
111. Wang Q, J Jiang, G Ying, XQ Xie, X Zhang, W Xu, X Zhang, E Song, H Bu, et al. (2018). Tamoxifen enhances stemness and promotes metastasis of ERalpha36(+) breast cancer by upregulating ALDH1A1 in cancer cells. Cell Res 28:336–358.
112. Bliss SA, S Paul, PW Pobiarzyn, S Ayer, G Sinha, S Pant, H Hilton, N Sharma, MF Cunha, et al. (2018). Evaluation of a developmental hierarchy for breast cancer cells to assess risk-based patient selection for targeted treatment. Sci Rep 8:367.
113. Ropper AE, DK Thakor, I Han, D Yu, X Zeng, JE Anderson, Z Aljuboori, SW Kim, H Wang, et al. (2017). Defining recovery neurobiology of injured spinal cord by synthetic matrix-assisted hMSC implantation. Proc Natl Acad Sci U S A 114:E820–E829.

Address correspondence to:
Dr. Yang D. Teng
Departments of Physical Medicine and Rehabilitation, and Neurosurgery
Harvard Medical School and Spaulding Rehabilitation Hospital Network
Brigham and Women's Hospital
Massachusetts General Hospital
Boston, MA 02115

E-mail: yang_teng@hms.harvard.edu

Received for publication June 15, 2018
Accepted after revision August 9, 2018
Prepublished on Liebert Instant Online XXXX XX, XXXX

JOURNAL OF NEUROTRAUMA 35:210–225 (January 15, 2018)

DOI: 10.1089/neu.2016.4953

Pathophysiological Bases of Comorbidity: Traumatic Brain Injury and Post-Traumatic Stress Disorder

Gary B. Kaplan,[1–3] Kimberly A. Leite-Morris,[2–4] Lei Wang,[5,6] Kendra K. Rumbika,[7] Stephen C. Heinrichs,[7] Xiang Zeng,[5,6] Liquan Wu,[5,6] Danielle T. Arena,[7] and Yang D. Teng[5,6]

Abstract

The high rates of traumatic brain injury (TBI) and post-traumatic stress disorder (PTSD) diagnoses encountered in recent years by the United States Veterans Affairs Healthcare System have increased public awareness and research investigation into these conditions. In this review, we analyze the neural mechanisms underlying the TBI/PTSD comorbidity. TBI and PTSD present with common neuropsychiatric symptoms including anxiety, irritability, insomnia, personality changes, and memory problems, and this overlap complicates diagnostic differentiation. Interestingly, both TBI and PTSD can be produced by overlapping pathophysiological changes that disrupt neural connections termed the ''connectome.'' The neural disruptions shared by PTSD and TBI and the comorbid condition include asymmetrical white matter tract abnormalities and gray matter changes in the basolateral amygdala, hippocampus, and prefrontal cortex. These neural circuitry dysfunctions result in behavioral changes that include executive function and memory impairments, fear retention, fear extinction deficiencies, and other disturbances. Pathophysiological etiologies can be identified using experimental models of TBI, such as fluid percussion or blast injuries, and for PTSD, using models of fear conditioning, retention, and extinction. In both TBI and PTSD, there are discernible signs of neuroinflammation, excitotoxicity, and oxidative damage. These disturbances produce neuronal death and degeneration, axonal injury, and dendritic spine dysregulation and changes in neuronal morphology. In laboratory studies, various forms of pharmacological or psychological treatments are capable of reversing these detrimental processes and promoting axonal repair, dendritic remodeling, and neurocircuitry reorganization, resulting in behavioral and cognitive functional enhancements. Based on these mechanisms, novel neurorestorative therapeutics using anti-inflammatory, antioxidant, and anticonvulsant agents may promote better outcomes for comorbid TBI and PTSD.

Keywords: comorbidity; excitotoxicity; neuroinflammation; oxidative stress; PTSD; TBI

Introduction

Traumatic brain injury (TBI) is a trauma-related condition that occurs after an external blunt or blast force produces a mild, moderate, or severe brain injury. Mild TBI (mTBI) is associated with a short period of loss of consciousness or a brief period of confusion or disorientation. In addition, a variety of physical symptoms develop with mTBI including headache, dizziness, tinnitus, and sensitivity to light and sound. Further, cognitive changes develop such as impaired concentration and memory, mental slowing, and speech changes. Concurrently, emotional changes also occur, including mood lability, anxiety, depression, and personality fluctuations.[1,2] Following a single mild or moderate TBI, a full recovery can occur within days to weeks; however, for many, symptoms persist. Patients with a history of multiple TBIs may experience more severe and persistent symptomatology. Mild to moderate TBI may cause immediate and sometimes lasting damage and dysfunction of brain cells, axonal stretching and injury and changes in neural plasticity. TBI is, therefore, a brain disease process, perpetuated by secondary molecular injuries that include neuroinflammation, oxidative damage, excitotoxicity, and other mechanisms. Moreover, a severe TBI can produce brain contusions, hemorrhages, axonal tears, and other more permanent damage to the brain that results in long-term and serious behavioral and/or neurological compromise and sometimes death.

[1]Mental Health Service, VA Boston Healthcare System, Brockton, Massachusetts.
Departments of [2]Psychiatry, and [3]Pharmacology and Experimental Therapeutics, Boston University School of Medicine, Boston, Massachusetts.
[4]Research Service, VA Boston Healthcare System, Jamaica Plain, Massachusetts.
[5]Division of Spinal Cord Injury Research, VA Boston Healthcare System, West Roxbury, Massachusetts.
[6]Departments of Physical Medicine and Rehabilitation and Neurosurgery, Harvard Medical School, Boston, Massachusetts.
[7]Research Service, VA Boston Healthcare System, West Roxbury, Massachusetts.

Post-traumatic stress disorder (PTSD) is caused by physical or emotional trauma that produces many signs and symptoms that overlap with TBI.[2] Like TBI, PTSD is a brain disease produced by white and gray matter damage via stress-related pathologies of neuroinflammation, oxidative damage, and excitotoxicity. PTSD develops after a person has experienced a highly disturbing event in which serious physical harm had occurred or was threatened; for example, after seeing someone injured or killed, or after sexual or physical assault, an accident, combat, or a natural disaster. PTSD often develops within a few months of the trauma and can continue for months or even years. During PTSD, psychological and/or physical trauma is followed by intrusion symptoms related to the event including disturbing memories, nightmares, dissociative reactions such as flashbacks, distress, and physical reactions at exposure to cues or contextual reminders of the trauma. Further, there is persistent avoidance of reminders of the trauma including people, places, and activities associated with it. Likewise, there are often cognitive changes such as amnesia and distortions to important trauma-related events such as negative beliefs about oneself and others, guilt, emotional disconnection from others, and loss of interest. PTSD also produces heightened arousal and reactivity such as irritability, self-destructive behaviors, hypervigilance, startle, inattention, and insomnia. To summarize, this review focuses on trauma-related pathologies and neurobiological underpinnings of TBI and PTSD and their comorbid condition in veterans and active duty military. It also describes characteristics of animal models, to study these pathologies and investigate new treatments for this comorbid disorder.

PTSD and mTBI have discernible overlaps in symptomatology which makes it difficult for a clinician to distinguish between these two conditions. For a majority of individuals with mTBI, symptoms resolve in days to months; however, a significant number ($\sim$ 15%) are estimated to have post-concussive syndrome 1 year post-injury.[1] Both mTBI and PTSD present with nonspecific symptoms such as generalized anxiety, irritability, insomnia, and memory problems, which further complicate diagnostic differentiation.[3] Somatic symptoms such as headache, hypersensitivity to light and sound, and dizziness are more specific to mTBI syndrome. Efforts to determine the diagnostic and neurobiological specificity of mTBI and PTSD, and their comorbid condition, are critical for understanding and effectively treating these post-traumatic disorders.

There has been a further enhanced interest in understanding and treating the comorbidity of TBI and PTSD because of its frequent occurrence in soldiers returning from Operation Enduring Freedom (OEF) in Afghanistan and Operation Iraqi Freedom (OIF) and Operation New Dawn (OND) in Iraq. The Armed Forces Health Surveillance reported that >1,800,000 service members were deployed in these conflicts, and that more than a third of these individuals were deployed at least twice.[4] During OIF and OEF, both the use of improvised explosive devices and continuous levels of threat during these operations contributed to the comorbidity of these conditions. In a sample of United States Army soldiers, 9% reported symptoms of mTBI, and >17% of those with mTBI screened positive for PTSD, whereas >31% screened positive for depression.[5] In a large cohort of returning OIF soldiers with TBI, of those reporting loss of consciousness, 43.9% also met criteria for PTSD.[6] In a large study of active duty Marine and Navy servicepersons who served in OIF or OEF, TBI doubled the likelihood of post-deployment PTSD symptoms.[7] In a study of >100,000 OEF/OIF veterans, one quarter received mental health diagnoses and more than half of these had two or more mental health diagnoses.[8] TBI has been linked to the serious consequence of ongoing suicidal ideation, which has been an epidemic for OIF/OEF veterans.[9] Whereas onsets of acute neuropsychological problems following mTBI often occur within 1–3 months after injury, current guidelines emphasize that a clinical diagnosis of PTSD should not be made until 6 months after the traumatic exposure of the patient. This fact suggests that the time courses of the development and recovery of PTSD and their pathophysiology have not been well understood. The delay in diagnosis and ineffective treatments caused by the complex symptomatology and presentation of the comorbid disorder may contribute to this inconsistent course of recovery.

Comorbid TBI/PTSD can present with a wide variety of neuropsychiatric signs and symptoms. The individual may endure a loss of consciousness from the head trauma but may also experience more subtle alterations of consciousness (feeling dazed), amnesia, or a transient neurologic deficit such as headache, weakness, or sensory or gait problems. When TBI does not result in a loss of consciousness, neuropsychiatric recovery is likely, although enduring cognitive changes worsen that prognosis.[10] TBI is also associated with other neuropsychiatric sequelae including depression, mania, or psychosis; substance use disorders; sleep disorders; and chronic pain. These conditions could directly result from the traumatic injury or from an emotional effect of the TBI on daily functioning.[11] In another study, patients with comorbid TBI and PTSD demonstrated increased health risks and cognitive impairments when compared with patients without PTSD.[12] The comorbidity of TBI and PTSD is associated with increased rates of neuropsychiatric health problems that complicate recovery.[13]

Both TBI and PTSD can be represented as brain disorders with disruptions in neural networks that communicate via long axonal pathways through white matter tracts, termed the ''connectome.''[14] We propose that both mTBI and PTSD are produced by insults to the connectome underlying neural circuits that subserve executive function, attentional control, motivational, behavioral inhibition, and fear responses. In both TBI and PTSD, the pathological mechanisms occur via a wide range of neuroinflammatory changes, excitotoxicity, and oxidative changes and result in neurodegeneration. Our central hypothesis is that TBI and PTSD result from a variety of pathophysiological mechanisms, resulting in dysfunction in overlapping neural circuits, and some common symptomatology. Further, we propose that the comorbid condition of TBI/PTSD produces more severe health consequences and is more resistant to treatment. A better understanding of the pathophysiological mechanisms and network dysfunctions for this devastating comorbid condition will lead to novel neurorestorative therapeutics.

In this review, relevant articles published between 1990 and 2017 were identified by searching MEDLINE®, using the following MeSH search terms that were cross-referenced: TBI, PTSD, comorbid, neuroimaging, glutamatergic excitotoxicity, oxidative damage, neuroinflammation, neurodegeneration, axonal injury, and dendritic plasticity. This search reflects the major topics that were reviewed and discussed. Both humans and other animals were considered.

Neuroimaging and Functional Circuitry of TBI and PTSD

Neuroimaging of TBI in military/veteran populations

The neurocircuitry disruptions in TBI, PTSD, and the comorbid disorder have been evaluated from clinical biospecimens. There are a variety of modalities used to assess the damage to these important circuits in TBI and PTSD, including structural and functional neuroimaging.[15,16] These modalities include CT, structural and functional MRI (sMRI and fMRI, respectively), transcranial Doppler

(TCD) (which measures vascular abnormalities), positron emission tomography (PET), single photon emission CT, arterial spin labeling (ASL) MRI, magnetic resonance spectroscopy (MRS), and electrophysiological techniques (magnetoencephalography [MEG] and electroencephalography [EEG]). CT or sMRI scanning have limited sensitivity to identify white matter lesions in TBI, and often have negative findings. Experts have concluded that CT or sMRI also have inadequate sensitivity for diffuse axonal injury (DAI) and associated vascular injuries.[15] Advanced MRI methods such as susceptibility weighted imaging (SWI) are able to detect DAI and are accessible in clinical practice. In one MRI study, chronic blast-induced mild and moderate TBI produced greater structural damage and cortical thinning in the right hemispheric insula, inferior temporal, and frontal lobes.[17] CT, sMRI, SWI, and TCD are the most accessible imaging tools in the clinical setting. No single imaging modality standard is sufficient for all patients, because of the heterogeneity of brain injury in TBI.[15] It is necessary to consider all these imaging techniques to gain a comprehensive visualization of the physical damage caused by TBI.

Diffusion tensor imaging (DTI) is a research tool utilized to identify DAI by measuring the diffusion properties of water to generate measures related to the structural integrity of specific white matter structures. DTI fractal anisotropy (FA) is used to measure neuronal fiber density, axonal diameter, and myelination in white matter. A lower FA measure suggests disruption of both white matter and neural circuitry connectivity. In a recent study of veteran cohorts from OIF, OEF, and/or OND, blast exposure effects on white matter tissue integrity using DTI was examined.[18] Interestingly, this study found a blast dose-response relationship between the number of blast exposures and the loss of white matter integrity. In addition, there was a negative relationship between FA and the length of time after injury, indicating greater disruption of white matter connectivity over time. In another DTI study of OIF/OEF/OND veterans exposed to a blast at close range (< 10 m), there was decreased connectivity of bilateral primary somatosensory and motor cortices compared with veterans with blast injury occurring beyond this distance.[19] Another DTI study compared soldiers with TBI with military controls and demonstrated white matter abnormalities in frontostriatal and frontolimbic circuits, fronto-parieto-occipital association tracts, brainstem and corpus callosum fibers.[20] In this study, there were asymmetries along the superior-inferior, anterior-posterior, and left and right hemispheric axes. This last study highlights the presence of diffuse and focal and asymmetrical white matter abnormalities in TBI. In another group of OIF/OEF veterans with TBI, lower FA was found in the corpus callosum and cingulum bundle, and this measure correlated with cognitive processing speed and executive functions.[21] Further, OIF/OEF veterans with blast injury and mTBI, and also a loss of consciousness, showed more spatially heterogeneous white matter abnormalities than veteran controls.[22] In this last study, decreasing FA was demonstrated in the left internal capsule as the number of blast exposures increased. In summary, DTI studies have shown that TBI results in asymmetrical cortical and subcortical tract abnormalities resulting in multiple circuit disruptions, and that DTI could be one of several important tools in assessing TBI in the clinical setting.

fMRI and electrophysiological studies using MEG have been performed in OIF/OEF veterans with TBI. An fMRI study was performed comparing blast-related TBI in a military population (OIF/OEF/OND veterans) to blunt force-induced TBI in civilians.[23] The study found that chronic TBI may cause abnormal patterns of brain activation to prevent mobilizing ''response inhibition,'' which describes a participant's capability to suppress an intended or already initiated manual action. It was concluded that such altered patterns of brain activation responsible for failure of executing ''response inhibition'' could be used to delineate military from civilian TBI. Other studies have examined MEG to detect neural changes in mTBI in OIF/OEF/OND veterans with blast injury.[24] This last study showed that abnormalities in the prefrontal cortex (PFC) were positively correlated with changes in mood lability, personality changes, concentration, and depression. It was hypothesized that MEG abnormalities may result from disconnection of multiple PFC circuits via axonal injury in TBI.

During the brain's resting state there are fluctuations in regional brain activity. The default mode network (DMN) involves discrete areas in the medial prefrontal, medial and lateral parietal, and medial and lateral temporal cortices.[25] Activation, deactivation, and connectivity within the DMN were shown to be altered in TBI and associated with cognitive impairment.[14] Patients with TBI have demonstrated sustained attention impairments that were associated with an increase in DMN activation, especially within the precuneus and posterior cingulate cortex.[26] These disruptions in DMN function in TBI were predicted by the amount of white matter damage in a tract connecting the right anterior insulae to the pre-supplementary motor area (SMA) and the dorsal anterior cingulate cortex.[27] *In summary, these findings suggest that TBI produces DAI, as demonstrated by cortical and subcortical white matter disruptions, and alterations in DMN functional circuits associated with neurocognitive, as well as emotional and behavioral, deficits that are characteristic of this condition.*

Neuroimaging of PTSD in military/veteran populations

Largely based on findings from basic science investigations, PTSD can be conceptualized as a cue- and context-associated fear conditioning (FC) process that is associated with amygdalar hyperresponsivity and prefrontal cortical impairments in fear inhibition.[28] It has been shown that fear-related sensory information is initially transmitted from cortical regions to the amygdala through the basolateral amygdala (BLA), which relays to the central nucleus of the amygdala (CeA) to activate fear responses through outputs to the hypothalamus and brainstem. By contrast, the infralimbic region within the PFC appears to be the primary candidate pathway to suppress fear responses via extinction learning.[29] The PFC inhibits the function of BLA by suppressing the conditioned fear responses after extinction training.[28–30] Although executive functions are maintained by widely distributed pathways, one key circuit in both disorders is the fronto-cingulo-parietal cognitive control network. Important hubs in this network have been associated with various executive function domains such as the anterior cingulate cortex involving cognitive control, the dorsolateral PFC mediating working memory, the inferior frontal gyrus and (pre-) SMA regulating response inhibition, and the parietal lobes involving attention and its control. Disruptions to this fronto-cingulo-parietal network could result in impairment in cognitive control, memory, attention, and inhibition of fear processing, which are relevant to PTSD and TBI.[31]

PTSD is associated with white matter changes and regional atrophy in the brain, resulting in emotional, behavioral, and functional deficits. Various subregions of the PFC, hippocampus, and amygdala that are involved in cognitive and behavioral regulation are important in the pathophysiology of PTSD. Neural changes in PTSD include a reduction in medial PFC gray matter volume, which may mediate behavioral disruption, personality changes, and impairments in cognitive control.[32,33] In an sMRI study, OIF/OEF

veterans with more severe PTSD symptoms showed gray matter volume loss in the temporal cortex, including the inferior temporal and parahippocampal gyrus regions.[34] Additionally, gray matter morphology in trauma-exposed individuals was compared in patients with and without PTSD.[35] The results of this meta-analysis demonstrated that there were consistent areas of gray matter volume reduction in the cingulate cortex, ventromedial PFC, temporal regions, and hippocampus in PTSD patients. In another study of structural and functional imaging, veterans with PTSD underwent ASL perfusion using MRI and DTI, in order to measure regional cerebral blood flow abnormalities and structural changes.[36] ASL-MRI findings demonstrated that veterans with PTSD had increased perfusion in the right parietal and superior temporal cortices, suggesting compensatory responses to regional volume losses. Using DTI, these individuals with PTSD showed reductions in white matter regions of the PFC, anterior cingulate cortex, and angular gyrus. In summary, these studies highlight the roles of the frontal, parietal, and temporal lobes in the pathophysiology of PTSD.

In PTSD, there are also distortions in traumatic memories that relate to dysfunction in the hippocampus.[37–40] Moreover, there have been findings of smaller hippocampal volumes in individuals with PTSD than in controls.[41] In male veterans with combat trauma, PTSD was associated with both smaller total hippocampal volumes and CA3/dentate gyrus subfield volumes, which may produce distorted contextual information.[40] There are also reports of hypothesized abnormalities in fear regulation from the BLA in PTSD. Following FC, veterans with PTSD (vs. combat controls) showed impairments in extinction learning and heightened amygdala activity as measured by fMRI in the safety context (i.e., the context in which extinction took place).[42] In contrast, in a fear danger context, these same veterans demonstrated lower activity in the amygdala than combat controls, suggesting dysregulation of fear in both safety and danger settings. In an fMRI study, decreases in ventral anterior cingulate cortical activation with repeated exposure to fearful stimuli predicted an increase in symptoms.[43] In summary, PTSD is associated with hyperactivity of the BLA producing fear responses, hypoactivity of the cingulate cortex resulting in mood regulation problems, and also smaller hippocampi associated with memory dysfunction.

PTSD severity was also associated with the extent of exposure to combat events, suggesting a potential dose-response relationship related to trauma.[44] In this last study of OEF/OIF combat veterans with PTSD, DTI and structural MRI and a variety of symptom scales were used. PTSD severity was associated with abnormal MRI findings and high FA on DTI. During the cognitive appraisal paradigm, the dorsolateral PFC appeared to be impaired in veterans with PTSD, who showed a lesser ability to activate this region, as measured by fMRI, than did combat controls.[45] Antidepressant treatment is known to enhance PFC function in PTSD. Veterans from OEF/OIF, with and without PTSD, were treated with the serotonin uptake inhibitor paroxetine, and underwent fMRI scans that were 12 weeks apart. An emotion regulation task was performed during each scan. Paroxetine treatment increased activation in both the left dorsolateral PFC and the SMA during emotion regulation and, therefore, was an effective treatment in this regard.[46] *In summary, impairments in function and volumes in the PFC, temporal cortex, and hippocampal regions may produce cognitive and memory changes in PTSD. These deficits along with cingulate cortical dysfunction may result in decreased top-down control of the amygdala, leading to increased sensitivity to fearful stimuli.*[28]

Only a few studies have examined neuroimaging alterations in the *comorbid condition of TBI and PTSD*. Davenport and coworkers used DTI to assess blast-related TBI injury and post-deployment PTSD in OIF/OEF service members.[47] The diagnosis of PTSD (with or without comorbid TBI) was associated with higher general FA and greater integrity of white matter fibers. In another study, OIF/OEF military veterans with mTBI and comorbid PTSD and depression were compared with non-TBI participants using high-angular resolution diffusion imaging.[48] There was a loss of white matter integrity that was associated with mTBI in a distributed pattern of major fiber bundles and smaller tracts. The diffuse loss of white matter integrity appears to be a consistent mechanism of damage specifically produced by blast injury. Amen and colleagues conducted a single photon emission computed tomography (SPECT) study of patients with either PTSD, TBI, or both conditions, compared with controls.[49] The study revealed that subjects with PTSD (compared with those with TBI) exhibited greater activity in the PFC and temporal lobes, cingulum, basal ganglia, insula, thalamus, and limbic regions. One interpretation of the relatively greater activation of these regions in PTSD patients may relate to the need to maintain normal function in damaged circuits from the TBI, producing a different signature of injury from that of either condition alone.

Other studies of *comorbid PTSD/TBI* have shown an array of functional network disruptions. In subjects with comorbid mTBI and PTSD, fMRI imaging showed that decoupling of hippocampal and PFC circuits might produce the disturbances of traumatic memories.[50] Another finding in this study was that the caudate/putamen was less connected to the PFC. These two network decouplings in PTSD/TBI may interact to regulate trauma memories, and any disconnection could contribute to this comorbid condition. In a SPECT study of veterans with *comorbid TBI and PTSD*, the DMN is differentially affected in those with PTSD and those with TBI. [51] This study showed that the DMN is hyperperfused in individuals diagnosed with PTSD and hypoperfused in patients diagnosed with TBI, providing a distinction between the two conditions. Further, individuals with the comorbid condition demonstrate perfusion to these regions that appears *intermediate* between PTSD and TBI. In another study of OEF/OIF/OND veterans with comorbid PTSD and mTBI who underwent sMRI, there were reductions in volume in the bilateral anterior amygdala in the comorbid group, compared with veterans with no history of either condition.[52] Amygdala volume reductions were predictive of poorer inhibitory control of behavior. The comorbid condition of TBI/PTSD appears to have a unique signature of neuroimaging findings.

To understand how these various gray and white matter deficits in mTBI and PTSD may produce their clinical impact, it is important to recognize the role of the ''connectome'' in brain injury. This term relates to the mapping and organization of neural pathways throughout the brain. These highly centralized long and short pathways integrate brain signals through gateway hubs from one region to another.[14] Even a small structural or cellular lesion that affects a major hub can be very disruptive to the functioning of a neural network, and thereby can affect associated behaviors and cognition. Wolf and Koch[14] hypothesized that damage to axons in TBI disrupts the timing of neural signals within and between brain networks in cortical and hippocampal cognitive circuits and limbic emotional regions. Loss of white matter integrity in mTBI in major fiber bundles and in smaller tracts, and structural and functional deficits in gray matter in frontal cortical, cingulate, hippocampal, and parietal cortices may produce the behavioral and cognitive dysfunction in comorbid TBI/PTSD. Additionally, there are perfusion deficits that are intermediate between PTSD and TBI, which may account for the overlapping and mixed clinical presentation between the two conditions.[51]

Translational Models in TBI, PTSD, and their Comorbidity

Using animal models enables better understanding of the pathophysiological mechanisms in TBI, PTSD and the comorbid condition. There is no single animal model for either TBI or PTSD that expresses the complexity of the human condition. However, widely utilized PTSD models, including fear conditioning/retention/extinction, inescapable stress, learned helplessness, prolonged immobilization, and others and have been well reviewed.[53] However, various stress or fear paradigms produce the behavioral and biological aspects of the PTSD phenotype including avoidant behavior, anxiety-like behavior, hyperarousal, cue- or context-induced fear responses, and alterations in brain or hypothalamic-pituitary-adrenal axis stress responses. FC and retention are often employed as an animal model for studying PTSD. FC has strong face validity in that fear cues and contexts become aversive and produce persistent fear behaviors, such as freezing and increased heartrate, startle, and avoidance, similar to PTSD symptoms. FC has good predictive validity as exposure/extinction treatments reduce clinical anxiety by exposing a patient to conditioned stimuli and extinguishing fear. The FC model has strong construct validity in that the theory of the disorder and the model converge through the formation of an association between a neutral and a threatening stimulus that produces cue and contextual fear responses. In the FC model, the fear cues and contexts recruit activation of a similar neurocircuitry, as seen in PTSD patients.[54]

There are several well-utilized models for blast and blunt trauma injury in rodent models that enable the study of their pathophysiology.[55] Blast models use the application of pressure waves to approximate blast TBI in humans. A blunt trauma is produced in the controlled cortical impact (CCI) model, in which an air- or electromagnetic-driven piston is used to penetrate the brain. The rodent fluid percussion injury (FPI) model is the most extensively utilized animal model of TBI that produces focal and diffuse brain injury dependent on the intensity of force applied to a cortical site of injury. Blast injury, CCI, and FPI models have strong face value, as they replicate the injury and behaviors of the human condition. They provide good construct validity, because the theory of the brain disorder and the model converge where the neurocircuitry disruption occurs in a fashion similarly to in TBI patients.

Only a few animal studies have modeled co-occurring disorders of TBI and PTSD. In one model, the PTSD paradigm used a combination of exposures to predator odor, repeated restraint, and inescapable footshock, whereas the mTBI component was concurrent CCI.[56] This study showed that these interventions produced unique signature of behavioral, inflammatory, pathological, and biochemical responses at acute time points. Another CCI model in rats produced loss of hippocampal and amygdala neurons, and also increased conditioned fear and anxiety-like behaviors.[57] This research group further developed a TBI model using CCI and a PTSD model of social defeat that produced greater anxiety-related behavior and fear behaviors within extinction sessions, compared with TBI and PTSD-only controls.[58] Further development of such animal models is essential for a greater understanding of the neurobiology, pathophysiological mechanisms, and treatment approaches to comorbid TBI/PTSD.

Pathophysiological Bases of TBI and PTSD

Primary and secondary injuries after TBI

TBI is initiated by a series of events beginning with a primary injury from the direct trauma, and results in a disruption of brain tissue.[59] The primary injury is produced by an external force; for example, a blast wave, a body or cranial impact, a projectile, and/or rapid acceleration-deceleration within the cranium. The primary brain injury produces cortical or subcortical contusions and lacerations, white matter hemorrhages, intracranial bleeding (subarachnoid hemorrhage or subdural hematoma), venous engorgement, vascular space enlargement, edema, and blood–brain barrier disruption.[59] DAI is the signature injury of TBI, is often caused by the acceleration-deceleration and angular forces on the brain, and is produced by stretching and shearing of axons. Shearing forces from the blast injury primarily produce lesions in the deep frontal white matter and subcortical structures while the common tensile effects produce axonal stretching.[60] *DAI has been hypothesized to be an interactive consequence of neuroinflammation and neurodegeneration, which is responsible for producing certain long-term complications of TBI.*[61,62]

TBI also produces cognitive and behavioral impairments through a process of secondary brain injuries to the critical neurocircuitry. Secondary molecular events follow primary injuries and represent metabolic, ischemic, cellular, oxidative, excitatory, and neuroinflammatory processes that produce neuronal injury and loss (see Fig. 1). These secondary injuries can occur within minutes, and can extend to months and perhaps years after the primary injury.[55] Additionally, these pathophysiological changes are associated with the synthesis and release of various neurochemicals that affect brain metabolism, cerebral blood flow, and ion homeostasis.[59,63] Mechanisms of neuronal and vascular damage include inflammation, calcium-mediated cell toxicity via proteolytic pathways, glutamate-mediated excitotoxicity, mitochondrial rupture, production of oxygen-free radicals, and release of apoptotic substances.[59,60] Notably, intra-axonal calcium increases activate the cysteine proteases, calpain and cathepsin, which produce protein degradation that damages the axon cytoskeleton. These changes further injure axons by producing swelling and disconnection and the signature pathology, DAI. Calpain in TBI and other neurodegenerative diseases is dysregulated, and produces neuronal injury and cell death, and, therefore, calpain inhibitors are possible neurotherapeutics for TBI.[64] These pathophysiological changes that produce axonal degeneration and disconnection and dendritic loss contribute to the associated cognitive and behavioral impairments. The apparent delays in TBI-induced disconnection via secondary injury mechanisms suggests that the process is amenable to therapeutic intervention.[60]

Neuroinflammatory pathologies in TBI

It has been established that neuroinflammation is a leading secondary injury mechanism following TBI.[65,66] Microglia are the innate immune cells of the CNS, and following TBI, these cells are activated. In addition, there is a breakdown of the blood–brain barrier, allowing further infiltration of neutrophils, macrophages, and lymphocytes into brain tissues. These inflammatory cells participate in phagocytosis and release pro- and/or anti-inflammatory cytokines and complement proteins that enclose foreign substances and limit local bleeding. As a result, there is an enhanced clearance of damaged cells and reduction of toxic effects accumulated by cellular degradation.[67] In addition to the well-known destructive and scavenging functions of the inflammatory process, recent studies have delineated a constructive role of neuroinflammatory cell responses in promoting brain tissue healing, restorative neuroplasticity, and cellular repair processes after TBI.[68–70] Specifically, distinct microglia/macrophage subpopulations can be defined

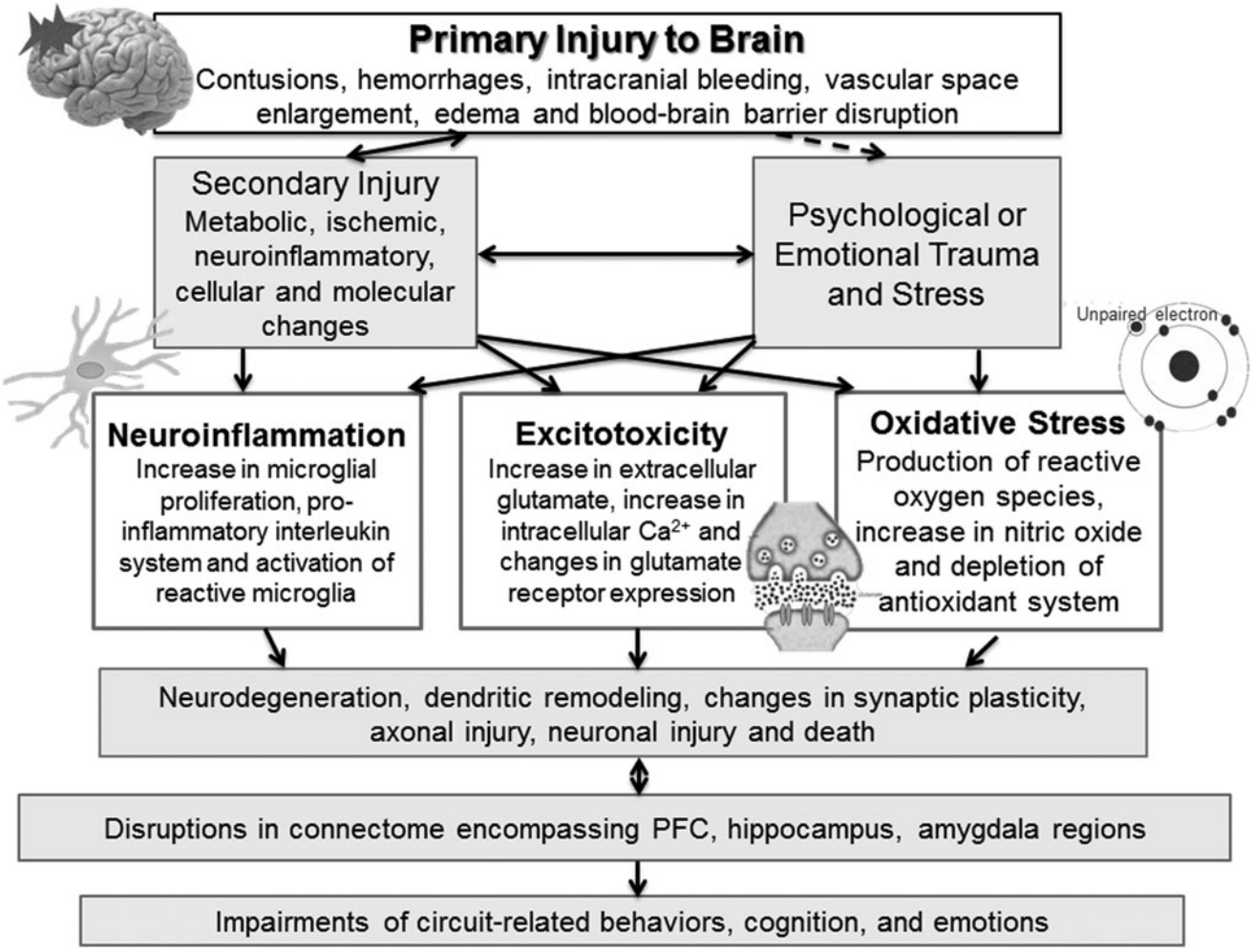

FIG. 1. Pathophysiological mechanisms leading to the brain circuit disruption and symptomatology of comorbid traumatic brain injury (TBI) and post-traumatic stress disorder (PTSD). Physical trauma may produce psychological trauma (broken line) and results in primary and secondary brain injuries. Primary injuries include brain contusions, hemorrhages, and vascular damage. Secondary injuries follow primary brain injuries and represent metabolic, ischemic, cellular, and molecular events, and produce neuronal injury. Secondary injury from TBI and from psychological trauma produces at least three major neuropathologies: oxidative stress, neuroinflammation, and glutamatergic excitotoxicity. These neural changes from physical and psychological trauma result in neurodegeneration, synaptic plasticity, dendritic remodeling, and neuronal injury and cell death in the prefrontal cortex (PFC), hippocampal, amygdalar, and other circuits. These changes in neural pathways mediating executive function, attentional and cognitive control, fear responses, and behavioral inhibition produce resultant neural dysfunction and symptoms characteristic of comorbid TBI and PTSD.

by unique surface antigens that correlate with different functions; that is, classically activated cells with cytotoxic and pro-inflammatory cytokine-releasing properties (M1 phenotype), alternative activated cells with pro-repair functions (M2A phenotype), immune regulatory cells (M2B phenotype), and deactivated cells (M2C phenotype).[71] The polarization continuum suggests that therapeutic strategies should aim to prevent over-polarization toward the M1 phenotype, but should enhance evolvement of the anti-inflammatory M2 phenotypes, to eventually install an optimal ratio of M1/M2 macrophages/microglia. Conversely, if TBI triggers chronically activated microglia, this causes damage to the neural cells and metabolism in the brain.[72,73] In a rat model of TBI, blood–brain barrier damage was confirmed by measuring immunoglobulin G (IgG) leakage, endothelial damage, activation of microglia (CD-68 expression), and reactive gliosis with heightened production of glial fibrillary acidic protein (GFAP). In a rat chronic TBI model (up to 3 months), myelin loss and microscopic bleeding that was co-localized with glial scars, and CD68 and IgG puncta staining of IgG and CD68, were observed.[74] In the last study, there were delayed increases in microvascular pathology after TBI that were associated with prolonged inflammation, blood–brain barrier disruption and progressive white matter degeneration. The cell surface marker of activated microglia, CD68, was also detected in the expanding cortical lesion 1 year after CCI in C57BL/6 mice.[75] It appears that in chronic TBI, there is long-term microglial activation that could be correlated with neural lesion expansion, continued neurodegeneration, and chronic demyelination.

TBI-initiated chronic activation of microglia has been shown to cause neural damage through the release of toxic substances such as pro-inflammatory cytokines, complement proteins, and proteases.[72] TBI generates time-dependent elevations of pro-inflammatory

cytokines of interleukin (IL)-1β, IL-6, and tumor necrosis factor-alpha (TNFα).[76–78] TNFα is involved in systemic inflammation, is produced by activated macrophage, and is highly relevant to TBI. A rodent model of FPI increased TNF-α mRNA expression at the site of injury in parietal cortex and its adjacent cortical regions, 1 and 6 h post-injury.[79] The increases in TNF-α mRNA and protein levels appeared to be dependent on the extent of injury in the ipsilateral cortex and hippocampus.[80] Complement proteins from neuroinflammatory processes can induce secondary neuropathology in TBI. Therefore, efforts to inhibit complements may reduce inflammation, neurodegeneration, and the resulting neurocircuitry disruptions. In experimental TBI, a novel anti-complement treatment was given after experimental TBI and applied to sites of injury.[81] Compared with placebo control treatment, this therapeutic approach reduced cortical neural cell membrane attack complexes, microglial proliferation, mitochondrial stress, cytokine production, and axonal damage, significantly improving neurological function.

Neuroinflammatory pathologies of PTSD

Neuroinflammation represents an important mechanism that causes neuronal damage and neurocircuitry disturbance in PTSD. Published literature shows evidence of neuroinflammatory responses in stress models and in PTSD models. Both acute and chronic stress increased microglial proliferation in the brain.[82] Stress-induced activation of microglial cells was produced in the hypothalamus, hippocampus, thalamus, substantia nigra, and central gray areas.[83] Moreover, chronic stress increased the number of activated microglia in multiple stress-sensitive brain regions possibly by augmenting their proliferation.[84] Predator stress exposure heightened levels of pro-inflammatory cytokine and NALP3 inflammasome proteins in the hippocampus and PFC.[85] Early life stressors were shown to sensitize microglial cells to induce exaggerated responses to stress later, which may contribute to the development of PTSD in the adulthood.[86] Another study reported that immobilization stress increased hypothalamic IL-1β mRNA expression in rats.[87]

Interleukins can promote neurodegeneration, disruption of neural networks, and consequent behavior disturbances, and have been investigated in stress and PTSD models. In a rat PTSD model, interleukin-beta (IL-1β) mRNA and protein levels were elevated in the hippocampus, PFC, and amygdala.[85] Intermittent footshock in rats caused changes in IL-6 in the hippocampus and cortex along with marked surges of IL-1β quantity in the hypothalamus.[88] Interestingly, psychosocial stressors also elevated IL-1β expression in the hypothalamus.[89] Conversely, IL-1β receptor knockout mice demonstrated a reduction of anxiety-related behaviors.[90] Clinically, cerebrospinal fluid (CSF) levels of IL-6 were found to be increased in veterans diagnosed with PTSD after returning from combat.[91] Further, compared with healthy controls, spontaneous production of IL-6 in white blood cells was detected in patients with PTSD and was correlated with PTSD symptom severity.[92] Lastly, levels of plasma IL-6 and norepinephrine were positively correlated in the PTSD group but not in controls.[91]

In one clinical[93] and two pre-clinical[94,95] studies, inflammatory responses were observed in the comorbid TBI/PTSD condition.[93,94] The clinical study evaluated 110 deployed, military personnel presenting with sleep disturbances related to TBI, PTSD, and depression. Logistic regression models were used to determine associations among blood plasma IL-6 level and quality of life ratings and service-related disorders. Quality of life was lower and plasma IL-6 concentrations were higher in military personnel with PTSD or depression. Military personnel with PTSD and depression were at higher risk for lower quality of life and higher plasma IL-6 concentrations. In a pre-clinical study of TBI/PTSD comorbidity using CCI and a predator stress model, rats demonstrated greater increases in activated microglial cells in the striatum, thalamus, and cerebral peduncle, compared with in those with PTSD alone or sham surgery controls.[94] Comparisons of levels of Ki-67-positive proliferating cells and DCX-positive migrating neural progenitor cells, as indicators of neuroinflammation and neurogenesis respectively, were made between TBI alone and TBI plus comorbid PTSD. This study revealed that PTSD did not further exacerbate the scales of the aforementioned neuropathological parameters relative to those of TBI-alone group.[94] Another study[95] examined anxiety and cognition changes in rats after repeated exposures to predator stress challenge alone or in combination with a single mild blast TBI. Rats with both TBI and stress exposures showed anxiety-related behaviors and spatial memory impairments that lasted up to 2 months. This TBI/PTSD group had a unique biochemical profile of elevated serum levels of stress and inflammatory biomarkers. *The combination of pre-clinical and clinical evidence indicate that the comorbidity of TBI/PTSD lowers quality of life of the patients, and that this may be partially caused by a shared pathophysiological process of neuroinflammation involving molecular, cellular, and network abnormalities that can be measured by specific biomarkers* (e.g., IL-1β, IL-6, TNFα, GFAP).

Glutamatergic pathologies of TBI

Glutamatergic dysregulation has been implicated in the pathophysiology of TBI. The most common of these include excitotoxicity from surges of extracellular glutamate and over-stimulation of glutamate receptors, and long-term potentiation (LTP)-related cerebral changes that impact cognition. Excitotoxicity during TBI results from an excessive stimulation of the glutamate *N*-methyl-D-aspartate (NMDA) and α-amino-3-hydroxy-5-methyl-4-isoxazolepropionic acid (AMPA) receptors that ultimately produce neuronal injury and cell death. Some of the most striking deficits of TBI are disruptions in attention, concentration, memory, and executive function related to the glutamate-mediated disturbances of neural networks and the loss of cognitive functioning.

Several animal and clinical studies have reported that TBI produces central glutamate-induced changes in extracellular glutamate, glutamate receptors, and related second messenger systems. In a human trauma study, transient increases in cerebral glutamate were seen daily after TBI, and these increases were associated with seizure activity.[96] Another study used a CCI model coupled with tissue microdialysis after moderate and severe TBI. This study also found several-fold increases in the level of frontal cortical glutamate.[97] In addition, a rat FPI model produced a short-term (4 day) decrease in glutamate NMDA NR2 subtype receptors, which was associated with alterations in calcium accumulation.[98] In other TBI models, there were decreases in AMPA receptor GluR2 subunit internalization, which enhanced calcium-permeable AMPA receptors and subsequently increased cellular vulnerability to excitotoxicity in the hippocampus.[99]

Glutamatergic effects resulting from TBI were also found to alter LTP, a cellular correlate of learning. Following FPI, LTP was blocked in brain slices from the hippocampal subregion CA1. This was associated with decreased NMDA potentials and glutamate-induced excitatory currents, and decreased expression of calcium calmodulin kinase II.[100] Patel and colleagues revealed that neuronal connectivity was altered by glutamatergic effects through specific

NMDA receptors in TBI.[101] In primary cortical neurons from rats after a TBI, individual neurons whose calcium oscillations were mostly caused by NMDA receptor subunit GluN2B, lost many of their functional targets after injury. After damage, activation of GluN2B receptors limited neural remodeling in response to a plasticity stimulus. In contrast, neurons with large GluN2A contributions or with high functional connectivity were protected against loss of connectivity. Thus, altered cortical glutamate NMDA receptor signaling appears to reshape neural networks in a receptor subtype-specific fashion in TBI models, and these cortical changes may impact cognition.

Another major mechanism for eliminating excessive glutamate is through uptake by excitatory amino acid transporters (EAAT) in astrocytes. Following TBI in humans, there was a decrease in the number of EAAT1-positive,[102] and EAAT2-positive cells.[103] The resultant reduction in glutamate uptake by astrocytes could be a major contributor to increased levels of extracellular glutamate and excitotoxic damage following TBI. There are many functional impacts of these glutamate-induced changes, including epileptiform activity. In a CCI model, cortical glutamate signaling were measured using glutamate biosensors along with cortical field potentials in brain slices.[104] In CCI-injured cortex, glutamate signaling increased electrical stimulation-evoked epileptiform field potentials, whereas markers for GABAergic interneurons were decreased. *In summary, TBI produces increases in cortical and hippocampal extracellular glutamate, reductions in glutamate transporters, and regulation of multiple glutamate receptors linked to increasing calcium flux. These alterations result in reduced GABAergic control, impairments in LTP, and increased epileptiform activity resulting in cell death. These neuronal changes may be linked to the cognitive impairments and increased seizure activity that follow TBI.*

Glutamate pathologies of PTSD

The glutamatergic system plays an important role in the pathophysiology of stress and PTSD. Restraint stress was reported to increase extracellular levels of glutamate in the medial PFC, hippocampus, striatum, and nucleus accumbens.[105] This glutamatergic enhancement was significantly higher in the PFC than in other brain regions. Subsequently, stress-induced production of glutamate in the PFC and hippocampus was reversed by adrenalectomy, whereas glucocorticoid replacement reversed this effect, demonstrating the role of stress hormones.[106] Acute restraint stress increased extracellular glutamate levels in amygdala subregions of the BLA and CeA, as measured by *in vivo* microdialysis.[107] Interestingly, stress-induced increases in BLA glutamate were reversed by the antidepressant tianeptine.[108] Additional studies found effects of stress on the phosphorylation states of specific serine residues on the AMPA receptor subunits GluA1 and GluA2, which regulate subcellular trafficking in the amygdala and medial PFC.[109] In this last study, stress increased GluA1 subunit phosphorylation, and post-stress administration of synthetic corticosteroid receptor antagonists reversed these effects. These stress-induced changes in glutamatergic transmission are hypothesized to mediate neuronal morphology remodeling and alter functional neurocircuitry and behavioral changes.[110]

In a recent study using a mouse model of comorbid mTBI (using CCI) and PTSD (using FC), there was enhanced acquisition of FC and delayed extinction in subjects with mTBI.[111] In this study, glutamate levels were increased, and the GABA/glutamate ratio was decreased in the ventral hippocampus. Further, GABA levels and GABA/glutamate ratios were both decreased in dorsal hippocampus. In a recent study using a murine modeling of mTBI and PTSD, it was demonstrated that BLA expression of NMDA receptors was significantly enhanced, coupling with decreases of GABAergic inhibitory neurotransmission in BLA and hippocampus.[112] These results support a notion that TBI may result in a loss of top-down control of PFC influence over the fear learning circuit and response to fear stimuli. *Therefore, glutamate/GABA balance in PFC, hippocampal and BLA circuits may be related to hippocampal memory function. A complete understanding of these neurochemical changes and how they relate to the fear circuit and memory is critical for the treatment of this comorbid condition.*

Oxidative stress and TBI

Free radicals can cause damage to proteins, DNA, and cell membranes by taking unpaired electrons from other molecules through oxidative processes. Oxidative damage results when toxic free radicals and reactive oxygen species (ROS) exceed the neural capacity to produce antioxidants to reverse these effects. The effects of oxidative damage on neuronal function following TBI are well documented in the literature (see Toklu and Tumer[113] for review). Additionally, oxidative stress increases blood–brain barrier permeability, and produces changes in synaptic plasticity, neurotransmission, and neural morphology.[114] Oxidative stress results in the reduction of a host of antioxidant enzymes, which contributes to the pathophysiology of TBI.[115] TBI produces ROS, such as the superoxide radicals and nitric oxide, which impair cerebral vascular function and produce ischemia. By enhancing ROS production, TBI reduces mitochondrial respiration and induces DNA deterioration, lipid peroxidation, protein and enzyme oxidation, and dysfunction. In one report, ROS changes produced impairments in the mitochondrial electron transport system and apoptosis, and all of these effects result in neuronal necrosis.[116] In this study, TBI resulted in mitochondrial fission, and treatment with a fission inhibitor improved hippocampal-dependent learning and memory, highlighting the utility of a mitochondrial approach. Because of the high rate of oxidative metabolism in the brain and its elevated levels of polyunsaturated lipids, which are the target of lipid peroxidation, neural circuits become vulnerable to oxidative stress. TBI-induced oxidative stress stimulates activation of neuroinflammatory cytokines and growth factors such as IL-1β, TNF-α, and transforming growth factor-beta (TGF-β).[117] In C57BL/6 mice with chronic TBI, long-term oxidative damage was found 1 year after injury, and was associated with lesion expansion, neural neurodegeneration, and demyelination.[75]

As mentioned, oxidative stress often overwhelms antioxidant responses involving the enzymes glutathione peroxidase, catalase, and superoxide dismutase. In a rat CCI model, hippocampal glutathione activity demonstrated a biphasic response that peaked at 12 h and again at 7 days.[118] Increased hippocampal catalase activity occurred steadily through the 1st week after injury, whereas hippocampal superoxide dismutase activity decreased initially after 6 h following injury and continued to decline through 14 days. These findings demonstrate a complex signature of antioxidant enzyme activity and synaptic proteins following TBI. In a CCI model, cortical tissues were analyzed for several antioxidants.[115] Antioxidant enzyme activity demonstrated a time-dependent increase in oxidative stress over hours and days. Because reduction in pre- and post-synaptic proteins (synapsin-I and PSD-95, respectively) also occurred early in this study, any concurrent depletion of antioxidant systems appeared to adversely affect synaptic function

and plasticity. Oxidative stress appears relevant in human TBI, as serial plasma oxidative and antioxidant markers were altered in patients with acute TBI versus controls.[119] In this last study, TBI patients showed increased serum glutathione levels and decreased erythrocyte superoxide dismutase levels. Using the Glascow Coma Scale as a behavioral outcome measure, serum glutathione and erythrocyte superoxide dismutase levels were higher in a subgroup with better functional outcomes than in a poor outcome subgroup. These findings highlight the pertinence and predictive nature of oxidative markers following human TBI.

Because the role of oxidative stress in TBI has been demonstrated in different models, there are a number of antioxidant therapeutic trials involving both experimental and clinical TBI. These trials utilize the ability of antioxidants to scavenge free radicals. A critical evaluation of evidence-based studies showed that antioxidant therapies such as amino acids, vitamins C and E, progesterone, *N*-acetylcysteine, and Enzogenol may serve as safe and effective adjunctive therapies in adult patients with TBI.[120] Although the impact of these treatments was limited, antioxidant therapies can be restorative, perhaps in combinatory therapies, because of their reversal of oxidative stress mechanisms.

Oxidative stress and PTSD

There is experimental evidence that increased oxidative stress is a factor in PTSD and in other stress models. In a rat model of inescapable footshocks, subjects displayed anxiety-like behavior, and showed enhanced fear acquisition and spatial memory deficits.[121] These behaviors were associated with increases in oxidation markers, nicotinamide adenosine dinucleotide phosphate (NADPH), oxidase 2 (NOX2), and 8-hydroxy-2-deoxyguanosine (8-OH-dG) in the hippocampus and PFC. In a model of single prolonged stress, rats displayed anxiety-like behaviors and enhancements in fear learning behavior that were associated with the increased expression of oxidation biomarkers of malondialdehyde, NOX2, and 4-hydroxynonenal in the hippocampus.[122] Additionally, in a predator stress model, there were increases in hippocampal, amygdala, and PFC levels of oxidative stress biomarkers such as superoxide, peroxynitrite, and total ROS.[85] Similarly, in human PTSD, a novel oxidative stress-related gene at the ALOX 12 locus moderated the association between PTSD and thinning of the right PFC.[123] This effect appeared to be localized to subregions including the middle frontal gyrus, superior frontal gyrus, anterior cingulate cortex, and medial orbitofrontal cortex. In summary, animal and human models of stress and PTSD show increases in oxidative stress biomarkers in the PFC, hippocampus, and amygdala. This oxidative damage in key neural circuits, along with neuroinflammation and excitotoxicity, results in changes in neural plasticity and morphology and disruption of neurotransmission.

One study examined neural oxidative damage in a comorbid model of repeated stress and mTBI.[124] Rats were divided into four groups that included naïve, repeated tail-shock stress, mTBI (using LFP), and a comorbid model of repeated stress followed by mTBI. After 1 week, repeated stress increased the expression of mitochondrial electron transport chain (ETC) complex protein subunits in the PFC, decreased pyruvate dehydrogenase (PDHE1α1) protein in the PFC and cerebellum, and decreased an ETC protein in the hippocampus. LFP alone decreased an ETC protein level in the ipsilateral hippocampus to the injury. The stress-mTBI group had its own synergistic profile of oxidative and mitochondrial damage. In summary, the comorbid TBI/PTSD condition has its own a unique profile of neuroinflammatory, oxidative damage and glutamatergic excitotoxicity damage in critical brain regions.

Neurodegeneration, Axonal Injury, and Dendritic Remodeling in TBI

Given these pathophysiological changes in PTSD, TBI, and their comorbid condition, we now discuss how neural structural changes develop in these disorders. TBI is associated with DAI, remodeling of dendritic connections, and spine loss. Dendritic spines provide the structural context for neuronal signaling and functional organization of synaptic connections. Therefore, any changes in neuronal morphology and dendritic spines have functional implications, as they reflect changes in synaptic strength.[125] Secondary molecular changes that are initiated in TBI, such as oxidative damage, glutamate excitotoxicity, and neuroinflammatory processes, interact with each other and produce neuronal damage and neurocircuitry dysfunction. Production of free oxygen radicals, superoxides, hydrogen peroxide, nitric oxide, and peroxynitrite impair the energy metabolism of the cells, impact membrane lipids, produce DNA fragmentation, and inhibit the mitochondrial electron transport system. This process induces apoptosis or necrosis of neural cells and neurites.[113] Activated microglia secrete various cytotoxic and neurotoxic factors that can lead to neuronal death. Microglia also release pro-inflammatory factors such as cytokines, and react to injury by secreting proteolytic enzymes that degrade the neuronal extracellular matrix and produce cellular debris (reviewed by Kou and VanderVord[126]). Finally, glutamate excitotoxicity with excessive activation of NMDA receptors produces neuronal damage. NMDA activation of sodium and calcium pathways, proteolytic enzymes, and initiation of cell death pathways are all mechanisms that produce cell damage and neurodegeneration.[127]

The loss of neurites is a consistent finding after TBI. In a CCI model in C57BL/6 mice, TBI acutely produced a 32% reduction of dendritic spines in the ipsilateral cortex and a 20% reduction in spines in the ipsilateral dentate gyrus. Additionally, there were >20% reductions in spines in the contralateral cortex and in the hippocampus.[128] These findings were replicated in another study in which spine density was reduced in ipsilateral cortical layers II and III and the dorsal dentate gyrus of the hippocampus.[129] TBI produced longer-term memory impairments accompanied by the shortening of PFC basal arbors at 4 months post-injury, and this occurred with findings of reduced density of both basal and apical spines in these neurons.[130] In contrast, another study indicated that at post-injury days 1, 7, and 28, brain-injured rats showed enhanced dendritic branch intersections in the BLA, as evidenced by Sholl analysis.[131]

There are physical and neurochemical mechanisms related to changes in neuronal morphology, neurites, and spine loss. An *in vitro* model of axonal stretch injury produced evidence of dendritic beading, and suggested that DAI alters dendrite structure and plasticity.[132] Another study used an electromechanical cell shearing device to produce strain injury in neurons or astrocytes in an extracellular matrix scaffold.[133] This study produced a range of strains and tracked fluorescent microbeads in an acellular matrix. Neuronal cell death and loss of neurites correlated with higher strain. Dendritic changes were also impacted indirectly through other mechanisms such as calcium dysregulation in TBI.[134] In this last study, TBI altered the calcium-sensitive phosphatase calcineurin and its effector cofilin, an actin-depolymerizing protein, and these changes coincided with dendritic synapse degeneration. In summary, there are direct physical insults and neurochemical factors that contribute to

TBI-induced dendritic and axonal injury. Cell death and dendrite degeneration in the cortex contribute to neural circuitry and behavioral dysfunctions in this condition.

DAI is the signature injury of TBI, and it results from the acute stretching and shearing of axons. This leads to disrupted axonal transport, axonal swelling, and secondary neuronal disconnection.[135] Data from studies of brain trauma in humans and on experimental brain trauma in animals indicate that DAI is a long-term process in which axons continue to degenerate and swell during an extended period. In the disconnected axons, both the β-amyloid precursor protein (β-APP) and other key enzymes (such as presenilin) for related amyloid-beta (Aβ) peptide generation accumulate in the swollen axonal bulbs.[136,137] After β-APP and Aβ are released from injured axons, accumulation occurs in the extracellular space as diffuse plaques.[137,138] Patients with TBI-related axonal injury produce an accumulation of β-amyloid proteins including β-APP and Aβ, and these are used as diagnostic markers of TBI.[139] Even a single brain trauma can result in the development of amyloid plaques, similar to those found in the brains of patients with other neurodegenerative diseases including Alzheimer's disease (AD), chronic traumatic encephalopathy (CTE), Dementia pugilistica, and amyotrophic lateral sclerosis (ALS).[140,136]

Neural Remodeling in PTSD

PTSD is a brain disorder that results from alterations in neural plasticity and dendritic remodeling, impacting neurocircuitry function and associated behaviors. Functionally, the amygdala has a central role in fear regulation, and PTSD may result from hyperactivity of neurons in the amygdala. This limbic hyperactivity may result from negative feedback impairments from the PFC, and atrophy of the hippocampal region.[141] In stress models, the aversive stimulus represented in sensory cortical circuits activates the CeA, which projects to brainstem monoaminergic cell body regions. This results in activation of widely disseminated serotoninergic, dopaminergic, and noradrenergic pathways that project to cortical and subcortical regions. In PTSD, cues and contexts associated with the aversive stimuli are represented in the PFC. Presentation of these cues and contexts activates PFC glutamatergic outputs, projecting to neurons in the BLA regulating the activation or inhibition of the amygdala.[142] Repeated FC and fear retention results in impairment of PFC inhibition of the BLA, producing long-term cue- and context-induced fear responses and stress responses of defensive behaviors, autonomic activity, hypothalamus–pituitary–adrenal axis activation, and limits on cognitive processes.[142,143]

Chronic stressors along with fear cues and contextual responses alter synaptic plasticity in rodent models. Electrophysiological studies have shown that stress modifies synaptic structure and function in the BLA, hippocampus, and PFC. Specifically, inescapable stress affects connections between the medial PFC and the BLA, and modifies both long-term depression (LTD) and LTP.[144] LTP persistently increases synaptic strength following repeated stimulation of a synapse, whereas LTD decreases synaptic strength. LTP is known to promote the formation of new spines and enhance dendritic complexity, whereas LTD reduces dendritic complexity or spines.[145] Exposure to inescapable stress reverses plasticity in the BLA, resulting in the promotion of LTP and the inhibition of LTD. After inescapable stress, LTP in the BLA is favored to encode memories of fear.[144] Moreover, stressed animals exhibit increased BLA plasticity as measured by neuronal firing rates and responsiveness.[146,147] In the PFC, some neurons respond during the occurrence of a stressor, whereas other neurons fire after the stress stops.[148]

There are neuronal morphological and dendritic changes associated with these plasticity changes in PTSD models. Pre-clinical studies have demonstrated that FC increased the rate of spine elimination in the frontal association cortex whereas fear extinction increased spine formation.[149] In contrast, FC increased dendritic spine density and dendritic morphology in the BLA, whereas subsequent extinction training reversed these effects.[150] Another study found that repeated stress increased spine numbers in lateral and basal amygdala subregions in distinct patterns, and increased dendritic length in the basal regions.[151] Repeated stress increased fear retention while it upregulated the density of total and mature dendritic spines in the dorsal hippocampus; this effect was reversed by anxiolytic treatment.[152] In summary, increases in BLA and hippocampal dendritic plasticity have been demonstrated in chronic stress or conditioned fear along with decreases in plasticity in PFC regions. This is hypothesized to produce increases in fear behaviors and fear memories and impairments in their extinction in PTSD. The molecular mechanisms underlying spine loss and dendritic retraction in chronically stressed animals have been reviewed recently.[153] Synaptic proteins including glutamatergic proteins, vesicular glutamate transporter 2, and GluR1, GluR2, NR1, NR2A, NR2B receptors, and many others play a role in the regulation of spine alterations and synaptic plasticity. Expression of these proteins in dendritic spines is influenced by chronic stress and fear conditioning.

There are few studies that have examined synaptic plasticity in comorbid models of TBI/PTSD. One study used footshock stress prior to TBI injury in C57BL/6 mice and examined synaptic plasticity in the lateral amygdala using whole-cell patch clamp electrophysiology.[154] In unstressed mice, TBI increased membrane excitability and spontaneous excitatory postsynaptic currents (sEPSCs) in lateral amygdala neurons, up to 3 months post-injury. Stress alone, in the absence of TBI, also increased sEPSC activity in these neurons. In the comorbid TBI/PTSD condition, sEPSC activity was *reduced* compared with in either condition alone, demonstrating different synaptic mechanisms in the comorbid condition. Another comorbid study showed that mice with mTBI demonstrated increased fear acquisition and delayed fear extinction.[111] In this study, mTBI/FC mice, showed a reduced GABA/glutamate ratio in the hippocampus at 25 days post-injury. These findings suggest that reductions in PFC plasticity and increases in BLA and hippocampal plasticity contribute to long-term fear retention and incomplete extinction. In another study examining TBI and post-injury behaviors at 7 and 30 days after a mild CCI injury, rats displayed greater anxiety-like behavior.[155] This combination of mTBI plus anxiety was associated with a loss of BLA GABAergic interneurons and reductions in spontaneous and miniature $GABA_A$-receptor-mediated inhibitory postsynaptic currents (IPSCs). These synaptic plasticity changes were associated with reduced BLA expression of inhibitory $\alpha 1$, $\beta 2$, and $\gamma 2$ $GABA_A$ receptor subunits, and with increases in the expression of excitation $\alpha 7$-nicotinic subunits. This suggests that reduction in inhibitory responses and increases in excitatory responses in the BLA may contribute to its hyperexcitability and to the development of fear-based disorders in comorbid TBI/PTSD. In this limited number of studies, comorbid TBI/PTSD produced a more unique synaptic and electrophysiological signature than either condition alone.

Translational Treatment Approaches and Conclusion

Despite intensive and extensive investment and the effort by basic or translational research to devise neuroprotective therapies

for brain trauma, the field has not been able to establish any standard treatment via randomized clinical trials. A meta-analysis examined the behavioral and cognitive effects of pharmacological treatments from 30 randomized controlled trials and open-label trials.[156] Only two trials showed some efficacy, one trial demonstrating that dopaminergic agonist methylphenidate produced improvements in irritability and aggression, whereas another trial showed that the cholinergic agent donepezil improved memory and attention. Certain other medications may benefit both conditions, such as antidepressants, stimulants, anticonvulsants, and hypnotics. In the clinic, great attention must be paid to the risks of each medication, and it is useful to start at a low dose, titrate slowly, and monitor side effects and benefits closely.

Based on the pathophysiological mechanisms reviewed in this article, there are several novel approaches that can be tested for TBI/PTSD, including the use of antioxidants, anti-inflammatory agents, and agents such as anticonvulsants that block excitoxicity. Antioxidants could be used to reduce inflammation, edema, the breakdown of the blood–brain barrier, expanding lesion size, and the associated neurological and behavioral deficits. Anti-inflammatory agents can suppress damaging response to astrocytes, microglia, monocytes or macrophages, neutrophils, and lymphocytes. In combination with other treatment agents targeting angiogenesis and neuroplasticity, they may synergistically increase therapeutic efficacy.[157] Anticonvulsant agents can be tested in order to block the epileptiform activity and seizures associated with TBI.

An example of a medication that reduces epileptiform activity and enhances the progression of neuroplasticity is the anticonvulsant agent valproic acid (VPA) (also known as sodium valproate and divalproex sodium). This commercially available histone deacetylase inhibitor (HDACi) produces transcriptional activation and neuronal dendritic sprouting, and enhances synaptic connectivity.[158,159] VPA also reduces the activation of microglia and other inflammatory markers after brain injury.[160] Several studies have demonstrated that VPA treatment is neuroprotective against glutamate excitotoxicity,[161] and ameliorates TBI-induced hippocampal damage.[162,163] Preliminary clinical studies suggest that VPA might be a useful treatment approach for the mood symptoms of TBI patients.[164,165] VPA reinforces fear extinction learning in human studies.[166] Our group has been studying VPA for its capacity to enhance learning, neuroprotection, neuroinflammation regulation, and synaptic plasticity. We demonstrated that VPA enhances extinction of fear responses in FC models,[150] and may be useful in a comorbid TBI/PTSD model.

In the clinic, the combination of TBI and PTSD produces persistent symptomatology, behavioral problems, and dysfunction for many veterans and civilians, and there is a need to develop better treatment approaches. Using animal models, investigators can examine the cognitive, behavioral, and neurobiological changes in this comorbid condition, and test the efficacy of new pharmacological and behavioral treatments. PTSD animal models can include fear conditioning, chronic unpredictable stress, immobilization stress, and others. Dependent measures of PTSD can include cue- and context-induced fear responses, and related measures of anxiety (e.g., elevated plus-maze, dark-light box), anhedonia (e.g., sucrose self-administration), depression (e.g., swim immobility), novelty responses, aggression, and other measures. TBI models can include FPI, CCI, blast injury, and others, and require some measurement of functional outcome (e.g., cognitive impairment). The temporal positioning of TBI or PTSD as the initial trauma event does not seem to make a significant difference in animal models in terms of triggering comorbid behavioral signs.[167] However, the impact of the sequential order of TBI and PTSD encountering on their comorbidity has not been systemically investigated in human cases. The comorbid modeling of TBI and PTSD can be quite complex, and decisions have to be made about the relevance of the models to the human condition and their sequence of onset as well as multiple behavioral, cognitive, and neurobiological outcomes and their time course.

The efficacies of therapeutic agents may be synergistically or additively enhanced by newly emerged combinatorial tactics that include multipotential drugs and even stem cell-based therapies.[168–170] Pharmacological trials have used pre-clinical models to suppress destructive neuroinflammatory responses, reverse oxidative damage and excitotoxicity, produce axonal and dendritic remodeling, initiate neurogenesis, and restore synapses in comorbid TBI/PTSD. Various forms of pharmacological and/or psychological training (extinction learning) reverse pathophysiological changes and produce axonal growth, dendritic remodeling, and neurocircuitry repair in TBI/PTSD. With further investigation, we hope to gain a better understanding of this devastating comorbid disorder in order to provide more efficacious, novel, and specific treatments.

Acknowledgments

This work was supported by Merit Review Award I01RX001144 from the United States Department of Veterans Affairs Rehabilitation Research and Development Service. The contents do not represent the views of the United States Department of Veterans Affairs or the United States Government. L.W., X.Z., and L.W. of Teng Lab were additionally supported by the Department of Defense (SC140194 to Y.D.T.), the Gordon Project of HMS, and China Scholarship Council, University of Wuhan Scholarship Fund, and Huazhang University of Science & Technology/Wuhan Union Hospital fellowships sponsored by Y.D.T. We thank Dr. David A. Williamson of Nexus Health Systems in Houston, Texas for his expertise in discussions of the psychiatric presentations of TBI and PTSD.

Author Disclosure Statement

No competing financial interests exist.

References

1. Stein, M.B., and McAllister, T.W. (2009). Exploring the convergence of posttraumatic stress disorder and mild traumatic brain injury. Am. J. Psychiatry 166, 768–776.
2. American Psychiatric Association (2013). *Diagnostic and Statistical Manual of Mental Disorders,* 5th ed. American Psychiatric Publishing: Washington, DC.
3. Howlett, J.R., and Stein, M.B. (2016). Prevention of trauma and stressor-related disorders: a review. Neuropsychopharmacology 41, 357–369.
4. Armed Forces Health Surveillance Center (US) (2011). Associations between repeated deployments to OEF/OIF/OND, October 2001–December 2010, and post-deployment illnesses and injuries, active component, U.S. Armed Forces. MSMR 18, 2–11.
5. Vasterling, J.J., and Dikmen, S. (2012). Mild traumatic brain injury and posttraumatic stress disorder: clinical and conceptual complexities. J. Int. Neuropsychol. Soc. 18, 390–393.
6. Hoge, C.W., McGurk, D., Thomas, J.L., Cox, A.L., Engel, C.C., and Castro, C.A. (2008). Mild traumatic brain injury in US soldiers returning from Iraq. N. Eng. J. Med. 358, 453–463.
7. Yurgil, K.A., Barkauskas, D.A., Vasterling, J.J., Nievergelt, C.M., Larson, G.E., Schork, N.J., Litz, B.T., Nash, W.P., and Baker, D.G. (2014). Association between traumatic brain injury and risk of posttraumatic stress disorder in active-duty Marines. JAMA Psychiatry 71, 149–157.

8. Seal, K.H., Bertenthal, D., Miner, C.R., Sen, S., and Marmar, C. (2007). Bringing the war back home: mental health disorders among 103,788 US veterans returning from Iraq and Afghanistan seen at Department of Veterans Affairs facilities. Arch. Intern. Med. 167, 476–482.
9. Wisco, B.E., Marx, B.P., Holowka, D.W., Vasterling, J.J., Han, S.C., Chen, M.S., Gradus, J.L., Nock, M.K., Rosen, R.C., and Keane, T.M. (2014). Traumatic brain injury, PTSD, and current suicidal ideation among Iraq and Afghanistan U.S. veterans. J. Trauma Stress 27, 244–248.
10. Belanger, H.G., Curtiss, G., Demery, J.A., Lebowitz B.K., and Vanderploeg, R.D. (2005). Factors moderating neuropsychological outcomes following mild traumatic brain injury: a meta-analysis. J. Int. Neuropsychol. Soc. 11, 215–227.
11. Capehart, B., and Bass, D. (2012). Review: managing posttraumatic stress disorder in combat veterans with comorbid traumatic brain injury. J. Rehabil. Res. Dev. 49, 789–812.
12. Zatzick, D.F., Rivara, F.P., Jurkovich, G.J., Hoge, C.W., Wang, J., Fan, M.Y., Russo, J., Trusz, S.G., Nathens, A., and Mackenzie, E.J. (2010). Multisite investigation of traumatic brain injuries, posttraumatic stress disorder, and self-reported health and cognitive impairments. Arch. Gen. Psychiatry 67, 1291–1300.
13. Vanderploeg, R.D., Belanger, H.G., and Curtiss, G. (2009). Mild traumatic brain injury and posttraumatic stress disorder and their associations with health symptoms. Arch. Phys. Med. Rehabil. 90, 1084–1093.
14. Wolf, J. A., and Koch, P.F. (2016). Disruption of network synchrony and cognitive dysfunction after traumatic brain injury. Front. Syst. Neurosci. 10, 43.
15. Amyot, F., Arciniegas, D.B., Brazaitis, M.P., Curley, K.C., Diaz-Arrastia, R., Gandjbakhche, A., Herscovitch, P., Hinds, S.R., Manley, G.T., Pacifico, A., and Razumovsky, A. (2015). A review of the effectiveness of neuroimaging modalities for the detection of traumatic brain injury. J. Neurotrauma 32, 1693–1721.
16. Wilde, E.A., Bouix, S., Tate, D.F., Lin, A.P., Newsome, M.R., Taylor, B.A., Stone, J.R., Montier, J., Gandy, S.E., Biekman, B., and Shenton, M.E. (2015). Advanced neuroimaging applied to veterans and service personnel with traumatic brain injury: state of the art and potential benefits. Brain Imaging Behav. 9, 367–402.
17. Michael, A.P., Stout, J., Roskos, P.T., Bolzenius, J., Gfeller, J., Mogul, D., and Bucholz, R. (2015). Evaluation of cortical thickness after traumatic brain injury in military veterans. J. Neurotrauma 32, 1751–1758.
18. Trotter, B.B., Robinson, M.E., Milberg, W.P., McGlinchey, R.E., and Salat, D.H. (2015). Military blast exposure, ageing and white matter integrity. Brain 138, 2278–2292.
19. Robinson, M.E., Lindemer, E.R., Fonda, J.R., Milberg, W.P., McGlinchey, R.E., and Salat, D.H. (2015). Close-range blast exposure is associated with altered functional connectivity in Veterans independent of concussion symptoms at time of exposure. Hum. Brain Mapp. 36, 911–922.
20. Yeh, P.H., Wang, B., Oakes, T.R., French, L.M., Pan, H., Graner, J., Liu, W., and Riedy, G. (2014). Postconcussional disorder and PTSD symptoms of military-related traumatic brain injury associated with compromised neurocircuitry. Hum. Brain Mapp. 35, 2652–2673.
21. Sorg, S.F., Schiehser, D.M., Bondi, M.W., Luc, N., Clark, A.L., Jacobson, M.W., Frank, L.R., and Delano-Wood, L. (2016). White matter microstructural compromise is associated with cognition but not posttraumatic stress disorder symptoms in military Veterans with traumatic brain injury. J. Head Trauma Rehabil. 31, 297–308.
22. Miller, D.R., Hayes, J.P., Lafleche, G., Salat, D.H., and Verfaellie, M. (2016). White matter abnormalities are associated with chronic postconcussion symptoms in blast-related mild traumatic brain injury. Hum. Brain Mapp. 37, 220–229.
23. Fischer, B.L., Parsons, M., Durgerian, S., Reece, C., Mourany, L., Lowe, M.J., Beall, E.B., Koenig, K.A., Jones, S.E., Newsome, M.R., and Scheibel, R.S. (2014). Neural activation during response inhibition differentiates blast from mechanical causes of mild to moderate traumatic brain injury. J. Neurotrauma 31, 169–179.
24. Huang, M.X., Nichols, S., Baker, D.G., Robb, A., Angeles, A., Yurgil, K.A., Drake, A., Levy, M., Song, T., McLay, R., and Theilmann, R.J. (2014). Single-subject-based whole-brain MEG slow-wave imaging approach for detecting abnormality in patients with mild traumatic brain injury. Neuroimage Clin. 5, 109–119.
25. Raichle, M.E. (2015). The brain's default mode network. Annu. Rev. Neurosci. 38, 433–447.
26. Bonnelle, V., Leech, R., Kinnunen, K.M., Ham, T.E., Beckmann, C.F., De Boissezon, X., Greenwood, R.J., and Sharp, D.J. (2011). Default mode network connectivity predicts sustained attention deficits after traumatic brain injury. J. Neurosci. 31, 13,442–13,451.
27. Bonnelle, V., Ham, T.E., Leech, R., Kinnunen, K.M., Mehta, M.A., Greenwood, R.J., and Sharp, D.J. (2012). Salience network integrity predicts default mode network function after traumatic brain injury. Proc. Natl. Acad. Sci. U. S. A. 109, 4690–4695.
28. Mahan, A.L., and Ressler, K.J. (2012). Fear conditioning, synaptic plasticity and the amygdala: implications for posttraumatic stress disorder. Trends Neurosci. 35, 24–35.
29. Quirk, G.J., and Mueller, D. (2008). Neural mechanisms of extinction learning and retrieval. Neuropsychopharmacology 33, 56–72.
30. Kim, J. J., and Jung, M.W. (2006). Neural circuits and mechanisms involved in Pavlovian fear conditioning: a critical review. Neurosci. Biobehav. Rev. 30,188–202.
31. Van Amelsvoort, T., and Hernaus, D. (2016). Effect of pharmacological interventions on the fronto-cingulo-parietal cognitive control network in psychiatric disorders: a transdiagnostic systematic review of fMRI studies. Front. Psychiatry 7, 82.
32. Rauch, S.L., Shin, L.M., Segal, E., Pitman, R.K., Carson, M.A., McMullin, K., Whalen, P.J., and Makris, N. (2003). Selectively reduced regional cortical volumes in post-traumatic stress disorder. Neuroreport 14, 913–916.
33. Yamasue, H., Kasai, K., Iwanami, A., Ohtani, T., Yamada, H., Abe, O., Kuroki, N., Fukuda, R., Tochigi, M., Furukawa, S., and Sadamatsu, M. (2003). Voxel-based analysis of MRI reveals anterior cingulate gray-matter volume reduction in posttraumatic stress disorder due to terrorism. Proc. Natl. Acad. Sci. U. S. A. 100, 9039–9043.
34. Aupperle, R.L., Connolly, C.G., Stillman, A.N., May, A.C., and Paulus, M.P. (2013). Deployment and post-deployment experiences in OEF/OIF veterans: relationship to gray matter volume. PLoS One 8, e75880.
35. Kuhn, S., and Gallinat, J. (2013). Gray matter correlates of posttraumatic stress disorder: a quantitative meta-analysis. Biol. Psychiatry 73, 70–74.
36. Schuff, N., Zhang, Y., Zhan, W., Lenoci, M., Ching, C., Boreta, L., Mueller, S.G., Wang, Z., Marmar, C.R., Weiner, M.W., and Neylan, T.C. (2011). Patterns of altered cortical perfusion and diminished subcortical integrity in posttraumatic stress disorder: an MRI study. Neuroimage 54, S62–S68.
37. Douglas, J. (1995). MRI-based measurement of hippocampal volume in patients with combat-related posttraumatic stress disorder. Am. J. Psychiatry 152, 973–998.
38. Gurvits, T.V., Shenton, M.E., Hokama, H., Ohta, H., Lasko, N.B., Gilbertson, M.W., Orr, S.P., Kikinis, R., Jolesz, F.A., McCarley, R.W., and Pitman, R.K. (1996). Magnetic resonance imaging study of hippocampal volume in chronic, combat-related posttraumatic stress disorder. Biol. Psychiatry 40, 1091–1099.
39. Gilbertson, M.W., Shenton, M.E., Ciszewski, A., Kasai, K., Lasko, N.B., Orr, S.P., and Pitman, R.K. (2002). Smaller hippocampal volume predicts pathologic vulnerability to psychological trauma. Nat. Neurosci. 5, 1242–1247.
40. Wang, Z., Neylan, T.C., Mueller, S.G., Lenoci, M., Truran, D., Marmar, C.R., Weiner, M.W., and Schuff, N. (2010). Magnetic resonance imaging of hippocampal subfields in posttraumatic stress disorder. Arch. Gen. Psychiatry 67, 296–303.
41. Karl, A., Schaefer, M., Malta, L.S., Dörfel, D., Rohleder, N., and Werner, A. (2006). A meta-analysis of structural brain abnormalities in PTSD. Neurosci. Biobehav. Rev. 30, 1004–1031.
42. Garfinkel, S.N., Abelson, J.L., King, A.P., Sripada, R.K., Wang, X., Gaines, L.M., and Liberzon, I. (2014). Impaired contextual modulation of memories in PTSD: an fMRI and psychophysiological study of extinction retention and fear renewal. J. Neurosci. 34, 13,435–13,443.
43. Stevens, J.S., Kim, Y.J., Galatzer-Levy, I.R., Reddy, R., Ely, T.D., Nemeroff, C.B., Hudak, L.A., Jovanovic, T., Rothbaum, B.O., and Ressler, K.J. (2016). Amygdala reactivity and anterior cingulate habituation predict posttraumatic stress disorder symptom maintenance after acute civilian trauma. Biol Psychiatry. [Epub ahead of print]
44. Bazarian, J.J., Donnelly, K., Peterson, D.R., Warner, G.C., Zhu, T., and Zhong, J. (2013). The relation between posttraumatic stress

disorder and mild traumatic brain injury acquired during Operations Enduring Freedom and Iraqi Freedom. J. Head Trauma Rehabil. 28, 1–12.
45. Rabinak, C.A., MacNamara, A., Kennedy, A.E., Angstadt, M., Stein, M.B., Liberzon, I., and Phan, K.L. (2014). Focal and aberrant prefrontal engagement during emotion regulation in veterans with posttraumatic stress disorder. Depress. Anxiety 31, 851–861.
46. MacNamara, A., Rabinak, C.A., Kennedy, A.E., Fitzgerald, D.A., Liberzon, I., Stein, M.B., and Phan, K.L. (2016). Emotion regulatory brain function and SSRI treatment in PTSD: neural correlates and predictors of change. Neuropsychopharmacology 41, 611–618.
47. Davenport, N.D., Lim, K.O., and Sponheim, S.R. (2015). White matter abnormalities associated with military PTSD in the context of blast TBI. Hum. Brain Mapp. 36, 1053–1064.
48. Morey, R.A., Haswell, C.C., Selgrade, E.S., Massoglia, D., Liu, C., Weiner, J., Marx, C.E., Cernak, I., and McCarthy, G. (2013). Effects of chronic mild traumatic brain injury on white matter integrity in Iraq and Afghanistan war veterans. Hum. Brain Mapp. 34, 2986–2999.
49. Amen, D.G., Raji, C.A., Willeumier, K., Taylor, D., Tarzwell, R., Newberg, A., and Henderson, T.A. (2015). Functional neuroimaging distinguishes posttraumatic stress disorder from traumatic brain injury in focused and large community datasets. PLoS One 10, e0129659.
50. Spielberg, J.M., McGlinchey, R.E., Milberg, W.P., and Salat, D.H. (2015). Brain network disturbance related to posttraumatic stress and traumatic brain injury in veterans. Biol. Psychiatry 78, 210–216.
51. Raji, C.A., Willeumier, K., Taylor, D., Tarzwell, R., Newberg, A., Henderson, T.A., and Amen, D.G. (2015). Functional neuroimaging with default mode network regions distinguishes PTSD from TBI in a military veteran population. Brain Imaging Behav. 9, 527–534.
52. Depue, B.E., Olson-Madden, J.H., Smolker, H.R., Rajamani, M., Brenner, L.A., and Banich, M.T. (2014). Reduced amygdala volume is associated with deficits in inhibitory control: a voxel- and surface-based morphometric analysis of comorbid PTSD/mild TBI. Biomed. Res. Int. 2014, 691505.
53. Yehuda, R. and Antelman, S.M. (1993). Criteria for rationally evaluating animal models of postraumatic stress disorder. Biol. Psychiatry 33, 479–486.
54. Vervliet, B., and Raes, F. (2013). Criteria of validity in experimental psychopathology: application to models of anxiety and depression. Psychol. Med. 43, 2241–2244.
55. Xiong, Y., Mahmood, A., and Chopp, M. (2013). Animal models of traumatic brain injury. Nat. Rev. Neurosci. 14, 128–142.
56. Ojo, J.O., Greenberg, M.B., Leary, P., Mouzon, B., Bachmeier, C., Mullan, M., Diamond, D.M., and Crawford, F. (2014). Neurobehavioral, neuropathological and biochemical profiles in a novel mouse model of co-morbid post-traumatic stress disorder and mild traumatic brain injury. Front. Behav. Neurosci. 8, 213.
57. Meyer, D.L., Davies, D.R., Barr, J.L., Manzerra, P., and Forster, G.L (2012). Mild traumatic brain injury in the rat alters neuronal number in the limbic system and increases conditioned fear and anxiety-like behaviors. Exp. Neurol. 235, 574–587.
58. Davies, D.R., Olson, D., Meyer, D.L., Scholl, J.L., Watt, M.J., Manzerra, P., Renner K.J., and Forster, G.L. (2016). Mild traumatic brain injury with social defeat stress alters anxiety, contextual fear extinction, and limbic monoamines in adult rats. Front. Behav. Neurosci. DOI: 10.3389/fnbeh.2016.00071.
59. Ray, S.K., Dixon, C.E., and Banik, N.L. (2002). Molecular mechanisms in the pathogenesis of traumatic brain injury. Histol. Histopathol. 17, 1137–1152.
60. Buki, A., and Povlishock, J.T. (2006). All roads lead to disconnection?—traumatic axonal injury revisited. Acta Neurochir. (Wien) 148, 181–194.
61. Goldstein, L.S. (2012). Axonal transport and neurodegenerative disease: can we see the elephant? Prog. Neurobiol. 99, 186–190.
62. Sharp, D.J., Scott, G., and Leech, R. (2014). Network dysfunction after traumatic brain injury. Nat. Rev. Neurol. 10, 156–166.
63. Risling, M., Plantman, S., Angeria, M., Rostami, E., Bellander, B.M., Kirkegaard, M., Arborelius, U., and Davidsson, J. (2011).Mechanisms of blast induced brain injuries, experimental studies in rats. Neuroimage 54, S89–S97.
64. Cagmat, E.B., Guingab-Cagmat, J.D., Vakulenko, A.V., Hayes, R.L., and Anagli, J. (2015). Potential use of calpain inhibitors as brain injury therapy, in: *Brain Neurotrauma: Molecular, Neuropsychological, and Rehabilitation Aspects*. F.H. Kobeissy (ed.). CRC Press/Taylor & Francis, Boca Raton, FL.
65. Dietrich, W.D., and Bramlett, H.M. (2015). Therapeutic hypothermia and targeted temperature management in traumatic brain injury: clinical challenges for successful translation. Brain Res. 1640, 94–103.
66. Witcher, K.G., Eiferman, D.S., and Godbout, J.P. (2015). Priming the inflammatory pump of the CNS after traumatic brain injury. Trends Neurosci. 38, 609–620.
67. Krishnamurthy, K., and Laskowitz, D.T. (2015). Cellular and molecular mechanisms of secondary neuronal injury following traumatic brain injury, in: *Translational Research in Traumatic Brain Injury*. D. Laskowitz, and G. Grant (eds.). CRC Press, Boca Raton, FL. pps. 97–126.
68. Burda, J.E., Bernstein, A.M., and Sofroniew, M.V. (2016). Astrocyte roles in traumatic brain injury. Exp. Neurol. 275, 305–315.
69. Myer, D.J., Gurkoff, G.G., Lee, S.M., Hovda, D.A., and Sofroniew, M.V. (2006). Essential protective roles of reactive astrocytes in traumatic brain injury. Brain 129, 2761–2772.
70. Donnelly, D.J., Gensel, J.C., Ankeny, D.P., van Rooijen, N., and Popovich, P.G. (2009). An efficient and reproducible method for quantifying macrophages in different experimental models of central nervous system pathology. J. Neurosci. Methods 181, 36–44.
71. Chhor, V., Le Charpentier, T., Lebon, S., Oré, M.V., Celador, I.L., Josserand, J., Degos, V., Jacotot, E., Hagberg, H., Sävman, K., and Mallard, C. (2013). Characterization of phenotype markers and neuronotoxic potential of polarised primary microglia in vitro. Brain Behav. Immun. 32, 70–85.
72. Dheen, S.T., Kaur, C., and Ling, E.A. (2007). Microglial activation and its implications in the brain diseases. Curr. Med. Chem. 14, 1189–1197.
73. Nagamoto-Combs, K., McNeal, D.W., Morecraft, R.J., and Combs, C.K. (2007). Prolonged microgliosis in the rhesus monkey central nervous system after traumatic brain injury. J. Neurotrauma 24, 1719–1742.
74. Glushakova, O.Y., Johnson, D., and Hayes, R.L. (2014). Delayed increases in microvascular pathology after experimental traumatic brain injury are associated with prolonged inflammation, blood–brain barrier disruption, and progressive white matter damage. J. Neurotrauma 31, 1180–1193.
75. Loane, D. J., Kumar, A., Stoica, B.A., Cabatbat, R., and Faden, A.I. (2014). Progressive neurodegeneration after experimental brain trauma: association with chronic microglial activation. J. Neuropathol. Exp. Neurol. 73, 14–29.
76. Ziebell, J.M., and Morganti-Kossmann, M.C. (2010). Involvement of pro- and anti-inflammatory cytokines and chemokines in the pathophysiology of traumatic brain injury. Neurotherapeutics 7, 22–30.
77. Morganti-Kossmann, M.C., Satgunaseelan, L., Bye, N., and Kossmann, T. (2007). Modulation of immune response by head injury. Injury 38, 1392–1400.
78. Lenzlinger, P.M., Morganti-Kossmann, M.C., Laurer, H.L., and McIntosh, T.K. (2001). The duality of the inflammatory response to traumatic brain injury. Mol. Neurobiol. 24, 169–181.
79. Fan, L., Young, P.R., Barone, F.C., Feuerstein, G.Z., Smith, D.H., and McIntosh, T.K. (1996). Experimental brain injury induces differential expression of tumor necrosis factor–α mRNA in the CNS. Mol. Brain Res. 36, 287–291.
80. Vitarbo, E.A., Chatzipanteli, K., Kinoshita, K., Truettner, J.S., Alonso, O.F., and Dietrich, W.D. (2004). Tumor necrosis factor α expression and protein levels after fluid percussion injury in rats: the effect of injury severity and brain temperature. Neurosurgery 55, 416–445.
81. Ruseva, M.M., Ramaglia, V., Morgan, B.P., and Harris, C.L. (2015). An anticomplement agent that homes to the damaged brain and promotes recovery after traumatic brain injury in mice. Proc. Natl. Acad. Sci. U. S. A. 112, 14,319–14,324.
82. Nair, A., and Bonneau, R.H. (2006). Stress-induced elevation of glucocorticoids increases microglia proliferation through NMDA receptor activation. J. Neuroimmunol. 171, 72–85.
83. Sugama, S., Fujita, M., Hashimoto, M., and Conti, B. (2007).Stress induced morphological microglial activation in the rodent brain: involvement of interleukin-18. Neuroscience 146, 1388–1399.
84. Tynan, R.J., Naicker, S., Hinwood, M., Nalivaiko, E., Buller, K.M., Pow, D.V., Day, T.A., and Walker, F.R. (2010). Chronic stress alters the density and morphology of microglia in a subset of stress-responsive brain regions. Brain Behav. Immun. 24, 1058–1068.

85. Wilson, C.B., McLaughlin, L.D., Nair, A., Ebenezer, P.J., Dange, R., and Francis, J. (2013). Inflammation and oxidative stress are elevated in the brain, blood, and adrenal glands during the progression of post-traumatic stress disorder in a predator exposure animal model. PLoS One 8, e76198.
86. Calcia, M.A., Bonsall, D.R., Bloomfield, P.S., Selvaraj, S., Barichello, T., and Howes, O.D. (2016). Stress and neuroinflammation: a systematic review of the effects of stress on microglia and the implications for mental illness. Psychopharmacology 233, 1637–1650.
87. Shintani, F., Nakaki, T., Kanba, S., Sato, K., Yagi, G., Shiozawa, M., Aiso, S., Kato, R., and Asai, M. (1995). Involvement of interleukin-1 in immobilization stress-induced increase in plasma adrenocorticotropic hormone and in release of hypothalamic monoamines in the rat. J. Neurosci. 15, 1961–1970.
88. Blandino, P., Barnum, C.J., Solomon, L.G., Larish, Y., Lankow, B.S., and Deak, T. (2009). Gene expression changes in the hypothalamus provide evidence for regionally-selective changes in IL-1 and microglial markers after acute stress. Brain Behav. Immun. 23, 958–968.
89. Barnum, C.J., Blandino, P., and Deak, T. (2008). Social status modulates basal IL-1 concentrations in the hypothalamus of pair-housed rats and influences certain features of stress reactivity. Brain Behav. Immun. 22, 517–527.
90. Koo, J.W., and Duman, R.S. (2009). Interleukin-1 receptor null mutant mice show decreased anxiety-like behavior and enhanced fear memory. Neurosci. Lett. 456, 39–43.
91. Baker, D.G., Ekhator, N.N., Kasckow, J.W., Hill, K.K., Zoumakis, E., Dashevsky, B.A., Chrousos, G.P., and Geracioti Jr, T.D. (2002). Plasma and cerebrospinal fluid interleukin-6 concentrations in post-traumatic stress disorder. Neuroimmunomodulation 9, 209–217.
92. Gola, H., Engler, H., Sommershof, A., Adenauer, H., Kolassa, S., Schedlowski, M., Groettrup, M., Elbert, T., and Kolassa, I.T. (2013). Posttraumatic stress disorder is associated with an enhanced spontaneous production of pro-inflammatory cytokines by peripheral blood mononuclear cells. BMC Psychiatry 13, 40.
93. Gill, J., Lee, H., Barr, T., Baxter, T., Heinzelmann, M., Rak, H., and Mysliwiec, V. (2014). Lower health related quality of life in US military personnel is associated with service-related disorders and inflammation. Psychiatry Res. 216, 116–122.
94. Acosta, S. A., Diamond, D.M., Wolfe, S., Tajiri, N., Shinozuka, K., Ishikawa, H., Hernandez, D.G., Sanberg, P.R., Kaneko, Y., and Borlongan, C.V. (2013). Influence of post-traumatic stress disorder on neuroinflammation and cell proliferation in a rat model of traumatic brain injury. PloS One 8, e81585.
95. Kwon, S.K., Kovesdi, E., Gyorgy, A.B., Wingo, D., Kamnaksh, A., Walker, J., Long, J.B., and Agoston, D.V. (2011). Stress and traumatic brain injury: a behavioral, proteomics, and histological study. Front. Neurol. 2, 12.
96. Vespa, P., Prins, M., Ronne-Engstrom, E., Caron, M., Shalmon, E., Hovda, D.A., Martin, N.A., and Becker, D.P. (1998). Increase in extracellular glutamate caused by reduced cerebral perfusion pressure and seizures after human traumatic brain injury: a microdialysis study. J. Neurosurg. 89, 971–982.
97. Palmer, A.M., Marion, D.W., Botscheller, M.L., Swedlow, P.E., Styren, S.D., and DeKosky, S.T. (1993). Traumatic brain injury-induced excitotoxicity assessed in a controlled cortical impact model. J. Neurochem. 61, 2015–2024.
98. Osteen, C. L., Giza, C.C., and Hovda, D.A. (2004). Injury-induced alterations in N-methyl-D-aspartate receptor subunit composition contribute to prolonged 45 calcium accumulation following lateral fluid percussion. Neuroscience 128, 305–322.
99. Bell, J. D., Park, E., Ai, J., and Baker, A.J. (2009). PICK1-mediated GluR2 endocytosis contributes to cellular injury after neuronal trauma. Cell Death Differ. 16, 1665–1680.
100. Schwarzbach, E., Bonislawski, D.P., Xiong, G., and Cohen, A.S. (2006). Mechanisms underlying the inability to induce area CA1 LTP in the mouse after traumatic brain injury. Hippocampus 16, 541–550.
101. Patel, T.P., Ventre, S.C., Geddes-Klein, D., Singh, P.K., and Meaney, D.F. (2014). Single-neuron NMDA receptor phenotype influences neuronal rewiring and reintegration following traumatic injury. J. Neurosci. 34, 4200–4213.
102. Beschorner, R., Dietz, K., Schauer, N., Mittelbronn, M., Schluesener, H.J., Trautmann, K., Meyermann, R., and Simon, P. (2007). Expression of EAAT1 reflects a possible neuroprotective function of reactive astrocytes and activated microglia following human traumatic brain injury. Histol. Histopathol. 22, 515–526.
103. Landeghem, F.K.V., Weiss, T., Oehmichen, M., and Deimling, A.V. (2006). Decreased expression of glutamate transporters in astrocytes after human traumatic brain injury. J. Neurotrauma 23, 1518–1528.
104. Cantu, D., Walker, K., Andresen, L., Taylor-Weiner, A., Hampton, D., Tesco, G., and Dulla, C.G. (2014). Traumatic brain injury increases cortical glutamate network activity by compromising GABAergic control. Cereb. Cortex 8, 2306–2320.
105. Moghaddam, B. (1993). Stress preferentially increases extraneuronal levels of excitatory amino acids in the prefrontal cortex: comparison to hippocampus and basal ganglia. J. Neurochem. 60, 1650–1657.
106. Moghaddam, B., Bolinao, M.L., Stein-Behrens, B., and Sapolsky, R. (1994). Glucocortcoids mediate the stress-induced extracellular accumulation of glutamate. Brain Res. 655, 251–254.
107. Reagan, L. P., Reznikov, L.R., Evans, A.N., Gabriel, C., Mocaër, E., and Fadel, J.R. (2012). The antidepressant agomelatine inhibits stress-mediated changes in amino acid efflux in the rat hippocampus and amygdala. Brain Res. 1466, 91–98.
108. Reznikov, L.R., Grillo, C.A., Piroli, G.G., Pasumarthi, R.K., Reagan, L.P., and Fadel, J. (2007). Acute stress-mediated increases in extracellular glutamate levels in the rat amygdala: differential effects of antidepressant treatment. Eur. J. Neurosci. 25, 3109–3114.
109. Caudal, D., Rame, M., Jay, T.M., and Godsil, B.P. (2016). Dynamic regulation of AMPAR phosphorylation in vivo following acute behavioral stress. Cell. Mol. Neurobiol. 36, 1331–1342.
110. Musazzi, L.,Treccani, G., and Popoli, M. (2015). Functional and structural remodeling of glutamate synapses in prefrontal and frontal cortex induced by behavioral stress. Front. Psychiatry 6, 60.
111. Schneider, B.L., Ghoddoussi, F., Charlton, J.L., Kohler, R.J., Galloway, M.P., Perrine, S.A., and Conti, A.C. (2016). Increased cortical gamma-aminobutyric acid precedes incomplete extinction of conditioned fear and increased hippocampal excitatory tone in a mouse model of mild traumatic brain injury. J. Neurotrauma 33, 1614–1624.
112. Reger, M.L., Poulos, A.M., Buen, F., Giza, C.C., Hovda, D.A., and Fanselow, M.S. (2012). Concussive brain injury enhances fear learning and excitatory processes in the amygdala. Biol. Psychiatry 71, 335–343.
113. Toklu, H.Z., and Tümer, N. (2015). Oxidative stress, brain edema, blood–brain barrier permeability, and autonomic dysfunction from traumatic brain injury, in: *Brain Neurotrauma: Molecular, Neuropsychological, and Rehabilitation Aspects*. F.H. Kobeissy (ed.). CRC Press/Taylor & Francis, Boca Raton, FL, pps. 7, 51–61.
114. Miller, M.W., and Sadeh, N. (2014). Traumatic stress, oxidative stress and post-traumatic stress disorder: neurodegeneration and the accelerated-aging hypothesis. Mol. Psychiatry, 11, 1156–1162.
115. Ansari, M.A., Roberts, K.N., and Scheff, S.W. (2008). Oxidative stress and modification of synaptic proteins in hippocampus after traumatic brain injury. Free Radic. Biol. Med. 45, 443–452.
116. Fischer, T.D., Hylin, M.J., Zhao, J., Moore, A.N., Waxham, M.N., and Dash, P.K. (2016). Altered mitochondrial dynamics and TBI pathophysiology. Front. Syst. Neurosci. 10, 29.
117. Fischer, T.D., Hylin, M.J., Zhao, J., Moore, A.N., Waxham, M.N., Dash, P.K., Abdul–Muneer, P. M., Chandra, N., and Haorah, J. (2015). Interactions of oxidative stress and neurovascular inflammation in the pathogenesis of traumatic brain injury. Mol. Neurobiol. 51, 966–979.
118. DeKosky, S.T., Taffe, K.M., Abrahamson, E.E., Dixon, C.E., Kochanek, P.M., and Ikonomovic, M.D. (2004). Time course analysis of hippocampal nerve growth factor and antioxidant enzyme activity following lateral controlled cortical impact brain injury in the rat. J. Neurotrauma 21, 491–500.
119. Wang, H.C., Lin, Y.J., Shih, F.Y., Chang, H.W., Su, Y.J., Cheng, B.C., Su, C.M., Tsai, N.W., Chang, Y.T., Kwan, A.L., and Lu, C.H. (2016). The role of serial oxidative stress levels in acute traumatic brain injury and as predictors of outcome. World Neurosurg. 87, 463–470.
120. Shen, Q., Hiebert, J.B., Hartwell, J., Thimmesch, A.R., and Pierce, J.D. (2016). Systematic review of traumatic brain injury and the impact of antioxidant therapy on clinical outcomes. Worldviews Evid. Based Nurs. 13, 380–389.
121. Sun, X. R., Zhang, H., Zhao, H.T., Ji, M.H., Li, H.H., Wu, J., Li, K.Y., and Yang, J.J. (2016). Amelioration of oxidative stress-induced phenotype loss of parvalbumin interneurons might contribute to the

beneficial effects of environmental enrichment in a rat model of post-traumatic stress disorder. Behav. Brain Res. 312, 84–92.
122. Liu, F.F, Yang, L.D., Sun, X.R., Zhang, H., Pan, W., Wang, X.M., Yang, J.J., Ji, M.H., and Yuan, H.M. (2015). NOX2 mediated-parvalbumin interneuron loss might contribute to anxiety-like and enhanced fear learning behavior in a rat model of post-traumatic stress disorder. Mol. Neurobiol. 53, 6680–6689.
123. Miller, M.W., Wolf, E.J., Sadeh, N., Logue, M., Spielberg, J.M., Hayes, J.P., Sperbeck, E., Schichman, S.A., Stone, A., Carter, W.C., and Humphries, D.E. (2015). A novel locus in the oxidative stress-related gene ALOX12 moderates the association between PTSD and thickness of the prefrontal cortex. Psychoneuroendocrinology 62, 359–365.
124. Xing, G., Barry, E.S., Benford, B., Grunberg, N.E., Li, H., Watson, W.D., and Sharma, P. (2013). Impact of repeated stress on traumatic brain injury-induced mitochondrial electron transport chain expression and behavioral responses in rats. Front. Neurol. 4, 196.
125. Schubert, V., and Dotti, C.G. (2007). Transmitting on actin: synaptic control of dendritic architecture. J. Cell Sci. 120, 205–212.
126. Kou, Z., and VandeVord, P.J. (2014). Traumatic white matter injury and glia activation: from basic science to clinics. Glia 62, 1831–1855.
127. Hardingham, G.E., and Bading, H. (2010). Synaptic versus extrasynaptic NMDA receptor signalling: implications for neurodegenerative disorders. Nat. Rev. Neurosci. 11, 682–696.
128. Winston, C.N., Chellappa, D., Wilkins, T., Barton, D.J., Washington, P.M., Loane, D.J., Zapple, D.N., and Burns, M.P. (2013). Controlled cortical impact results in an extensive loss of dendritic spines that is not mediated by injury-induced amyloid-beta accumulation. J. Neurotrauma 30, 1966–1972.
129. Campbell, J.N., Register, D., and Churn, S.B. (2012). Traumatic brain injury causes an FK506-sensitive loss and an overgrowth of dendritic spines in rat forebrain. J. Neurotrauma 29, 201–217.
130. Hoskison, M.M., Moore, A.N., Hu, B., Orsi, S., Kobori, N., and Dash, P.K. (2009). Persistent working memory dysfunction following traumatic brain injury: evidence for a time-dependent mechanism. Neuroscience 159, 483–491.
131. Hoffman, A.N., Paode, P.R., May, H.G., Ortiz, J.B., Kemmou, S., Lifshitz, J., Conrad, C.D., and Currier Thomas, T. (2017). Early and persistent dendritic hypertrophy in the basolateral amygdala following experimental diffuse traumatic brain injury. J. Neurotrauma 34, 213–219.
132. Monnerie, H., Tang-Schomer, M.D., Iwata, A., Smith, D.H., Kim, H.A., and Le Roux, P.D. (2010). Dendritic alterations after dynamic axonal stretch injury in vitro. Exp. Neurol. 224, 415–423.
133. LaPlaca, M. C., Cullen, D.K., McLoughlin, J.J., and Cargill, R.S. (2005). High rate shear strain of three-dimensional neural cell cultures: a new in vitro traumatic brain injury model. J. Biomech. 38, 1093–1105.
134. Campbell, J.N., Low, B., Kurz, J.E., Patel, S.S., Young, M.T., and Churn, S.B. (2012). Mechanisms of dendritic spine remodeling in a rat model of traumatic brain injury. J. Neurotrauma 29, 218–234.
135. Blennow, K., Hardy, J., and Zetterberg, H. (2012). The neuropathology and neurobiology of traumatic brain injury. Neuron 76, 886–899.
136. Gupta, R., and Sen, N. (2016). Traumatic brain injury: a risk factor for neurodegenerative diseases. Rev. Neurosci. 27, 93–100.
137. Gentleman, S.M., Nash, M.J., Sweeting, C.J., Graham, D.I., and Roberts, G.W. (1993). Beta-amyloid precursor protein (beta APP) as a marker for axonal injury after head injury. Neurosci. Lett. 160, 139–144.
138. Sherriff, F.E., Bridges, L.R., and Sivaloganathan, S. (1994). Early detection of axonal injury after human head trauma using immunocytochemistry for beta-amyloid precursor protein. Acta Neuropathol. 87, 55–62.
139. Ekmark-Lewen, S., Flygt, J., Kiwanuka, O., Meyerson, B.J., Lewén, A., Hillered, L., and Marklund, N. (2013). Traumatic axonal injury in the mouse is accompanied by a dynamic inflammatory response, astroglial reactivity and complex behavioral changes. J. Neuroinflammation 10, 44.
140. Chauhan, N.B. (2014). Chronic neurodegenerative consequences of traumatic brain injury. Restor. Neurol. Neurosci. 32, 337–365.
141. Apfel, B.A., Ross, J., Hlavin, J., Meyerhoff, D.J., Metzler, T.J., Marmar, C.R., Weiner, M.W., Schuff, N., and Neylan, T.C. (2011). Hippocampal volume differences in Gulf War veterans with current versus lifetime posttraumatic stress disorder symptoms. Biol. Psychiatry 69, 541–548.
142. Licznerski, P., and Duman, R.S. (2013). Remodeling of axo-spinous synapses in the pathophysiology and treatment of depression. Neuroscience 251, 33–50.
143. Pitman, R.K., Rasmusson, A.M., Koenen, K.C., Shin, L.M., Orr, S.P., Gilbertson, M.W., Milad, M.R., and Liberzon, I. (2012). Biological studies of post-traumatic stress disorder. Nat. Rev. Neurosci. 13, 769–787.
144. Maroun, M. (2006). Stress reverses plasticity in the pathway projecting from the ventromedial prefrontal cortex to the basolateral amygdala. Eur. J. Neurosci. 24, 2917–2922.
145. Bosch, M., and Hayashi, Y. (2012). Structural plasticity of dendritic spines. Curr. Opin. Neurobiol. 22, 383–388.
146. Kavushansky, A., Vouimba, R.M., Cohen, H., and Richter-Levin, G. (2006). Activity and plasticity in the CA1, the dentate gyrus, and the amygdala following controllable vs. uncontrollable water stress. Hippocampus 16, 35–42.
147. Manzanares, P.A.R., Isoardi, N.A., Carrer, H.F., and Molina, V.A. (2005). Previous stress facilitates fear memory, attenuates GABAergic inhibition, and increases synaptic plasticity in the rat basolateral amygdala. J. Neurosci. 25, 8725–8734.
148. Jackson, M.E., and Moghaddam, B. (2006). Distinct patterns of plasticity in prefrontal cortex neurons that encode slow and fast responses to stress. Eur. J. Neurosci. 24, 1702–1710.
149. Lai, C.S., Franke, T.F., and Gan, W.B. (2012). Opposite effects of fear conditioning and extinction on dendritic spine remodelling. Nature 483, 87–91.
150. Heinrichs, S.C., Leite-Morris, K.A., Guy, M.D., Goldberg, L.R., Young, A.J., and Kaplan, G.B. (2013). Dendritic structural plasticity in the basolateral amygdala after fear conditioning and its extinction in mice. Behav. Brain Res. 248, 80–84.
151. Padival, M.A., Blume, S.R., and Rosenkranz, J.A. (2013). Repeated restraint stress exerts different impact on structure of neurons in the lateral and basal nuclei of the amygdala. Neuroscience 246, 230–242.
152. Giachero, M., Calfa, G.D., and Molina, V.A. (2013). Hippocampal structural plasticity accompanies the resulting contextual fear memory following stress and fear conditioning. Learn. Mem. 20, 611–616.
153. Qiao, H., Li, M.X., Xu, C., Chen, H.B., An, S.C., and Ma, X.M. (2016). Dendritic spines in depression: what we learned from animal models. Neural Plast. 51, 1–26.
154. Klein, R. C., Acheson, S.K., Qadri, L.H., Dawson, A.A., Rodriguiz, R.M., Wetsel, W.C., Moore, S.D., Laskowitz, D.T., and Dawson, H.N. (2015). Opposing effects of traumatic brain injury on excitatory synaptic function in the lateral amygdala in the absence and presence of preinjury stress. J. Neurosci. Res. 94, 579–589.
155. Almeida-Suhett, C.P., Prager, E.M., Pidoplichko, V., Figueiredo, T.H., Marini, A.M., Li, Z., Eiden, L.E., and Braga, M.F. (2014). Reduced GABAergic inhibition in the basolateral amygdala and the development of anxiety-like behaviors after mild traumatic brain injury. PLoS One 9, e102627.
156. Wheaton, P., Mathias, J.L., and Vink, R. (2011). Impact of pharmacological treatments on cognitive and behavioral outcome in the postacute stages of adult traumatic brain injury: a meta-analysis. J. Clin. Psychopharmacol. 31, 745–57.
157. Corps, K.N., Roth, T.L., and McGavern, D.B. (2015). Inflammation and neuroprotection in traumatic brain injury. JAMA Neurol. 72, 355–362.
158. Lattal, K.M., Barrett, R.M., and Wood, M.A. (2007). Systemic or intrahippocampal delivery of histone deacetylase inhibitors facilitates fear extinction. Behav. Neurosci. 121, 1125–1131.
159. Lattal, K.M., and Wood, M.A. (2013). Epigenetics and persistent memory: implications for reconsolidation and silent extinction beyond the zero. Nat. Neurosci. 16, 124–129.
160. Lu, W.H., Wang, C.Y., Chen, P.S., Wang, J.W., Chuang, D.M., Yang, C.S., and Tzeng, S.F. (2013). Valproic acid attenuates microgliosis in injured spinal cord and purinergic P2X4 receptor expression in activated microglia. J. Neurosci. Res. 91, 694–705.
161. Leng, Y., and Chuang, D.M. (2006). Endogenous alpha-synuclein is induced by valproic acid through histone deacetylase inhibition and participates in neuroprotection against glutamate-induced excitotoxicity. J. Neurosci. 26, 7502–7512.
162. Yu, F., Wang, Z., Tanaka, M., Chiu, C.T., Leeds, P., Zhang, Y., and Chuang, D.M. (2013). Posttrauma cotreatment with lithium and

valproate: reduction of lesion volume, attenuation of blood–brain barrier disruption, and improvement in motor coordination in mice with traumatic brain injury. J. Neurosurg. 119, 766–773.
163. Dash, P.K., Orsi, S.A., Zhang, M., Grill, R.J., Pati, S., Zhao, J., and Moore, A.N. (2010). Valproate administered after traumatic brain injury provides neuroprotection and improves cognitive function in rats. PLoS One 5, e11383.
164. Beresford, T.P., Arciniegas, D., Clapp, L., Martin, B., and Alfers, J. (2005). Reduction of affective lability and alcohol use following traumatic brain injury: a clinical pilot study of anti-convulsant medications. Brain Inj. 19, 309–313.
165. Jorge, R., and Robinson, R.G. (2003). Mood disorders following traumatic brain injury. Int. Rev. Psychiatry 15, 317–327.
166. Kuriyama, K., Honma, M., Soshi, T., Fujii, T., and Kim, Y. (2011).Effect of D-cycloserine and valproic acid on the extinction of reinstated fear-conditioned responses and habituation of fear conditioning in healthy humans: a randomized controlled trial. Psychopharmacology 218, 589–597.
167. Sierra-Mercado, D., McAlliste, L.M., Lee, C.C., Milad, M.R., Eskandar, E.N., and Whalen, M.J. (2015). Controlled cortical impact before or after fear conditioning does not affect fear extinction in mice. Brain Res. 1606, 133–141.
168. Teng, Y.D., Yu, D., Ropper, A.E., Li, J., Kabatas, S., Wakeman, D.R., Wang, J., Sullivan, M.P., Redmond Jr, E., Langer, R., and Snyder, E.Y. (2011). Functional multipotency of stem cells: a conceptual review of neurotrophic factor-based evidence and its role in translational research. Curr. Neuropharmacol. 9, 574–585.
169. Snyder, E.Y., and Teng, Y.D. (2012). Stem cells and spinal cord repair. N. Engl. J. Med. 366, 1940–1942.
170. Teng, Y.D., and Eve, D.J. (2014). The future potential of regenerative medicine for neural therapy and repair: introduction to the ASNTR special issue from the 2014 meeting. Cell Transplant. 24, 589–590.

Address correspondence to:
Gary B. Kaplan, MD
VA Boston Healthcare System
940 Belmont Street
Brockton, MA 02301

E-mail: Gary.Kaplan@va.gov

Establishing an Organotypic System for Investigating Multimodal Neural Repair Effects of Human Mesenchymal Stromal Stem Cells

Devang K. Thakor,[1,2,5] Lei Wang,[1,2,3,5] Darcy Benedict,[1,2] Serdar Kabatas,[1,2,4] Ross D. Zafonte,[1] and Yang D. Teng[1,2,6]

[1]Departments of Physical Medicine & Rehabilitation and Neurosurgery, Harvard Medical School/Spaulding Rehabilitation Hospital Network, Brigham and Women's Hospital, and Massachusetts General Hospital, Boston, Massachusetts
[2]Division of Spinal Cord Injury Research, VA Boston Healthcare System, Boston, Massachusetts
[3]Department of Neurosurgery, Wuhan Union Hospital, Huazhong University of Science and Technology, Wuhan, Hubei, China
[4]Department of Neurosurgery, Taksim Education and Teaching Hospital, University of Healthsciences, Istanbul, Turkey
[5]These authors contributed equally to this work
[6]Corresponding author: *yang_teng@hms.harvard.edu*

Human mesenchymal stromal stem cells (hMSCs) hold regenerative medicine potential due to their availability, *in vitro* expansion readiness, and autologous feasibility. For neural repair, hMSCs show translational value in research on stroke, spinal cord injury (SCI), and traumatic brain injury. It is pivotal to establish multimodal *in vitro* systems to investigate molecular mechanisms underlying neural actions of hMSCs. Here, we describe a platform protocol on how to set up organotypic co-cultures of hMSCs (alone or polymer-scaffolded) with explanted adult rat dorsal root ganglia (DRGs) to determine neural injury and recovery events for designing implants to counteract neurotrauma sequelae. We emphasize *in vitro* hMSC propagation, polymer scaffolding, hMSC stemness maintenance, hMSC-DRG interaction profiling, and analytical formulas of neuroinflammation, trophic factor expression, DRG neurite outgrowth and tropic tracking, and *in vivo* verification of tailored implants in rodent models of SCI.

Keywords: human mesenchymal stem cells • spinal cord injury • dorsal root ganglion • polymer • organotypic culture

How to cite this article:
Thakor, D. K., Wang, L., Benedict, D., Kabatas, S., Zafonte, R. D., & Teng, Y. D. (2018). Establishing an organotypic system for investigating multimodal neural repair effects of human mesenchymal stromal stem cells. *Current Protocols in Stem Cell Biology*, e58. doi: 10.1002/cpsc.58

INTRODUCTION

Neurotrauma presents a significant clinical challenge due to severe pathological consequences and the exceedingly limited spontaneous regenerative capacity of the adult central nervous system (CNS). Multipotent human mesenchymal stromal stem cells (hMSCs) have been applied to animal models and to human patients with traumatic brain injury and spinal cord injury (SCI), with some functional benefits observed

Current Protocols in Stem Cell Biology e58
Published in Wiley Online Library (wileyonlinelibrary.com).
doi: 10.1002/cpsc.58

(Archambault et al., 2018; Parr, Tator, & Keating, 2007; Suzuki et al., 2014; Yoon et al., 2007; Zhang, Guan, Zhang, Zhang, & Dai, 2008). Specific neural recovery mechanisms of hMSCs, however, have not been systematically defined. Understanding how hMSCs promote neural repair is highly desirable because it would identify therapeutic targets and develop novel therapies. As such, studies have investigated how hMSCs and other types of non-neural progenitor cells facilitate neurite regeneration, promote recovery of neural plasticity, mitigate host neural cell or donor cell death and axon demyelination, modulate autoimmune response and astrogliosis, and impede neuroinflammation (Archambault et al., 2018; Garbuzova-Davis, Ehrhart, & Sanberg, 2017; Parr et al., 2007; Srivastava, Bulte, Shats, Walczak, & Bulte, 2016; Ulrich, do Nascimento, Bocsi, & Tárnok, 2015).

Given the diversity of potential therapeutic mechanisms engendered by the functional multipotency of stem cells (Garbuzova-Davis et al., 2017; Srivastava et al., 2016; Teng et al., 2008, 2011; Ulrich et al., 2015), it is imperative to devise screening platforms that recapitulate the essential complexity of the neurobiological environment while allowing controlled experimental manipulation and the analysis of key components and responses of neural pathophysiology (e.g., axotomy, neuroinflammation, apoptosis, reactive gliosis, trophic or tropic effect, neurite outgrowth, etc.). Explanted dorsal root ganglia (DRGs) are commonly used as a model of neural lesion and neuritogenesis (Thakor, Teng, & Tabata, 2009; Tonge et al., 2008), because they impose a self-contained neural organ that can be cultured in whole-mount preparations. The explantation procedure *per se* results in axotomy of the DRG neurons, which allows the quality and quantity of neurite regeneration to be evaluated in an *ex vivo* tissue culture setting (Neumann, Skinner, & Basbaum, 2005; Thakor et al., 2009). DRGs comprise sensory neuronal somata, satellite glial cells, Schwann cells, and macrophages (Costigan, Scholz, & Woolf, 2009). These cells and their physiological and pathophysiological interactions function in normal and repair/regenerative responses to nerve injury that can be investigated mechanistically (Scholz & Woolf, 2007; Thakor et al., 2009). In a recent study (Ropper et al., 2017), we experimented with hMSC-DRG co-cultures by plating hMSCs over adult rat DRG explants embedded in trophic factor reduced matrigel, a gelatinous protein mixture initially produced by Engelbreth-Holm-Swarm (EHS) mouse sarcoma cells (i.e., Matrigel®, manufactured and marketed by Corning Life Sciences and BD Biosciences). We found that proper matrigel plating introduced a substrate that was suitable for examining profiles of DRG neuritogenesis (Leclere et al., 2007; Thakor et al., 2009), whereas direct seeding of hMSCs enabled both physical and chemical communication with DRGs. Therefore, we hypothesized that establishing organotypic co-cultures of hMSCs and DRGs (with or without polymer scaffolding) would offer a unique system that could be specifically tailored to analyze cell neurogenic behaviors (e.g., neurite outgrowth, turning, innervation, synaptic formation) and their related molecular mechanisms (e.g., trophic or tropic factor release). This system can be used to investigate therapeutic effects of MSCs, neural stem cells (NSCs), or other types of stem cells on neurotrauma relevant outcomes, including axotomy, cell death, neuroinflammation, reactive gliosis, cell stemness maintenance, and regenerative responses. The events can be recapitulated directly by using a DRG following surgical removal, or with further manipulation *in vitro* to investigate selective targets (e.g., exposure to specific trophic or tropic factor, and proinflammatory or anti-inflammatory molecules). Importantly, desirable stem cell or polymer scaffolding features determined by this platform technology may be used to design stem cell-based multimodal implants to investigate or offer repair and regenerative mechanisms *in vivo* for the injured or diseased spinal cord or brain (Kaplan et al., 2018; Ropper et al., 2017; Teng et al., 2002, 2011, 2012; Yu et al., 2009).

Here we provide protocols for establishing a unique organotypic hMSC-DRG co-culture system and provide two leads of its application in the neurotropic and trophic assessment

and neuroinflammatory investigation of hMSCs and DRG cells (e.g., primary sensory neurons, satellite cells and endothelial cells). Basic Protocol 1 describes characterization, propagation, and scaffold incorporation of hMSCs; Basic Protocol 2 describes how to prepare and analyze hMSC-DRG co-cultures; and Basic Protocol 3 describes an effective *in vivo* hMSC transplant strategy and analysis of neural repair in rat SCI models. Investigators with a background or experience in stem cell biology, neuroscience, and working with rodents will be able to effectively set up the organotypic co-culture system and rat SCI models.

NOTE: All cells are cultured in a humidified 37°C, 5% CO_2 incubator. The following procedures using live cells are performed in sterile equipment and solutions aseptically.

NOTE: Strictly follow chemical and biological safety rules in performing all laboratory tasks.

NOTE: All animal procedures should be performed in accordance with institutional animal care and use committee (IACUC) approved protocols that are in full compliance with NIH (or NIH equivalent institutions in other countries) guidelines.

NOTE: Strict aseptic technique is essential during animal surgery to prevent perisurgical infection and consequential loss of the subjects.

hMSC PREPARATION AND POLYMER SCAFFOLD INCORPORATION

BASIC PROTOCOL 1

This protocol details procedures for hMSC maintenance, biodegradable polymer fabrication, and seeding polymers with hMSCs.

Materials

hMSC line: e.g., normal human bone marrow-derived mesenchymal stem cells (ATCC®, cat. no. PCS-500-012™)

Any established hMSC line can be characterized following the procedures and parameters described in protocol. For our original studies, hMSC lines were established from cells obtained from either a 26-year-old male donor (7023-R) or a 29-year-old female donor (7038-L) at the Tulane University Center for Gene Therapy, an NIH-funded cell distribution center (Haragopal et al., 2015; Ropper et al., 2017).

hMSC lines derived from donors must be systematically examined for their cell biological features. In our own studies, we did not observe any difference between the two cell lines and used the cells in approximately equal numbers in the assays.

Dulbecco's Modified Eagle Medium with high glucose (HG-DMEM, Thermo Fisher Scientific, cat. no. 11965084)

10,000 U/mL Penicillin-Streptomycin (Thermo Fisher Scientific, cat. no. 15140148)

100 × MEM non-essential amino acids solution (Thermo Fisher Scientific, cat. no. 11140050)

Fetal bovine serum (FBS, Thermo Fisher Scientific, cat. no. 10438034)

Recombinant human basic fibroblast growth factor (bFGF; 146 aa) protein (R&D Systems, cat. no. 233-FB-025)

0.25% trypsin/1 M EDTA (Thermo Fisher Scientific, cat. no. 25200056)

0.05% trypsin/0.5 mM EDTA (Thermo Fisher Scientific, cat. no. 25300-054)

Cell dissociation medium (Accutase®; Innovative Cell Technologies, cat. no. AT104)

0.4% trypan blue solution (ThermoFisher Scientific, cat. no. 15250061)

Phosphate buffered saline (PBS; Boston Bioproduct, cat. no. BM-220)

4% paraformaldehyde (PFA; Sigma-Aldrich, cat. no. 158127) in PBS

Primary antibodies (Table 1) and secondary antibodies (Table 2) for immunocytochemistry (ICC) and immunohistochemistry (IHC)
Anti-fading medium containing DAPI (Vector laboratories, cat. no. H1200)
StemPro™ Adipogenesis Differentiation Kit (Thermo Fisher Scientific, cat. no. A1007001)
StemPro™ Osteogenesis Differentiation Kit (Thermo Fisher Scientific, cat. no. A1007201)
StemPro™ Chondrogenesis Differentiation Kit (Thermo Fisher Scientific, cat. no. A1007101)
Von Kossa kit for calcium stain (Abcam, cat. no. ab150687)
Alizarin Red S (Sigma-Aldrich, cat. no. A5533)
Oil Red O (Sigma-Aldrich, cat. no. O0625)
Alcian Blue (Sigma-Aldrich, cat. no. A3157)
Phosphate buffer (PB; Sigma-Aldrich, cat. no. P3619)
Poly(lactide-co-glycolide) (PLGA; Sigma-Aldrich, cat. no. P2191), 50:50 lactide:glycolide, Mn 30,000 to 60,000 Da
PLGA-polylysine (PLGA-PLL; PolySciTech, cat. no. AI028): PLGA block Mn ~30,000 Da, polylysine block Mn ~10,000 Da
Chloroform (Sigma-Aldrich, cat. no. CX1050)
Salt particles, 350- to 500-μm diameter (made from rock salt; Thermo Fisher Scientific, cat. no. S71989)

6- and 12-well tissue culture plates (Sigma-Aldrich, cat. nos. CLS3506 and CLS3512)
Glass coverslips (Fisher Scientific, cat. no. 22-293232)
CKX31 inverted tissue culture microscope (Olympus Life Science)
Zeiss Axiovert 200 microscope equipped with an Axiocam CCD camera (Carl Zeiss Microscopy)
Glass vials for casting PLGA scaffold (Sigma-Aldrich, cat. no. Z256161).
Parafilm® (Sigma-Aldrich, cat. no. P7793)

hMSC propagation, quality control, and characterization

1a. Plate passage 2 (P2) or passage 3 (P3) hMSCs at 5×10^3 cells/cm^2 in MSC culture medium composed of HG-DMEM supplemented with 0.1 mM nonessential amino acids, 1% penicillin/streptomycin, 10% (v/v) MSC-qualified FBS, and 1 ng/ml bFGF.

Cultures can be grown in T75, T175, or T225 flasks, depending on the number of cells required.

1b. For ICC assays, plate hMSCs onto glass coverslips in 12-well plates at 5×10^3 cells/cm^2 and incubate the culture for 1 week at 37°C, 5% CO_2.

2. Incubate cultures at 37°C, 5% CO_2.

3. Change the medium every other day, and split cultures 1:2 in MSC culture medium every 6 or 7 days, when cultures reach 80% to 90% confluence.

Double the volume of medium when the density reaches >60%.

4. Dissociate the cells for 5 to 15 min using 0.05% trypsin/0.5 mM EDTA or "Cell Dissociation Medium" (Accutase®) at 37°C, split cultures 1:2 in fresh MSC culture medium.

Use 0.25% trypsin/1M EDTA for more firmly attached cells.

5. Perform a trypan blue exclusion test to check cell viability at each passage. Viability rates should be >98%.

a. Measure the cell density of the cell line suspension using a hemacytometer.
b. Prepare a 0.4% solution of trypan blue in PBS (pH 7.2 to 7.3).
c. Add 0.1 ml trypan blue stock solution to 0.1 ml of cells.
d. Load a hemocytometer and examine immediately under a microscope at low magnification. Count the number of trypan blue-stained cells and the total number of cells. Cell viability should be >98%.

Note: % viable cells = [1.00 – (no. blue cells ÷ no. total cells)] × 100.

6a. To control for quality of stemness, quantify the fraction of hMSCs in the culture by FACS analysis. At least 90% of the cells in the culture should be positive for hMSC markers (e.g., HLA-I, CD147, CD90, CD105, CD49c, CD29, etc.) and negative for non-hMSC markers (e.g., CD36, CD34, CD19, CD11b, etc.). Include non-labeled cells as a control group, run FACS analysis for marker identification (i.e., positive selection population vs. negative selection population vs. no label cells). Lastly, determine the presence and proportions of the cell populations qualified for use.

We recommend first developing FACS protocols to detect combinations of described surface or intracellular (e.g., HLA-I, etc.) markers. After harvesting the hMSCs, label the candidate surface antigens, then fix, permeabilize, and label intracellular antigens.

Antibodies (see Table 1 for primary antibodies and Table 2 for secondary antibodies) can be validated by immunocytochemistry (ICC) assays that require relatively small quantities of hMSCs. Always examine cell images systematically using a high quality microscope (e.g., Zeiss Axiovert 200 microscope or other models with equivalent or enhanced functions).

hMSC cultures should be >90% positive for the positive markers and <10% for non-hMSC markers. Specifically, for passage 2 cells, more than 95% of cells should express CD90, CD105, CD49c, CD29, CD59, CD73a, and CD44. Ninety to 95% should express CD147 and HLA-I. Fewer than 5% should express CD36, CD34, CD19, CD11b, CD45, CD117, CD3, CD14, CD79a, CD271, or CD106. Five to 10% should express CD49b or CD184.

6b. For ICC assays, fix cultured cells on coverslips for 30 min with 4% paraformaldehyde (PFA) in PBS at 37°C. Stemness can be confirmed by ICC using antibodies against the cell surface markers CD90 (1:200) and CD105 (1:200). As a negative control, stain one sample with secondary antibody alone. Mount the coverslips with stained cells onto slides in an antifade mounting medium containing DAPI.

7. A qualified hMSC line should possess the ability to differentiate into a variety of cell types, including osteoblasts, chondrocytes, and adipocytes. For example, phenotypic multipotency of hMSCs at P2 or P3 can be characterized by (i) standard Von Kossa stain assay or Alizarin Red S, which should stain >60% of cells after osteogenic differentiation; and (ii) standard Oil Red O histochemical assay, which should stain >60% of cells after adipogenic differentiation; or (iii) Alcian blue stain, which should stain >60% of cells after for chondrogenesic differentiation.

Differentiation kits are available from StemPro (see Materials list).

8. Use P5 to P12 hMSC cultures for *in vitro* and *in vivo* experiments (Haragopal et al., 2015; Ropper et al., 2017).

Prepare PLGA scaffold

Based on our previous work (Lavik et al., 2002; Pritchard et al., 2010; Teng et al., 2002; Yu et al., 2009), we use the following refined protocol to fabricate PLGA scaffolds

Table 1 Primary Antibodies

Target	Supplier	Cat. No.	Dilution
GFAP	Millipore Sigma	G3893	1:1,000
CD11b	Bio-Rad	MCA275R	1:250
CD68	Chemicon	MABF216	1:250
Nitrotyrosine	Santa Cruz	SC-32757	1:250
Nestin	Santa Cruz	SC-21249	1:200
Doublecortin	Santa Cruz	SC-8066	1:250
Laminin	Sigma-Aldrich	L9393	1:60-100
CD31	Santa Cruz	SC-1506	1:250
IL-10	Santa Cruz	SC-365858	1:250
5HT	Immunostar	20080	1:10K-20K
Synapsin	Abcam	Ab64581	1:500
Synaptophysin	Thermofisher Scientific	PA1-1043	1:100
STRO-1	Thermofisher Scientific	398401	1:200
Collagen I	Thermofisher Scientific	MA1-26771	1:2,000
Collagen II	Novus Biologicals	NBP1-77795	1:200
Collagen IV	Thermofisher Scientific	MA5-13437	1:50
ALP	Santa Cruz	SC-373737	1:250
CD90	Santa Cruz	SC-6071	1:300
CD90	BD Pharmingen	BD 555593;	1:200
CD105	Thermofisher Scientific	12-1051-82	1:200
Human Mitochondria Antigen	Millipore Sigma	MAB1273	1:100-250
Human Laminin a5	Millipore Sigma	MAB1924	1:1,000
Laminin a2 (human or mouse)	Sigma-Aldrich	L0663	1:1,000
β3-tubulin	BioLegend	MRB-435P	1:300
Neurofilament M	Millipore Sigma	AB5735	1:1000
Human Heat Shock Protein 27	Enzo Life Sciences	ADI-SPA-800	1:250-300
BDNF	Abcam	108319	1:300
BDNF	Promega	G1641	1:250
GDNF	Abcam	ab18956	1:400-600
vGlutT1	Millipore Sigma	MABS132	1:1,000
vGlutT2	Millipore Sigma	AB2251	1:6,000

tailored with unique porous, soft, and smooth features to maintain the stemness biology of hMSCs (Ropper et al., 2017).

Synthesize the hMSC scaffolds from a blend of 75% PLGA:25% PLGA-PLL (by weight). Fabricate the porous scaffold through a salt-leaching process as described (Teng et al., 2002, and Lavik, Teng, Snyder, & Langer, 2002).

9. Prepare a 0.03% to 0.1% (w/v, which defines the degree of softness) solution of the polymer blend in chloroform, and cast the polymer blend over salt with a particle diameter range of 350 to 500 μm inside a glass vial to ~2:1 volume ratio (salt:PLGA solution).

Table 2 Secondary Antibodies

Target	Vender	Cat. No.	Dilution
Donkey anti-mouse Texas Red IgG	Jackson ImmunoResearch	715-075-151	1:250
Donkey anti-mouse Texas Red IgG	Sigma-Aldrich	SAB3701111	1:200
Goat anti-mouse Texas Red IgG	Abcam	Ab6787	1:1000-5000
Donkey anti-mouse FITC IgG	Jackson ImmunoResearch	715-095-150	1:250
Donkey anti-rabbit FITC IgG	Jackson ImmunoResearch	715-095-152	1:250
Donkey anti-goat DyLight 594 IgG	Jackson ImmunoResearch	705-515-003	
Donkey anti-chicken Texas Red IgG	Jackson ImmunoResearch	703-075-155	1:250
Donkey anti- rabbit Texas Red IgG	Jackson ImmunoResearch	715-075-152	1:250
Donkey anti-rabbit FITC IgG	Jackson ImmunoResearch	715-095-152	1:200-250
Donkey anti-guinea pig FITC IgG	Jackson ImmunoResearch	706-095-148	1:250

Note: FITC: Fluorescein

10. Allow the solvent to evaporate under an organic solvent-resistant desiccator in a contained environment (Grayson, Cima, & Langer, 2005).

11. After drying the construct, cut/shave the salt/PLGA layer off the glass. Leach the salt from the construct by soaking overnight in sterilized distilled water followed by a series of washes with fresh sterile distilled water the next morning, or vice versa.

12. Place scaffolds in sterile Petri dishes and air-dry in a laminar flow hood for a few hours (with germicidal lamp turned off). Trim scaffolds to the designed sizes and shapes (1 × 2 × 3 mm for *in vitro* assay and 1 × 2 × 4 mm for *in vivo* implantation), and store individual scaffolds in a –20°C freezer inside Parafilm®-sealed microcentrifuge tubes.

    Note: Importantly, PLGA scaffolds in harder texture, more rigid and uneven fabrication patterns, and smaller pore sizes can induce mesenchymal phenotypic differentiation of hMSCs even under regular maintenance medium incubation. Try to avoid this outcome in neural therapeutic investigations or applications of scaffolded hMSCs in the CNS.

Incorporate hMSCs into PLGA scaffold

13. Treat the scaffolds with 100% FBS overnight to promote cell adhesion (Kang et al., 2012).

14. Wash the pretreated scaffolds with MSC culture medium and place them in a low-adhesion 6-well plate.

15. Suspend hMSCs at 2×10^7 cells/ml in MSC culture medium, add 6 μl of hMSC suspension onto each scaffold, and incubate scaffolds for 3 hr at 37°C, 5% CO_2, to permit hMSC attachment.

    During this time, scaffolds should be frequently and carefully observed, ideally at intervals not greater than 10 to 15 minutes, and additional 6-μl aliquots of MSC culture medium are added when scaffolds begin to dry.

16. After 3 hr, add 2 ml MSC culture medium into the wells, and incubate overnight at 37°C, 5% CO^2. Repeat the seeding procedure the following day, and maintain MSC-incorporated scaffolds in MSC culture medium at 37°C, 5% CO^2 until use.

17. To confirm hMSC seeding, fix hMSC-incorporated scaffolds for 3 hr in 4% paraformaldehyde in 0.1 M PB or PBS (pH 7.4), cryosection the scaffolds at 50 μm, perform a standard hematoxylin and eosin staining, and microscopically confirm that the construct meets the required qualifications (Thakor, Spigelman, Tabata, & Nishimura, 2007).

BASIC PROTOCOL 2

DRG EXTRACTION AND CO-CULTURE WITH hMSCs ALONE OR SEEDED IN SCAFFOLD

Technical and operational specifics together with study design logistics are demonstrated here to ensure productive applications for establishing an organotypic system of DRG and hMSC co-cultures to investigate neural repair actions of adult hMSCs.

Materials *(also see Basic Protocol 1)*

Adult female and male rats (235 to 250 g)
Ketamine hydrochloride (Putney, cat. no. 045-290)
Xylazine hydrochloride (Lloyd Inc., cat. no. 139-236)
Matrigel matrix, growth factor reduced basement membrane matrix (Corning, cat. no. 356230); free of viruses, including lactose dehydrogenase elevating virus
hMSCs (Basic Protocol 1)
1 × 2 × 3-mm PLGA scaffolds, with and without hMSCs (Basic Protocol 1)
Lipopolysaccharides (LPS; Sigma-Aldrich, cat. no. L4391)
Phosphate buffer (PB; Sigma-Aldrich, cat. no. P3619)
Normal donkey serum (Jackson ImmunoResearch, cat. no. 017-000-121)
Primary antibodies (Table 1) and secondary antibodies (Table 2) for ICC and IHC detection of β3-tubulin; neurofilament M; human heat shock protein 27, brain-derived neurotrophic factor (BDNF), and glial cell line-derived trophic factor (GDNF)
Tumor necrosis factor α (TNFα) Quantikine ELISA kit (R&D System, cat. no. DTA00C)
BDNF Quantikine ELISA kit (R&D System, cat. no. DBNT00)
RNAqueous™ Total RNA Isolation Kit (RNAqueous kit, Thermo Fisher Scientific, cat. no. AM1912)
SuperScript™ III Platinum™ One-Step qRT-PCR Kit (Thermo Fisher Scientific, cat. no. 11732088)
Fast SYBR™ Green Master Mix (Thermo Fisher Scientific, cat. no. 43-856-12)

Stemi SV 11 stereomicroscopes (Carl Zeiss Microscopy)
Surgical tools, including: tissue scissors, needle holder, and surgical blades for general incision, dissection, and sutures; curved rongeur 0.7 mm (Fine Science Tools, cat. no. 16121-14); curved Moria spring scissors (Fine Science Tools, cat. no. 15396-01); Agricola retractors (Fine Science Tools, cat. no. 17005-04); Alm retractor with blunt teeth (Fine Science Tools, cat. no. 17009-07); Adson forceps (Fine Science Tools, cat. no. 11027-12); Curved Vannas spring scissors (Fine Science Tools, cat. no. 15071-08)
24-well plates (Sigma-Aldrich, cat. no. CLS3524)
Transwell inserts (Sigma-Aldrich, cat. no. CLS3450)
Nikon Eclipse TE300 inverted microscope (Nikon) equipped with a Spot RT-Slider CCD camera (Diagnostic Instruments Inc., model RT910)
NIS-Elements AR 4.30.0 System (Nikon) for confocal imaging analysis
Zeiss Axiovert 200 microscope equipped with an Axiocam CCD camera (Carl Zeiss)

Zeiss LSM1 confocal microscope (Carl Zeiss)
Adobe Photoshop CS4 11.0.1 or a further updated version (Adobe)
ImageJ software (NIH, Bethesda, MD)
7900HT Fast Real-Time PCR System (Thermo Fisher Scientific, cat. no. 4329001)

DRG extraction

1. Deeply anesthetize adult female and male rats (235 to 250 g) with 75 mg/kg ketamine and 10 mg/kg xylazine administered by intraperitoneal injection.
2. Under a stereomicroscope, make a vertical incision from T5 (thoracic level 5) to S1 (sacral level 1) after standard skin disinfection. Remove the muscular tissue and carefully perform laminectomy from T6 to L5 by using a fine tipped rongeur.
3. Expose bilateral DRGs from T6 to L5 and harvest them gently by cutting the neural fibers at both ending and existing zones of the distal and proximal nerve roots of the DRG using curved Moria spring scissors (Fig. 1A).

   Similar procedures can be used to dissect and remove mouse DRGs for establishing organotypic systems (Sleigh, Greg, Weir, & Schiavo, 2016).

4. Place the DRGs in ice-cold DRG culture medium, composed of DMEM supplemented with 10% FBS, and incubate floating culture for 12 hr at 37°C, 5% CO_2 before plating.

Co-culture of DRGs with hMSCs

5. Direct co-culture (**Fig.** 1**B-I**):

   a. Coat a set of 6-well plates with a thin layer of matrigel: add a small pool of growth factor reduced matrigel to the center of each well and then aspirate to leave a thin layer.
   b. Place one DRG onto the center of each well, incubate for 10 min at 37°C, 5% CO_2, and then fill the well with 2 ml DRG culture medium.
   c. Plate hMSCs onto DRG-containing wells at 3×10^5 hMSCs/well, co-culture for 24 to 72 hr at 37°C, 5% CO_2.
   d. Evaluate neurite outgrowth, and measure secretion of BDNF (or CNTF: ciliary neurotrophic factor) and proinflammatory or anti-inflammatory cytokines. To measure BDNF and cytokine levels, remove 2 ml media for ELISA (enzyme-linked immunosorbent assay) assays and follow test kit protocols.

6. Indirect co-cultures: Plate hMSCs into 6-well plates, and plate DRGs into the center of transwell inserts designed for 6-well plates. The inserts are then placed into the wells of the hMSC-containing plates, and co-cultures are maintained in 4 ml DRG culture medium at 37°C, 5% CO_2.

Co-culture of DRGs with scaffolded MSCs

7. Coat twelve-well plates with matrigel (25 to 50 μl/well of a 12-well plate).
8. Seed a single DRG into the center of each well.
9. Quickly place a $1 \times 2 \times 3$-mm piece of hMSC-incorporated PLGA scaffold in the pool of matrigel, and before the matrigel sets, use forceps to position the hMSC-PLGA scaffold 2 mm away from the DRG and at a ~45° angle from either the proximal or distal axotomy of the DRG.

   Alternate the placement of hMSC-incorporated scaffolds to control for potential differences in neuritogenic capacity between proximal and distal axotomy of the DRG (Fig. 1B and C).

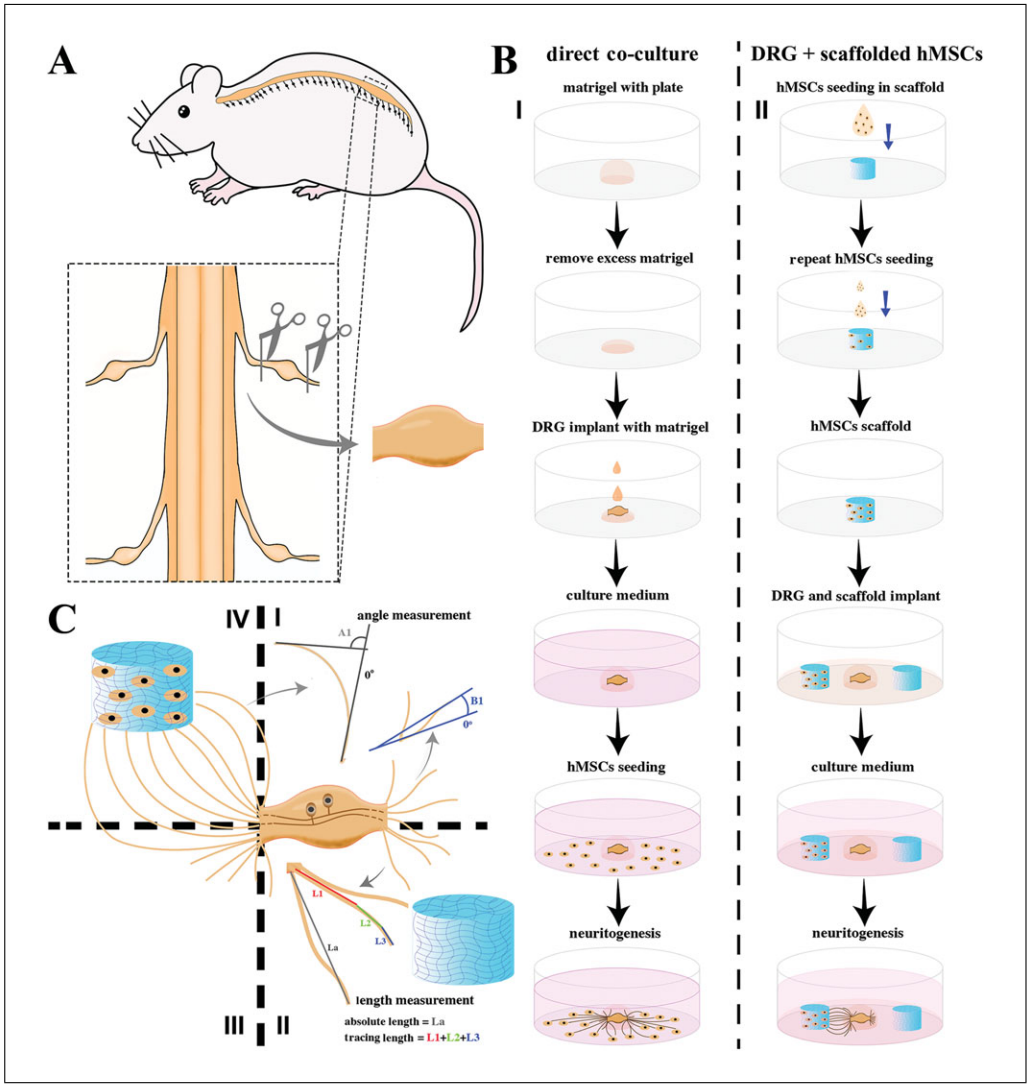

Figure 1 Platform design of an organotypic system for co-culturing hMSCs and explanted adult rat DRGs. (**A**) A schematic presentation of the anatomical location and surgical procedure for adult rat DRG collection. Please refer to surgery methods for anesthesia and operation details. (**B**) Bench workflow charts of procedures for setting up direct co-cultures of an explanted DRG with hMSCs only (**B-I**) or co-cultures for an explanted DRG with polymer-scaffolded hMSCs (**B-II**; anticipated DRG neurite outgrowth patterns are illustrated). (**C**) Schematic illustrations of formulas used to calculate the primary turning angle of a regrowing DRG neurite. The angle derived between nerve fiber A's two segments is 97.10°, and 11.70° for nerve fiber B (**c-I**). The two methods to compute the "tracing length" and the "absolute length" of a DRG neurite are shown in **C-II**. Schematic images show that neurites of an adult rat DRG neurons grow more robustly from the axotomy side proximal to the scaffolded hMSCs (i.e., neurotrophic effect; **IV**) and preferentially tracking human MSCs after 48 hr of co-culture (i.e., neurotropic effect; **III**). By contrast, neurites on the opposite side of the DRG, proximal to a control polymer scaffold (no hMSCs), showed limited regrowth of nerve fibers that project in a more random trajectory (**II**).

10. Place an unseeded scaffold (with or without coating of medium conditioned by hMSC culture, depending on the purpose and design of the assay) in the pool near the opposite axotomy, so that each DRG can be used as its own control (Fig. 1B and C).

11. Gently apply 75 µl of matrigel to coat the entire assembly, and incubate 15 min at 37°C, 5% CO_2, to permit the matrigel to solidify.

12. Add 1 ml DRG culture medium to each well, and maintain co-cultures under the same condition for the desired amount of time. This allows the generation of co-cultures with a fixed distance between the scaffolded hMSCs and DRG.

    We typically incubate up to 48 hr to observe neurite outgrowth.

13. For neuroinflammatory experiments, plate DRGs in growth factor reduced matrigel in 24-well plates, and place a 1 × 2 × 3-mm piece of hMSC-seeded PLGA scaffold into the matrigel next to the DRG. After the matrigel has set, add 500 µl DRG culture medium to each well, and culture at 37°C, 5% CO_2. At 24 hr after plating, replace the medium with serum-free DRG culture medium containing various concentrations of LPS to induce neuroinflammation. Examine the effects of LPS at a pre-determined time point based on the hypothesis to be tested (Ropper et al., 2017).

    Dissolve LPS in distilled water at a stock concentration of 200 µg/µl and then add it to the culture medium to generate different final concentrations at 10, 50, or 100 µg/ml.

Immunocytochemical assays for co-cultures

14. Fix co-cultures in situ—inside the wells—for 2 to 3 hr in 4% paraformaldehyde in 0.1 M PB at 37°C, wash with PBS, and block co-cultures for 1 hr at room temperature with 1% to 2% (v/v) donkey serum in PBS.

15. Incubate fixed co-culture samples overnight with primary antibodies against β3-tubulin (1:300), neurofilament M (1:1000), human heat shock protein 27 (1:300), and BDNF (1:300) or GDNF (1:500) at room temperature or 4°C.

16. Wash the wells containing the fixed and stained co-cultures with PBS, and incubate with FITC- and Texas Red-labeled secondary antibodies (1:200) for 2 to 3 hr at room temperature.

17. Immediately image the wells containing the co-cultures after the final PBS wash, while the samples are immersed in PBS.

    Mount slides the multi-well plates on the microscope carefully due to the 3-dimensional structure of the co-cultures and the fragility of the matrigel after fixation and washing.

Quantification of neurite turning behavior and neurite length

Quantify neurite turning behavior by using a modification of a procedure described by Nishiyama et al. (2003).

18. Use the "measure angle" function of ImageJ software to evaluate the angle between the direction of neurite extension at the point of emergence from the DRG and the point of termination at the growth cone (Fig. 1C-I).

19. Take the angle between neurite trajectories at these two points as a measure of neurotropism. Straight radial extensions would result in an angle measurement of 0°, and the angle will increase as the path of neurite regeneration diverges from the original trajectory (Fig. 1C-I).

20. Measure neurite length as previously described (Thakor et al., 2009) using the "segmented line" function in ImageJ. Utilize the pseudounipolar morphology of adult DRG neurons in the explants to evaluate the length of regenerated neurites, and define length as the length along the neurite from the point of emergence from the DRG to the point of termination at the growth cone (Fig. 1C-II: Tracing Length). Moreover, measure the absolute neurite length by determining the straight line distance between a neurite's beginning and ending points (Fig. 1C-II: Absolute Length). Lastly, quantify the total number of neurites growing from each DRG to assess the overall neurotrophic effect of hMSCs (or other types of cells).

Table 3 Primers Used in Real Time-PCR

Target	Forward (5′-3′)	Reverse (5′-3′)
Adiponectin	TATGATGGCTCCACT GGTA	GAGCATAGCCTTGTC CTTCT
CNTF	GGACCTCTGTAGCCG CTCTA	TGGGATCCCAGTCTG ATGAG
BDNF	TAACGGCGGCAGAC AAAAAGA	GAAGTATTGCTTCA GTTGGCCT
GDNF	ATGAAGTTATGGGATG TCGTGGCTG	ACCGTTTAGCGGAATG CTTTCTTAG
GADPH	GCCAAGGTCATCCAT GACAAC	GTCCACCACCCTGTT GCTGTA

Measure angle and length of neurite only if the point of origin and point of termination are clearly visible.

BDNF and TNFα enzyme-linked immunosorbent assay (ELISA)

21. Collect 2-ml supernatants from co-cultures, snap-freeze in liquid nitrogen, and store at –80°C.

22. Quantify TNFα and BDNF using enzyme-linked immunosorbent assay kits according to the manufacturer's instructions with minor modifications. Measure optical density at a wavelength of 450 nm and a reference wavelength of 570 nm. Correlate density values linearly with the concentrations of cytokine standards.

Real-time PCR

23. At predetermined times after the application of LPS, remove the medium from each well, and freeze the plates at –80°C.

24. While still frozen, remove DRG and scaffolded hMSCs from the well plates with forceps and place in the RNAqueous lysis buffer from the RNAqueous kit.

25. Extract total RNA following the manufacturer's instructions, precipitate with sodium acetate and linear acrylamide in ethanol, and suspend RNA pellets in 15 μl elution solution, as described in RNAqueous instructions. Treat the RNA with DNase to remove any genomic DNA.

26. Prepare first-strand cDNA using the SuperScript III reverse transcription kit following the manufacturer's instructions.

27. Perform real-time PCR using Fast SYBR Green Master Mix per manufacturer's instructions and an Applied Biosystems 7900HT Fast Real-Time PCR system. Perform a dissociation curve analysis to confirm the specificity of the reaction and the lack of primer-dimer formation.

Select PCR primers from previous reports or designed with Primer Express software.

Target gene primer sequences are provided in Table 3.

28. Quantify the amplification data using with the ΔΔCt method (Han et al., 2016), which is an efficient way to analyze the relative changes in gene expression from real-time quantitative PCR experiments.

We recommend using glyceraldehyde 3-phosphate dehydrogenase (GAPDH) as the housekeeping gene to normalize gene expression of RT-PCR analysis due to the stability of its expression in DRG and peripheral nerve injury tissue samples. Since real-time PCR

assays determine a positive reaction via detecting accumulation of a fluorescent signal, define the Ct (cycle threshold) as the number of cycles required for the fluorescent signal to be above the threshold of background signal. Ct levels are inversely proportional to the amount of target nucleic acid in the sample.

Relative quantification compares the PCR signal of the target gene transcript in a treatment group to that of an untreated control: $\Delta Ct_{SOI} = Ct_{SSI} - Ct_{SCS}$ and $\Delta Ct_{RS} = Ct_{CSS} - Ct_{CRS}$. Thus, $\Delta\Delta Ct = \Delta Ct_{SOI} - \Delta Ct_{RS}$. For the exponential nature of PCR, calculate signal fold change as $2^{-(\Delta\Delta Ct)}$ (SOI: sequence of interest for sample; SSI: sample sequence of interest; SCS: sample control sequence; RS: reference sequence; CSS: control sample sequence; CRS: control reference sequence). Express fold-differences produced by the $\Delta\Delta Ct$ method as a range, which is a result of incorporating the standard deviation of the $\Delta\Delta Ct$ value into the fold-difference calculation: Fold Change $\pm$ S.D. (Livak & Schmittgen, 2001).

RAT SCI MODELING AND hMSC TRANSPLANTATION

BASIC PROTOCOL 3

This protocol specifies all critical experimental steps and procedures needed for creating rodent SCI models. In addition, we have presented in-depth information in regards to how to effectively investigate hMSC-based implant, which is tailored by the mechanistic insights obtained from the organotypic system, in the injured rodent spinal cord *in vivo* to uncover neurobiology and neural recovery mechanisms.

Materials *(also see Basic Protocols 1 and 2)*

Prograf/Tacrolimus (Astellas Pharma)
hMSCs
1 × 2 × 4-mm PLGA scaffolds, with and without hMSCs (Basic Protocol 1)
Ringer's lactate solution (Baxter, cat. no. 2B2324X)
Ketoprofen (also called Anafen; Merial)
NeuroTrace™ BDA (Biotinylated dextran amine)-10,000 Neuronal Tracer Kit (Thermo Fisher, cat. no. 7167)
Gelfoam® (Pfizer/Pharmacia and Upjohn Company; Baxter, cat. no. 1501341)
Fluoro-Gold (Fluorochrome LLC)
DiI stain: 1,1′-Dioctadecyl-3,3,3′,3′-Tetramethylindocarbocyanine Perchlorate (Thermo Fisher Scientific, cat. no. D282)
Fast blue (Polysciences Inc., cat. no. 17740-5)
Sucrose (Sigma-Aldrich, cat. no. S0389)
Isopentane
Tissue-Tek Optimal Cutting Temperature Compound (OCT, Sakura Finetek, cat. no. 4583)
Harris-modified hematoxylin solution (Sigma-Aldrich, cat. no. HHS16)
Alcoholic Eosin Y solution (Sigma-Aldrich, cat. no. HT110116)
Solvent blue
VECTASTAIN® Elite® ABC-HRP Kit (Vector Laboratories, cat. no. PK-6100)
Bovine serum albumin (BSA)

NYU contusion SCI device (Teng et al., 2004); compression SCI device (Ropper et al., 2015); or a modified curved angioclips (Fine Science Tools, cat. no. 18055-05): jaw dimensions: 6 × 1 mm; size: medium; length: 17 mm; force: 35 to 100 g
Injection pipette
Small animal stereotaxic instrument (David Kopf Instruments, Model 900)

Immunosuppress rats and assign treatment groups

1. Immunosuppress adult female and male rats by daily administering 1 mg/kg Prograf in drinking water (or 1 to 3 μg/kg subcutaneously) starting 5 days before injury.

2. Randomly assign rats to pre- or post-injury treatment groups, with group size carrying adequate statistical power (Ropper et al., 2015, 2017; Teng et al., 2002, 2004).

Compression SCI

3. Anesthetize a rat by intraperitoneal injection with a solution of 75 mg/kg ketamine and 10 mg/kg xylazine, and perform laminectomy to expose the T9 and T10 vertebrae.

4. Under a stereomicroscope, generate injuries to the T9-T10 spinal cord by mild weight-drop contusion (NYU Device; Teng et al., 2004), standardized hemisection (Teng et al., 2002), or moderate static compression (Ropper et al., 2015), or by applying a modified curved angioclip across the dorsal-ventral axis with a 1-mm gap on closure to exert 35 g (or up to 100 g) force for 1 min (Poon, Gupta, Shoichet, & Tator, 2007).

5. An independent observer—blinded from the experimental group design—should confirm the adequacy and consistency of the contusion or compression injury by assessing the length and breadth of the lesion bruise. Only then should the surgeon be informed of the particular treatment (e.g., hMSC suspension solution, vehicle solution, polymer-scaffolded hMSCs, or plain polymer) to be administered locally.

6. Immediately following contusion and static or angioclip compression injury, inject 150,000 hMSCs in 3 μl PBS/per locus, with one injection into the lesion site and two injections into the spinal cord parenchyma, 1-mm caudal and 1-mm rostral to the injury site, over a 3 min interval. Keep the injection pipette tip in place (at a depth ~1.20 mm below the T9-T10 dorsal surface) for another 2 min before slow removal to prevent backflow of the cells.

Segmental hemisection SCI

7. For segmental hemisection SCI, make a midline incision with a no. 11 sharp-tip scalpel, and perform transverse hemisections plus myelotomy to complete a unilateral (left- or right-sided) segmental hemisection, measuring 4-mm rostral-caudal.

8. After hemostasis is achieved and lesion size consistency is confirmed by a surgery assistant, have an independent observer (blinded to the block design) randomly select the treatment to be administered into the hemisection by the surgeon. Treatments should include PLGA scaffold seeded with hMSCs (~5.0×10^5 hMSCs per scaffold), hMSCs alone (~5.0×10^5 hMSCs/100 μl medium; i.e., hMSC-alone control), polymer alone, or 100 μl hMSC-conditioned culture medium (i.e., lesion-only control).

9. Approximate and close the spinal musculature and fascia with a 4-0 nonabsorbable suture. Close the skin with standard wound clips, and remove the clips 5 to 7 days after surgery.

10. Let the SCI rat recover in a cage with clean bedding materials on a heating pad until it awakens fully.

11. Administer 5.0 to 10.0 ml Ringer's lactate solution and ketoprofen (5 mg/kg; s.c.) daily for 5 to 7 days post-operation. When injury affects spontaneous micturition reflex, have a trained investigator or research facility staff member manually evacuate the bladder twice daily until a so-called "reflex bladder" function is established.

12. Alternatively, perform transplantation at 3 to 10 days after injury to evaluate reciprocal interaction outcomes between the implant and host in a subacute phase.

Behavioral evaluation

13. Behavioral analysis should be conducted by two observers who are blinded to the treatment identity. Evaluate coordinated motor activity with the Basso, Beattie, Bresnahan locomotor rating scale (scored on a 21-point scale; Basso, Beattie, & Bresnahan, 1995). Assess ability to maintain stable body position on an inclined plane, with the highest degree of inclination defined as that at which the animal could maintain its position for 5 s on two consecutive trials. Perform reflex tests—e.g., toe spread; withdrawal reflexes to extension, pain, and pressure; and placing and righting—and grade the results as described (Teng, Mocchetti, Taveira-DaSilva, Gillis, & Wrathall, 1999). For more detailed sensory measurement, perform a barrage of sensory tests by applying standard 2-g and 10-g Semmes-Weinstein filament stimulation to the T9-T10 dermatomes weekly to detect "at-level neuropathic pain"-like hypersensitivity response (i.e., an avoidance response). Test each rat on the first postoperative day and weekly thereafter throughout the study.

Evaluate repair of damaged spinal cords

14. Evaluate whether the treatments with hMSC-seeded scaffolds have enhanced the repair of damaged spinal cords using tracers.

    a. At 2 to 4 weeks before termination of the study, anesthetize a study rat as described in step 3 above and place it on a Kopf stereotaxic frame.
    b. Anterograde tracer: Inject 10% (w/v) biotinylated dextran amine (BDA in PBS) into the sensorimotor cortex bilaterally for contusion and compression SCI or identified anatomically contralateral to the lesioned T9–T10 side for tracing of the corticospinal tract as previously described (Ropper et al., 2017; Teng et al., 2002).
    c. Retrograde tracer: Soak 1-mm^3 Gelfoam cubes in 2% (w/v) Fluoro-Gold solution (FG in PBS) and insert them or a few crystals of DiI through two small incisions on each side of the hindlimb, respectively, into the quadriceps.

15. For a subset of rats, perform intramuscular administration of retrograde tracers, fast blue (FB), DiI, or FG. Together with synaptophysin ICC (see below), retrograde tracers can be used to investigate the integrity of intraspinal proprioceptive neuronal projections.

    a. At 4 to 8 weeks post-injury, anesthetize rats as described in step 3 above, and expose the left latissimus dorsi and left pectoralis major, muscles that are innervated by the C7, C8, and T1 nerve roots.
    b. Implant 1-mm^3 Gelfoams soaked in 1.5 μl of 2% (w/v) DiI in dimethyl sulfoxide or 2% (w/v) FG aqueous solution, or FB crystals into four different locations within each muscle at an approximate depth of 2 mm.
    c. To trace T6–T8 motor nerve roots, implant 1-mm^3 Gelfoams soaked in 1.5 μl of 2% FB or FG in distilled water or FB crystals into four different locations within the left external intercostal muscles and anterior abdominus muscle.
    d. Close the soft tissue and skin with sutures and standard wound clips, respectively.

Perfusion and Tissue Processing

16. At the end of the study—8 to 10 days (for subacute responses), 4 to 8 weeks (for early chronic responses), or 13 to 16 weeks (for chronic outcomes) after injury or implantation—deeply anesthetize rats and perform transcardial perfusion with 4% paraformaldehyde in 0.1 M PB (pH 7.4).

17. Dissect the spinal cord, brain, and internal organs (i.e., liver, spleen, lungs, gastrointestinal system, kidneys, and bladders), and postfix overnight in 4% PFA.

18. Dehydrate in 10% sucrose solution for 2 hr at room temperature, 20% sucrose solution for 2 hr at room temperature, and then 30% sucrose overnight at 4°C.

Tissue will sink in sucrose solution when dehydration is completed properly.

19. Freeze the samples in –50°C isopentane.

20. Embed two-centimeter blocks of the thoracic region of the cords, including injury epicenters, in Tissue-Tek OCT compound, and cryosection at a 20-μm slice thickness.

21. Stain sections with H&E and solvent blue, image sections with a standard Zeiss upright microscope to take digital photographs.

22. Analyze images with Adobe Photoshop CS4 11.0.1 or ImageJ software to quantify lesion volume, white matter sparing, and the number of ventral horn motor neurons from rats in each treatment group ($n \geq 3$ rats per group, or a group size required for proper power analysis) whose behavior values most closely approximate the mean for each group. Approximate lesion volume and white matter sparing by comparing pixel numbers for the targeted regions. Count motor neurons in the ventral horn on each side of the spinal cord, as described by Teng et al. (1998, 1999).

23. Perform IHC on 20-μm sections prepared in step 20 above, using the following primary antibodies (Table 1) to assess:

    Inflammatory markers: glial fibrillary acidic protein (rabbit anti-GFAP; 1:1000), CD11b (mouse anti-CD11b; 1:250), CD68 (mouse anti-CD68; 1:250), and nitrotyrosine (mouse anti-NT; 1:250).

    Spinal cord endogenous neural stem cell activity: nestin (mouse anti-nestin; 1:200) and doublecortin (goat anti-DCX; 1:250).

    Angiogenesis: laminin (pan anti-laminin antibody L9393; 1:60 to 1:100) and CD31 (goat anti-CD31; 1:400).

    Neurotrophic factors in the transplants: brain-derived neurotrophic factor (chicken anti-BDNF; 1:250) and IL-10 (mouse anti-IL-10; 1:250)

    Neural plasticity: descending serotonin axons (5HT), synaptic vesicles (rabbit anti-synapsin I (1:500), and rabbit anti-synaptophysin (1:100).

    Donor cell fate: STRO-1 (sc-47733; 1:200), collagen 1 (rabbit anticol1), collagen 2 (mouse anti-col2), collagen 4 (mouse anti-col4), and anti-ALP (1:250), as well as to stain lipids with Oil Red O.

    Costain for human CD90 (goat anti-CD90; 1:300), human heat shock protein (rabbit anti-HSP 27; 1:250), and human mitochondria antigen (anti-mitochondria: mouse MAB1273; 1:100 to 1:200).

    When costaining CD90 and for laminin, use CD90 (1:400) together with anti-human lamininα5 chain (clone LAM-89; 1:1000) or anti-human laminin α2 chain (clone 5H2; 1:1000), with the appropriate fluorophore-conjugated antibodies to achieve dual visualization, e.g., green (FITC) for CD90 and red (Texas Red or DyLight594) for laminin. (see Table 2).

    vGluT1 is the primary proprioceptive terminal glutamate transporter interacting with propriospinal interneurons (PSNs) in Rexed's Laminae (RL) IV–VIII and RL IX motor neurons, and vGluT2 is a primary marker of rubrospinal tract (RST) terminals. vGluT1 and vGluT2 expression are evaluated to identify changes in propriospinal plasticity and rubrospinal regeneration, respectively.

    To detect vGluT1, use mouse monoclonal antibody against vGluT1 (1:1000; MABS132) plus goat polyclonal secondary antibody to mouse IgG (1:1000 to 1:5000; ab6787; Texas Red); for vGlut2, use guinea pig anti-vGluT2 polyclonal antibody (1:6,000; AB2251) and secondary antibody of FITC-goat anti-guinea pig IgG (AP108F).

24. Block the tissue samples for 1 hr in donkey serum (or serum from species that matches secondary antibody) containing 5% (w/v) BSA at room temperature.

25. In general, incubate samples for 1 to 2 hr with primary antibodies at 4°C overnight, and secondary antibodies at room temperature for 1 to 2 hr.

26. Capture images using a Nikon Eclipse TE300 (or equivalent) microscope equipped with a Spot RT-Slider CCD camera, a Zeiss Axiovert 200 microscope equipped with an Axiocam CCD camera, or a Zeiss LSM1 confocal microscope equipped with Zeiss Zen 2011 software set, with appropriate filters for FITC, Texas Red, and DAPI.

27. For semi-quantification of IHC, obtain signal intensity above a determined threshold level and divide it by the total pixel count or units of the area measured, to yield a percentage above threshold, or relative signal value in an arbitrary unit.

COMMENTARY

Background Information

In vitro cell cultures are a very prominent technique for studying specific biological questions in a well-controlled and systematically designed environment. Over the past ~100 years, the *in vitro* culturing of dissociated primary neural cells (i.e., neurons, astrocytes, and oligodendrocytes), endothelial cells, epithelial cells, and more recently, stem cells has been instrumental in allowing scientists to explore and understand cellular and molecular events, particularly those related to survival, morphology, and basic functions under either physiological or pathological/toxic conditions. However, cultured primary cells do not recapitulate the essential features of the original organ or organism due to the drastic loss of systemic cytoarchitecture, intercellular contact, system formation, and specific niche. To overcome these deficits, investigators have devised combinatorial *in vitro* culture systems (i.e., organotypic cultures) that maintain and manipulate organs or organ slices *ex vivo*, aiming to preserve *in vivo* anatomical and functional characteristics of the original tissue.

Organotypic (from organo + typic) describes tissue samples or organs that, after being removed, continue to develop as they would *in vivo*. The term was first published in 1954 to show a design that supported *in vitro* differentiation of the chick embryo eye (Reinbold, 1954). Buoyed by the success of culturing living vertebral nerve tissues outside the body in Harrison's hanging drop design in 1959 (Harrison, 1959), the first organotypic neural tissue culture was made feasible for rat hypophysis by Bousquet and Meunier in 1962, in which the structural and synaptic organizations of the neurons were largely preserved (Bousquet and Meunier, 1962). Although the field still lacks uniform *in vitro* settings that fully recapitulate the *in vivo* features of the CNS, advances in cell, tissue, and organ culture technologies (e.g., 3D cultures, bioreactors, organotypic roller-tube cultures, microfluidic devices) have enabled investigators to glean mechanisms of developmental biology, physiology, pathophysiology, pathogenesis, organ preservation, bioengineering, and therapeutic inventions.

Here we have reported a new organotypic explant system to study hMSC-derived multimodal effects in a neurological setting. Whole-mount tissue explants offer an investigative bridge between primary cells and *ex vivo* neural organs. Our protocols and published results suggest that such multicomponent 3-dimensional microenvironments are more comprehensive and powerful for mechanistic studies and drug screening endeavors, relative to the conventional homogenous monolayer cultures (Haragopal et al., 2015; Ropper et al., 2017). Several previous studies used neural explant systems to evaluate the effects of MSCs or MSC conditioned medium on neurite growth from embryonic chick or juvenile mouse DRGs (Crigler, Robey, Asawachaicharn, Gaupp, & Phinney, 2006; Sasaki et al., 2009; Wright, Griffiths, & Johnson, 2010), including engineering laminin, an extracellular matrix molecule secreted by MSCs, via covalently coupling to agarose hydrogel using the bifunctional cross-linking reagent to significantly enhance neurite extension from 3D cultured embryonic day 9 chick DRGs (Yu, Dillon, & Bellamkonda, 1999). Our system has the following unique aspects. First, the adult rat DRG is used. Modeling neurotrauma and neuroinflammation using adult rats is especially important, because trophic factor requirements and effects in neural tissues such as the brain, spinal cord, and DRG

change with maturity (Tonge, Edstrom, & Ekstrom, 1998). Second, our studies have generated related but distinct co-culture systems for qualitative and quantitative analyses of specific neurotrophic (i.e., neurite growth and neuroprotection) and neurotropic (i.e., neurite turning and targeting) effects. Third, the application of our system extends beyond the investigation of regenerative neuritogenic effects to include the ability to examine neuroinflammatory responses, which often trigger or promote additional degeneration or repair processes.

MSCs reportedly enhance axonal regeneration in rat traumatic SCI (Sasaki et al., 2009), and they exert immunomodulatory and anti-inflammatory effects in mouse models of stroke (Ohtaki et al., 2008) and experimental autoimmune encephalomyelitis (Morando et al., 2012). Our observations of neurite tracking to hMSCs as well as hMSC-derived neuritogenic and anti-inflammatory effects might thus represent an *in vitro* recapitulation of *in vivo* therapeutic mechanisms of hMSCs (Ropper et al., 2017). At least 10 rodent studies of traumatic SCI have shown varying degrees of functional improvement when MSCs were injected at about one week after SCI (Archambault et al., 2017; Parr et al., 2007). Observed benefits of MSCs in animal SCI models have spurred human clinical trials (Suzuki et al., 2014; Yoon et al., 2007). However, at least 3 rodent studies have shown no motor improvement (Ankeny, McTigue, & Jakeman, 2004; Mothe et al., 2011; Yoshihara et al., 2006). Thus, it is imperative for the field to determine optimal modalities for hMSC transplantation by understanding specific molecular events responsible for ameliorating corresponding pathologies post SCI. The presented protocol, including the preliminary analytical formulas of DRG interaction-influenced BDNF secretion from hMSCs, demonstrates that explant-based *in vitro* modeling can be used to further elucidate processes required to maximize the multimechanistic therapeutic effects of hMSC implant on experimental SCI prior to lifting the technology to clinical translations (Ropper et al., 2017; Teng et al., 2008, 2011).

Critical Parameters and Troubleshooting

Cell quality control

For hMSC-related research, it is vital to maintain basic stemness biology (i.e., MSCness) throughout the experiment (Fig. 2A to J). However, maintaining hMSCs in a stable multipotent state during repeated propagations is a challenge. We recommend preserving enough vials of frozen hMSCs from early passages, and in each experiment, setting up parallel hMSCs cultures for both cryostorage and quality control, which can be readily examined by using immunocytochemical FACS or staining (e.g., CD90, CD105, etc.) and differentiation tests (Fig. 2A and 2B).

Generation of SCI models

For the lower thoracic SCI models, consistency of the hindlimb locomotor deficit of a particular model is the best indicator of its replicability. To reach this goal, is pivotal to focus quality control on uniformity of anesthesia depth, laminectomy size, severity of spinal cord lesion, post-care quality, mitigation of complications, and behavioral evaluation. To obtain unbiased outcomes produced by a specific treatment, evaluators must be kept blind to the treatment design and execution till all data is collected.

Statistical analyses

Perform statistics with SPSS software version 19 (IBM Corp; or equivalent software). Perform comparisons of behavioral data, motor neuron quantifications, and semi-quantification of pixels (for histopathology, ICC and IHC) among ≥ 3 study groups with repeated-measures ANOVA or one-way ANOVA, followed with Tukey's *post hoc* test. Determine statistical difference between two study groups using the Student *t*-test. To compare proportional differences, use Fisher's exact test. Set statistical significance commonly at $P < 0.05$.

Understanding results

The key features of the outcomes from the protocol-based studies are clearly described in the following section. It is critical for the investigators to design and include proper control groups that can help to determine specific effects of hMSC or DRG, relative to those that can be derived from growth factor-reduced matrigel, conditioned medium (e.g., supernatant from hMSC culture solution), and polymer only, respectively.

Anticipated Results

MSCs have been widely investigated for their potential in neural repair and neuroglial functional recovery. However, these endeavors have been designated following two mainstreams of academic reasoning: (1) direct cell replacement possibilities derived from the potential neural trans-differentiation capacity of MSCs (Shakhbazau & Potapnev, 2016);

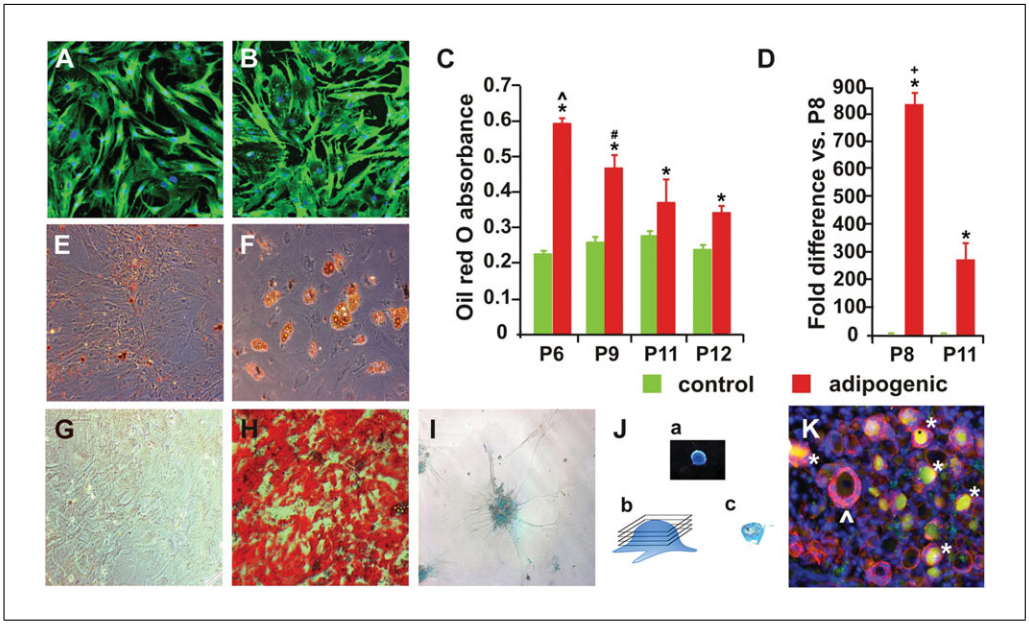

Figure 2 hMSC quality control. (**A** and **B**) Immunostaining of MSC markers CD105 (A) and CD90 (B) for passage 12 (P12) hMSCs. (**C**) Oil Red O staining of adipogenic differentiation of P6 to P12 hMSCs ($n = 6$ per group; *, differentiation vs. control, $P < 0.05$, Student's *t*-test; ^, P6 vs. P9 to P12 and #, P9 vs. P11 and P12; $n = 6$; $P < 0.05$, one-way ANOVA with Tukey's *post hoc* test). (**D**) Real-time PCR showed mean expression levels of adiponectin (an adipogenic marker) in P8 and P11 hMSCs cultured in adipogenic or control medium (+, P8 vs. P11; statistical method per **C**). The real-time PCR finding was corroborated by Oil Red O staining of P12 and P6 hMSC-derived adipogenic cells shown in **E** and **F**, respectively. Alizarin Red S staining confirmed osteogenic capability of hMSCs. Whereas P9 hMSCs cultured in control conditions showed no reactivity (**G**), the cells had high osteogenic yield after differentiation medium induction (**H**). Alcian Blue staining showed P9 cells with chondrogenic differentiation (**I**), and one of the intact chondrogenic pellets derived from hMSCs (**J**-a) that was cut (**J**-b) into 50-μm sections (**J**-c). (**K**) Immunohistochemical signs of neuroinflammation in a tissue section of an explanted dorsal root ganglion (DRG) after 12 to 18 hr exposure to 10 μg/ml lipopolysaccharides (LPS). Immunostains of GFAP (red: arrowhead) and nitrotyrosine (i.e., protein nitration; yellow: asterisk) depicted reactive activation of satellite cells (i.e., GFAP immunoreactivity augmentation) and neuronal reactive nitrogen species damage (i.e., nitrotyrosine immunoreactivity; yellow: asterisk), respectively. Blue shows DAPI staining of nuclei.

and (2) therapeutic effects produced by functional multipotency of stem cells (Srivastava et al., 2016; Teng et al., 2008, 2011; Ulrich et al., 2015). Whether MSCs can directly differentiate into neurons, oligodendrocytes, and astrocytes without reentering the pluripotency phase (i.e., neural trans-differentiation) remains uncertain; however, accumulating evidence shows that functionally multipotent MSCs produce factors (e.g., trophic factors, cytokines, exosomes, and microRNAs) that support the establishment or restoration of homeostasis via their pro-healing/repair, anti-inflammatory, and pro-neurogenic actions. Such innate developmental capacity of MSCs evidently should be systematically studied not only for increasing translational opportunities, but also for advancing our understanding of fundamental stem cell biology. Thus, the hMSC-DRG co-culture system for evaluating neuritogenesis, neuroinflammation, and neural repair offers excellent scientific value.

As examples, in neuritogenesis angle analysis, control DRGs cultured alone showed some non-radial extension, as the average neurite trajectory angle was 48.15°. However, DRGs co-cultured with hMSCs showed a significantly increased average neurite trajectory angle of 59.25°, aiming at hMSCs (see details in Ropper et al., 2017). This indicates that regenerating neurites changed their path to track hMSCs (see schematic illustration in Fig. 2C-III and 2C-IV). Using scaffolded hMSCs-DRG co-culture system, we observed a significant increase in the mean length of regenerated neurites on either side of DRGs exposed to hMSC-incorporated scaffolds when compared to control scaffolds (Ropper et al., 2017). The data suggest that hMSCs possess neurotropic and neurotrophic

effects that are maintained in hMSCs seeded onto polymer scaffolds, a feature which holds potential for neural tissue repair *in vivo*. Our mechanistic exploration revealed that hMSC-DRG co-cultures triggered significantly increased amounts of secreted BDNF, confirmed immunocytochemically to be originate from hMSCs. Secreted levels of BDNF were further increased in culture supernatants collected after 96 hr of co-culture, as compared to those collected at 48 hr, suggesting that BDNF secretion was constitutive and responsive to DRG co-culturing (Ropper et al., 2017).

Work in the past 3 decades demonstrated that inflammation plays pivotal dual roles in cell damage and scavenging, and in tissue and functional repair as well. The presented organotypic models provide an effective conduit to investigating the complex facets of neuroinflammation in neurotrauma. In DRGs cultured alone as a model and in DRGs cultured with cell-free PLGA scaffolds as a control, treatment with 10 μg/ml LPS markedly increased secreted TNFa levels in the culture supernatant and other interstitial inflammatory responses (e.g., reactive gliosis and protein nitration) (Fig. 2K). However, treatment of co-cultures of PLGA-scaffolded MSCs and DRGs with 10 μg/ml LPS did not trigger a discernible elevation of secreted TNFα, suggesting that the co-culture system could serve as an *in vitro* model for evaluating interactive molecular events of neuroinflammation, and immunomodulation. In addition, hMSCs can be investigated for their anti-inflammatory effect and homeostatic impact when interacting with *ex vivo* DRG in an inflammatory environment (Ropper et al., 2017).

Regarding *in vivo* investigation of the neural repair effects of scaffolded hMSCs (designed per information obtained from our organotypic system) implanted acutely in a rat T9-10 hemisection SCI model, we demonstrated that a properly tailored PLGA-scaffolding maintained hMSC stemness and engraftment, and induced robust motosensory improvement, mitigation of neuropathic pain and tissue damage, and preservation of myelin. The scaffolded non-trans-differentiated hMSCs exerted multimodal effects of neurotrophism, angiogenesis, neurogenesis, anti-autoimmunity, and anti-inflammation. Hindlimb locomotion was restored by reestablished integrity of submidbrain circuits of serotonergic reticulospinal innervation at lumbar levels, the propriospinal projection network, neuromuscular junction, and central pattern generator, thus providing a platform for investigating molecular events underlying the *in vivo* repair impact of non-differentiated hMSCs (Ropper et al., 2017).

Quality control and characterization of hMSCs

As described above, the hMSC cells we used were systematically characterized for phenotypical markers at passages 2 and 3, which were re-checked for their stemness biology features in higher passages up to passage 12 (Fig. 2A to J). To ensure that hMSCs used in the *in vitro* and *in vivo* studies retain essential MSC stemness biology (i.e., MSC-ness), we recommend to perform parallel differentiation assays for osteogenesis, adipogenesis, and chondrogenesis, as per our recent report (Haragopal et al., 2015; Ropper et al., 2017), for hMSCs to be used for implantation (e.g., from passage 6 populations in our study). In summary, it is extremely important for the investigators to ensure that all hMSCs, especially those in higher passages retain basic "MSCness" by using our formula of maintenance and monitoring.

Time Considerations

Basic Protocol 1

hMSCs characterization and quality control

1. Adipogenesis with Oil Red O staining: 7 to 14 days;
2. Osteogenesis with Alizarin Red S staining: ≥21 days;
3. Chondrogenesis with Alcian blue: ∼14 to 21 days.

hMSC propagation and preparation: The expansion (and maintenance) of hMSCs is a dynamic process that is dependent on the growth rate of the cells. hMSCs cultures can be split 1:2 every 5 to 7 days when they reach 80% to 90% confluency and with >98% viability.

PLGA scaffold preparation: 2 to 3 d.

Scaffold incorporation of hMSCs: PLGA need to be coated with FBS or hMSC-conditioned medium one day prior to cell incorporation. The incorporation of hMSCs should be repeated on the following day.

Basic Protocol 2

DRG extraction: After achieving satisfactory anesthesia, 30 to 50 min per animal.

Co-culture of DRGs with hMSCs: 2 to 5 days.

ICC, IHC, and imaging of co-cultures: 2 days for each round of staining and imaging.

Quantification of neurite turning behavior and neurite length: about 20 to 40 min for each imaging field.

BDNF and TNFα enzyme-linked immunosorbent assay (ELISA): ∼2 days each.

Basic Protocol 3

Animal surgery:

1. SCI modeling with immediate hMSCs cell transplant: After satisfactory anesthesia, 20 to 50 min per animal, depending on operator's skills and experiences.

2. hMSCs seeded in scaffold or in suspension can be transplanted immediately after SCI or at different times after injury (e.g., 3 days post-injury). Except for acute implantations, later phase transplantations require establishing satisfactory general anesthesia first, which together with implantation usually takes about 30 to 50 min for each animal.

Systemic fixative perfusion: ∼30 min per mouse; ∼50 min per rat.

Tissue harvesting: 20 to 30 min per animal.

Post-fixation and dehydration: 3 to 5 days.

Tissue embedding and cryosection: Variable timeline depending on the number of samples.

Immunostaining of tissue slides: 2 days per round of staining plus initial imaging evaluation.

Acknowledgements

The authors do not hold any COI for the presented protocol. D.K.T. thanks Drs. A. Soto-Gutierrez, H. Yagi, M. Yarmush, and D. Yu for their technical help in the preparatory phase of the method development. Support for this work was provided to Dr. Teng's laboratory by U.S. VA RRD Grant 1-I01-RX000308-01A1, CIMIT-DoD Grant W81XWH-09-2-0001 and W81XWH-15-1-0621, and a grant from the Ellen R. and Melvin J. Gordon Center for the Cure and Treatment of Paralysis established by the Cele H. and William B. Rubin Family Fund, Inc. L.W. was also supported by a Wuhan Union Hospital/HZUST fellowship and S. K. by a Turkish government fellowship (Y.D.T. project sponsor).

Literature Cited

Ankeny, D. P., McTigue, D. M., & Jakeman, L. B. (2004). Bone marrow transplants provide tissue protection and directional guidance for axons after contusive spinal cord injury in rats. *Experimental Neurology*, *190*, 17–31. doi: 10.1016/j.expneurol.2004.05.045.

Archambault, J., Moreira, A., McDaniel, D., Winter, L., Sun, L., & Hornsby, P. (2017). Therapeutic potential of mesenchymal stromal cells for hypoxic ischemic encephalopathy: A systematic review and meta-analysis of preclinical studies. *PLoS ONE*, *12*, e0189895. doi: 10.1371/journal.pone.0189895 eCollection 2017.

Basso, D. M., Beattie, M. S., & Bresnahan, J. C. (1995). A sensitive and reliable locomotor rating scale for open field testing in rats. *Journal of Neurotrauma*, *12*, 1–21. doi: 10.1089/neu.1995.12.1.

Bousquest, J., & Meunier, J. M. (1962). Organotypic culture, on natural and artificial media, of fragments of the adult rat hypophysis. *Comptes Rendus des Seances de la Societe de Biologie et de Ses Filiales*, *156*, 65–67.

Costigan, M., Scholz, J., & Woolf, C. J. (2009). Neuropathic pain: A maladaptive response of the nervous system to damage. *Annual Review of Neuroscience*, *32*, 1–32. doi: 10.1146/annurev.neuro.051508.135531.

Crigler, L., Robey, R. C., Asawachaicharn, A., Gaupp, D., & Phinney, D. G. (2006). Human mesenchymal stem cell subpopulations express a variety of neuro-regulatory molecules and promote neuronal cell survival and neuritogenesis. *Experimental Neurology*, *198*, 54–64. doi: 10.1016/j.expneurol.2005.10.029.

Garbuzova-Davis, S., Ehrhart, J., & Sanberg, P. R. (2017). Cord blood as a potential therapeutic for amyotrophic lateral sclerosis. *Expert Opinion on Biological Therapy*, *17*, 837–851. doi: 10.1080/14712598.2017.1323862.

Grayson, A. C., Cima, M. J., & Langer, R. (2005). Size and temperature effects on poly(lactic-co-glycolic acid) degradation and microreservoir device performance. *Biomaterials*, *26*, 2137–2145.

Han, I. B., Kim, M., Lee, S. H., Kim, J. K., Kim, S. H., Chang, J. H., & Teng, Y. D. (2016). Down-regulation of MicroRNA-126 in Glioblastoma and its Correlation with Patient Prognosis: A Pilot Study. *Anticancer Research*, *36*, 6691–6697.

Haragopal, H., Yu, D., Zeng, X., Kim, S. W., Han, I. B., Ropper, A. E., ... Teng, Y. D. (2015). Stemness enhancement of human neural stem cells following bone marrow MSC co-culture. *Cell Transplantation*, *24*, 645–659. doi: 10.3727/096368915X687561.

Harrison, R. G. (1959). The outgrowth of the nerve fiber as a mode of protoplasmic movement. *Journal of Experimental Zoology*, *142*, 5–73. doi: 10.1002/jez.1401420103.

Kang, K. N., Kim, D. Y., Yoon, S. M., Lee, J. Y., Lee, B. N., Kwon, J. S., ... Kim, M. S. (2012). Tissue engineered regeneration of completely transected spinal cord using human mesenchymal stem cells. *Biomaterials*, *33*, 4828–4835. doi: 10.1016/j.biomaterials.2012.03.043.

Kaplan, G. B., Leite-Morris, K. A., Wang, L., Rumbika, K. K., Heinrichs, S. C., Zeng, X., ... Teng, Y. D. (2018). Pathophysiological bases of comorbidity: Traumatic brain injury and post-traumatic stress disorder. *Journal of Neurotrauma*, *35*, 210–225. doi: 10.1089/neu.2016.4953.

Lavik, E., Teng, Y. D., Snyder, E., & Langer, R. (2002). Seeding neural stem cells on scaffolds of PGA, PLA, and their copolymers. *Methods in Molecular Biology*, *198*, 89–97. doi: 10.1385/1-59259-186-8:89.

Leclere, P. G., Norman, E., Groutsi, F., Coffin, R., Mayer, U., Pizzey, J., & Tonge, D. (2007). Impaired axonal regeneration by isolectin B4-binding dorsal root ganglion neurons in vitro. *Journal of Neuroscience*, *27*, 1190–1199. doi: 10.1523/jneurosci.5089-06.2007.

Livak, K. J., & Schmittgen, T. D. (2001). Analysis of relative gene expression data using real-time quantitative PCR and the $2^{-\Delta\Delta CT}$ method. *Methods*, *25*, 402–408. doi: 10.1006/meth.2001.1262.

Morando, S., Vigo, T., Esposito, M., Casazza, S., Novi, G., Principato, M. C., ... Uccelli, A. (2012). The therapeutic effect of mesenchymal stem cell transplantation in experimental autoimmune encephalomyelitis is mediated by peripheral and central mechanisms. *Stem Cell Research & Therapy*, *3*, 3. doi: 10.1186/scrt94.

Mothe, A. J., Bozkurt, G., Catapano, J., Zabojova, J., Wang, X., Keating, A., & Tator, C. H. (2011). Intrathecal transplantation of stem cells by lumbar puncture for thoracic spinal cord injury in the rat. *Spinal Cord*, *49*, 967–973. doi: 10.1038/sc.2011.46.

Neumann, S., Skinner, K., & Basbaum, A. I. (2005). Sustaining intrinsic growth capacity of adult neurons promotes spinal cord regeneration. *Proceedings of the National Academy of Sciences of the United States of America*, *102*, 16848–16852. doi: 10.1073/pnas.0508538102.

Nishiyama, M., Hoshino, A., Tsai, L., Henley, J. R., Goshima, Y., Tessier-Lavigne, M., ... Hong, K. (2003). Cyclic AMP/GMP-dependent modulation of Ca2+ channels sets the polarity of nerve growth-cone turning. *Nature*, *423*, 990–995. doi: 10.1038/nature01751.

Ohtaki, H., Ylostalo, J. H., Foraker, J. E., Robinson, A. P., Reger, R. L., Shioda, S., & Prockop, D. J. (2008). Stem/progenitor cells from bone marrow decrease neuronal death in global ischemia by modulation of inflammatory/immune responses. *Proceedings of the National Academy of Sciences of the United States of America*, *105*, 14638–14643. doi: 10.1073/pnas.0803670105.

Parr, A. M., Tator, C. H., & Keating, A. (2007). Bone marrow-derived mesenchymal stromal cells for the repair of central nervous system injury. *Bone Marrow Transplantation*, *40*, 609–619. doi: 10.1038/sj.bmt.1705757.

Poon, P. C., Gupta, D., Shoichet, M. S., & Tator, C. H. (2007). Clip compression model is useful for thoracic spinal cord injuries: Histologic and functional correlates. *Spine (Phila Pa 1976)*, *32*, 2853–2859. doi: 10.1097/BRS.0b013e31815b7e6b.

Pritchard, C. D., Slotkin, J. R., Yu, D., Dai, H., Lawrence, M. S., Bronson, R. T., ... Langer, R. S. (2010). Establishing a model spinal cord injury in the African green monkey for the preclinical evaluation of biodegradable polymer scaffolds seeded with human neural stem cells. *Journal of Neuroscience Methods*, *188*, 258–269. doi: 10.1016/j.jneumeth.2010.02.019.

Reinbold, R. (1954). Organotypic differentiation of the eye of the chick embryo in vitro. *Comptes Rendus Des Seances De La Societe De Biologie Et De Ses Filiales*, *148*, 1493–1495.

Ropper, A. E., Thakor, D. K., Han, I., Yu, D., Zeng, X., Anderson, J. E., ... Teng, Y. D. (2017). Defining recovery neurobiology of injured spinal cord by synthetic matrix-assisted hMSC implantation. *Proceedings of the National Academy of Sciences of the United States of America*, *114*, E820–e829. doi: 10.1073/pnas.1616340114.

Ropper, A. E., Zeng, X., Anderson, J. E., Yu, D., Han, I., Haragopal, H., & Teng, Y. D. (2015). An efficient device to experimentally model compression injury of mammalian spinal cord. *Experimental Neurology*, *271*, 515–523. doi: 10.1016/j.expneurol.2015.07.012.

Sasaki, M., Radtke, C., Tan, A. M., Zhao, P., Hamada, H., Houkin, K., ... Kocsis, J. D. (2009). BDNF-hypersecreting human mesenchymal stem cells promote functional recovery, axonal sprouting, and protection of corticospinal neurons after spinal cord injury. *Journal of Neuroscience*, *29*, 14932–14941. doi: 10.1523/jneurosci.2769-09.2009.

Scholz, J., & Woolf, C. J. (2007). The neuropathic pain triad: Neurons, immune cells and glia. *Nature Neuroscience*, *10*, 1361–1368. doi: 10.1038/nn1992.

Shakhbazau, A., & Potapnev, M. (2016). Autologous mesenchymal stromal cells as a therapeutic in ALS and epilepsy patients: Treatment modalities and ex vivo neural differentiation. *Cytotherapy*, *18*, 1245–1255. doi: 10.1016/j.jcyt.2016.06.001.

Sleigh, J. N., Greg, A., Weir, G. A., & Schiavo, G. (2016). A simple, step-by-step dissection protocol for the rapid isolation of mouse dorsal root ganglia. *BMC Research Notes*, *9*, 82. doi: 10.1186/s13104-016-1915-8.

Srivastava, A. K., Bulte, C. A., Shats, I., Walczak, P., & Bulte, J. W. (2016). Co-transplantation of syngeneic mesenchymal stem cells improves survival of allogeneic glial-restricted precursors in mouse brain. *Experimental Neurology*, *275*, 154–161. doi: 10.1016/j.expneurol.2015.10.008.

Suzuki, Y., Ishikawa, N., Omae, K., Hirai, T., Ohnishi, K., Nakano, N., ... Ide, C. (2014). Bone marrow-derived mononuclear cell transplantation in spinal cord injury patients by lumbar puncture. *Restorative Neurology and Neuroscience*, *32*, 473–482. doi: 10.3233/rnn-130363.

Teng, Y. D., Benn, S. C., Kalkanis, S. N., Shefner, J. M., Onario, R. C., Cheng, B., ... Snyder, E. Y. (2012). Multimodal actions of neural stem cells in a mouse model of ALS: A meta-analysis. *Science Translational Medicine*, *4*, 165ra164. doi: 10.1126/scitranslmed.3004579.

Teng, Y. D., Choi, H., Onario, R. C., Zhu, S., Desilets, F. C., Lan, S., ... Friedlander, R.

M. (2004). Minocycline inhibits contusion-triggered mitochondrial cytochrome c release and mitigates functional deficits after spinal cord injury. *Proceedings of the National Academy of Sciences of the United States of America*, *101*, 3071–3076. doi: 10.1073/pnas.0306239101.

Teng, Y. D., Lavik, E. B., Qu, X., Park, K. I., Ourednik, J., Zurakowski, D., ... Snyder, E. Y. (2002). Functional recovery following traumatic spinal cord injury mediated by a unique polymer scaffold seeded with neural stem cells. *Proceedings of the National Academy of Sciences of the United States of America*, *99*, 3024–3029. doi: 10.1073/pnas.052678899.

Teng, Y. D., Mocchetti, I., Taveira-DaSilva, A. M., Gillis, R. A., & Wrathall, J. R. (1999). Basic fibroblast growth factor increases long-term survival of spinal motor neurons and improves respiratory function after experimental spinal cord injury. *Journal of Neuroscience*, *19*, 7037–7047. doi: 10.1523/JNEUROSCI.19-16-07037.1999.

Teng, Y. D., Mocchetti, I., & Wrathall, J. R. (1998). Basic and acidic fibroblast growth factors protect spinal motor neurones in vivo after experimental spinal cord injury. *European Journal of Neuroscience*, *10*, 798–802. doi: 10.1046/j.1460-9568.1998.00100.x.

Teng, Y. D., Santos, F. N., Black, P. M., Konya, D., Park, K. I., Sidman, R. L., & Snyder, E. Y. (2008). Chapter 18: Neural stem cells: Multipotency beyond self-renewal and phenotypic differentiation. In: A. Atala, R. Lanza, J. A. Thomson, & R. M. Nerem (Eds.). *Principles of Regenerative Medicine*, (1st ed., pp. 300–317). San Diego: Elsevier, Inc.

Teng, Y. D., Yu, D., Ropper, A. E., Li, J., Kabatas, S., Wakeman, D. R., ... Sidman, R. L. (2011). Functional multipotency of stem cells: A conceptual review of neurotrophic factor-based evidence and its role in translational research. *Current Neuropharmacology*, *9*, 574–585. doi: 10.2174/157015911798376299.

Thakor, D., Spigelman, I., Tabata, Y., & Nishimura, I. (2007). Subcutaneous peripheral injection of cationized gelatin/DNA polyplexes as a platform for non-viral gene transfer to sensory neurons. *Molecular Therapy*, *15*, 2124–2131. doi: 10.1038/sj.mt.6300256.

Thakor, D. K., Teng, Y. D., & Tabata, Y. (2009). Neuronal gene delivery by negatively charged pullulan-spermine/DNA anioplexes. *Biomaterials*, *30*, 1815–1826. doi: 10.1016/j.biomaterials.2008.12.032.

Tonge, D., Chan, K., Zhu, N., Panjwani, A., Arno, M., Lynham, S., ... Pizzey, J. (2008). Enhancement of axonal regeneration by in vitro conditioning and its inhibition by cyclopentenone prostaglandins. *Journal of Cell Science*, *121*, 2565–2577. doi: 10.1242/jcs.024943.

Tonge, D., Edstrom, A., & Ekstrom, P. (1998). Use of explant cultures of peripheral nerves of adult vertebrates to study axonal regeneration in vitro. *Progress in Neurobiology*, *54*, 459–480. doi: 10.1016/S0301-0082(97)00072-5.

Ulrich, H., do Nascimento, I. C., Bocsi, J., & Tárnok, A. (2015). Immunomodulation in stem cell differentiation into neurons and brain repair. *Stem Cell Reviews*, *11*, 474–486. doi: 10.1007/s12015-014-9556-6.

Wright, K. T., Griffiths, G. J., & Johnson, W. E. (2010). A comparison of high-content screening versus manual analysis to assay the effects of mesenchymal stem cell-conditioned medium on neurite outgrowth in vitro. *Journal of Biomolecular Screening*, *15*, 576–582. doi: 10.1177/1087057110367959.

Yoon, S. H., Shim, Y. S., Park, Y. H., Chung, J. K., Nam, J. H., Kim, M. O., ... Ha, Y. (2007). Complete spinal cord injury treatment using autologous bone marrow cell transplantation and bone marrow stimulation with granulocyte macrophage-colony stimulating factor: Phase I/II clinical trial. *Stem Cells*, *25*, 2066–2073. doi: 10.1634/stemcells.2006-0807.

Yoshihara, H., Shumsky, J. S., Neuhuber, B., Otsuka, T., Fischer, I., & Murray, M. (2006). Combining motor training with transplantation of rat bone marrow stromal cells does not improve repair or recovery in rats with thoracic contusion injuries. *Brain Research*, *1119*, 65–75. doi: 10.1016/j.brainres.2006.08.080.

Yu, D., Neeley, W. L., Pritchard, C. D., Slotkin, J. R., Woodard, E. J., Langer, R., & Teng, Y. D. (2009). Blockade of peroxynitrite-induced neural stem cell death in the acutely injured spinal cord by drug-releasing polymer. *Stem Cells*, *27*, 1212–1222. doi: 10.1002/stem.26.

Yu, X., Dillon, G. P., & Bellamkonda, R. B. (1999). A laminin and nerve growth factor-laden three-dimensional scaffold for enhanced neurite extension. *Tissue Engineering*, *5*, 291–304. doi: 10.1089/ten.1999.5.291.

Zhang, Z. X., Guan, L. X., Zhang, K., Zhang, Q., & Dai, L. J. (2008). A combined procedure to deliver autologous mesenchymal stromal cells to patients with traumatic brain injury. *Cytotherapy*, *10*, 134–139. doi: 10.1080/14653240701883061.

Experimental Neurology 311 (2019) 135–147

Contents lists available at ScienceDirect

Experimental Neurology

journal homepage: www.elsevier.com/locate/yexnr

Review Article

Spinal cord astrocytomas: progresses in experimental and clinical investigations for developing recovery neurobiology-based novel therapies

Yang D. Teng[a,*], Muhammad Abd-El-Barr[a,b,1], Lei Wang[a,1], Hadi Hajiali[a], Liqun Wu[a], Ross D. Zafonte[a]

[a] Departments of Physical Medicine & Rehabilitation and Neurosurgery, Harvard Medical School, Spaulding Rehabilitation Hospital and Brigham and Women's Hospital, Division of Spinal Cord Injury Research, VA Boston Healthcare System, Boston, MA, USA
[b] Current affiliation: Department of Neurosurgery, Duke University School of Medicine, Durham, NC, USA

ARTICLE INFO

Keywords:
Spinal cord astrocytoma
Glioma
Glioblastoma
Intramedullary spinal cord tumor
Cancer stem cell
Tumor survival cell
Gene-directed enzyme prodrug therapy
Recovery neurobiology

ABSTRACT

Spinal cord astrocytomas (SCAs) have discernibly unique signatures in regards to epidemiology, clinical oncological features, genetic markers, pathophysiology, and research and therapeutic challenges. Overall, there are presently very limited clinical management options for high grade SCAs despite progresses made in validating key molecular markers and standardizing tumor classification. The endeavors were aimed to improve diagnosis, therapy design and prognosis assessment, as well as to define more effective oncolytic targets. Efficacious treatment for high grade SCAs still remains an unmet medical demand. This review is therefore focused on research state updates that have been made upon analyzing clinical characteristics, diagnostic classification, genetic and molecular features, tumor initiation cell biology, and current management options for SCAs. Particular emphasis was given to basic and translational research endeavors targeting SCAs, including establishment of experimental models, exploration of unique profiles of SCA stem cell-like tumor survival cells, characterization of special requirements for effective therapeutic delivery into the spinal cord, and development of donor stem cell-based gene-directed enzyme prodrug therapy. We concluded that precise understanding of molecular oncology, tumor survival mechanisms (e.g., drug resistance, metastasis, and cancer stem cells/tumor survival cells), and principles of Recovery Neurobiology can help to create clinically meaningful experimental models of SCAs. Establishment of such systems will expedite the discovery of efficacious therapies that not only kill tumor cells but simultaneously preserve and improve residual neural function.

1. Introduction

Gliomas are tumors that arise from glial cells. They make up about 30% of all brain and spinal cord (i.e., the central nervous system: CNS) tumors. Intramedullary spinal cord tumors (IMSCTs: tumors within the parenchyma) are the rarest of primary spinal cord tumors with high grade ones causing severe neurologic deterioration, functional deficit or death. IMSCTs comprise 8 to 10% of all primary spinal cord tumors, which in turn account for 2 to 4% of all CNS tumors (Chamberlain and Tredway, 2011; Minehan et al., 2009) (**Fig. 1**). This is in contrast to intracranial gliomas, which comprise ~80% of all malignant tumors in the brain. Spinal cord gliomas can be sub-classified based on their cellular origin, with 60 to 70% classified as ependymomas and 30 to 40% classified as astrocytomas, followed by hemangioblastomas and other rare lesions (Babu et al., 2014; Milano et al., 2010).

Astrocytomas are a group of cancers derived from presently defined tumorigenic astrocytes of the CNS. Based on the most commonly used grading system established by the World Health Organization (WHO), astrocytomas are graded from I (least advanced disease with best prognosis) to IV (most advanced disease with worst prognosis). High grade SCAs fortunately are rare relative to other types of CNS cancers in humans. However, to date they remain to be the most difficult entities for clinical management due to their tenacious growth/metastasis, poor response to chemoradiotherapy, and difficulties or outcome uncertainty for surgical interventions (Abd-El-Barr et al., 2016). Although there are many similarities between astrocytomas of the spinal cord and those of the brain, there are important differences. These differences account for both the variations in tumor cell behaviors and importantly, in the tactics of devising research strategies to develop targeted therapies. For these reasons the review is mainly focused on high grade SCAs, with

* Corresponding author.
E-mail address: yang_teng@hms.harvard.edu (Y.D. Teng).
[1] Equal contribution authors.

https://doi.org/10.1016/j.expneurol.2018.09.010
Received 26 July 2018; Received in revised form 7 September 2018; Accepted 16 September 2018
Available online 21 September 2018
0014-4886/

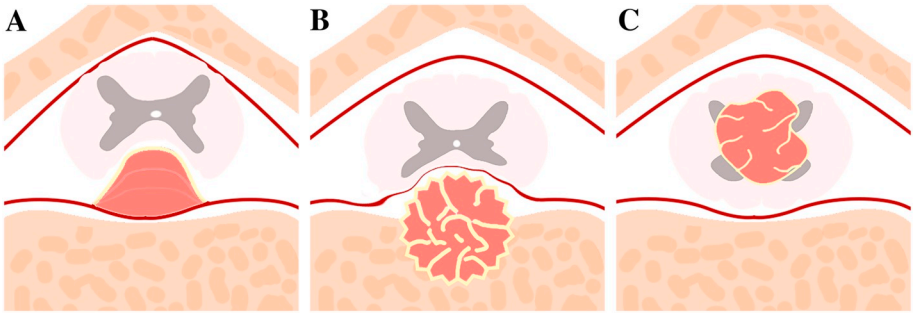

Fig. 1. The three general pathological types of spinal tumors.
(A) Extradural neoplasms: The majority of neoplastic lesions (~ 60%) grow extradurally and originate from the vertebrae, for which metastasis is the most frequent cause. (B) Extramedullary neoplasms: Intradural tumors are relatively rare with the extramedullary tumors being the more common type (~30%). Lastly, (C) intramedullary neoplasms: Intramedullary tumors are the least common (~10%) among all spinal tumors. However, they occur most often in the cervical levels of the spinal cord and comprise predominantly gliomas (i.e., infiltrative astrocytomas and ependymomas), imposing tenacious resistance to conventional treatments.

highlights shed on molecular oncologic genetics, research advances, and the different therapies that are currently used or under development for the management of SCAs.

2. Epidemiology

To judiciously design translational research approaches to treating high grade SCAs, it is important for laboratory investigators to first grasp the specific epidemiology feature of this group of tumors. Primary spinal cord gliomas occur in a very low incidence rate of 0.22 per 100,000 person-years (Milano et al., 2010; Schellinger et al., 2008). In regards to age preference, ependymomas are more common in adult spinal cord, while astrocytomas comprise 90% of IMSCTs in pediatric patients (Karsy et al., 2015; Ostrom et al., 2014b), showing a possible inclination of astrocytoma cells to grow in the biochemical and signaling regulation environment of the developing spinal cord. For SCAs, a recent examination of the Surveillance, Epidemiology and End Results (SEER) database revealed that most patients presented their first clinical signs during the first 3 decades of life and most had low grade lesions (Grades I or II) at time of diagnosis (Milano et al., 2010). Ependymomas, by contrast, were more likely to present between the ages of 40 and 59, with a majority being Grade I. A large retrospective review of all primary SCAs seen at the Mayo Clinic over 40 years uncovered an average age of 35 years at disease presentation, with 60% of patients being male (Minehan et al., 2009). The clinical manifestation of spinal cord gliomas is determined in large part by the location and growth profile of the tumor (**Fig. 1**). However, pain appears to be the predominant symptom in the majority of cases (~70%), which can be presented as back pain, radicular pain, or central pain (Raco et al., 2005). The next most common presentation is sensory deficit (~65%), followed by motor deficit (~50%). The duration of symptoms before diagnosis is usually protracted due to the nonspecific nature of the symptoms, with one large series uncovering an average symptom duration of 3 years (Raco et al., 2005). The occurring sites of these tumors are nearly evenly divided amongst cervical, thoracic and lumbar segments (Abdel-Wahab et al., 2006; Raco et al., 2005).

For WHO's conventional grading of astrocytomas, Grade I describes juvenile pilocytic astrocytoma or cystic cerebellar astrocytoma (and its variant juvenile pilomyxoid astrocytoma) that occurs more often in children and young adults (i.e., in the first 20 years of life). Astrocytoma Grade II (also called Low-Grade Astrocytoma) are diffuse tumor types such as fibrillary, gemistocytic, protoplasmic astrocytoma that tend to invade surrounding tissue and grow at a relatively slow pace. Grade III consists of anaplastic astrocytomas that are malignant and grow more aggressively. They often trigger seizures, neurologic deficits, headaches, or changes in mental status. Lastly, Grade IV comprises glioblastoma multiforme (GBM) that is the most malignant with poorest prognosis (Louis et al., 2007; Parsa et al., 2005; Zadnik et al., 2013). In its most current iteration, the WHO has incorporated molecular parameters in addition to histological grading in its classification schema (Louis et al., 2016). Noticeably, IMSCTs only account for 2% to 10% of all CNS tumors and for ~15% of primary intradural spinal tumors in adults (Heo et al., 2012; Sturm et al., 2012; Yang et al., 2012). Among them, about 70% are tumors of low malignant potential, such as low-grade astrocytomas and ependymomas (Schwartzentruber et al., 2012). However, a report on primary spinal cord tumors diagnosed between 1998 and 2002 showed that about 31% were Grade III or IV malignant tumors and 69% were Grades I or II non-malignant tumors (Schellinger et al., 2008).

2.1. Molecular biology and genetics of SCAs

Since standard treatment of SCAs involves maximal safe resection, followed by chemoradiation and there has been conflicting evidence for surgery efficacies, the reality has made tissue availability much scarcer for enabling systematically designed genetic and genomic studies to be carried out. For what have been published, the role of isocitrate dehydrogenase 1 (*IDH1)* and *IDH2* genes has become important in the understanding of tumorigenesis and prognosis of SCAs, which were used effectively for generating the 2016 WHO classification of astrocytomas (Sturm et al., 2012; Zadnik et al., 2013). The mutations lead to abnormal DNA methylation as they cause an abnormal production of 2-hydroxyglutarate that normally inhibits histone demethylases (Yang et al., 2012). The rate of IDH1 mutations in SCAs is presently not clear despite frequent detections of IDH1 mutations in autopsy samples of SCAs (Heo et al., 2012).

An important gene regulating methylation is the histone 3 variant H3.3 (H3F3A), which has been implicated in the tumorigenesis of both intracranial and spinal cord astrocytomas (Schwartzentruber et al., 2012; Wu et al., 2012). Two mutations, Lys27Met and Gly34Arg in H3F3A have been identified in nearly 80% of glioblastomas (i.e., Grade IV astrocytoma) in the brainstem, an anatomical structure that connects the spinal cord with the brain (Schwartzentruber et al., 2012; Wu et al., 2012). The Lys27 residue was found to be abnormally methylated in *IDH1* mutant glioblastoma – underlying the importance of epigenetic modification in CNS tumorigenesis (Sturm et al., 2012; Yang et al., 2012; Zadnik et al., 2013). The mutation of H3F3A K27M is predominantly detected in malignant astrocytomas arising in structures of the midline of the body, including the thalamus, brain stem, and spinal cord and was listed as a separate entity in the 2016 WHO classification (Louis et al., 2016; Solomon et al., 2016). Worth noting is the suggestion that the K27M mutation may be a marker of primary astrocytoma in the spinal cord and hence an indicator of the worst prognosis probability (Nagaishi et al., 2016).

Also on the list of important tumor markers is the BRAF gene (Schindler et al., 2011; von Deimling et al., 2011). BRAF is a member of the mitogen-activated protein kinase (MAPK) pathway which is important for cell survival including cellular division, cell cycle progression and excessive growth (i.e., malignant transformation; Penman et al., 2015). It has been shown that in a majority of pilocytic astrocytomas, a previously uncharacterized gene, KIAA1549, and the BRAF gene form a fusion oncogene that causes constitutive BRAF kinase activation (Jones et al., 2008). Detailed mutational analysis of the BRAF gene determined a valine to glutamate substitution at position 600

(BRAF V600E), resulting in constant activation of the MAPK pathway (Davies et al., 2002). The combination of the V600E mutation and a homozygous deletion of CDKN2A, which encodes P14ARF and P16INK4A, in human neural progenitor cells have been demonstrated to induce tumor cell transformation that manifested morphologic and pathologic features most close to those of malignant astrocytomas (Huillard et al., 2012). These mutations thus carry important prognostic and therapeutic impact, with fusion-negative patients showing better length of survival (LOS) and progression-free survival (PFS) compared to fusion-positive patients (Horbinski et al., 2012; Penman et al., 2015). In fact, numerous studies have uncovered that supratentorial pilocytic astrocytomas are more likely to harbor the BRAF V600E mutation, while posterior fossa and spinal cord pilocytic astrocytomas are more likely to harbor fusion oncogenes (Horbinski et al., 2012). A multi-institutional study of SCAs found that 80% of Grade I astrocytomas harbored mutations in the BRAF genes, among which 40% harboring the BRAF-KIAA1549 translocation and the other 60% having a BRAF copy number gain (Shankar et al., 2016). Interestingly, none of their specimens harbored the *BRAF* V600E mutation. The same study also found a preponderance of the K27M mutation in their series of Grade III and IV SCAs, suggesting that occurrences of the BRAF and H3F3A may segregate based on the grading of the astrocytoma, which should be additionally examined to establish possible prognostic utilities (Shankar et al., 2016).

Based on the profiles of the clinical manifestations and molecular causal factors of SCAs *we hypothesized that these marker genes are primarily involved in regulating cell survival endeavors; when functioning in pathological scales they drive intractable growth of high grade SCAs*. Our postulation is supported by outcomes of a systematic analysis of representative oncogenes of spinal cord astrocytoma (**Table 1**) that shows that most of the genes (i.e., in orange and red color zones) that have been established for clinical diagnosis and progression utility are indeed in charge of cell survival, not conventionally defined stemness biology (Teng et al., 2018). This conclusion suggests that cancer cell survivology mechanisms, in addition to stemness events that may be related to cancer occurrence, should be targeted for developing clinically meaningful therapeutics (Teng et al., 2018). As the field moves forward from histopathological grading of both intracranial and spinal cord gliomas into molecular grading, the efficacy of accurate experimental tumor modeling, and clinical tumor diagnosis, prognosis assessment and therapeutic plan design for SCAs will continuously be improved. The advancement has been additionally strengthened by validation of regulatory roles of microRNA (miR: small non-coding ribonucleic acid molecules that function primarily in RNA silencing and/or post-transcriptional regulation of gene expression) in cancer diagnosis and prognosis. This approach has been widely used in basic science settings and especially for evaluating clinical prognosis of SCAs (**Table 2**), further enriching the repertoire and sophistication of clinical diagnosis, prognosis assessment, academic reasoning, and research tactics to tackle SCAs.

Additionally benefited from this technology advancement is clinical efficiency since less tissue is needed for performing molecular diagnoses versus conventional histopathologic assays (Shankar et al., 2016). As a result, all the previously known problems concerning spinal cord tissue inadequacy and possibility of worsening neurological function due to biopsy procedures are and will be further mitigated.

2.2. Current therapeutic approaches for SCAs

Surgical treatment: There is currently no consensus on the best treatment for infiltrating SCAs. Oftentimes, there is a real need of tissue biopsy for diagnostic purpose as radiology imaging itself cannot differentiate between the different types of IMSCTs or other pathologies such as transverse myelitis, demyelination, infection, or even spinal cord infarction. For both intracranial and spinal cord astrocytoma cases, there is evidence that the extent of the surgical resection positively influences the patient LOS and PFS (Garces-Ambrossi et al., 2009; Karikari et al., 2015; McGirt et al., 2008). However, this correlation is tempered by surgery-triggered onset of neurological worsening that has been associated with poorer clinical outcomes (McGirt et al., 2009; Rahman et al., 2017). The latter has been considered as a very serious challenge regarding treatment plan formation for this category of tumors, which was caused by the conventional goal of cancer treatment (i.e., to remove tumor mass as much as possible). Unlike intracranial astrocytomas, the extreme functional eloquence of the spinal cord and its associated axonal tracts make the surgery utterly difficult, if not impossible to achieve a gross total resection (GTR) of SCA without causing additional permanent neurological deficits to the patient. Accumulated data suggested that histological grading, which affects infiltrative nature of the astrocytoma appears to be the most important factor to predict whether or not a dissection plane between the tumor and the spinal cord can be found and hence whether or not a GTR can be achieved (Toktas et al., 2018; Abd-El-Barr et al., 2016; Karikari et al., 2011). Indeed, for low-grade gliomas, especially grade I pilocytic astrocytomas, often a dissection plane could be determined for carrying out a GTR without subjecting the patient to a neurological deficit. In these cases, aggressive surgical approaches under intraoperative magnetic resonance imaging assistance are normally advised in order to give the patient the best chance of increased survival and lower the risk of recurrence (Toktas et al., 2018). By contrast, for Grade III or IV SCAs, such a dissection plane simply does not exist; thus, aggressive surgical resection is not recommended as this will subject the patient to more neurological deteriorations with some of them frequently being permanent. For those cases, surgical options are truly limited and qualitatively improved prognosis relies on targeted cancer therapy that has been under development (Ropper et al., 2016; Zeng et al., 2016). Typically, a biopsy with expansile duraplasty is used as the safest option to establish a definitive diagnosis and the space created may temporally alleviate clinical signs caused by continued growth of the tumor. Even for biopsy intraoperative neuromonitoring is strongly advised to assist the surgeons to mitigate possibilities of causing complications and to strive to remove as little tissue as is needed to enable a diagnosis (Verla et al., 2016). Similar to advances being made in intracranial mapping techniques, newer intraoperative neuromonitoring techniques are designated to helping to identify safer passages to these intramedullary tumors for surgical approaches without triggering neurological deficits (Deletis and Sala, 2008; Nair et al., 2014). Although presently surgery intervention is not recommended for treating patients with high grade and infiltrating SCAs, rapid intraoperative diagnosis of molecular markers and histopathologic profiles via glioma biopsy is a promising direction of development in the immediate future as we are learning more about the oncological features of these different subtypes of malignant tumors for designing targeted therapies (see details below; Shankar et al., 2015).

Radiation therapy and chemotherapy: The role of radiotherapy for managing SCAs remains debatable and controversial. Although adjuvant or postsurgical radiotherapy has been adopted worldwide, the exact effects on SCAs have not been systematically examined and validated. Conceivably, for low grade SCAs, only limited benefits can be speculated for postoperative radiotherapy due to the spontaneous low recurrent rates of the tumors that argue against any real necessity for the patients to have radiation exposure for its known side effects (Epstein et al., 1992; Rodrigues et al., 2000). Rather, radiotherapy is indicated postoperatively for cases of partial resection and high grade SCAs (Jyothirmayi et al., 1997). Nevertheless, some research data suggested that a slight advantage of overall survival may be attainable for radiotherapy of low grade astrocytomas via enhanced control of tumor growth (Jyothirmayi et al., 1997; Santi et al., 2003). This effect may be true particularly for patients under 25 years old (Guss et al., 2013). Conversely, the risk of secondary malignancy and growth retardation that have been indicated in pediatric patients radiotherapy should be factored in except, perhaps in very special circumstances such as cancer recurrence (Kutluk et al., 2015).

Table 1
Common molecular markers used to diagnose spinal cord astrocytomas (SCAs)

Gene	Full Name	Wide Type Protein	Function	Mutation Protein	Oncological Features
IDH	Isocitrate Dehydrogenase	IDH1 (Cytoplasm)	NADPH production; Defense against oxidative stress (Jo et al., 2001)	IDH1 R132H (R132S, R132C, R132G, and R132L)	D-2-hydroxyglutarate (D-2HG) accumulation in tumor cells, which contributes to tumorigenesis, cell growth and survival (Zhao et al., 2009); Remodeling the methylome of DNA and establishing glioma-specific G-CIMP (Turcan et al., 2012).
		IDH2 (Mitochondria)		IDH2 R172K	
H3F3A	H3 histone family member 3A	H 3.3 (Nucleus)	Nucleosome structure of the chromatin. It supports chromosomal heterochromatic structures, which maintains genome integrity during mammalian development (Jang et al., 2015).	Lys27Met Gly34Arg K27M G34R/G34V	Cancer cell migration (Park et al., 2016) and DNA hypomethylation (Bender et al., 2013); Alternatively lengthening of telomeres; Affecting specific gene expressions (Schwartzentruber et al., 2012) and tumorigenesis (Bjerke et al., 2013).
TP53	Tumor protein p53	p53 (Nucleus and/or cytoplasm)	Initiating apoptosis, activating DNA repair, arresting growth by cell cycle regulation, and inhibiting angiogenesis, cellular renew and differentiation (Ryan et al., 2001).	Deletion	Tumor development and radioresistance (Squatrito et al., 2010).
CDKN2A	Cyclin Dependent Kinase Inhibitor 2A	p16INK4a and p14ARF (Nucleus)	Cell cycle regulation (Ichimura et al., 2000), inhibition of cell proliferation and telomerase activity (Fuxe et al., 2000).	Point Mutation Deletion	Cell proliferation (Mistry et al., 2015) Resistance of antimetabolite agents (Iwadate et al., 2000)
CDKN2B	Cyclin Dependent Kinase Inhibitor 2B	p15INK4b (Nucleus)	Regulating cell growth and the cell cycle G1-S progression (Wrensch et al., 2009b). It has been recognized as an effective “backup” for loss of CDKN2A (Krimpenfort et al., 2007).	Point mutation Deletion	Tumorigenesis and cell proliferation (Simon et al., 1999). Its variants are associated with high-grade glioma susceptibility (Wrensch et al., 2009a).
PTEN	Phosphatase and tensin homolog	PTEN (Cytoplasm)	Inhibitor of PI3K/AKT signaling pathway: maintaining genomic stability, and suppressing cell survival and cell proliferation (Yin and Shen, 2008).	Point Mutation Deletion	Activation of PI3K/AKT pathway, angiogenesis, tumorigenesis (Cheney et al., 1998; Smith et al., 2001).
NF1	Neurofibromin 1	Neurofibromin (Cytoplasm)	GTPase-activating protein and negative regulation of RAS/MAPK pathway activity (Johannessen et al., 2005)	Mutation (R1391S, R1513*, e25-1, e29 +1, etc.) Heterozygous deletions	Inactivation of neurofibromin, activation of RAS/MAPK pathway, and suppression of apoptosis (Johannessen et al., 2005; Tanic et al., 2012).
BRAF	B-Raf Proto-Oncogene, Serine/Threonine Kinase	BRAF (Cytoplasm)	Regulation of the MAP kinase/ERK signaling pathway, which controls cell cycle entry, proliferation, and integration of mitogen and stress signals for proliferation (Yang et al., 2017).	BRAF V600E (R461I, I462S, G463E, G463V, G465A, G465E, etc.) KIAA1549-BRAF	Activate MAPK/ERK signaling pathway; Promote cell proliferation and transformation, or formation of anchorage independent colonies (Liu et al., 2007).
EGFR	Epidermal growth factor receptor	EGFR (Cell membrane)	Cellular proliferation, growth, differentiation, and survival (Oda et al., 2005; Reddy et al., 2016).	vIII mutants	Constitutive activation of EGFR and its downstream proproliferative and antiapoptotic pathway. Cell proliferation and invasion (Micallef et al., 2009). Radioresistance and DNA repair (Lammering et al., 2003).

(continued on next page)

Table 1 (*continued*)

Note: Color coding: Green zone genes and molecules mainly regulate cell metabolism and proliferation, or repair DNA damages (i.e., tumor suppressors); their mutations can trigger SCA occurrence. Orange zone genes and molecules largely promote cell proliferation and cell survival under physiological condition. Red zone genes are those with mutations such as genetic deletion, which turns on their ability to promote cell survival by augmenting cell proliferation, migration and drug-tolerance, as well as by suppressing apoptosis (Bender et al., 2013; Bjerke et al., 2013; Cheney et al., 1998; Fuxe et al., 2000; Ichimura et al., 2000; Iwadate et al., 2000; Jang et al., 2015; Jo et al., 2001; Johannessen et al., 2005; Krimpenfort et al., 2007; Lammering et al., 2003; Liu et al., 2007; Micallef et al., 2009; Mistry et al., 2015; Oda et al., 2005; Park et al., 2016; Reddy et al., 2016; Ryan et al., 2001; Simon et al., 1999; Smith et al., 2001; Squatrito et al., 2010; Tanic et al., 2012; Turcan et al., 2012; Wrensch et al., 2009a; Wrensch et al., 2009b; Yang et al., 2017; Yin and Shen, 2008; Zhao et al., 2009).

For high grade SCAs that generally have low sensitivity to radiation treatment, a recent systematic review of overall survival in a pediatric series showed that adjuvant radiotherapy improved general outcome of primary spinal glioblastoma multiforme (Konar et al., 2017), which is different from results from previous studies (Fakhreddine et al., 2013; Santi et al., 2003). Given the lack of large multicenter studies, it appears that prospective clinical trials are needed to further clarify the role of radiotherapy, with a focus on differing results in different pathological types, molecular grade of SCAs, and patient profiles (e.g., age, gender, clinical history, etc.).

Currently, established chemotherapy regimens are also considered to have limited value in the treatment of SCAs. It is commonly reserved

Table 2
micro RNAs (miRs) currently used as prognostic indicators for spinal cord astrocytomas (SCAs)

MicroRNAs	Full Name	Function	Clinical Value
miR-126	MicroRNA-126	Likely having effect on suppressing angiogenesis (Han et al., 2016)	Potential marker for postsurgical prognosis evaluation for patients with brain glioblastoma (Han et al., 2016)
miR-106a	MicroRNA-106a	Suppress cell proliferation and induce apoptosis (Zhang et al., 2012)	Independent and significant predictor of prognosis in glioblastoma patients (Zhao et al., 2013)
miR-130a	MicroRNA-130a	Suppress angiogenesis (Chen et al., 2008), and promote cancer migration, invasion and proliferation (Jiang et al., 2015)	Marker of favorable prognosis (Qiu et al., 2013)
miR-181d	MicroRNA-181d	MiR-181d directly regulates MGMT post-transcriptionally (Zhang et al., 2012)	Biomarker to predict temozolomide response (Zhang et al., 2012)
miR-326	MicroRNA-326	Regulate cell survival (Kefas et al., 2010)	Marker of favorable prognosis; An important candidate as a tumor suppressor (Wang et al., 2013)
hTERT mRNA	Telomerase messenger ribonucleic acid	Maintenance of telomeric DNA at the ends of chromosomes (Kang et al., 2016)	A potential prognostic factor and diagnosis marker (Shervington et al., 2007; Lötsch et al., 2013)
MiR-21	MicroRNA-21	Suppress cell apoptosis (Chan et al., 2005)	Poor prognostic marker (Hemansen et al., 2013)
miR-155	MicroRNA-155	Regulate cell invasion and chemosensitivity (Liu et al., 2015)	Poor prognostic marker (Qiu et al., 2013)
miR-182	MicroRNA-182	Facilitate cell migration and promote cell survival (Segura et al., 2009)	Prognostic marker for glioma progression and patient survival (Jiang et al., 2010)
miR-210	MicroRNA-210	Promote a hypoxic phenotype and radioresistance (Grosso et al., 2013)	Poor prognostic marker (Qiu et al., 2013)
miR-215	MicroRNA-215	Promote tumor growth by activating the CTNNBIP1/β-catenin pathway (Tong et al., 2015)	Poor prognostic marker (Tong et al., 2015)
miR-637	MicroRNA-637	Promote cell growth, migration and invasion via direct targeting Akt1 (Que et al., 2015)	Poor prognostic marker (Que et al., 2015)

Note: Green color-coded miRs are associated with more favorable prognosis; red color-coded miRs and mRNA are associated with poor outcomes of SCAs (Chan et al., 2005; Chen and Gorski, 2008; Grosso et al., 2013; Han et al., 2016; Hermansen et al., 2013; Jiang et al., 2010; Jiang et al., 2015; Kang et al., 2016; Kefas et al., 2010; Liu et al., 2015; Lötsch et al., 2013; Qiu et al., 2013; Que et al., 2015; Segura et al., 2009; Shervington et al., 2007; Tong et al., 2015; Wang et al., 2013; Zhang et al., 2012; Zhao et al., 2013).

for patients with tumor recurrences after surgery and radiotherapy. Temozolomide, an oral methylating agent, has become standard therapy in newly diagnosed adult intracranial GBM (Hegi et al., 2005; Stupp et al., 2005). There are, however, small study series that have shown encouraging results for low-grade SCAs, with 18% of patients having a partial response and no major adverse reactions (Chamberlain, 2008). For high-grade astrocytomas, small retrospective series have shown some benefits, with ~40% of patients showing a partial response, albeit more hematological side effects were noted (Kaley et al., 2012; Kim et al., 2011). In addition, antiangiogenic treatments have also shown certain effects. Bevacizumab is such an antiangiogenic agent that targets vascular endothelial growth factor (VEGF). Small size retrospective studies have suggested a palliative impact for the use of bevacizumab in spinal cord gliomas that manifested persistent progression despite surgical resection, radiation therapy and temozolomide therapy (Chamberlain and Johnston, 2011).

Kaley et al. reported that administration of temozolomide and bevacizumab may be beneficial in the recurrence of spinal cord high-grade gliomas after radiotherapy (Kaley et al., 2012). A pilot study assessing the long term outcome of combinatorial chemoradiation treatments suggested that the approach was feasible and could serve as a therapeutic option (Corradini et al., 2016). But due to the small size of the patient population, different origins of tumors and limitations of retrospective investigations, convincing evidence remains lacking to standardize chemoradiation for SCAs (Corradini et al., 2016).

2.3. Experimental investigation and therapy development

Based on the afore-described data, it is clear that SCAs are extremely difficult oncologic entities to treat. This is partly attributable to the inherently aggressive biology of these tumors, but also due to the eloquent structures of the spinal cord, making aggressive surgical treatment – an important intervention, not applicable in SCAs, especially for infiltrating neoplastic lesions. Thereby, basic science investigations and experimental therapies should become the focal point in order to eventually overcome SCAs. However, most experimental endeavors have to date been carried out for the research and treatment development of intracranial gliomas, leaving IMSCTs as an understudied topic. Consequently, there are very few experimental models being established for investigating SCAs in vivo. In the next section, we reviewed some of the promising investigations, comprising establishing clinically relevant models, stem-cell therapies, gene therapies and immunotherapies, all aiming to devising targeted treatments, with emphasis on how to effectively eliminate the diffusely infiltrating astrocytoma cells and preserve the residual neural network in the spinal cord, particularly for the segments that sustain vital functions (e.g., cervical spinal cord for respiratory and circulation functions).

2.4. Experimental models of IMSCTs

The migratory and diffuse growth feature of high grade astrocytoma cells in the spinal cord and brain often renders surgical treatment *per se* insufficient and not feasible. A powerful approach to changing this situation is to first set up experimental models of IMSCTs with high clinical face value. Prior to our work that was published in 2016, there had been only 3 articles describing how to design rat models of intramedullary spinal cord gliomas. All three protocols reported reproducible intramedullary growth of glioma by directly injecting 9L gliosarcoma, 98L glioma, or glioblastoma multiforme neurosphere cells into the middle or lower thoracic spinal cord level (Caplan et al., 2006; Hsu et al., 2012; Ren et al., 2010). The lower thoracic spinal cord tumors produced hindlimb locomotion deficits, which were used for testing standard behavioral batteries to define the survival duration of the affected rats.

However, in humans the cervical and cervicothoracic junction regions of the spinal cord with enriched autonomic neural components are more common sites for the multitude of growth of intramedullary astrocytomas. Thus, autonomic disorders are often presented by the patients, which, sometimes, have life-threatening consequences (Furlan et al., 2003; Krassioukov et al., 2009; Osborn et al., 1990; Teasell et al., 2000). More research effort is therefore needed to establish cervical spinal cord models of high grade SCAs. We recently designed a rat C6 model of SCAs by implanting G55 or U87 human astrocytoma cells, and characterized the pathophysiological profile by assessing positive correlations between the scale of C6 tumor growth with degrees of abnormality in the somatomotor and sensory systems, respiratory function, blood pressure, heart rate, body temperature, and body weight (Ropper et al., 2016). Furthermore, we investigated whether human NSCs (hNSCs; see below for details) could be genetically engineered into effector cells to carry out gene-directed enzyme prodrug therapy (GDEPT) for controlling midcervical SCAs, tapping into hNSC's chemotactic capability to track cancer cells following the chemical concentration gradients of the ligands (e.g., VEGF, CXCL-12, etc.) produced by the tumor and/or inflammatory cells (Ropper et al., 2016; Teng et al., 2011; Schmidt et al., 2005). In our model, the non-treated control C6 SCA rats showed significantly decreased respiratory rate and correspondingly increased inspiration time phase during the late stage of tumor growth. The data of respiratory change was consistent with clinical observation in patients with cervical SCAs-related bilateral diaphragm weakness who often show the so-called "poor inspiratory effort" because about 70% of tidal volume in humans is normally attributable to the inspiratory work of the diaphragm, in contrast to rodent's breathing activity that is driven more by the force derived from the intercostal and abdominal muscles (McCool, 2012; Teng et al., 1999). C6 SCA model also exhibited progressive disturbance of blood pressure and body temperature. For example, beginning at the third week after G55 astrocytoma cell transplantation, rats without receiving effective treatment showed significantly decreased group average systolic arterial blood pressure (SP). Their group mean arterial blood pressure (MAP = DP + 1/3 x [SP – DP]; DP: diastolic blood pressure) reduced significantly at the terminal stage when they could not consistently perform body weight-bearing locomotion (Ropper et al., 2016). The MAP data suggested that the cervical tumor growth might have compromised systemic tissue blood perfusion in the C6 SCA rats (Teng and Wrathall, 1996). This notion was corroborated by changes of body temperature in the same set of rats; we observed more severe hypothermia in the C6 SCA rats starting in the third week after tumor cell injection (Ropper et al., 2016). Academically, the C6 SCA model was also investigated in an innovative way to understand adult mammalian spinal cord neurobiology through characterizing its functional adaptation in response to the gradually escalated assaults and damages of infiltrating tumor cell growth to the axonal tracts and neurons. We hope that the approaches will ignite more research investment to research and therapeutic development for SCAs and other currently intractable metastatic diseases (Ropper et al., 2016).

2.5. Stem Cell-based gene directed enzyme prodrug therapy (GDEPT)

Neural stem cells (NSCs) are multipotent cells that are capable of generating gliogenic or neurogenic progeny (Teng et al., 2017; Llorens-Bobadilla and Martin-Villalba, 2017). There are generally four main sources for mammalian (including primate) NSCs to be isolated or derived for basic research and translational study applications: the neurogenesis niches of the subgranular zone (SGZ) of the young or adult hippocampal dentate gyrus, the subventricular zone (SVZ) of the lateral ventricles or the hypothalamus in developmental and adult brains, the embryonic stem cells (ESCs), and the inducible pluripotent stem cells (iPSCs) (Aboody et al., 2011). One of the functional multipotency features of NSCs is that these cells possess an exquisite tumor-tropism property that is enabled by their developmental capability of chemotactic migration (Aboody et al., 2000; Kim et al., 2005; Teng et al., 2011, 2012, 2017). Thereby, NSCs are able not only to track down and

move close to clusters or individual astrocytoma cells *in vitro* they can also track and infiltrate tumor masses *in vivo* (Aboody et al., 2000; Schmidt et al., 2005; Kim et al., 2005; Ropper et al., 2016). These properties of NSCs make them powerful vehicles to locally deliver anti-cancer genes and drugs with minimized systemic side effects. Buoyed by this innate biology of stem cells, many genetic engineering strategies have been formulated to equip NSCs with molecular mechanisms such as synthesis of a particular enzyme (i.e., GDEPT) that can convert a specific non-toxic prodrug into an oncolytic compound (Aboody et al., 2000; Ropper et al., 2016; Zeng et al., 2016). Hence, after the NSCs have migrated into the cancer cell's vicinity, a benign prodrug can be systemically administered for killing cancer cells via the afore-described "bystander effect" (Aboody et al., 2000; Ropper et al., 2016; Zeng et al., 2016).

Following completion of many well-designed animal studies, there was a recently published report on a phase-I clinical study that evaluated safety of applying an immortalized human NSC system in brain glioma cases (Portnow et al., 2017). Briefly, 15 patients with recurrent brain glioblastomas were treated with a one-time intracranial administration of the genetically engineered NSCs that expressed cytosine deaminase (HB1.F3.CD.C21) that converts the prodrug 5-fluorocytosine (5-FC) to the cytotoxic 5-fluororacil (5-FU). Investigators found no evidence of dose limiting toxicity (DLT) due to the injected CD-NSCs. However, there was one case of DLT (i.e., transaminitis) occurrence, which was considered to be likely caused by 5-FC (Portnow et al., 2017). Microdialysis evaluation revealed that the cytotoxic drug 5-FU was produced in the brain in a 5-FC dose-dependent manner and autopsy results from 2 patients deceased from disease progression revealed that the donor NSCs migrated to infiltrate distant tumor sites without donor-related tumorigenic signs. Although the primary end point in this study was safety and the sample size was very small, efficacy could be loosely inferred by the fact that those patients receiving higher doses of the NSCs were found to have a longer median overall survival compared to those patients that received lower doses. However, based on our observation of the significantly diminished functional deficits in C6 SCA rats that received hNSC-based GDEPT and the functional multipotency of NSCs (e.g., production of trophic factors, etc.), it is important to examine whether the administered hNSCs also enhanced residual brain tissue preservation and function by activating alternative neural circuits (Ropper et al., 2016, 2017; Teng et al., 2011, 2017) or even through the potential of forming new neurons to integrate into the neurocircuit (Teng et al., 2017). Encouragingly, the same technology has been successfully used to engineer human mesenchymal stromal stem cells (hMSCs) to investigate and treat brain glioblastoma (Chung et al., 2016). However, more work is needed to reveal molecular specifics for the widely recognized pro- and anti-oncogenic properties of hMSCs in order to judiciously apply them for tumor control purposes (Chulpanova et al., 2018). We reiterate that integration of such Recovery Neurobiology principle (i.e., augmenting residual neural tissue sparing and function, or activating alternative neural pathways; Ropper et al., 2017) into the conventional oncolytic approach that solely focuses on killing tumor cells may synergistically increase the overall efficacy of cancer therapy.

In our premiere study, a clonal hNSC line (i.e., F3.hNSC) was engineered to express either cytosine deaminase gene only (i.e., F3.CD) or dual genes of CD and thymidine kinase (i.e., F3.CD-TK) to carry out GDEPT in a rat model of midcervical SCA (Ropper et al., 2016). F3.CD or F3.CD-TK cells were injected into the tumor epicenter 7 days after C6 tumor seeding. The C6 SCA rats that received the treatment of the F3.CD-TK NSCs plus systemic administration of 5-FC and Ganciclovir (GCV), prodrug of 5-FU and GCV triphosphate that are converted by CD and TK, respectively, lived significantly longer than those received F3.CD only or F3.hNSC debris followed with the same formula of 5-FC and GCV treatment (Ropper et al., 2016). Since the U.S. Food and Drug Administration lately approved the first clinical study evaluating a CD-engineered hNSC therapy for recurrent high-grade glioblastomas in the brain (Portnow et al., 2017), we are currently investigating more oncolytic strategies in newly established experimental models following the Recovery Neurobiology principles, aiming to ultimately translate our findings for treating patients suffering from high grade astrocytoma (Karikari et al., 2011; Snyder and Teng, 2012; Ropper et al., 2016, 2017).

2.6. Direct gene therapy and gene editing

Traditionally, gene therapy has been defined by the addition of new genes to human cells. Nevertheless, a new paradigm has emerged with the advent of genome-editing techniques, where the human genome can be retailored to achieve a therapeutic effect (Friedmann and Roblin, 1972; Maeder and Gersbach, 2016; Maguire et al., 2014). The major catalyst behind the genome-editing techniques was the discovery that targeted DNA double stranded breaks (DSBs) could be used to "hijack" the cell's endogenous cellular repair mechanisms to delete deleterious genes or re-express lost genes that are therapeutically needed (Takata et al., 1998). Maeder and Gersbach reviewed the four primary methods of causing targeted DSBs – Zinc finger nucleases, transcription activator-like effector (TALE)-nucleases (TALENs), meganucleases, and the most recent CRISPR/Cas system (Maeder and Gersbach, 2016). Description of the specifics of these different methods is beyond the scope of this paper. It is worth noting that the CRISPR/Cas mechanism is derived from a system that was evolved in bacteria; it is a prokaryotic immune system that provides defense to foreign genetic molecules such as those present within plasmids and phages. The fact clearly indicates that even in the 21st century the knowledge and capability of humans to biotechnologically simulate nature's basic ways of maintaining genetic homeostasis still remain in a very early stage of development (Barrangou et al., 2007; Horvath and Barrangou, 2010; Wiedenheft et al., 2012).

Logically, as these technologies begin to capture attention in the science and clinical communities, their safety-related questions and potential ethic issues are also arising. Among them, how to control and reach the designed specificity of the genome-editing or gene delivery in using these genome-editing tools is one of the top concerns (Maeder and Gersbach, 2016). For now data obtained from intracranial glioblastoma studies suggested that a convergence of methods, rather than exclusive methods may be a better approach to overcoming the adaptive mechanisms used by glioblastomas to evade a conventionally standardized treatment (O'Duibhir et al., 2017).

2.7. Targeted immunotherapy

The role of the immune system in cancer tumorigenesis has long been recognized, from the empirical observation that immunosuppressive regimens or immunosuppressive states are accompanied with an increase in the incidence of malignancy (Calinescu et al., 2015; Doll and Kinlen, 1970). Conversely, both solid and hematologic cancers have been shown to progress more slowly or even gradually disappear when a targeted immune response is elicited (Burnet, 1967; Calinescu et al., 2015; Ostrom et al., 2014a). From these observations, the concept of immune surveillance was born, where it was hypothesized that the immune system is responsible for the continuous monitoring and elimination of cells harboring neoplastic mutations. Reciprocally, it has been observed that cancer cells are capable of producing immunosuppressive cytokines, which could lead to their escape from immune surveillance. With its regards to the CNS, there has long been a dogma that the CNS is immunoprivileged (Fecci et al., 2014). This was first suggested based on experiments in the 1940s in which skin grafts transplanted into the brain of experimental animals avoided rejection (Medawar, 1948). However, subsequent studies have modified this dogma: instead of absolute immunologic privilege, a concept that CNS has its distinct immunological processes was formed (Dunn et al., 2012).

Due to the demand in medical practice, most of the preclinical and clinical efforts on developing immunotherapy for CNS gliomas have so far targeted Grade-IV astrocytomas. In general, the major categories of these therapies comprised surface-directed passive immunotherapies, adoptive lymphocytic transfer, cancer vaccines, and immune checkpoint blockade (Calinescu et al., 2015; Fecci et al., 2014). For surface-directed passive immunotherapies, the goal is to bind a therapeutic reagent to a specific molecule on the tumor surface in order to block important tumor growth/survival pathways (e.g., EGFR-mediated signaling) or to activate tumoricidal toxins. Effective surface molecules that have shown overexpression in glioblastomas include EGFR, tenascin, transferri, IL13 and I4 receptors (Calinescu et al., 2015; Fecci et al., 2014). The two major limitations to this methodology are the relative impermeability of the blood brain barrier (BBB) to these large protein constructs, which often require direct injection into the resection cavity and the fact that the response is limited by the half-life of the agent delivered (Fecci et al., 2014; Platten et al., 2016; Sampson et al., 2010). Two other mechanisms likely have also mitigated the efficacy of this methodology, which are the heterogeneity of the surface target expression and the ability of these tumors to adapt to this mode of attack (Furnari et al., 2015; Platten et al., 2016).

Adoptive lymphocyte transfer uses T-cells that are harvested and expanded and sensitized *ex vivo* against glioblastoma for autologous cell transfer back to patients, often with other immune cells, such as dendritic cells (Fecci et al., 2014; Han et al., 2015; Prins et al., 2008; Samaha et al., 2015). To ensure generation of large amounts of functional T-cells, a recent technology development that has shown promise is to genetically modify T-cells to enable expression of a chimeric antigen receptor (CAR), which can bind to tumor antigens in an MHC-unrestricted manner to activate T-cells (Gross et al., 1989; Han et al., 2015).

Also surging is the interest in developing vaccines that are made from antigens (e.g., proteins) expressed almost exclusively by a particular type of cancer cells to activate immune system recognition for selective elimination. Presently, there are five categories of tumor antigen vaccines: (1) *antigen vaccines* that are made from special protein antigens in cancer cells. Since the genetic codes of different cancer cell specific proteins have been uncovered, these vaccines can be made in large quantities; (2) *whole cell vaccines* that are made from the whole cancer cell from the patient, another person, or cancer cells that cultured in the laboratory; (3) *dendritic cell (DC) vaccines* that help the immune system to recognize and attack cancer cells. Often autologous DCs maintained *ex vivo* are pulsed with tumor antigens before injecting back into patients. After stimulation, DCs mature and migrate to draining lymph nodes where they induce immune responses to assault cancer cells; (4) *DNA vaccines* that are made with bits of DNA from cancer cells. Following administration of the vaccines the immune system can be stimulated to destroy the cancer cells; and (5) *anti-idiotype vaccines* are made of antibodies that detect other antibodies as the antigen and bind to it. The vaccines can stimulate the body to produce antibodies against tumor cells. These strategies have been used individually or in combination with additional molecular manipulations to enhance efficacy, as per the following studies discussed. Similar to human papillomavirus (HPV) and hepatitis B that were found to be causative of cervical and hepatocellular carcinoma, respectively (Benvegnu et al., 1994; Walboomers et al., 1999), potential roles of cytomegalovirus (CMV) in triggering glioblastoma and pediatric glioma were also investigated. In spite of some controversial findings, certain evidence suggested that the viruses may be etiological in the oncogenicity of those tumors (Cobbs, 2013; Mitchell et al., 2008; Wakefield et al., 2015). These possible tumorigenic connections can provide specific antigenic epitopes for developing targeted immune therapies. For example, it was reported that pre-conditioning the vaccine site with a potent recall antigen (i.e., tetanus/diphtheria toxoid: Td) could significantly improve the lymph node homing and potency of tumor-antigen-specific DCs. In randomized patients with glioblastoma who received pre-conditioning with either mature DCs or Td unilaterally before bilateral vaccination with DCs pulsed with Cytomegalovirus phosphoprotein 65 (pp65: expressing in > 90% of glioblastoma specimens but not in normal brain), those given Td had enhanced DC migration bilaterally and significantly improved survival (Mitchell et al., 2015).

Immune checkpoints are important signaling mechanisms that prevent autoimmune reactions and allow for self-tolerance by decreasing normal T-cell-mediated immune responses (Calinescu et al., 2015). It has become increasingly recognized that tumors, including glioblastoma can damp immune checkpoints to limit host T-cell mediated attack (Fecci et al., 2007; Pardoll, 2012; Platten et al., 2016). Major advances in understanding immune checkpoint inhibition have been made in the treatment of melanoma, where antibodies against CTLA-4 and PD-1 have shown promising results clinically (Hamid et al., 2013; Hodi et al., 2010). Encouraging outcomes have also been reported for preclinical test of immune checkpoint inhibitors in murine models of glioblastoma, and there are several phase I-III trials to determine whether the efficacy may be translated to the clinical realm (Agarwalla et al., 2012; Kim et al., 2017; Wainwright et al., 2014).

2.8. Special considerations for therapeutic delivery to the Spinal cord

Many of the more recent experimental therapies for intracranial gliomas require direct application of these therapies close to the affected area during resection of primary or recurrent gliomas. This is due to the impermeability of the blood-brain barrier (BBB) and blood-spinal cord barrier (BSCB) to large and/or charged (i.e., hydrophilic) molecules such as proteins and the increased effectiveness of the required immune responses following direct injection (Dunn et al., 2012; Hulou et al., 2016; Mitchell et al., 2015). Thus, for therapeutic delivery to SCAs, there have been numerous challenges. First, due to the anatomical fragileness of the spinal cord, gross total resection of high grade spinal cord gliomas is often not possible without subjecting patients to neurological deficits. Overall, data to date remains insufficient regarding detailed permeability and metabolic differences between the BSCB and BBB, particularly in terms of unique changes under different diseases and trauma conditions (Bartanusz et al., 2011). Such specific information, if available, would be highly valuable in designing tailored therapies to treat spinal cord tumors and other pathological conditions. Mannitol and other substances have been used to disrupt BSCB in animal models (Prockop et al., 1995). These methods however failed to gain traction in clinical trials, as it was reported that the methods increased the permeability of tumor vasculature by 25%, but increased normal vascular permeability by 10-fold higher, leading to the leakage of proteins, etc. to trigger unwanted systemic effects (Garg et al., 2015; Kroll and Neuwelt, 1998). To overcome uncertainties imposed by the BSCB and BBB, local delivery strategies for conventional therapeutics or stem cells have been extensively investigated. Among the innovative approaches, biodegradable polymers have shown impactful promise in treating both spinal cord and intracranial diseases. Brem et al. first proposed using a biodegradable polymer (poly [bis(p-carboxyphenoxy)]propane-sebacic acid) as a method to administer interstitial chemotherapy in the treatment of primary and recurrent intracranial gliomas (Brem et al., 1995). For therapeutic NSC delivery into the spinal cord, in a joint pioneer study with MIT's Langer Lab we tested a biodegradable polymer construct that was seeded with either murine or human NSCs in the injured rat and non-human primate (i.e., African green monkey) spinal cord, respectively (Teng et al., 2002; Pritchard et al., 2010). The results of these preclinical studies have led to FDA's approval of applying a scaffold alone design as the first implantable therapeutic device for an early phase clinical trial for patients with ASI-A acute thoracic spinal cord injury (see details in: https://clinicaltrials.gov/ct2/show/NCT02138110). In addition, a report has shown some intriguing results of releasing paclitaxel, a chemotherapeutic agent from ReGel, a thermal gel depot-based delivery system in a rat model of

gliosarcoma (Tyler et al., 2012). We anticipate that future endeavors will concern how to use polymer for controlled release of genetically engineered stem cells or drugs to maximize the initial success we obtained in GDEPT treatment for experimental SCAs (Ropper et al., 2016).

To improve intraparenchymal drug distribution, convection-enhanced delivery (CED) was first presented in 1994 (Bobo et al., 1994) as a method to overcome the diffusion-limited application of chemotherapeutics in the brain. It involves the use of pump connected to an infusion catheter and maintains a pressure gradient, aiming to sustain more diffuse and homogeneous drug concentrations, with results showing improved drug administration in the spinal cord (Endo et al., 2015; Lonser et al., 1998). Interestingly, due to the different anistropic properties, the gray matter and white matter of the spinal cord exhibit distinct characteristics of drug distribution by CED. Whereas the ratio of the volume of distribution to the volume of infusion in the gray matter was comparable to that of the white matter, drugs remained in the white matter tract and rarely infused into the adjacent gray matter. Conversely, when drugs were injected into the gray matter, they infiltrated laterally into the white matter tract and traveled longitudinally and preferably along the white matter funiculi. At the infusion center, the areas of drug presence were generally larger in the gray matter CED than in the white matter (Endo et al., 2015). The findings have therapeutic implications in the drug delivery to treat spinal cord gliomas, which grow in both the white matter and the gray mater (Ropper et al., 2016).

Lastly, the use of intrathecal delivery has been adopted for the treatment of both brain and spinal cord disorders (Garg et al., 2015; Nance et al., 1995; Sampson et al., 2002; Yu et al., 2013). For long-term release of therapeutic substances, electrical or osmotic pumps connected to an intrathecal catheter have become widespread, especially in the treatment of spasticity or neuropathic pain after spinal cord trauma (Garg et al., 2015; Yu et al., 2013). It should be noted that such systems when used clinically may be susceptible to complications, mostly related to the catheter's physicochemical impact and possible infection (Draulans et al., 2013).

2.9. Summary notes

Although being relatively rare, SCAs are exceedingly difficult clinical entities to treat. This challenge is borne by the fact that many patients present with infiltrative tumors that are not amenable to satisfactory resection or even applying surgical intervention due to the functional eloquence of the axonal tracts and neuronal circuits that carry crucial vital functions of the spinal cord. In our assessment, newly emerged therapies such as genetically engineered stem cell-based GDEPT, direct gene therapy, and targeted immunotherapy are promising domains of therapeutic development that have provided and will continuously offer medical caregivers with more efficacious treatments for patients suffering from high grade SCAs. Importantly, to eventually conquer spinal cord malignant tumors, future interventions must be able to selectively track and ablate the so-called cancer stem cells (CSCs)/tumor survival cells (TSCs). We have shown that CSCs/TSCs of SCAs are more resilient to oncolytic assault than those in brain glioblastoma, as F3.CD NSC implantation plus 5-FC injection was effective in a murine intracranial glioblastoma model but not impactful on C6 SCA in rats (Aboody et al., 2000; Ropper et al., 2016). In addition, hyperthermia preconditioning increased numbers of human glioblastoma cells that expressed CSC/TSC markers and facilitated their engrafting in the adult rat spinal cord (Zeng et al., 2016). Therefore, future therapeutic designs for SCAs should factor in mechanisms that can specifically target the most critical features of the disease in regards of tumorigenesis, malignant grade, lethality, functional anatomy of the spinal cord, pharmacokinetics, and synergistic combination of treatment modalities.

Acknowledgement

Research work at Dr. Teng's Lab has been supported by NIH, United States Departments of Defense and Veterans Affairs, The Gordon Project to Treat Clinical Paralysis, The Rubin Family Fund, The Center for the Advancement of Science in Space, and The National Aeronautics and Space Administration.

Disclosure

There is no conflict of interest to disclose. FDA device and drug status are not applicable for this paper.

References

Abd-El-Barr, M.M., Huang, K.T., Chi, J.H., 2016. Infiltrating spinal cord astrocytomas: Epidemiology, diagnosis, treatments and future directions. J. Clin. Neurosci. 29, 15–20.
Abdel-Wahab, M., Etuk, B., Palermo, J., Shirato, H., Kresl, J., Yapicier, O., Walker, G., Scheithauer, B.W., Shaw, E., Lee, C., Curran, W., Thomas, T., Markoe, A., 2006. Spinal cord gliomas: A multi-institutional retrospective analysis. Int. J. Radiat. Oncol. Biol. Phys. 64, 1060–1071.
Aboody, K.S., Brown, A., Rainov, N.G., Bower, K.A., Liu, S., Yang, W., Small, J.E., Herrlinger, U., Ourednik, V., Black, P.M., Breakefield, X.O., Snyder, E.Y., 2000. Neural stem cells display extensive tropism for pathology in adult brain: evidence from intracranial gliomas. Proc. Natl. Acad. Sci. U. S. A. 97, 12846–12851.
Aboody, K., Capela, A., Niazi, N., Stern, J.H., Temple, S., 2011. Translating stem cell studies to the clinic for CNS repair: current state of the art and the need for a Rosetta stone. Neuron 70, 597–613.
Agarwalla, P., Barnard, Z., Fecci, P., Dranoff, G., Curry Jr., W.T., 2012. Sequential immunotherapy by vaccination with GM-CSF-expressing glioma cells and CTLA-4 blockade effectively treats established murine intracranial tumors. J. Immunother. 35, 385–389.
Babu, R., Karikari, I.O., Owens, T.R., Bagley, C.A., 2014. Spinal cord astrocytomas: a modern 20-year experience at a single institution. Spine (Phila Pa 1976) 39, 533–540.
Barrangou, R., Fremaux, C., Deveau, H., Richards, M., Boyaval, P., Moineau, S., Romero, D.A., Horvath, P., 2007. CRISPR provides acquired resistance against viruses in prokaryotes. Science 315, 1709–1712.
Bartanusz, V., Jezova, D., Alajajian, B., Digicaylioglu, M., 2011. The blood-spinal cord barrier: morphology and clinical implications. Ann. Neurol. 70, 194–206.
Bender, S., Tang, Y., Lindroth, A.M., Hovestadt, V., Jones, D.T., Kool, M., Zapatka, M., Northcott, P.A., Sturm, D., Wang, W., Radlwimmer, B., Hojfeldt, J.W., Truffaux, N., Castel, D., Schubert, S., Ryzhova, M., Seker-Cin, H., Gronych, J., Johann, P.D., Stark, S., Meyer, J., Milde, T., Schuhmann, M., Ebinger, M., Monoranu, C.M., Ponnuswami, A., Chen, S., Jones, C., Witt, O., Collins, V.P., von Deimling, A., Jabado, N., Puget, S., Grill, J., Helin, K., Korshunov, A., Lichter, P., Monje, M., Plass, C., Cho, Y.J., Pfister, S.M., 2013. Reduced H3K27me3 and DNA hypomethylation are major drivers of gene expression in K27M mutant pediatric high-grade gliomas. Cancer Cell 24, 660–672.
Benvegnu, L., Fattovich, G., Noventa, F., Tremolada, F., Chemello, L., Cecchetto, A., Alberti, A., 1994. Concurrent hepatitis B and C virus infection and risk of hepatocellular carcinoma in cirrhosis. A prospective study. Cancer 74, 2442–2448.
Bjerke, L., Mackay, A., Nandhabalan, M., Burford, A., Jury, A., Popov, S., Bax, D.A., Carvalho, D., Taylor, K.R., Vinci, M., Bajrami, I., McGonnell, I.M., Lord, C.J., Reis, R.M., Hargrave, D., Ashworth, A., Workman, P., Jones, C., 2013. Histone H3.3. mutations drive pediatric glioblastoma through upregulation of MYCN. Cancer Discov 3, 512–519.
Bobo, R.H., Laske, D.W., Akbasak, A., Morrison, P.F., Dedrick, R.L., Oldfield, E.H., 1994. Convection-enhanced delivery of macromolecules in the brain. Proc. Natl. Acad. Sci. U. S. A. 91, 2076–2080.
Brem, H., Piantadosi, S., Burger, P.C., Walker, M., Selker, R., Vick, N.A., Black, K., Sisti, M., Brem, S., Mohr, G., et al., 1995. Placebo-controlled trial of safety and efficacy of intraoperative controlled delivery by biodegradable polymers of chemotherapy for recurrent gliomas. The Polymer-brain Tumor Treatment Group. Lancet 345, 1008–1012.
Burnet, F.M., 1967. Immunological aspects of malignant disease. Lancet 1, 1171–1174.
Calinescu, A.A., Kamran, N., Baker, G., Mineharu, Y., Lowenstein, P.R., Castro, M.G., 2015. Overview of current immunotherapeutic strategies for glioma. Immunotherapy 7, 1073–1104.
Caplan, J., Pradilla, G., Hdeib, A., Tyler, B.M., Legnani, F.G., Bagley, C.A., Brem, H., Jallo, G., 2006. A novel model of intramedullary spinal cord tumors in rats: functional progression and histopathological characterization. Neurosurgery 59, 193–200 discussion 193-200.
Chamberlain, M.C., 2008. Temozolomide for recurrent low-grade spinal cord gliomas in adults. Cancer 113, 1019–1024.
Chamberlain, M.C., Johnston, S.K., 2011. Recurrent spinal cord glioblastoma: salvage therapy with bevacizumab. J. Neuro-Oncol. 102, 427–432.
Chamberlain, M.C., Tredway, T.L., 2011. Adult primary intradural spinal cord tumors: a review. Curr Neurol Neurosci Rep 11, 320–328.
Chan, J.A., Krichevsky, A.M., Kosik, K.S., 2005. MicroRNA-21 is an antiapoptotic factor in human glioblastoma cells. Cancer Res. 65, 6029–6033.
Chen, Y., Gorski, D.H., 2008. Regulation of angiogenesis through a microRNA (miR-130a)

that down-regulates antiangiogenic homeobox genes GAX and HOXA5. Blood 111, 1217–1226.
Cheney, I.W., Johnson, D.E., Vaillancourt, M.-T., Avanzini, J., Morimoto, A., Demers, G.W., Wills, K.N., Shabram, P.W., Bolen, J.B., Tavtigian, S.V., Bookstein, R., 1998. Suppression of Tumorigenicity of Glioblastoma Cells by Adenovirus-mediated < em > MMAC1/PTEN < /em > Gene Transfer. Cancer Res. 58, 2331–2334.
Chulpanova, D.S., Kitaeva, K.V., Tazetdinova, L.G., James, V., Rizvanov, A.A., Solovyeva, V.V., 2018. Application of Mesenchymal Stem Cells for Therapeutic Agent Delivery in Anti-tumor Treatment. Front. Pharmacol. 9, 259.
Chung, T., Na, J., Kim, Y.I., Chang, D.Y., Kim, Y.I., Kim, H., Moon, H.E., Kang, K.W., Lee, D.S., Chung, J.K., Kim, S.S., Suh-Kim, H., Paek, S.H., Youn, H., 2016. Dihydropyrimidine Dehydrogenase Is a Prognostic Marker for Mesenchymal Stem Cell-Mediated Cytosine Deaminase Gene and 5-Fluorocytosine Prodrug Therapy for the Treatment of Recurrent Gliomas. Theranostics 6, 1477–1490.
Cobbs, C.S., 2013. Cytomegalovirus and brain tumor: epidemiology, biology and therapeutic aspects. Curr. Opin. Oncol. 25, 682–688.
Corradini, S., Hadi, I., Hankel, V., Ertl, L., Ganswindt, U., Belka, C., Niyazi, M., 2016. Radiotherapy of spinal cord gliomas : A retrospective mono-institutional analysis. Strahlenther. Onkol. 192, 139–145.
Davies, H., Bignell, G.R., Cox, C., Stephens, P., Edkins, S., Clegg, S., Teague, J., Woffendin, H., Garnett, M.J., Bottomley, W., Davis, N., Dicks, E., Ewing, R., Floyd, Y., Gray, K., Hall, S., Hawes, R., Hughes, J., Kosmidou, V., Menzies, A., Mould, C., Parker, A., Stevens, C., Watt, S., Hooper, S., Wilson, R., Jayatilake, H., Gusterson, B.A., Cooper, C., Shipley, J., Hargrave, D., Pritchard-Jones, K., Maitland, N., Chenevix-Trench, G., Riggins, G.J., Bigner, D.D., Palmieri, G., Cossu, A., Flanagan, A., Nicholson, A., Ho, J.W., Leung, S.Y., Yuen, S.T., Weber, B.L., Seigler, H.F., Darrow, T.L., Paterson, H., Marais, R., Marshall, C.J., Wooster, R., Stratton, M.R., Futreal, P.A., 2002. Mutations of the BRAF gene in human cancer. Nature 417, 949–954.
Deletis, V., Sala, F., 2008. Intraoperative neurophysiological monitoring of the spinal cord during spinal cord and spine surgery: a review focus on the corticospinal tracts. Clin. Neurophysiol. 119, 248–264.
Doll, R., Kinlen, L., 1970. Immunosurveillance and cancer: epidemiological evidence. Br. Med. J. 4, 420–422.
Draulans, N., Vermeersch, K., Degraeuwe, B., Meurrens, T., Peers, K., Nuttin, B., Kiekens, C., 2013. Intrathecal baclofen in multiple sclerosis and spinal cord injury: complications and long-term dosage evolution. Clin. Rehabil. 27, 1137–1143.
Dunn, G.P., Fecci, P.E., Curry, W.T., 2012. Cancer immunoediting in malignant glioma. Neurosurgery 71, 201–222 discussion 222-203.
Endo, T., Fujii, Y., Sugiyama, S.I., Zhang, R., Ogita, S., Funamoto, K., Saito, R., Tominaga, T., 2015. Properties of convective delivery in spinal cord gray matter: laboratory investigation and computational simulations. J Neurosurg Spine 1–8.
Epstein, F.J., Farmer, J.P., Freed, D., 1992. Adult intramedullary astrocytomas of the spinal cord. J. Neurosurg. 77, 355–359.
Fakhreddine, M.H., Mahajan, A., Penas-Prado, M., Weinberg, J., McCutcheon, I.E., Puduvalli, V., Brown, P.D., 2013. Treatment, prognostic factors, and outcomes in spinal cord astrocytomas. Neuro-Oncology 15, 406–412.
Fecci, P.E., Ochiai, H., Mitchell, D.A., Grossi, P.M., Sweeney, A.E., Archer, G.E., Cummings, T., Allison, J.P., Bigner, D.D., Sampson, J.H., 2007. Systemic CTLA-4 blockade ameliorates glioma-induced changes to the CD4+ T cell compartment without affecting regulatory T-cell function. Clin. Cancer Res. 13, 2158–2167.
Fecci, P.E., Heimberger, A.B., Sampson, J.H., 2014. Immunotherapy for primary brain tumors: no longer a matter of privilege. Clin. Cancer Res. 20, 5620–5629.
Friedmann, T., Roblin, R., 1972. Gene therapy for human genetic disease? Science 178, 648–649.
Furlan, J.C., Fehlings, M.G., Halliday, W., Krassioukov, A.V., 2003. Autonomic dysreflexia associated with intramedullary astrocytoma of the spinal cord. Lancet Oncol. 4, 574–575.
Furnari, F.B., Cloughesy, T.F., Cavenee, W.K., Mischel, P.S., 2015. Heterogeneity of epidermal growth factor receptor signalling networks in glioblastoma. Nat. Rev. Cancer 15, 302–310.
Fuxe, J., Akusjarvi, G., Goike, H.M., Roos, G., Collins, V.P., Pettersson, R.F., 2000. Adenovirus-mediated overexpression of p15INK4B inhibits human glioma cell growth, induces replicative senescence, and inhibits telomerase activity similarly to p16INK4A. Cell Growth Differ. 11, 373–384.
Garces-Ambrossi, G.L., McGirt, M.J., Mehta, V.A., Sciubba, D.M., Witham, T.F., Bydon, A., Wolinksy, J.P., Jallo, G.I., Gokaslan, Z.L., 2009. Factors associated with progression-free survival and long-term neurological outcome after resection of intramedullary spinal cord tumors: analysis of 101 consecutive cases. J Neurosurg Spine 11, 591–599.
Garg, T., Bhandari, S., Rath, G., Goyal, A.K., 2015. Current strategies for targeted delivery of bio-active drug molecules in the treatment of brain tumor. J. Drug Target. 23, 865–887.
Gross, G., Waks, T., Eshhar, Z., 1989. Expression of immunoglobulin-T-cell receptor chimeric molecules as functional receptors with antibody-type specificity. Proc. Natl. Acad. Sci. U. S. A. 86, 10024–10028.
Grosso, S., Doyen, J., Parks, S.K., Bertero, T., Paye, A., Cardinaud, B., Gounon, P., Lacas-Gervais, S., Noël, A., Pouysségur, J., Barbry, P., Mazure, N.M., Mari, B., 2013. MiR-210 promotes a hypoxic phenotype and increases radioresistance in human lung cancer cell lines. Cell Death Dis. 4 e544.
Guss, Z.D., Moningi, S., Jallo, G.I., Cohen, K.J., Wharam, M.D., Terezakis, S.A., 2013. Management of pediatric spinal cord astrocytomas: outcomes with adjuvant radiation. Int. J. Radiat. Oncol. Biol. Phys. 85, 1307–1311.
Hamid, O., Robert, C., Daud, A., Hodi, F.S., Hwu, W.J., Kefford, R., Wolchok, J.D., Hersey, P., Joseph, R.W., Weber, J.S., Dronca, R., Gangadhar, T.C., Patnaik, A., Zarour, H., Joshua, A.M., Gergich, K., Elassaiss-Schaap, J., Algazi, A., Mateus, C., Boasberg, P., Tumeh, P.C., Chmielowski, B., Ebbinghaus, S.W., Li, X.N., Kang, S.P., Ribas, A., 2013. Safety and tumor responses with lambrolizumab (anti-PD-1) in melanoma. N. Engl. J. Med. 369, 134–144.
Han, J., Chu, J., Keung Chan, W., Zhang, J., Wang, Y., Cohen, J.B., Victor, A., Meisen, W.H., Kim, S.H., Grandi, P., Wang, Q.E., He, X., Nakano, I., Chiocca, E.A., Glorioso 3rd, J.C., Kaur, B., Caligiuri, M.A., Yu, J., 2015. CAR-Engineered NK Cells Targeting Wild-Type EGFR and EGFRvIII Enhance Killing of Glioblastoma and Patient-Derived Glioblastoma Stem Cells. Sci. Rep. 5, 11483.
Han, I.B., Kim, M., Lee, S.H., Kim, J.K., Kim, S.H., Chang, J.H., Teng, Y.D., 2016. Down-regulation of MicroRNA-126 in Glioblastoma and its Correlation with Patient Prognosis: A Pilot Study. Anticancer Res. 36, 6691–6697.
Hegi, M.E., Diserens, A.C., Gorlia, T., Hamou, M.F., de Tribolet, N., Weller, M., Kros, J.M., Hainfellner, J.A., Mason, W., Mariani, L., Bromberg, J.E., Hau, P., Mirimanoff, R.O., Cairncross, J.G., Janzer, R.C., Stupp, R., 2005. MGMT gene silencing and benefit from temozolomide in glioblastoma. N. Engl. J. Med. 352, 997–1003.
Heo, D.H., Kim, S.H., Yang, K.M., Cho, Y.J., Kim, K.N., Yoon, D.H., Kang, T.C., 2012. A histopathological diagnostic marker for human spinal astrocytoma: expression of glial fibrillary acidic protein-delta. J. Neuro-Oncol. 108, 45–52.
Hermansen, S.K., Dahlrot, R.H., Nielsen, B.S., Hansen, S., Kristensen, B.W., 2013. MiR-21 expression in the tumor cell compartment holds unfavorable prognostic value in gliomas. J. Neuro-Oncol. 111, 71–81.
Hodi, F.S., O'Day, S.J., McDermott, D.F., Weber, R.W., Sosman, J.A., Haanen, J.B., Gonzalez, R., Robert, C., Schadendorf, D., Hassel, J.C., Akerley, W., van den Eertwegh, A.J., Lutzky, J., Lorigan, P., Vaubel, J.M., Linette, G.P., Hogg, D., Ottensmeier, C.H., Lebbe, C., Peschel, C., Quirt, I., Clark, J.I., Wolchok, J.D., Weber, J.S., Tian, J., Yellin, M.J., Nichol, G.M., Hoos, A., Urba, W.J., 2010. Improved survival with ipilimumab in patients with metastatic melanoma. N. Engl. J. Med. 363, 711–723.
Horbinski, C., Nikiforova, M.N., Hagenkord, J.M., Hamilton, R.L., Pollack, I.F., 2012. Interplay among BRAF, p16, p53, and MIB1 in pediatric low-grade gliomas. Neuro-Oncology 14, 777–789.
Horvath, P., Barrangou, R., 2010. CRISPR/Cas, the immune system of bacteria and archaea. Science 327, 167–170.
Hsu, W., Siu, I.M., Pradilla, G., Gokaslan, Z.L., Jallo, G.I., Gallia, G.L., 2012. Animal model of intramedullary spinal cord glioma using human glioblastoma multiforme neurospheres. J Neurosurg Spine 16, 315–319.
Huillard, E., Hashizume, R., Phillips, J.J., Griveau, A., Ihrie, R.A., Aoki, Y., Nicolaides, T., Perry, A., Waldman, T., McMahon, M., Weiss, W.A., Petritsch, C., James, C.D., Rowitch, D.H., 2012. Cooperative interactions of BRAFV600E kinase and CDKN2A locus deficiency in pediatric malignant astrocytoma as a basis for rational therapy. Proc. Natl. Acad. Sci. U. S. A. 109, 8710–8715.
Hulou, M.M., Cho, C.F., Chiocca, E.A., Bjerkvig, R., 2016. Experimental therapies: gene therapies and oncolytic viruses. Handb. Clin. Neurol. 134, 183–197.
Ichimura, K., Bolin, M.B., Goike, H.M., Schmidt, E.E., Moshref, A., Collins, V.P., 2000. Deregulation of the p14ARF/MDM2/p53 pathway is a prerequisite for human astrocytic gliomas with G1-S transition control gene abnormalities. Cancer Res. 60, 417–424.
Iwadate, Y., Mochizuki, S., Fujimoto, S., Namba, H., Sakiyama, S., Tagawa, M., Yamaura, A., 2000. Alteration of CDKN2/p16 in human astrocytic tumors is related with increased susceptibility to antimetabolite anticancer agents. Int. J. Oncol. 17, 501–505.
Jang, C.W., Shibata, Y., Starmer, J., Yee, D., Magnuson, T., 2015. Histone H3.3 maintains genome integrity during mammalian development. Genes Dev. 29, 1377–1392.
Jiang, L., Mao, P., Song, L., Wu, J., Huang, J., Lin, C., Yuan, J., Qu, L., Cheng, S.Y., Li, J., 2010. miR-182 as a prognostic marker for glioma progression and patient survival. Am. J. Pathol. 177, 29–38.
Jiang, H., Yu, W.-W., Wang, L.-L., Peng, Y., 2015. miR-130a acts as a potential diagnostic biomarker and promotes gastric cancer migration, invasion and proliferation by targeting RUNX3. Oncol. Rep. 34, 1153–1161.
Jo, S.H., Son, M.K., Koh, H.J., Lee, S.M., Song, I.H., Kim, Y.O., Lee, Y.S., Jeong, K.S., Kim, W.B., Park, J.W., Song, B.J., Huh, T.L., 2001. Control of mitochondrial redox balance and cellular defense against oxidative damage by mitochondrial NADP+-dependent isocitrate dehydrogenase. J. Biol. Chem. 276, 16168–16176.
Johannessen, C.M., Reczek, E.E., James, M.F., Brems, H., Legius, E., Cichowski, K., 2005. The NF1 tumor suppressor critically regulates TSC2 and mTOR. Proc. Natl. Acad. Sci. U. S. A. 102, 8573–8578.
Jones, D.T., Kocialkowski, S., Liu, L., Pearson, D.M., Backlund, L.M., Ichimura, K., Collins, V.P., 2008. Tandem duplication producing a novel oncogenic BRAF fusion gene defines the majority of pilocytic astrocytomas. Cancer Res. 68, 8673–8677.
Jyothirmayi, R., Madhavan, J., Nair, M.K., Rajan, B., 1997. Conservative surgery and radiotherapy in the treatment of spinal cord astrocytoma. J. Neuro-Oncol. 33, 205–211.
Kaley, T.J., Mondesire-Crump, I., Gavrilovic, I.T., 2012. Temozolomide or bevacizumab for spinal cord high-grade gliomas. J. Neuro-Oncol. 109, 385–389.
Kang, H.-J., Cui, Y., Yin, H., Scheid, A., Hendricks, W.P., Schmidt, J., Sekulic, A., Kong, D., Trent, J.M., Gokhale, V., 2016. A pharmacological chaperone molecule induces cancer cell death by restoring tertiary DNA structures in mutant hTERT promoters. J. Am. Chem. Soc. 138, 13673–13692.
Karikari, I.O., Nimjee, S.M., Hodges, T.R., Cutrell, E., Hughes, B.D., Powers, C.J., Mehta, A.I., Hardin, C., Bagley, C.A., Isaacs, R.E., Haglund, M.M., Friedman, A.H., 2011. Impact of tumor histology on resectability and neurological outcome in primary intramedullary spinal cord tumors: a single-center experience with 102 patients. Neurosurgery 68, 188–197 discussion 197.
Karikari, I.O., Nimjee, S.M., Hodges, T.R., Cutrell, E., Hughes, B.D., Powers, C.J., Mehta, A.I., Hardin, C., Bagley, C.A., Isaacs, R.E., Haglund, M.M., Friedman, A.H., 2015. Impact of tumor histology on resectability and neurological outcome in primary intramedullary spinal cord tumors: a single-center experience with 102 patients.

Neurosurgery 76 (Suppl 1), S4–S13 discussion S13.
Karsy, M., Guan, J., Sivakumar, W., Neil, J.A., Schmidt, M.H., Mahan, M.A., 2015. The genetic basis of intradural spinal tumors and its impact on clinical treatment. Neurosurg. Focus. 39, E3.
Kefas, B., Comeau, L., Erdle, N., Montgomery, E., Amos, S., Purow, B., 2010. Pyruvate kinase M2 is a target of the tumor-suppressive microRNA-326 and regulates the survival of glioma cells. Neuro-Oncology 12, 1102–1112.
Kim, S.K., Cargioli, T.G., Machluf, M., Yang, W., Sun, Y., Al-Hashem, R., Kim, S.U., Black, P.M., Carroll, R.S., 2005. PEX-producing human neural stem cells inhibit tumor growth in a mouse glioma model. Clin. Cancer Res. 11, 5965–5970.
Kim, W.H., Yoon, S.H., Kim, C.Y., Kim, K.J., Lee, M.M., Choe, G., Kim, I.A., Kim, J.H., Kim, Y.J., Kim, H.J., 2011. Temozolomide for malignant primary spinal cord glioma: an experience of six cases and a literature review. J. Neuro-Oncol. 101, 247–254.
Kim, J.E., Patel, M.A., Mangraviti, A., Kim, E.S., Theodros, D., Velarde, E., Liu, A., Sankey, E.W., Tam, A., Xu, H., Mathios, D., Jackson, C.M., Harris-Bookman, S., Garzon-Muvdi, T., Sheu, M., Martin, A.M., Tyler, B.M., Tran, P.T., Ye, X., Olivi, A., Taube, J.M., Burger, P.C., Drake, C.G., Brem, H., Pardoll, D.M., Lim, M., 2017. Combination Therapy with Anti-PD-1, Anti-TIM-3, and Focal Radiation Results in Regression of Murine Gliomas. Clin. Cancer Res. 23, 124–136.
Konar, S.K., Bir, S.C., Maiti, T.K., Nanda, A., 2017. A systematic review of overall survival in pediatric primary glioblastoma multiforme of the spinal cord. J Neurosurg Pediatr 19, 239–248.
Krassioukov, A., Warburton, D.E., Teasell, R., Eng, J.J., 2009. A systematic review of the management of autonomic dysreflexia after spinal cord injury. Arch. Phys. Med. Rehabil. 90, 682–695.
Krimpenfort, P., Ijpenberg, A., Song, J.Y., van der Valk, M., Nawijn, M., Zevenhoven, J., Berns, A., 2007. p15Ink4b is a critical tumour suppressor in the absence of p16Ink4a. Nature 448, 943–946.
Kroll, R.A., Neuwelt, E.A., 1998. Outwitting the blood-brain barrier for therapeutic purposes: osmotic opening and other means. Neurosurgery 42, 1083–1099 discussion 1099-1100.
Kutluk, T., Varan, A., Kafali, C., Hayran, M., Soylemezoglu, F., Zorlu, F., Aydin, B., Yalcin, B., Akyuz, C., Buyukpamukcu, M., 2015. Pediatric intramedullary spinal cord tumors: a single center experience. Eur. J. Paediatr. Neurol. 19, 41–47.
Lammering, G., Hewit, T.H., Valerie, K., Contessa, J.N., Amorino, G.P., Dent, P., Schmidt-Ullrich, R.K., 2003. EGFRvIII-mediated radioresistance through a strong cytoprotective response. Oncogene 22, 5545–5553.
Liu, D., Liu, Z., Condouris, S., Xing, M., 2007. BRAF V600E Maintains Proliferation, Transformation, and Tumorigenicity of BRAF-Mutant Papillary Thyroid Cancer Cells. J. Clin. Endocrinol. Metab. 92, 2264–2271.
Liu, Q., Zou, R., Zhou, R., Gong, C., Wang, Z., Cai, T., Tan, C., Fang, J., 2015. miR-155 Regulates Glioma Cells Invasion and Chemosensitivity by p38 Isforms In Vitro. J. Cell. Biochem. 116, 1213–1221.
Llorens-Bobadilla, E., Martin-Villalba, A., 2017. Adult NSC diversity and plasticity: the role of the niche. Curr. Opin. Neurobiol. 42, 68–74.
Lonser, R.R., Gogate, N., Morrison, P.F., Wood, J.D., Oldfield, E.H., 1998. Direct convective delivery of macromolecules to the spinal cord. J. Neurosurg. 89, 616–622.
Lötsch, D., Ghanim, B., Laaber, M., Wurm, G., Weis, S., Lenz, S., Webersinke, G., Pichler, J., Berger, W., Spiegl-Kreinecker, S., 2013. Prognostic significance of telomerase-associated parameters in glioblastoma: effect of patient age. Neuro-Oncology 15, 423–432.
Louis, D.N., Ohgaki, H., Wiestler, O.D., Cavenee, W.K., Burger, P.C., Jouvet, A., Scheithauer, B.W., Kleihues, P., 2007. The 2007 WHO classification of tumours of the central nervous system. Acta Neuropathol. 114, 97–109.
Louis, D.N., Perry, A., Reifenberger, G., von Deimling, A., Figarella-Branger, D., Cavenee, W.K., Ohgaki, H., Wiestler, O.D., Kleihues, P., Ellison, D.W., 2016. The 2016 World Health Organization Classification of Tumors of the Central Nervous System: a summary. Acta Neuropathol. 131, 803–820.
Maeder, M.L., Gersbach, C.A., 2016. Genome-editing Technologies for Gene and Cell Therapy. Mol. Ther. 24, 430–446.
Maguire, C.A., Ramirez, S.H., Merkel, S.F., Sena-Esteves, M., Breakefield, X.O., 2014. Gene therapy for the nervous system: challenges and new strategies. Neurotherapeutics 11, 817–839.
McCool, F.D., 2012. Chapter 99. Diseases of the diaphragm, chest wall, pleura, and mediastinum. In: Cecil, R.L.F., Goldman, L., Schafer, A.I. (Eds.), Goldman's Cecil Medicine. Elsevier Saunders, Philadelphia, PA, pp. 603.
McGirt, M.J., Goldstein, I.M., Chaichana, K.L., Tobias, M.E., Kothbauer, K.F., Jallo, G.I., 2008. Extent of surgical resection of malignant astrocytomas of the spinal cord: outcome analysis of 35 patients. Neurosurgery 63, 55–60 discussion 60-51.
McGirt, M.J., Mukherjee, D., Chaichana, K.L., Than, K.D., Weingart, J.D., Quinones-Hinojosa, A., 2009. Association of surgically acquired motor and language deficits on overall survival after resection of glioblastoma multiforme. Neurosurgery 65, 463–469 discussion 469-470.
Medawar, P.B., 1948. Immunity to homologous grafted skin; the fate of skin homografts transplanted to the brain, to subcutaneous tissue, and to the anterior chamber of the eye. Br. J. Exp. Pathol. 29, 58–69.
Micallef, J., Taccone, M., Mukherjee, J., Croul, S., Busby, J., Moran, M.F., Guha, A., 2009. Epidermal growth factor receptor variant III-induced glioma invasion is mediated through myristoylated alanine-rich protein kinase C substrate overexpression. Cancer Res. 69, 7548–7556.
Milano, M.T., Johnson, M.D., Sul, J., Mohile, N.A., Korones, D.N., Okunieff, P., Walter, K.A., 2010. Primary spinal cord glioma: a Surveillance, Epidemiology, and End Results database study. J. Neuro-Oncol. 98, 83–92.
Minehan, K.J., Brown, P.D., Scheithauer, B.W., Krauss, W.E., Wright, M.P., 2009. Prognosis and treatment of spinal cord astrocytoma. Int. J. Radiat. Oncol. Biol. Phys. 73, 727–733.
Mistry, M., Zhukova, N., Merico, D., Rakopoulos, P., Krishnatry, R., Shago, M., Stavropoulos, J., Alon, N., Pole, J.D., Ray, P.N., Navickiene, V., Mangerel, J., Remke, M., Buczkowicz, P., Ramaswamy, V., Stucklin, A.G., Li, M., Young, E.J., Zhang, C., Castelo-Branco, P., Bakry, D., Laughlin, S., Shlien, A., Chan, J., Ligon, K.L., Rutka, J.T., Dirks, P.B., Taylor, M.D., Greenberg, M., Malkin, D., Huang, A., Bouffet, E., Hawkins, C.E., Tabori, U., 2015. BRAF Mutation and CDKN2A Deletion Define a Clinically Distinct Subgroup of Childhood Secondary High-Grade Glioma. J. Clin. Oncol. 33, 1015–1022.
Mitchell, D.A., Xie, W., Schmittling, R., Learn, C., Friedman, A., McLendon, R.E., Sampson, J.H., 2008. Sensitive detection of human cytomegalovirus in tumors and peripheral blood of patients diagnosed with glioblastoma. Neuro-Oncology 10, 10–18.
Mitchell, D.A., Batich, K.A., Gunn, M.D., Huang, M.N., Sanchez-Perez, L., Nair, S.K., Congdon, K.L., Reap, E.A., Archer, G.E., Desjardins, A., Friedman, A.H., Friedman, H.S., Herndon 2nd, J.E., Coan, A., McLendon, R.E., Reardon, D.A., Vredenburgh, J.J., Bigner, D.D., Sampson, J.H., 2015. Tetanus toxoid and CCL3 improve dendritic cell vaccines in mice and glioblastoma patients. Nature 519, 366–369.
Nagaishi, M., Nobusawa, S., Yokoo, H., Sugiura, Y., Tsuda, K., Tanaka, Y., Suzuki, K., Hyodo, A., 2016. Genetic mutations in high grade gliomas of the adult spinal cord. Brain Tumor Pathol 33, 267–269.
Nair, D., Kumaraswamy, V.M., Braver, D., Kilbride, R.D., Borges, L.F., Simon, M.V., 2014. Dorsal column mapping via phase reversal method: the refined technique and clinical applications. Neurosurgery 74, 437–446 discussion 446.
Nance, P., Schryvers, O., Schmidt, B., Dubo, H., Loveridge, B., Fewer, D., 1995. Intrathecal baclofen therapy for adults with spinal spasticity: therapeutic efficacy and effect on hospital admissions. Can J Neurol Sci 22, 22–29.
Oda, K., Matsuoka, Y., Funahashi, A., Kitano, H., 2005. A comprehensive pathway map of epidermal growth factor receptor signaling. Mol. Syst. Biol. 1, 2005.0010.
O'Duibhir, E., Carragher, N.O., Pollard, S.M., 2017. Accelerating glioblastoma drug discovery: Convergence of patient-derived models, genome editing and phenotypic screening. Mol. Cell. Neurosci. 80, 198–207.
Osborn, J.W., Taylor, R.F., Schramm, L.P., 1990. Chronic cervical spinal cord injury and autonomic hyperreflexia in rats. Am. J. Phys. 258, R169–R174.
Ostrom, Q.T., Bauchet, L., Davis, F.G., Deltour, I., Fisher, J.L., Langer, C.E., Pekmezci, M., Schwartzbaum, J.A., Turner, M.C., Walsh, K.M., Wrensch, M.R., Barnholtz-Sloan, J.S., 2014a. The epidemiology of glioma in adults: a "state of the science" review. Neuro-Oncology 16, 896–913.
Ostrom, Q.T., Gittleman, H., Liao, P., Rouse, C., Chen, Y., Dowling, J., Wolinsky, Y., Kruchko, C., Barnholtz-Sloan, J., 2014b. CBTRUS statistical report: primary brain and central nervous system tumors diagnosed in the United States in 2007-2011. Neuro-Oncology 16 (Suppl. 4), iv1–63.
Pardoll, D.M., 2012. The blockade of immune checkpoints in cancer immunotherapy. Nat. Rev. Cancer 12, 252–264.
Park, S.M., Choi, E.Y., Bae, M., Kim, S., Park, J.B., Yoo, H., Choi, J.K., Kim, Y.J., Lee, S.H., Kim, I.H., 2016. Histone variant H3F3A promotes lung cancer cell migration through intronic regulation. Nat. Commun. 7.
Parsa, A.T., Chi, J.H., Acosta Jr., F.L., Ames, C.P., McCormick, P.C., 2005. Intramedullary spinal cord tumors: molecular insights and surgical innovation. Clin. Neurosurg. 52, 76–84.
Penman, C.L., Faulkner, C., Lowis, S.P., Kurian, K.M., 2015. Current Understanding of BRAF Alterations in Diagnosis, Prognosis, and Therapeutic Targeting in Pediatric Low-Grade Gliomas. Front. Oncol. 5, 54.
Platten, M., Bunse, L., Wick, W., Bunse, T., 2016. Concepts in glioma immunotherapy. Cancer Immunol. Immunother. 65, 1269–1275.
Portnow, J., Synold, T.W., Badie, B., Tirughana, R., Lacey, S.F., D'Apuzzo, M., Metz, M.Z., Najbauer, J., Bedell, V., Vo, T., Gutova, M., Frankel, P., Chen, M., Aboody, K.S., 2017. Neural Stem Cell-Based Anticancer Gene Therapy: A First-in-Human Study in Recurrent High-Grade Glioma Patients. Clin. Cancer Res. 23, 2951–2960.
Prins, R.M., Shu, C.J., Radu, C.G., Vo, D.D., Khan-Farooqi, H., Soto, H., Yang, M.Y., Lin, M.S., Shelly, S., Witte, O.N., Ribas, A., Liau, L.M., 2008. Anti-tumor activity and trafficking of self, tumor-specific T cells against tumors located in the brain. Cancer Immunol. Immunother. 57, 1279–1289.
Pritchard, C.D., Slotkin, J.R., Yu, D., Dai, H., Lawrence, M.S., Bronson, R.T., Reynolds, F.M., Teng, Y.D., Woodard, E.J., Langer, R.S., 2010. Establishing a model spinal cord injury in the African green monkey for the preclinical evaluation of biodegradable polymer scaffolds seeded with human neural stem cells. J. Neurosci. Methods 188, 258–269.
Prockop, L.D., Naidu, K.A., Binard, J.E., Ransohoff, J., 1995. Selective permeability of [3H]-D-mannitol and [14C]-carboxyl-inulin across the blood-brain barrier and blood-spinal cord barrier in the rabbit. J Spinal Cord Med 18, 221–226.
Qiu, S., Lin, S., Hu, D., Feng, Y., Tan, Y., Peng, Y., 2013. Interactions of miR-323/miR-326/miR-329 and miR-130a/miR-155/miR-210 as prognostic indicators for clinical outcome of glioblastoma patients. J. Transl. Med. 11, 10.
Que, T., Song, Y., Liu, Z., Zheng, S., Long, H., Li, Z., Liu, Y., Wang, G., Liu, Y., Zhou, J., Zhang, X., Fang, W., Qi, S., 2015. Decreased miRNA-637 is an unfavorable prognosis marker and promotes glioma cell growth, migration and invasion via direct targeting Akt1. Oncogene 34, 4952.
Raco, A., Esposito, V., Lenzi, J., Piccirilli, M., Delfini, R., Cantore, G., 2005. Long-term follow-up of intramedullary spinal cord tumors: a series of 202 cases. Neurosurgery 56, 972–981 discussion 972-981.
Rahman, M., Abbatematteo, J., De Leo, E.K., Kubilis, P.S., Vaziri, S., Bova, F., Sayour, E., Mitchell, D., Quinones-Hinojosa, A., 2017. The effects of new or worsened post-operative neurological deficits on survival of patients with glioblastoma. J. Neurosurg. 127, 123–131.
Reddy, R.J., Gajadhar, A.S., Swenson, E.J., Rothenberg, D.A., Curran, T.G., White, F.M., 2016. Early signaling dynamics of the epidermal growth factor receptor. Proc. Natl.

Acad. Sci. 113, 3114–3119.
Ren, T.J., Wang, Z.C., Zhang, Y.Z., Li, D., Wang, H.Y., Li, Z.Z., 2010. Establishment of intramedullary spinal cord glioma model in rats. Chin. Med. J. 123, 2580–2585.
Rodrigues, G.B., Waldron, J.N., Wong, C.S., Laperriere, N.J., 2000. A retrospective analysis of 52 cases of spinal cord glioma managed with radiation therapy. Int. J. Radiat. Oncol. Biol. Phys. 48, 837–842.
Ropper, A.E., Zeng, X., Haragopal, H., Anderson, J.E., Aljuboori, Z., Han, I., Abd-El-Barr, M., Lee, H.J., Sidman, R.L., Snyder, E.Y., Viapiano, M.S., Kim, S.U., Chi, J.H., Teng, Y.D., 2016. Targeted Treatment of Experimental Spinal Cord Glioma With Dual Gene-Engineered Human Neural Stem Cells. Neurosurgery 79, 481–491.
Ropper, A.E., Thakor, D.K., Han, I., Yu, D., Zeng, X., Anderson, J.E., Aljuboori, Z., Kim, S.W., Wang, H., Sidman, R.L., Zafonte, R.D., Teng, Y.D., 2017. Defining recovery neurobiology of injured spinal cord by synthetic matrix-assisted hMSC implantation. Proc. Natl. Acad. Sci. U. S. A. 114, E820–E829.
Ryan, K.M., Phillips, A.C., Vousden, K.H., 2001. Regulation and function of the p53 tumor suppressor protein. Curr. Opin. Cell Biol. 13, 332–337.
Samaha, H., El Naggar, S., Ahmed, N., 2015. Armed hunter killers: discerning the role of adoptive T-cell transfer for glioblastoma. Immunotherapy 7, 481–485.
Sampson, F.C., Hayward, A., Evans, G., Morton, R., Collett, B., 2002. Functional benefits and cost/benefit analysis of continuous intrathecal baclofen infusion for the management of severe spasticity. J. Neurosurg. 96, 1052–1057.
Sampson, J.H., Heimberger, A.B., Archer, G.E., Aldape, K.D., Friedman, A.H., Friedman, H.S., Gilbert, M.R., Herndon 2nd, J.E., McLendon, R.E., Mitchell, D.A., Reardon, D.A., Sawaya, R., Schmittling, R.J., Shi, W., Vredenburgh, J.J., Bigner, D.D., 2010. Immunologic escape after prolonged progression-free survival with epidermal growth factor receptor variant III peptide vaccination in patients with newly diagnosed glioblastoma. J. Clin. Oncol. 28, 4722–4729.
Santi, M., Mena, H., Wong, K., Koeller, K., Olsen, C., Rushing, E.J., 2003. Spinal cord malignant astrocytomas. Clinicopathologic features in 36 cases. Cancer 98, 554–561.
Schellinger, K.A., Propp, J.M., Villano, J.L., McCarthy, B.J., 2008. Descriptive epidemiology of primary spinal cord tumors. J. Neuro-Oncol. 87, 173–179.
Schindler, G., Capper, D., Meyer, J., Janzarik, W., Omran, H., Herold-Mende, C., Schmieder, K., Wesseling, P., Mawrin, C., Hasselblatt, M., Louis, D.N., Korshunov, A., Pfister, S., Hartmann, C., Paulus, W., Reifenberger, G., von Deimling, A., 2011. Analysis of BRAF V600E mutation in 1,320 nervous system tumors reveals high mutation frequencies in pleomorphic xanthoastrocytoma, ganglioglioma and extracerebellar pilocytic astrocytoma. Acta Neuropathol. 121, 397–405.
Schmidt, N.O., Przylecki, W., Yang, W., Ziu, M., Teng, Y.D., Kim, S.U., Black, P.M., Aboody, K.S., Carroll, R.S., 2005. Brain tumor tropism of transplanted human neural stem cells is induced by vascular endothelial growth factor. Neoplasia 7, 623–629.
Schwartzentruber, J., Korshunov, A., Liu, X.Y., Jones, D.T., Pfaff, E., Jacob, K., Sturm, D., Fontebasso, A.M., Quang, D.A., Tonjes, M., Hovestadt, V., Albrecht, S., Kool, M., Nantel, A., Konermann, C., Lindroth, A., Jager, N., Rausch, T., Ryzhova, M., Korbel, J.O., Hielscher, T., Hauser, P., Garami, M., Klekner, A., Bognar, L., Ebinger, M., Schuhmann, M.U., Scheurlen, W., Pekrun, A., Fruhwald, M.C., Roggendorf, W., Kramm, C., Durken, M., Atkinson, J., Lepage, P., Montpetit, A., Zakrzewska, M., Zakrzewski, K., Liberski, P.P., Dong, Z., Siegel, P., Kulozik, A.E., Zapatka, M., Guha, A., Malkin, D., Felsberg, J., Reifenberger, G., von Deimling, A., Ichimura, K., Collins, V.P., Witt, H., Milde, T., Witt, O., Zhang, C., Castelo-Branco, P., Lichter, P., Faury, D., Tabori, U., Plass, C., Majewski, J., Pfister, S.M., Jabado, N., 2012. Driver mutations in histone H3.3 and chromatin remodelling genes in paediatric glioblastoma. Nature 482, 226–231.
Segura, M.F., Hanniford, D., Menendez, S., Reavie, L., Zou, X., Alvarez-Diaz, S., Zakrzewski, J., Blochin, E., Rose, A., Bogunovic, D., 2009. Aberrant miR-182 expression promotes melanoma metastasis by repressing FOXO3 and microphthalmia-associated transcription factor. Proc. Natl. Acad. Sci. 106, 1814–1819.
Shankar, G.M., Francis, J.M., Rinne, M.L., Ramkissoon, S.H., Huang, F.W., Venteicher, A.S., Akama-Garren, E.H., Kang, Y.J., Lelic, N., Kim, J.C., Brown, L.E., Charbonneau, S.K., Golby, A.J., Sekhar Pedamallu, C., Hoang, M.P., Sullivan, R.J., Cherniack, A.D., Garraway, L.A., Stemmer-Rachamimov, A., Reardon, D.A., Wen, P.Y., Brastianos, P.K., Curry, W.T., Barker 2nd, F.G., Hahn, W.C., Nahed, B.V., Ligon, K.L., Louis, D.N., Cahill, D.P., Meyerson, M., 2015. Rapid Intraoperative Molecular Characterization of Glioma. JAMA Oncol 1, 662–667.
Shankar, G.M., Lelic, N., Gill, C.M., Thorner, A.R., Van Hummelen, P., Wisoff, J.H., Loeffler, J.S., Brastianos, P.K., Shin, J.H., Borges, L.F., Butler, W.E., Zagzag, D., Brody, R.I., Duhaime, A.C., Taylor, M.D., Hawkins, C.E., Louis, D.N., Cahill, D.P., Curry, W.T., Meyerson, M., 2016. BRAF alteration status and the histone H3F3A gene K27M mutation segregate spinal cord astrocytoma histology. Acta Neuropathol. 131, 147–150.
Shervington, A., Patel, R., Lu, C., Cruickshanks, N., Lea, R., Roberts, G., Dawson, T., Shervington, L., 2007. Telomerase subunits expression variation between biopsy samples and cell lines derived from malignant glioma. Brain Res. 1134, 45–52.
Simon, M., Koster, G., Menon, A.G., Schramm, J., 1999. Functional evidence for a role of combined CDKN2A (p16-p14(ARF))/CDKN2B (p15) gene inactivation in malignant gliomas. Acta Neuropathol. 98, 444–452.
Smith, J.S., Tachibana, I., Passe, S.M., Huntley, B.K., Borell, T.J., Iturria, N., O'Fallon, J.R., Schaefer, P.L., Scheithauer, B.W., James, C.D., Buckner, J.C., Jenkins, R.B., 2001. PTEN Mutation, EGFR Amplification, and Outcome in Patients With Anaplastic Astrocytoma and Glioblastoma Multiforme. JNCI: Journal of the National Cancer Institute 93, 1246–1256.
Snyder, E.Y., Teng, Y.D., 2012. Stem cells and spinal cord repair. N. Engl. J. Med. 366, 1940–1942.
Solomon, D.A., Wood, M.D., Tihan, T., Bollen, A.W., Gupta, N., Phillips, J.J., Perry, A., 2016. Diffuse Midline Gliomas with Histone H3-K27M Mutation: A Series of 47 Cases Assessing the Spectrum of Morphologic Variation and Associated Genetic Alterations. Brain Pathol. 26, 569–580.
Squatrito, M., Brennan, C.W., Helmy, K., Huse, J.T., Petrini, J.H., Holland, E.C., 2010. Loss of ATM/Chk2/p53 Pathway Components Accelerates Tumor Development and Contributes to Radiation Resistance in Gliomas. Cancer Cell 18, 619–629.
Stupp, R., van den Bent, M.J., Hegi, M.E., 2005. Optimal role of temozolomide in the treatment of malignant gliomas. Curr Neurol Neurosci Rep 5, 198–206.
Sturm, D., Witt, H., Hovestadt, V., Khuong-Quang, D.A., Jones, D.T., Konermann, C., Pfaff, E., Tonjes, M., Sill, M., Bender, S., Kool, M., Zapatka, M., Becker, N., Zucknick, M., Hielscher, T., Liu, X.Y., Fontebasso, A.M., Ryzhova, M., Albrecht, S., Jacob, K., Wolter, M., Ebinger, M., Schuhmann, M.U., van Meter, T., Fruhwald, M.C., Hauch, H., Pekrun, A., Radlwimmer, B., Niehues, T., von Komorowski, G., Durken, M., Kulozik, A.E., Madden, J., Donson, A., Foreman, N.K., Drissi, R., Fouladi, M., Scheurlen, W., von Deimling, A., Monoranu, C., Roggendorf, W., Herold-Mende, C., Unterberg, A., Kramm, C.M., Felsberg, J., Hartmann, C., Wiestler, B., Wick, W., Milde, T., Witt, O., Lindroth, A.M., Schwartzentruber, J., Faury, D., Fleming, A., Zakrzewska, M., Liberski, P.P., Zakrzewski, K., Hauser, P., Garami, M., Klekner, A., Bognar, L., Morrissy, S., Cavalli, F., Taylor, M.D., van Sluis, P., Koster, J., Versteeg, R., Volckmann, R., Mikkelsen, T., Aldape, K., Reifenberger, G., Collins, V.P., Majewski, J., Korshunov, A., Lichter, P., Plass, C., Jabado, N., Pfister, S.M., 2012. Hotspot mutations in H3F3A and IDH1 define distinct epigenetic and biological subgroups of glioblastoma. Cancer Cell 22, 425–437.
Takata, M., Sasaki, M.S., Sonoda, E., Morrison, C., Hashimoto, M., Utsumi, H., Yamaguchi-Iwai, Y., Shinohara, A., Takeda, S., 1998. Homologous recombination and non-homologous end-joining pathways of DNA double-strand break repair have overlapping roles in the maintenance of chromosomal integrity in vertebrate cells. EMBO J. 17, 5497–5508.
Tanic, N., Milovanovic, Z., Tanic, N., Dzodic, R., Juranic, Z., Susnjar, S., Plesinac-Karapandzic, V., Tatic, S., Dramicanin, T., Davidovic, R., Dimitrijevic, B., 2012. The impact of PTEN tumor suppressor gene on acquiring resistance to tamoxifen treatment in breast cancer patients. Cancer Biology & Therapy 13, 1165–1174.
Teasell, R.W., Arnold, J.M., Krassioukov, A., Delaney, G.A., 2000. Cardiovascular consequences of loss of supraspinal control of the sympathetic nervous system after spinal cord injury. Arch. Phys. Med. Rehabil. 81, 506–516.
Teng, Y.D., Wrathall, J.R., 1996. Evaluation of cardiorespiratory parameters in rats after spinal cord trauma and treatment with NBQX, an antagonist of excitatory amino acid receptors. Neurosci. Lett. 209, 5–8.
Teng, Y.D., Mocchetti, I., Taveira-DaSilva, A.M., Gillis, R.A., Wrathall, J.R., 1999. Basic fibroblast growth factor increases long-term survival of spinal motor neurons and improves respiratory function after experimental spinal cord injury. J. Neurosci. 19, 7037–7047.
Teng, Y.D., Lavik, E.B., Qu, X., Park, K.I., Ourednik, J., Zurakowski, D., Langer, R., Snyder, E.Y., 2002. Functional recovery following traumatic spinal cord injury mediated by a unique polymer scaffold seeded with neural stem cells. Proc. Natl. Acad. Sci. U. S. A. 99, 3024–3029.
Teng, Y.D., Yu, D., Ropper, A.E., Li, J., Kabatas, S., Wakeman, D.R., Wang, J., Sullivan, M.P., Redmond Jr., D.E., Langer, R., Snyder, E.Y., Sidman, R.L., 2011. Functional multipotency of stem cells: a conceptual review of neurotrophic factor-based evidence and its role in translational research. Curr. Neuropharmacol. 9, 574–585.
Teng, Y.D., Benn, S.C., Kalkanis, S.N., Shefner, J.M., Onario, R.C., Cheng, B., Lachyankar, M.B., Marconi, M., Li, J., Yu, D., Han, I., Maragakis, N.J., Lládo, J., Erkmen, K., Redmond Jr., D.E., Sidman, R.L., Przedborski, S., Rothstein, J.D., Brown Jr., R.H., Snyder, E.Y., 2012. Multimodal actions of neural stem cells in a mouse model of ALS: a meta-analysis. Sci. Transl. Med. 4, 165ra164.
Teng, Y.D., Snyder, E.Y., Zeng, X., Anderson, J.E., Han, I.B., 2017. Multimodal Neural Stem Cell Research Protocols for Experimental Spinal Cord Injuries. In: Srivastava, A.K., Snyder, E.Y., Teng, Y.D. (Eds.), Stem Cell Technologies in Neuroscience. Springer, San Diego, CA.
Teng, Y.D., Wang, L., Kabatas, S., Ulrich, H., Zafonte, R., 2018. Cancer stem cells or tumor survival cells. Stem Cell Dev *In press*.
Toktas, Z.O., Yılmaz, B., Eksi, M.S., Wang, L., Akakın, A., Yener, Y., Konakcı, M., Ayan, E., Kılıc, T., Konya, D., Teng, Y.D., 2018. An ioMRI-assisted Case of Cervical Intramedullary Diffuse Glioma Resection. Cancer Manag. Res In press.
Tong, Y.Q., Liu, B., Zheng, H.-Y., Gu, J., Liu, H., Li, F., Tan, B.H., Hartman, M., Song, C., Li, Y., 2015. MiR-215, an activator of the CTNNBIP1/β-catenin pathway, is a marker of poor prognosis in human glioma. Oncotarget 6, 25024–25033.
Turcan, S., Rohle, D., Goenka, A., Walsh, L.A., Fang, F., Yilmaz, E., Campos, C., Fabius, A.W.M., Lu, C., Ward, P.S., Thompson, C.B., Kaufman, A., Guryanova, O., Levine, R., Heguy, A., Viale, A., Morris, L.G.T., Huse, J.T., Mellinghoff, I.K., Chan, T.A., 2012. IDH1 mutation is sufficient to establish the glioma hypermethylator phenotype. Nature 483, 479–483.
Tyler, B.M., Hdeib, A., Caplan, J., Legnani, F.G., Fowers, K.D., Brem, H., Jallo, G., Pradilla, G., 2012. Delayed onset of paresis in rats with experimental intramedullary spinal cord gliosarcoma following intratumoral administration of the paclitaxel delivery system OncoGel. J Neurosurg Spine 16, 93–101.
Verla, T., Fridley, J.S., Khan, A.B., Mayer, R.R., Omeis, I., 2016. Neuromonitoring for Intramedullary Spinal Cord Tumor Surgery. World Neurosurg 95, 108–116.
von Deimling, A., Korshunov, A., Hartmann, C., 2011. The next generation of glioma biomarkers: MGMT methylation, BRAF fusions and IDH1 mutations. Brain Pathol. 21, 74–87.
Wainwright, D.A., Chang, A.L., Dey, M., Balyasnikova, I.V., Kim, C.K., Tobias, A., Cheng, Y., Kim, J.W., Qiao, J., Zhang, L., Han, Y., Lesniak, M.S., 2014. Durable therapeutic efficacy utilizing combinatorial blockade against IDO, CTLA-4, and PD-L1 in mice with brain tumors. Clin. Cancer Res. 20, 5290–5301.
Wakefield, A., Pignata, A., Ghazi, A., Ashoori, A., Hegde, M., Landi, D., Gray, T., Scheurer, M.E., Chintagumpala, M., Adesina, A., Gottschalk, S., Hicks, J., Powell, S.Z., Ahmed, N., 2015. Is CMV a target in pediatric glioblastoma? Expression of CMV proteins, pp65 and IE1-72 and CMV nucleic acids in a cohort of pediatric glioblastoma

patients. J. Neuro-Oncol. 125, 307–315.
Walboomers, J.M., Jacobs, M.V., Manos, M.M., Bosch, F.X., Kummer, J.A., Shah, K.V., Snijders, P.J., Peto, J., Meijer, C.J., Munoz, N., 1999. Human papillomavirus is a necessary cause of invasive cervical cancer worldwide. J. Pathol. 189, 12–19.
Wang, S., Lu, S., Geng, S., Ma, S., Liang, Z., Jiao, B., 2013. Expression and clinical significance of microRNA-326 in human glioma miR-326 expression in glioma. Med. Oncol. 30, 373.
Wiedenheft, B., Sternberg, S.H., Doudna, J.A., 2012. RNA-guided genetic silencing systems in bacteria and archaea. Nature 482, 331–338.
Wrensch, M., Jenkins, R.B., Chang, J.S., Yeh, R.-F., Xiao, Y., Decker, P.A., Ballman, K.V., Berger, M., Buckner, J.C., Chang, S., Giannini, C., Halder, C., Kollmeyer, T.M., Kosel, M.L., LaChance, D.H., McCoy, L., O'Neill, B.P., Patoka, J., Pico, A.R., Prados, M., Quesenberry, C., Rice, T., Rynearson, A.L., Smirnov, I., Tihan, T., Wiemels, J., Yang, P., Wiencke, J.K., 2009a. Variants in the CDKN2B and RTEL1 regions are associated with high-grade glioma susceptibility. Nat. Genet. 41, 905.
Wrensch, M., Jenkins, R.B., Chang, J.S., Yeh, R.F., Xiao, Y., Ballman, K.V., Berger, M., Buckner, J.C., Chang, S., Decker, P.A., Giannini, C., Halder, C., Kollmeyer, T.M., Kosel, M.L., LaChance, D.H., McCoy, L., O'Neill, B., Patoka, J., Pico, A.R., Prados, M., Quesenberry, C., Rice, T., Rynearson, A., Smirnov, I., Tihan, T., Wiemels, J., Yang, P., Wiencke, J.K., 2009b. Variants in the CDKN2B and RTEL1 regions are associated with high grade glioma susceptibility. Nat. Genet. 41, 905–908.
Wu, G., Broniscer, A., McEachron, T.A., Lu, C., Paugh, B.S., Becksfort, J., Qu, C., Ding, L., Huether, R., Parker, M., Zhang, J., Gajjar, A., Dyer, M.A., Mullighan, C.G., Gilbertson, R.J., Mardis, E.R., Wilson, R.K., Downing, J.R., Ellison, D.W., Zhang, J., Baker, S.J., 2012. Somatic histone H3 alterations in pediatric diffuse intrinsic pontine gliomas and non-brainstem glioblastomas. Nat. Genet. 44, 251–253.
Yang, H., Ye, D., Guan, K.L., Xiong, Y., 2012. IDH1 and IDH2 mutations in tumorigenesis: mechanistic insights and clinical perspectives. Clin. Cancer Res. 18, 5562–5571.
Yang, H.W., Chung, M., Kudo, T., Meyer, T., 2017. Competing memories of mitogen and p53 signalling control cell-cycle entry. Nature 549, 404–408.
Yin, Y., Shen, W.H., 2008. PTEN: a new guardian of the genome. Oncogene 27, 5443.
Yu, D., Thakor, D.K., Han, I., Ropper, A.E., Haragopal, H., Sidman, R.L., Zafonte, R., Schachter, S.C., Teng, Y.D., 2013. Alleviation of chronic pain following rat spinal cord compression injury with multimodal actions of huperzine A. Proc. Natl. Acad. Sci. U. S. A. 110, E746–E755.
Zadnik, P.L., Gokaslan, Z.L., Burger, P.C., Bettegowda, C., 2013. Spinal cord tumours: advances in genetics and their implications for treatment. Nat. Rev. Neurol. 9, 257–266.
Zeng, X., Han, I., Abd-El-Barr, M., Aljuboori, Z., Anderson, J.E., Chi, J.H., Zafonte, R.D., Teng, Y.D., 2016. The Effects of Thermal Preconditioning on Oncogenic and Intraspinal Cord Growth Features of Human Glioma Cells. Cell Transplant. 25, 2099–2109.
Zhang, W., Zhang, J., Hoadley, K., Kushwaha, D., Ramakrishnan, V., Li, S., Kang, C., You, Y., Jiang, C., Song, S.W., Jiang, T., Chen, C.C., 2012. miR-181d: a predictive glioblastoma biomarker that downregulates MGMT expression. Neuro-Oncology 14, 712–719.
Zhao, S., Lin, Y., Xu, W., Jiang, W., Zha, Z., Wang, P., Yu, W., Li, Z., Gong, L., Peng, Y., Ding, J., Lei, Q., Guan, K.L., Xiong, Y., 2009. Glioma-Derived Mutations in IDH1 Dominantly Inhibit IDH1 Catalytic Activity and Induce HIF-1α. Science 324, 261–265.
Zhao, S., Yang, G., Mu, Y., Han, D., Shi, C., Chen, X., Deng, Y., Zhang, D., Wang, L., Liu, Y., Hou, X., Wang, C., Wu, J., Liu, H., Wang, L., Zhang, G., Qi, J., Fang, X., Shi, C., Ai, J., 2013. MiR-106a is an independent prognostic marker in patients with glioblastoma. Neuro-Oncology 15, 707–717.